Exploring the nervous system architecture of the Chaetognatha: A new morphological approach to help resolving the phylogeny of an enigmatic taxon

Inauguraldissertation

zur

Erlangung des akademischen Grades

doctor rerum naturalium (Dr. rer. nat.)

an der Mathematisch-Naturwissenschaftlichen Fakultät

der

Ernst-Moritz-Arndt-Universität Greifswald

vorgelegt von Verena Rieger

geboren am 03.02.1982

in Stuttgart-Bad Cannstatt

Greifswald, November 2012

Dekan: Prof. Dr. Klaus Fesser

1. Gutachter: Prof. Dr. Steffen Harzsch

2. Gutachter: Prof. Dr. Roland Melzer

Tag der Promotion: 26.04.2013

Table of contents

Summary 4

Zusammenfassung 6

1. General Introduction 8

1.1 Introduction to a taxon: the Chaetognatha 8
1.2 Chaetognath history and phylogeny 10
1.3 Chaetognath behavior 11
1.4 Chaetognath morphology 12
1.5 Chaetognath sensory organs and nervous system 13
1.6 Research topic, motivation, and scope of this study 13

2. The development of the nervous system in *Spadella cephaloptera* 16

2.1 Tubulin & RFamide 16
2.2 BrdU 17

3. The nervous system of adult *Spadella cephaloptera* 18

3.1 The cephalic nervous system 18
3.2 The ventral nervous system 19
3.3 Additional immunohistochemical tests 20
3.3.1 Primary antibodies and phalloidin 20
3.3.2 Secondary antibodies and nuclear staining 25
3.3.3 Discussion 26
3.4 Ciliary receptors 27

4. Interspecific variances of chaetognath nervous systems 30

4.1 Results 30
4.2 Discussion 40

5. Outgroup comparisons with an emphasis on Gnathostomulida 44

5.1 New data of the Gnathostomulid nervous system 44
5.2 Discussion 50

6. Literature 58

7. Authors contributions/ Anteil der Eigenleistung 65

8. Publications.. 67

  8.1 Harzsch et al. 2009 67
  8.2 Rieger et al. 2010 91
  8.3 Rieger et al. 2011 121
  8.4 Perez et al. 2013..143
  8.5 Müller et al. submitted..161

9. Selbständigkeitserklärung..211

10. Acknowledgements 213

11. Appendix..214

  11.1 Material & Methods..214
  11.2 List of abbreviations..221

Summary

Chaetognaths are a fascinating taxon with unique features and a great impact on marine food webs as primary predators of zooplankton. Their phylogenetic position has been subject to many speculations ever since their discovery and even contemporary phylogenomic methods have not yet been able to suggest a stable hypothesis on their phylogenetic position within the Bilateria. Neuroanatomical studies may contribute new aspects to this discussion. This study aims to provide new insights into the chaetognath nervous system using a fresh set of methods to determine characters for a phylogenetic discussion. The method of choice in this case was immunohistochemistry combined with confocal microscopy. Experiments were conducted with a host of antibodies. The most effective target antigenes were RFamides (a family of neuropeptides), synapsins (synaptic proteins), tyrosinated tubulin (a cytoskeletal element, especially in neurites) and BrdU (bromodeoxyuridin, a proliferation marker). Each of those markers was of great use in highlighting certain aspects of the nervous system.

A fresh look at the development of juvenile chaetognaths shortly after hatching revealed that the ventral nerve center (VNC) is developing earlier than the brain and that the production of neurotransmitters has already started at hatching. Specifically, some neurons exhibit RFmide-like immunoreactivity (ir). Neurogenesis continues for about five days after hatching and the mode of division in the neuronal stemcells is asymmetrical. In adult chaetognaths, the brain is divided into a stomatogastric anterior and a sensory posterior neuropil domain. It contains a set of individually identifiable neurons that exhibit RFamide-like ir. The study highlights the interspecific variation of brain architecture between representatives of spadellids and sagittids. The VNC consists of two lateral bands of somata that flank a central neuropil. Within the VNC exists a serial arrangement of neurons with RFamide-like ir. A variety of other neurotransmitters and related substances are also present in both, the brain and the VNC. More interspecific differences and similarities were explored in another part of the study, comparing even more different chaetognath species and focusing on the VNC and its internal structure. The two species of *Krohnitta* have an unusual distribution of nuclei that is not clearly separated into two lateral bands like in other species. Many of the sagittid species exhibit a striation pattern of the neuropil that is mostly absent in other groups and some of their nerve nets show varying degrees of order as opposed to the rather disorganized nerve net in other groups.

In addition, immunohistochemical methods were applied to several specimens of Gnathostomula sp. in order to test one of the many hypotheses about the chaetognaths phylogenetic position, a sister-group relationship to gnathostomulids. A comparison between the two taxa, taking into account also other gnathifera and platyhelminthes, makes a sistergroup relationship between chaetognaths and gnathostomulids very unlikely. In conclusion, chaetognaths remain in an enigmatic phylogenetic position and likely branched off close to the deuterostome/protostome split.

Zusammenfassung

Die Chaetognathen sind ein faszinierendes Taxon mit einzigartigen Eigenschaften. Da sie zu den primären Predatoren von Zooplankton gehören, haben sie großen Einfluss auf marine Nahrungsnetzte. Ihre phylogenetische Position ist seit ihrer Entdeckung die Ursache verschiedenster Spekulationen. Sogar mit phylogenomischen Methoden ist es bisher nicht möglich ihre phylogenetische Position innerhalb der Bilateria zu klären. Neuroanatomische Untersuchungen könnten ein Weg sein diese Fragestellung zu lösen. Die vorliegende Studie hat zum Ziel neue Einblicke ins Nervensystem der Chaetognathen zu ermöglichen und daraus Charakteristika für eine phylogenetische Diskussion zu ziehen. Die Methode der Wahl war in diesem Fall die Immunhistochemie in Kombination mit konfokaler Mikroskopie. Es wurden Experimente mit einer ganzen Reihe von primären Antikörpern durchgeführt, aber die besten Ergebnisse erzielten Antikörper gegen RFamide (eine Familie von Neuropeptiden), Synapsine (synaptische Proteine), tyrosiniertes Tubulin (ein Cytoskelettbaustein vor allem in Neuriten) und BrdU (Bromodeoxyuridin, ein Proliferationsmarker). Diese Marker waren sehr hilfreich bei dem Versuch verschiedene Aspekte des Nervensystems zu ergründen.

Eine neue Analyse der Entwicklung von juvenilen Chaetognathen kurz nach dem Schlupf zeigte, dass sich das ventrale Nervenzentrum (ventral nerve center, VNC) früher entwickelt als das Gehirn. Die Produktion von Neurotransmittern hat beim Schlüpfen bereits begonnen, was sich durch einige Neurone mit RFamide-artiger Immunreaktivität zeigt. Die Neurogenese geht noch etwa fünf Tage nach dem Schlüpfen weiter und die Art der Teilung bei neuronalen Stammzellen ist asymmetrisch.

In erwachsenen Chaetognathen ist das Gehirn in eine stomatogastrische anteriore und eine sensorische posteriore Neuropildomäne getrennt. Es enthält eine Anzahl von individuell identifizierbaren Neuronen mit RFamid-artiger Immunreaktivität. Die Studie geht auch besonders auf die interspezifischen Variationen der Gehirnarchitektur zwischen Spadelliden und Sagittiden ein. Das VNC besteht aus zwei lateralen Clustern von Somata die ein zentrales Neuropil begrenzen. Im VNC selbst finden sich seriell angeordnete Neurone mit RFamide-artiger Immunreaktivität. Zusätzlich finden sich sowohl im Gehirn als auch im VNC eine Reihe von zusätzlichen Neurotransmittern und anderen neuronalen Markern.

In einem weiteren Teil der Studie wurden noch mehr verschiedene Arten von Chaetognathen auf interspezifische Unterschiede und Gemeinsamkeiten untersucht, wobei der Fokus auf dem VNC und seinen internen Strukturen liegt. Die zwei untersuchten Arten von *Krohnitta* haben eine ungewöhnliche Verteilung von Zellkernen, da diese nicht klar in

zwei laterale Cluster aufgeteilt sind, wie das in anderen Arten der Fall ist. Viele Vertreter der Sagittiden verfügen über eine Streifung des Neuropils das in anderen Arten zum größten Teil fehlt. Einige ihrer Nervennetze weisen unterschiedliche Grade von Organisation auf, im Gegensatz zu anderen Gruppen, deren Nervennetze ziemlich desorganisiert erscheinen.

Zusätzlich wurden mehrere Vertreter von *Gnathostomula* sp. mit immunhistochemischen Methoden untersucht. Ziel war es eine bestimmte Hypothese zur phylogenetischen Zugehörigkeit der Chaetognathen, die mögliche Verwandtschaft zu den Gnathostomuliden, zu untersuchen. Ein Vergleich zwischen den beiden Taxa, unter Berücksichtigung anderer Vertreter der Gnathifera sowie der Platyhelminthes, führt zu der Schussfolgerung, dass ein Schwesterngruppenverhältnis zwischen Chaetognathen und Gnathostomuliden sehr unwahrscheinlich ist. Alles in allem bleibt die genau phylogenetische Position der Chaetognathen weiterhin unbestimmt, vermutlich aber haben sie sich in etwa zur Zeit der Trennung von Proto- und Deuterostomiern von den restlichen Taxa abgespaltet.

1. General Introduction

1.1 Introduction to a taxon: the Chaetognatha

Chaetognaths are predatory, marine animals that are present in great abundance in all marine habitats. The scientific name Chaetognatha is based on the characteristic grasping spines of the head (Fig. 1A). It is derived from the Greek words *'khaitē',* translating to bristle or seta, and *'gnathos',* meaning jaw. The commonly used name arrowworms (dt. Pfeilwürmer) refers to the shape of a chaetognath body, which resembles an arrow with its slightly triangular head, elongated trunk and tail and posterior fins that remind of the feathers on an arrows shaft. The number and size of the fins as well as the relative proportions of trunk and tail vary depending on the species. Chaetognaths are bilaterally symmetrical and mostly translucent. The taxon Chaetognatha comprises several genera with over 120 different species. The actual number of species, however, is very likely higher than that, and descriptions of newly discovered species are published frequently, e.g. *Spadella interstitialis* (KAPP & GIERE, 2005) and *Spadella valsalinae* (WINKELMANN ET AL, 2012).

▶ Fig. 1: (A) Live specimen of *Spadella cephaloptera*; (B,C) *Sagitta bipunctata*, immunoreactivity against tyrosinated tubulin (red), counterstained against nuclei (blue, HOECHST), (B) ventral view of the trunk, (C) dorsal view of the head; (D) Possible phylogenetic relationships of the chaetognaths proposed by molecular studies. 1: Zrzavý et al. (1998); 2:Halanych (1996), Peterson & Eernisse (2001); 3: Paps et al. (2009); 4: Mallatt & Winchell (2002); 5: Littlewood et al. (1998); 6: Matus et al. (2006), Papillon et al. (2004), Dunn et al. (2008), and Philippe et al. (2011); 7: Giribet et al. (2000), Helfenbein et al. (2004), and Marlétaz et al. (2006); 8: Telford & Holland (1993) and Papillon et al. (2003). (from Rieger et al. 2011, modified from Harzsch & Müller 2007); (E) General nervous system architecture of a chaetognath (modified from Kapp 2007). Abbreviations: cc, corona ciliata; cn, caudal nerve; con, coronal nerve; e, eye; fc, frontal connective; fr, fence receptor; gs, grasping spines; int, intestine; lf, lateral fin; mc, main connectives; on, optical nerve; rs, receptaculum seminis; sv, seminal vesicle; tf, tail fin; vg, vestibular ganglion; VNC, ventral nerve center. Scale bars: A: 100µm, B: 500µm, C: 200µm.

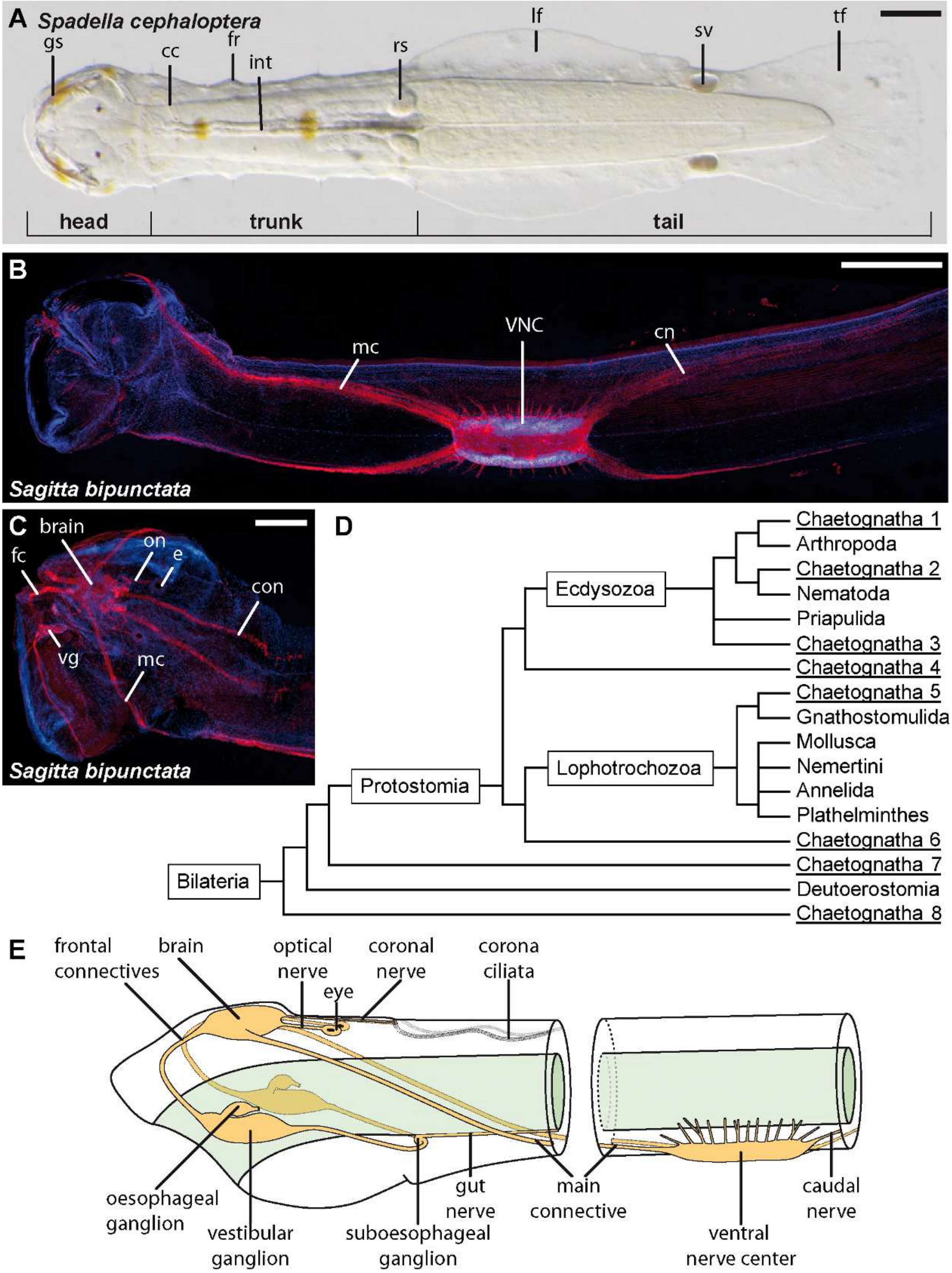
A
Spadella cephaloptera
gs
cc
fr
int
rs
lf
sv
tf
head
trunk
tail
B
mc
VNC
cn
Sagitta bipunctata
C
brain
fc
on
e
con
vg
mc
Sagitta bipunctata
D
Chaetognatha 1
Arthropoda
Chaetognatha 2
Nematoda
Priapulida
Chaetognatha 3
Chaetognatha 4
Chaetognatha 5
Gnathostomulida
Mollusca
Nemertini
Annelida
Plathelminthes
Chaetognatha 6
Chaetognatha 7
Deutoerostomia
Chaetognatha 8
Ecdysozoa
Lophotrochozoa
Protostomia
Bilateria
E
frontal connectives
brain
optical nerve
eye
coronal nerve
corona ciliata
oesophageal ganglion
vestibular ganglion
suboesophageal ganglion
gut nerve
main connective
ventral nerve center
caudal nerve

1.2 Chaetognath history and phylogeny

Animals that can be clearly recognized as chaetognaths can be found in the fossil record, dating back about 500 million years (Chen & Huang 2002; Szaniawski 2005). Furthermore what was originally described as a species called 'protochonodonts' was recently reevaluated and is now believed to be evidence for the presence of chaetognaths (Szaniawski 2002). There is a striking similarity of the so called protochonodonts to the grasping spines of recent chaetognaths. On this basis, the author suggests that the chitinous grasping spines were fossilized while the soft body tissue of the chaetognaths was not preserved and subsequently the fossilized parts appeared as a different, unrelated, taxon. The first recent chaetognath was described by Slabber in 1778. Since then, a variety of chaetognath species has been described and studied. However, to this day their phylogenetic relationship with other taxa remains controversial (Fig. 1D). Many of the early theories, like a close relation to molluscs or arthropods (reviewed for example by Ghirardelli 1968), have since been discredited. But even with modern methods, molecular as well as morphological, the position of the chaetognaths is still an enigma. A recent review by Perez et al. (submitted) summarizes the current state of knowledge on this topic. Molecular studies have proposed several possible positions for the Chaetognatha (Fig. 1D, reviewed in Rieger et al. 2011) dependent on a variety of different approaches. Among the different approaches were several analyzes of ribosomal genes, for example most recently by Papillon et al. (2006) and Mallatt et al. (2012), other single genes (Erber et al. 1998, Matus et al. 2006) or a integrated approach containing sequences of several genes (recently e.g. Dunn et al., 2008, Marletaz et al. 2008, Marletaz and Le Parco 2008, Philippe et al. 2011) or even larger amount of sequenced data like for example complete mitochondrial genomes (Helfenbein et al. 2004, Papillon et al. 2004, Miyamoto et al. 2010).The most recent inclusion in a phylogenetic analysis places them within the Ecdysozoa, although the authors themselves expressed serious doubts about the validity of this position (Mallatt et al. 2012). However, the majority of these studies link the chaetognaths to the protostomes (compare Fig. 1D) as opposed to the previously prevalent assumption that chaetognaths are deuterostomes, which was mainly based on their mode of development (reviewed e.g. by Rieger et al. 2011). Chaetognath morphology has also been responsible for a number of different hypotheses since it is unique in several aspects like their overall appearance, their grasping spines, musculature, epidermis, and of course their nervous system (see Ghirardelli 1968, Nielsen 2012). All of these factors point to a long history of independent development that set them apart from other known species and obscure their phylogenetic affinities. Currently, chaetognaths are presumed to have a close affiliation with the Protostomia, either as an early offshoot or as a sister-group to the Ecdysozoa or the Lophotrochozoa (Rieger et al.

2011, Nielsen 2012). The internal phylogeny of the Chaetognatha is disputed, as summed up by Papillion et al. (2006) who tackled this problem with an extensive molecular study (Papillon et al. 2006). However, there is a broad consensus that chaetognaths can be divided into the Aphragmophora and the Phragmophora depending on the absence or presence of transverse musculature.

1.3 Chaetognath behavior

Despite the number of described chaetognath species, behavioral studies have focused on only a few of them, mainly due to a lack of accessibility and difficulties in rearing.

Most chaetognath species are pelagic, often migrating within the water column (Pierrot-Bults & Nair 1991). Some spadellids however are epibenthic, like *Spadella cephaloptera* (BUSCH, 1851), or even interstitial, like the recently discovered *Spadella interstitialis* (Kapp & Giere 2005). Chaetognaths are a major component of marine plankton communities and primary predators of zooplankton. An examination of the stomach contents of several species sheds light on their feeding preferences. The favorite prey is copepods, various larvae, and other small, planctonic animals. Many species also exhibit cannibalistic behavior

(Feigenbaum 1991). To observe the hunting behavior, it is necessary to keep live animals in the lab which can be difficult for the pelagic deep sea species, and has mostly been done with more accessible species. *S. cephaloptera,* for example, is an ambush predator, waiting attached to a piece of seaweed for a prey organism to swim by in close distance. *S. cephaloptera* then attacks with a short but very fast forward movement, simultaneously spreading the hook-like grasping spines on its head. These spines grab the prey and are then used to shove it down the pharynx and into the gut (Feigenbaum 1991). The pelagic species *Ferosagitta hispida* (CONANT, 1895) has a similar approach, passively sinking through the water column, waiting for prey, although this species periodically uses directed swimming to regain height as described by Feigenbaum and Reeve (1977). Also, these authors report that some pelagic species have been seen swimming forward towards a prey organism for about 20mm but this could not be reproduced in controlled experiments. No other form of a more active hunting behavior has been reported so far. For most chaetognath species, mating has not been observed or described and it is therefore unclear whether these species exhibit a specific mating behavior or not. However, a rather elaborate mating ritual has been described for *Paraspadella schizoptera* (CONANT, 1895; Goto & Yoshida 1985). A sperm packet is positioned on the mating partner's body and the sperm migrates towards the female reproductive organs. Fertilized eggs are either released freely into the water, like in most species of *Sagitta*, or they are attached to a surface, like done by for example *S.*

cephaloptera (Pearre Jr 1991). The chaetognath embryonic development is direct (Kapp 2000). Hatchlings already resemble the adult and just grow in size during maturation, although some organ systems are not yet functional at hatching. More information on the development is summarized in Rieger et al. (2011).

1.4 Chaetognath morphology

Several authors have reviewed the state of knowledge on the basic chaetognath anatomy (Kapp 1991; Shinn 1997; Kapp 2004). The elongated chaetognath body has three discernible regions: head, trunk and tail (Fig. 1A). The tail is separated from the trunk by the transversal septum. One or two pairs of rayed fins are positioned laterally along trunk and tail and a rayed tailfin is present at the posterior end of the animal. The epidermis on the fins is single layered like it is on the ventral part of the head and few other places. Otherwise, chaetognaths have a multilayered epidermis. In some species, the epidermis of the neck region contains alveolar tissue, what is sometimes referred to as 'colarette'. A part of the epidermis, the hood, covers the grasping spines to reduce water drag when the animal is resting or swimming. The hood gets pulled back rapidly when the animal attacks a prey organism. Throughout the trunk four prominent longitudinal muscles enable the movement required for the attack movements and swimming. Transverse muscles are only present in a part of the taxon, the Phragmophora. A complex system of muscles is present in the head that operates the hood, grasping spines, and mouth. The grasping spines are one of the most notable characteristics of the chaetognath body. They are arranged laterally on both sides of the head and are spread during an attack. In addition, the animals possess one or two paired rows of teeth. They are probably used to puncture the cuticle or epidermis of prey organisms to enable paralyzing venom to enter the prey's bodies. It is known that some chaetognaths use tetrodotoxin to paralyze their prey, which is produced by associated bacteria (Thuesen 1991). The mouth opens to the pharynx which connects to the intestine. The gut is a straight tube positioned centrally within the body and extends along the entire trunk. The anus is positioned medially on the ventral surface, just anterior to the transversal septum. All chaetognaths are protandric hermaphrodites (Pearre Jr. 1991). The ovaries are located in the trunk on either side of the gut. The receptaculum seminis, through which sperm enters the female reproductive tract and through which the eggs are released, are located laterally on either side of the body close to the transversal septum. The testes are located in the tail. Spermatocytes are produced and mature inside the tail cavity. Mature sperm is released through the seminal vesicles, which are positioned laterally in between the lateral fins and the tailfin.

1.5 Chaetognath sensory organs and nervous system

The nervous system (Fig. 1B,C,E) was the main focus point of my study and there are more detailed descriptions available in the enclosed publications or in the publications of e.g. Goto and Yoshida (1987), Bone and Goto (1991), or Shinn (1997).

Chaetognaths have two major centralized nervous system structures: The brain, located in the dorsal part of the head with an associated chain of smaller ganglia that encircle the esophagus (Fig. 1C,E), and the ventral nerve center (VNC), located ventrally on the trunk(Fig. 1B,E) . These two are linked by the main connectives (Fig. 1B,C,E). The posterior part of the trunk and the tail contain the paired lateral caudal nerves which are directly linked to the VNC (Fig. 1B,E). Several lateral nerves connect these centralized parts to other organ systems either through directly, like the eyes or corona ciliata, or via the nerve net (Fig. 1C,E), a plexus of neurites that covers the body. It can be separated into two portions, the subepidermal plexus, that is located at the basis of the epidermis, and the intraepidermal plexus, that is distributed throughout the multilayered epidermis. Chaetognaths possess a variety of organs, which are known or speculated to be sensory. A pair of eyes on the dorsal side of the head allow for phototaxis (Fig. 1A,C,E). The two biggest ciliary sensory organs are the mechanosensory ciliary fence receptors (Fig. 1 A) and the corona ciliata (Fig. 1A,E), for which several functions have been proposed including chemo- and mechanoreception, a secretory function, and a nephridium-like function (reviewed by Ghirardelli 1968). The retrocerebral organ, also with an unknown function, is located at the posterior end of the brain, and there are putative sensory organs in the mouth region.

1.6 Research topic, motivation, and scope of this study

My project focused on several aspects of the nervous system in order to derive new morphological characteristics that may help to narrow down the range of possible phylogenetic positions proposed for the Chaetognatha. This approach is known as neurophylogeny as explained by e.g. Harzsch and Müller (2007). The nervous system is especially suited for morphological comparisons, since its complex interactions require a high degree of evolutionary conservation. In addition to the traditional morphological studies, immunohistochemical methods have previously been shown to provide interesting new characters, like individually identifiable neurons (Harzsch & Müller 2007). This study tries to further assess the value of neuronal characteristics in a broader spectrum by including various other mayor metazoan taxa.

I used mainly immunohistochemical techniques combined with modern microscopic methods. During the course of my thesis I applied a variety of antibodies, mainly against neuronal structures. Some markers proved especially useful: anti-RFamide labels single neurons that contain neuropeptides that belong to the family of the RFamides, a group of peptides that are structurally similar. RFamides have already been detected and examined in a broad range of metazoan taxa (reviewed by Walker 2009), making them uniquely suited for the task at hand. Anti-synapsin labels entire neuropils and anti-tyrosin-tubulin proved to be an excellent marker for neurites and thus both are very useful to explore for the overall structure of the nervous system, from mayor components like the VNC to the single neurites found in the nerve net. BrdU gives a picture of prolific activity in hatchlings and as a result also of the mode of division of neuroblasts during development.

The following thesis covers a variety of topics, starting with the development of the nervous system of *Spadella cephaloptera* after hatching. The two main aspects in this chapter are the onset and development of neurotransmitter expression (Chapter 2.1 Tubulin & RFamide; Rieger et al. 2011) and the mitotic activity that results in the great number of cells in the nervous system, especially the ventral nerve center (Chapter 2.2 BrdU; Perez et al. 2013).

The next mayor topic is the adult nervous, mainly of *Spadella cephaloptera*. I focused on the cephalic nervous system (Chapter 3.1 The cephalic nervous system; Rieger et al. 2010), the VNC (Chapter 3.2 The ventral nervous system; Harzsch et al. 2009), and tried to identify transmitter systems other than RFamides (Chapter 3.3 Additional immunohistochemical tests). I also revisited two of the most prominent sensory structures, the corona ciliata and the ciliary fence receptors, with immunohistochemical methods (Chapter 3.4 Ciliary receptors; Müller et al. submitted)

The third section is dedicated to interspecific variation of the main components of the nervous system by broadening the range of studied species (Chapter 4 Interspecific variances of chaetognath nervous systems).

Finally, I broaden the scope of the study and discuss the impact of my findings when compared to other metazoan taxa that are candidates for a close phylogenetic relationship. This section also includes data on one further group, the gnathostomulids, to test a specific phylogenetic hypothesis proposed by Nielsen (2001), who once suggested a close relationship of gnathostomulids and chaetognaths (Chapter 5 Outgroup comparisons with an emphasis on Gnathostomulida).

2. The development of the nervous system in *Spadella cephaloptera*

2.1 Tubulin & RFamide

“Chaetognaths (arrow worms) play an important role as predators in planktonic food webs. Their phylogenetic position is unresolved, and among the numerous hypotheses, affinities to both protostomes and deuterostomes have been suggested. Many aspects of their life history, including ontogenesis, are poorly understood and, though some aspects of their embryonic and postembryonic development have been described, knowledge of early neural development is still limited. This study sets out to provide new insights into neurogenesis of newly hatched *Spadella cephaloptera* and their development during the following days, with attention to the two main nervous centers, the brain and the ventral nerve center. These were examined with immunohistological methods and confocal laser-scan microscopic analysis, using antibodies against tubulin, FMRFamide, and synapsin to trace the emergence of neuropils and the establishment of specific peptidergic subsystems. At hatching, the neuronal architecture of the ventral nerve center is already well established, whereas the brain and the associated vestibular ganglia are still rudimentary. The development of the brain proceeds rapidly over the next 6 days to a state that resembles the adult pattern. These data are discussed in relation to the larval life style and behaviors such as feeding. In addition, we compare the larval chaetognath nervous system and that of other bilaterian taxa in order to extract information with phylogenetic value. We conclude that larval neurogenesis in chaetognaths does not suggest an especially close relationship to either deuterostomes or protostomes, but instead displays many apomorphic features.” (Rieger et al. 2011).

For more information on this topic see Rieger et al. (2011), page 121.

2.2 BrdU

“Emerging evidence suggests that Chaetognatha represent an evolutionary lineage that is the sister group to all other Protostomia thus promoting these animals as a pivotal model for our understanding of bilaterian evolutionary history. We have analyzed the proliferation of neuronal stem cells in the developing ventral nerve centre of *Spadella cephaloptera* hatchlings by *in vivo* incorporation of the s-phase specific mitosis marker bromodeoxyuridine (BrdU). Our experiments provide evidence for a high level of mitotic activity in the ventral nerve centre for ca. 3 days after hatching. Neurogenesis is carried by asymmetrically dividing neuronal stem cells that cycle rapidly (ca. 1.5 h), and are arranged in a distinct grid-like geometrical pattern including about 35 transverse rows. Considering chaetognaths to be an early offshoot of the protostome lineage we conclude that the presence of stem cells with asymmetric division seems to be a feature that is rooted deeply in the Metazoa. In the light of previous evidence indicating the presence of serially iterated peptidergic neurons with individual identities in the chaetognath ventral nerve centre we discuss if these neuronal stem cells give rise to distinct lineages. Furthermore, we evaluate the serially iterated arrangement of the stem cells in the light of evolution of segmentation.” (Perez et al. 2013)

For more information on this topic see Perez et al. 2013), page 143.

3. The nervous system of adult *Spadella cephaloptera*

3.1 The cephalic nervous system

“We examined the brain architecture in different species of Chaetognatha using immunofluorescence methods with a set of nervous system markers and confocal laser-scan microscopic analysis. These markers include antibodies against synaptic proteins, RFamide-related peptides, and tyrosinated tubulin, as well as a marker of cell nuclei. Furthermore, we present a 3D reconstruction based on histological section series. Our results expand the previous knowledge on neuroanatomy in Chaetognatha. We suggest a structural and functional subdivision of the rather complex chaetognath brain into two domains, a posterior domain that may be primarily involved in the integration of sensory input, and an anterior domain that may be involved in the control of the mouthparts and the anterior part of the digestive system. Immunolocalization of a neuropeptide suggests the presence of an identifiable group of neurons associated with the brain of all species examined here. However, our data also reveal a certain degree of interspecific variation and divergence within the Chaetognatha concerning, for example, the pattern of nerves branching off the brain and the proportional sizes of the various neuropil compartments. We compare our data to brain architecture in various other representatives of Protostomia and Deuterostomia. The chaetognath brain fits within the range of structural variation encountered in protostomian brains, and we cannot find any brain characteristics that would argue in favor of placing chaetognaths outside of the Protostomia. Rather, we see the circumoral arrangement of their cephalic nervous system as an argument that suggests protostome affinities.” (Rieger et al. 2010)

For more information on this topic see Rieger et al. (2010), page 91.

3.2 The ventral nervous system

“The enigmatic arrow worms (Chaetognatha) are marine carnivores and among the most abundant planktonic organisms. Their phylogenetic position has been heavily debated for a long time. Most recent molecular studies still provide a diverging picture and suggest arrow worms to be some kind of basal protostomes. In an effort to understand the organization of the nervous system in this clade for a broad comparison with other Metazoa we analysed the ultrastructure of the ventral nerve centre in *Spadella cephaloptera* by transmission electron microscopy. We were able to identify six different types of neurons in the bilateral somata clusters by means of the cytoplasmic composition (regarding the structure of the neurite and soma including the shape and eu-/heterochromatin ratio within the nucleus) as well as the size and position of these neurons. Furthermore, our study provides new insights into the neuropil composition of the ventral nerve centre and several other fine structural features. Our second goal was to examine if individually identifiable neurons are present in the ventral nerve centres of four chaetognath species, *Sagitta setosa*, *Sagitta enflata*, *Pterosagitta draco*, and *Spadella cephaloptera*. For that purpose, we processed whole mount specimens of these species for immunolocalization of RFamide-related neuropeptides and analysed them with confocal laser-scanning microscopy. Our experiments provide evidence for the interspecific homology of individual neurons in the ventral nerve centres of these four chaetognath species suggesting that the potential to generate serially arranged neurons with individual identities is part of their ground pattern.” (Harzsch et al. 2009)

For more information on this topic see Harzsch et al. (2009), page 67.

3.3 Additional immunohistochemical tests

A variety of antibodies was applied against neurotransmitters in an attempt to identify some of the numerous neurons in the VNC, and a fluorescent probe (phalloidin) was used to detect actin, all in adult *Spadella cephaloptera.* Although most antibodies reacted, only a small number of somata were labeled and sometimes only non-neuronal structures showed a signal. For this reason these experiments were not repeated or continued. The following results should therefore be taken with caution, since sometimes the quality of the staining was far from ideal.

3.3.1 Primary antibodies and phalloidin

Several of the tested antibodies did not produce any detectable signal, namely antibodies against Gamma-AminoButyric Acid *(*GABA), Glutamate, Octopamine, small cardiac peptide B (SCPb), and Substance P (SubP) (For details, see page 217, table 3). Anti-histamine immunohistochemistry did not work either, and further experiments were not possible, since the animals reacted very negatively to the necessary prefixative EDAC. The use of phalloidin and the following antibodies resulted in a detectable signal:

anti-Allatostatin (ASTA)

The use of anti-allatostatin produces a faint labeling in the VNC. One pair of somata is located bilaterally in the anterior part of the VNC, projecting towards the midline, maybe to the contralateral site. Several longitudinal neurites are distinguishable. One neurite to either side of the midline extends along the whole VNC and a median pair of neurites extends a little less far posteriorly. All longitudinal neurites are crossed anteriorly by the transversal projections (Fig. 3G). No immunoreactivity (ir) is observed in the main connectives or the brain. In addition ASTA-like ir is detected on the adhesive papillae, which are mostly distributed along the ventral side of the tail. The signal appears like a cap on the tip of the single papillae (Fig. 2C).

anti-Aspartate

Next to the signal in the sensory organs described in Rieger et al. (submitted) aspartate-like ir is present in the VNC. There are two bilateral pairs of somata, one in the median and one in the posterior part of the VNC. Their neurites extend primarily in an anterior direction, although the posterior pair has a small branch that extends posteriorly. The main anterior projection leaves the VNC laterally at about the level of the second pair of somata. The projections from this more anterior pair can not be traced beyond the borders of the VNC (Fig. 3F).

anti-CCAP (crustacean cardioactive peptide)

The use of an antibody against CCAP results in an unexpected pattern seen in the epidermis. Very small ring-shaped patterns are associated with the cell nuclei of the epidermis, about two or three of the rings with each nucleus (Fig. 2B).

anti-GLWamids

GLWamids-like immunoreactivity is visible in the brain and VNC of *S. cephaloptera*. However, the experiment results in a very weak signal. It has not been repeated, since the results did not look promising. A mass of neuropil in the brain is weakly labeled. In the VNC, two longitudinal neurites are positioned bilaterally of and very close to the midline in the neuropil part of the VNC (Fig. 3H).

anti-PSK (Perisulfakinin)

Antibodies against perisulfakinin produce extensive labeling in the brain (Fig. 2E) and the VNC (Fig. 3B). The pattern in parts resembles the one found with anti-RFamide antibodies as described by Harzsch and Müller (2007). However, it has not been analyzed whether any of the cells labeled with anti-perisulfakinin would also have co-labeled with anti-RFamide. In the brain, one pair of somata is located posterior, and slightly lateral, to the core neuropil. A roughly V-shaped band of projections within the core neuropil exhibits PSK-like ir, and parts of these neurites extend past the borders of the posterior neuropil domain into the main connectives and probably the VNC. There appears to be no labeling in the anterior neuropil domain (Fig. 2E). The pattern in the VNC consists of several bilateral pairs of somata that projected medially and several longitudinal neurite bundles. The most anterior pair of somata is labeled very weakly and it is also the most laterally positioned PSK-like ir pair. It is followed slightly more posterior by a pair of large and intensely labeled somata and then again by a smaller pair. Next follow five pairs of small somata that are distributed evenly along the longitudinal axis, just lateral to the most lateral fibers. A sixth pair of similar size is located even more medially. Most posterior there is a group of three brightly labeled somata on each side. The longitudinal neurites are grouped into one median and a pair of more lateral bundles, with intensive PSK-like ir. At the lateral edges of the VNC's neuropil extends another bilateral pair of single neurites. The three neurite bundles are interconnected at several points, most notably anterior, at the level of the third pair of somata, and posterior, at the level of the last pair of somata. The median bundle fans out at the posterior end of the VNC (Fig. 3B). It is not possible to detect whether any neurites left the VNC either anteriorly or posteriorly, due to an extreme, unspecific signal that occurred sometimes during staining (see section Secondary antibodies).

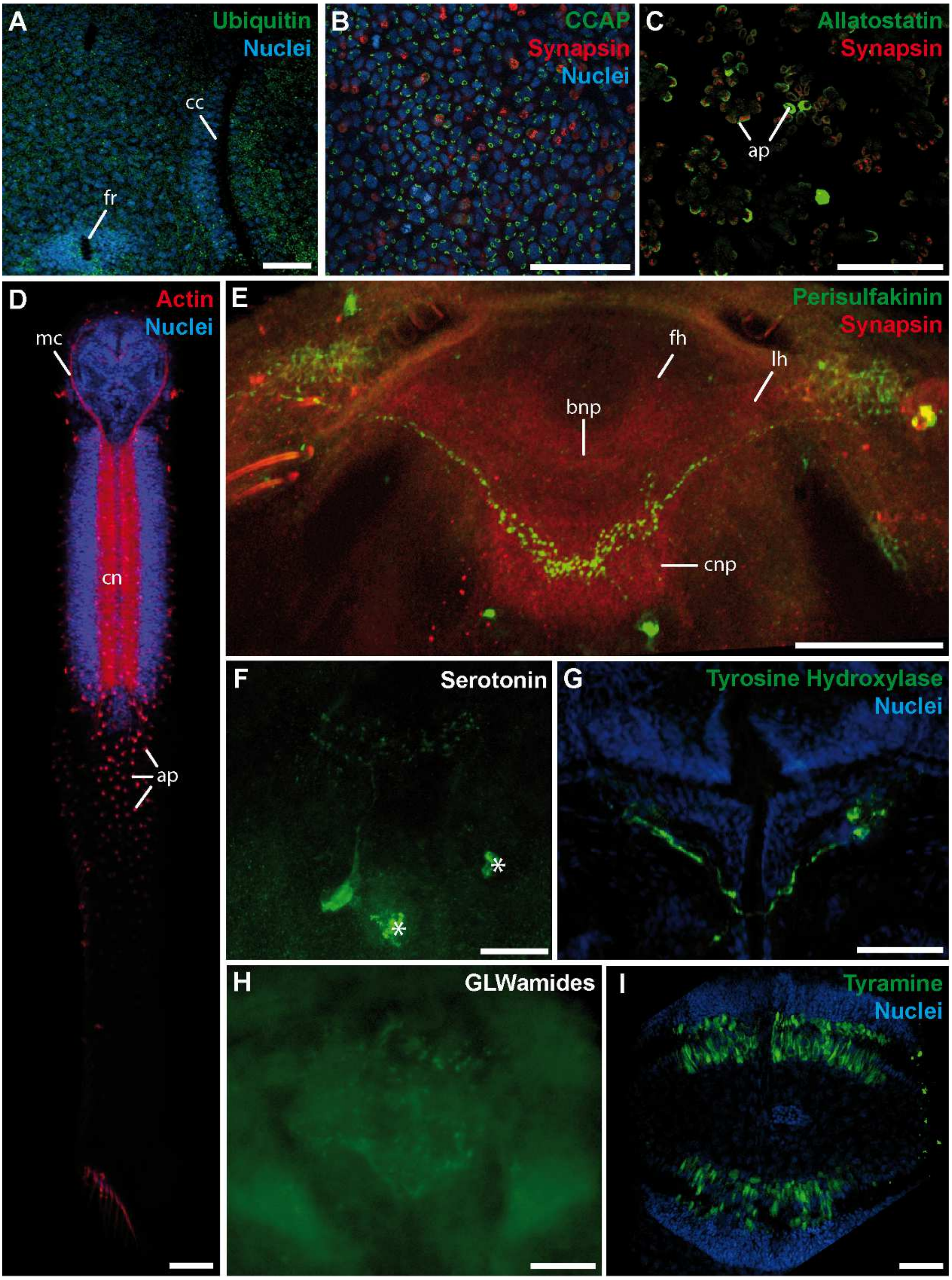
A
Ubiquitin
Nuclei
cc
fr
B
CCAP
Synapsin
Nuclei
C
Allatostatin
Synapsin
ap
D
Actin
Nuclei
mc
cn
ap
E
Perisulfakinin
Synapsin
fh
lh
bnp
cnp
F
Serotonin
*
*
G
Tyrosine Hydroxylase
Nuclei
H
GLWamides
I
Tyramine
Nuclei

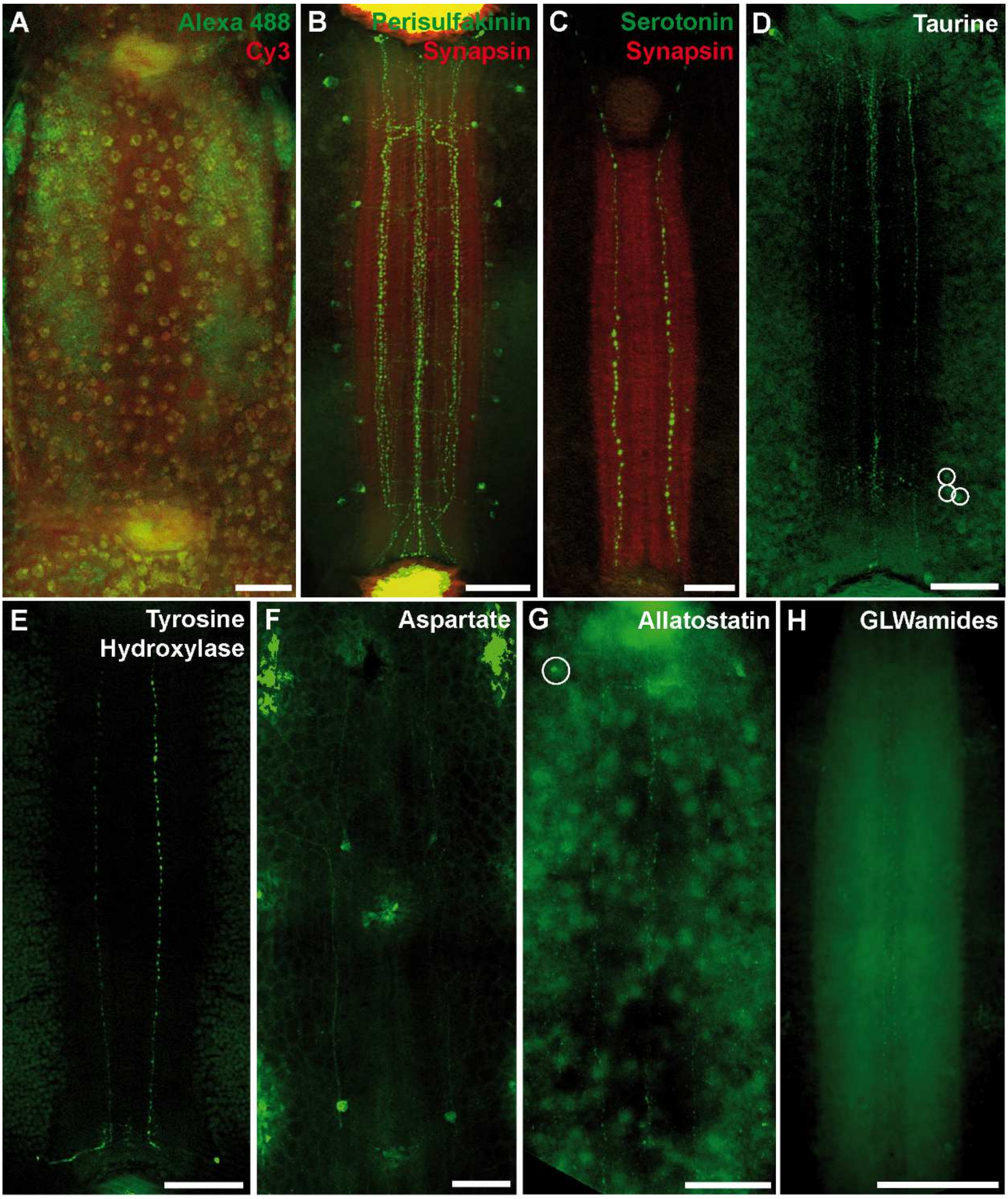
A
Alexa 488
Cy3
B
Perisulfakinin
Synapsin
C
Serotonin
Synapsin
D
Taurine
E
Tyrosine
Hydroxylase
F
Aspartate
G
Allatostatin
H
GLWamides

▲ Fig. 3: Immunoreactivity against various antibodies in the VNC of *S. cephaloptera*. The corresponding antigenes are indicated in the images, nuclei were labeled with HOECHST. All scale bars: 50µm.

◀ Fig. 2: Immunoreactivity of *S. cephaloptera* against various antibodies on the body (A,B) the adhesive papillae (C), in the brain (E-H), and the corona ciliata(I). The corresponding antigenes are indicated in the images. Actin (D) was detected in a hatchling using phalloidin conjugated with a fluorochrome, nuclei were labeled with HOECHST. Abbreviations: ap, adhesive papillae; bnp, bridge neuropil; cc, corona ciliata; cn, central neuropil; cnp, core neuropil; fh, frontal horn; fr, fence receptor; lh, lateral horn; mc, main connectives. Scale bars: A-E, G,I: 50µm; F: 20µm; H: 10µm.

anti-Serotonin

The serotonergic system in chaetognaths is not very elaborate. It consists of a single cell located medially in the brain posterior to the central core neuropil. It projects anteriorly into the core neuropil and branches out heavily (Fig. 2F). Within the VNC, no labeled somata are found and only one pair of labeled neurites is visible within the neuropil portion of the VNC. These neurites are positioned longitudinally and can be traced into the main connectives at the anterior end, while posteriorly they end at the border of the VNC (Fig. 3C). It can not be determined, if the fibers in the VNC are connected to the cell located in the brain.

anti-Taurine

Taurine-like ir is found in the VNC only. A single bilateral pair of somata is located very anteriorly and laterally, projecting in a median-posterior direction. Several other somata might be present: Three pairs of somata in the posterior half and a single soma pair at the posterior end. However, these supposed somata are labeled very faintly and they cannot be identified without a doubt due to a heavy background staining. Several longitudinal neurite bundles are present in the VNC. One very prominent bundle is located along the midline. On both sides, two single neurites run parallel along the VNC. The longitudinal neurites are connected anteriorly by a single transverse link, which is formed by the most lateral pair of neurites. On the level of the possible group of posterior somata, scattered Taurine-like ir labeling is visible in the neuropil part (Fig. 3D).

anti-Tyramine

The only structure labeled by anti-tyramine is the corona ciliata. Tyramine-like ir is found only in the inner circle of elongated somata (Fig. 2I).

anti-Tyrosine Hydroxylase

Tyrosine-hydroxylase-like ir is present in the head and the VNC. Two bilateral pairs of somata are located in the posterior cell-cluster of the brain. Their projections run medio-ventral, leaving the brain and joining at the midline (Fig. 2G). In the VNC only two longitudinal neurites show a signal. They extend along the complete VNC and curve laterally at the posterior end (Fig. 3E).

anti-Ubiquitin

Immunoreactivity to ubiquitin-like substances is found ubiquitous in the epidermis. It appears to be present in every cell within the cytoplasm (Fig. 2A).

Actin (Phalloidin)

The phalloidin staining does not work in adult specimens of *Spadella cephaloptera*. Some hatchlings, however, are labeled and phalloidin stains the fibrous parts of the central nervous system. At this young age, this means the neuropil part of the VNC, the main connectives and the loop in the head that will give rise to the brain. Actin is also present in the adhesive papillae on the ventral surface of the animal (Fig. 2D).

3.3.2 Secondary antibodies and nuclear staining

The secondary antibodies Alexa 488 goat anti-rabbit and Cy3 goat anti mouse were the most frequently applied secondary antibodies. They were applied together with a nuclear marker. During one experiment the primary antibodies were switched with PBS-TX secondary antibodies to test specificity. The concentrations, especially of the nuclear markers were adjusted when necessary, based on experience from prior experiments.

Secondary antibodies

Without primary antibodies, the secondary antibodies label neither somata nor neurites. The camera still picks up a background level of emissions and the adhesive papillae on the body surface seem labeled (Fig. 3A). Sometimes, both secondary antibodies produce heavy signals anterior and posterior to the VNC. This is not visible in the blue channel, which detects the nuclear marker, so this signal is not caused by auto-fluorescence but is clearly an unspecific signal of the secondary antibodies (Fig. 3A,B,G).

Nuclear marker

Both nuclear markers, HOCHST and YOYO-1 reliably label nuclei. The signal emitted by the nuclear marker HOECHST is sometimes still detected when using the filters that are meant to detect the emitted spectra of Alexa 488 (see Fig. 13). In this case, the nuclear staining is regarded as background staining, but in extreme cases this effect can partly obscure the actually labeled structures, e.g. in the case of Allatostatin (Fig. 3G).

3.3.3 Discussion

Most of the antigenes that were tested for are present in *S. cephaloptera,* but most of them only in very few cells. Some of the substances are restricted to the central nervous system. With the exception of the single serotonergic neuron in the brain, all neural structures are bilateral symmetrical. Unexpected results like for anti-CCAP beg the question, whether the immunoreactive components are actually related to CCAP-like peptides or just somewhat structurally similar. Chaetognaths and crustaceans are not closely related and a western blot or HPLC (*High-performance liquid chromatography*) would be needed to determine the similarity of the labeled peptides.

Replacing the primary antibody with PBS-TX and applying only secondary antibodies demonstrates that somata and neurites visible in other experiments are, in fact, specific signals. It also shows that a slight amount of background fluorescence is to be expected and that the adhesive papillae on the ventral surface of the body are prone to unspecific staining. However, the level of background staining is, under most circumstances, not problematic and specifically labeled structures are easy to discern. In some cases, the nuclear staining with Hoechst is showing in the green channel, most likely because the nuclear staining is too intense and fluorescence is still detectable using the green filter due to the bisbenzimide emission spectra and the properties of the filter (cross-talk between the channels; see Fig. 13). This phenomenon is especially problematic when the antibody-specific labeling is weak and requires a long camera exposure-time, like in the case of taurine, tyrosin-hydroxylase and allatostatin. The heavy fluorescence observed at either end of the VNC is also unspecific and has only been observed in *S. cephaloptera*. It is mostly visible in experiments with very fresh material, prolonged fixation seems to weaken or eliminate this staining. The location is the same as for the small brownish structures observed in live animals of *S. cephaloptera* (see Fig. 1A). The contents of this structure are not known, and require a closer examination, e.g. by ultrastructural methods.

Extensive testing still resulted in very little knowledge of the transmitters used by the majority of the VNC's large number of neurons. It might be a yet untested or unsuccessfully tested for transmitter, or maybe even a transmitter unique to chaetognaths. Ultimately, this question can only be resolved with further experiments.

3.4 Ciliary receptors

“This study sets out to explore details of structure and innervation of multicellular ciliary sense organs in Chaetognatha, highly abundant marine predators which effectively prey on zooplankton in various depths and habitats. We examined the epibenthic species *Spadella cephaloptera* and *Spadella valsalinae* as well as the pelagic species *Parasagitta setosa* by immunohistofluorescence with confocal laser-scan microscopy to detect tubulin and cell nuclei in whole mount preparations. Furthermore, we used scanning and transmission electron microscopy to analyse ultrastructural details of multicellular ciliary sense organs (including a further pelagic species, *Sagitta bipunctata*) and a mitosis marker to detect proliferating cells. Chaetognaths, and in particular the examined species, are equipped with several epidermal sensory organs including the three types of ciliary sense organs that are the focus of the present study: the transversally oriented ciliary fence organs (1), the longitudinally (parallel to the anterior-posterior axis) oriented ciliary tuft organs (2) and a ciliary loop, the corona ciliata (3). The outer shape of those sense organs, especially the corona ciliata, may vary widely among Chaetognatha. Shape, number and distribution of the ciliary fence organs and the corona ciliata are species-specific and can be easily highlighted by immunohistochemical techniques making these a useful tool for taxonomic studies. Two different types of multilayered and partly pooled receptor cells constitute the ciliary fence and ciliary tuft organs. Each receptor cell extends a single, non-locomotory cilium from the narrow apex so that multiple rows of highly ordered cilia are formed. The ciliary fence and ciliary tuft organs are distributed in large numbers along the entire body. They are known to have a mechanosensory function, detecting hydrodynamic stimuli to initiate attack or escape movements. Their axons project in bundles towards the ventral nerve centre. The corona ciliata consists of numerous ciliary cells forming a loop on the animal’s dorsal neck region and shows an extensive and intricate pattern of innervation. Many of the cells in the corona ciliata of adult specimens of *S. cephaloptera* show mitotic activity suggesting a turnover of cells. In *S. cephaloptera* and *S. valsalinae,* the corona ciliate shares a nearly identical cellular architecture. The outer cellular population of the corona ciliata comprises epithelial cells with a single motile cilium, whereas the larger inner cell population contains two types of epithelial cells: absorptive cells extending two or several cilia and sensory cells with a single cilium. TEM studies show that the two latter ciliary cell types surround an annular extracellular cavity which is, although almost completely enclosed, accessible by water from outside.

The axons of the sensory cells become bundled to the centre of the corona ciliata, where they pass into the dorsomedian coronal nerves that house approximately 400 neurites and project into the posterior area of the brain. Synapses are found throughout the coronal nerves, close to the ECM and the subjacent longitudinal dorsomedian musculature of the trunk. The function of the corona ciliata is not yet known, but the new insights into the microscopic architecture strengthens speculations of a sensory function, and suggest that it is most likely a chemosensory organ.” (Müller et al. submitted)

For more information on this topic see Müller et al. (submitted), page 161.

4. Interspecific variances of chaetognath nervous systems

Antibodies against RFamide were previously applied to several species and results were published in Rieger et al. (2010). Several other species were obtained other during various trips (see chapter 12.1 Material & Methods). However, for reasons unknown, the reaction with anti-RFamide did not produce a specific signal and this approach was abandoned in favor of the more stable anti-tyrosinated tubulin staining combined with a marker for nuclei (Fig. 4). Most descriptions and measurements given below are based on either one or two specimens of one species only, and may therefore be not be completely representative of the respective species.

4.1 Results

Brain

The brain architecture of several species was discussed in Rieger et al. (2010). Tyrosin-tubulin-ir did not work on the brain in the additional species. Therefore, no new data is presented here.

VNC

The properties of the ventral nerve center (VNC) in different species are summarized in table 5. The most striking observations are addressed below.

Nuclei

The distribution of nuclei in the VNC of examined members of the krohnittids differs from those of other chaetognath species. In spadellids and sagittids the nuclei are clearly divided into two masses on either side of the central neuropil with few nuclei spread out in small clusters along the midline. However, in the krohnittids, *Krohnitta subtilis* (GRASSI, 1881) and *Krohnitta pacifica* (AIDA, 1897), this distinction is not as prominent. Although most nuclei are located in the lateral bands, there is also a continuous layer of nuclei in between them (Fig. 5C,D). The same is probably true for Eukrohnittids as indicated by a single damaged individual of *Eukrohnia fowleri* (RITTER-ZÁHONY, 1909) (data not shown). In this specimen only the anterior tip of the VNC was still present, but it contained a continuous layer of nuclei.

Anti-tyrosine-tubulin

As described by Harzsch & Müller (2007), a very clear horizontal striation is visible in the core neuropil of the VNC in *Parasagitta setosa* (MÜLLER, 1847) when using synapsin antibodies. Similar patterns could be detected in various other sagittids with tyrosin-tubulin-ir.

However, this striation was less clear or almost nonexistent in the examined species of *Spadella* and in the krohnittids. *Spadella valsalinae* shows slight striation within the neuropil, with fine horizontal and longitudinal bundles of neurites embedded in a rather homogeneous neuropil (Fig. 6B). The horizontal elements are even less pronounced in the VNC of *Spadella cephaloptera, K. pacifica* and *K. subtilis* (Fig. 6A,C,D). They have no visible striation in the middle of the neuropil, although at the border of the core neuropil and the lateral portion of the nuclei, a slight striation can be found in *S. cephaloptera* and *K. subtilis.* In comparison, *Pseudosagitta lyra* (KROHN, 1853), *Flaccisagitta enflata* (GRASSI, 1881), and *Serratosagitta tasmanica* (THOMPSON, 1947; Fig. 6E,F,I) have well defined bundles of horizontal neurites and the surrounding tissue is structured into longitudinal stripes. In other *Sagittids* the structures are less pronounced, but still present (Fig. 6). Unfortunately, no data on the VNC is available for any species of *Eukrohnia* due to tissue damage in the available *Eukrohnia* specimens. The main connectives, the lateral and the caudal nerves were also heavily damaged. The overall structure of the VNC in most species is very symmetrical, not only between the two sides, but also concerning the anterior and posterior halves (Fig. 5). This is especially the case when the main connectives and the caudal nerves have a very similar look, to the point where it is impossible to discern the anterior or posterior end when only the VNC and its immediate surroundings are visible. The lateral nerves are more or less condensed neurite bundles that connect to the nerve net surrounding the VNC (Fig. 5). They often appear rather short, but since the nerve net is intraepidermal, and the epidermis is often damaged during processing, the appearance might have been altered. The caudal nerves are usually broad, condensed neurite bundles that run laterally along the body between the VNC and the tip of the tail. They split into a ventral and a dorsal part. Portions of the caudal nerves branch off diagonally to innervate the nerve net in the tail. The nerve net or plexus, as mentioned above, is often damaged and data is only present for part of the species (Fig. 7). There are great differences in the organization of the nerve net: In *S. cephaloptera, K. subtilis* and *S. tasmanica* the plexus is chaotic, without any obvious arrangement (Fig. 7A,B,G), whereas in some species like *Flaccisagitta hexaptera* (D'ORBIGNY, 1836) and *Serratosagitta serratodentata* (KROHN, 1853) the neurites of the nerve net are arranged in straight horizontal and longitudinal rows and columns (Fig. 7E,H). In other species an ordered arrangement is partly present, but not as clear (Fig. 7C,D).

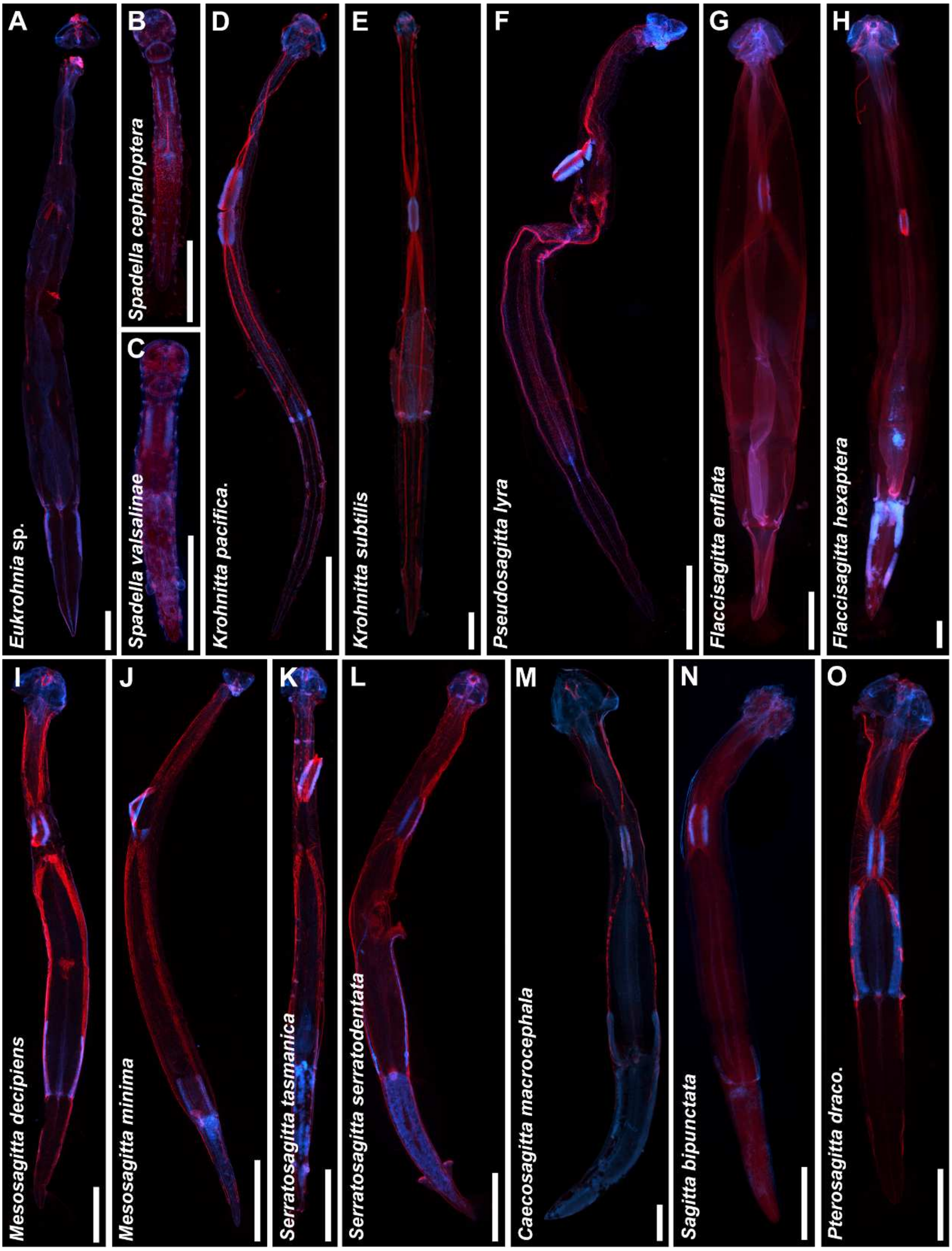
A
B
C
D
E
F
G
H
I
J
K
L
M
N
O
Eukrohnia sp.
Spadella cephaloptera
Spadella valsalinae
Krohnitta pacifica.
Krohnitta subtilis
Pseudosagitta lyra
Flaccisagitta enflata
Flaccisagitta hexaptera
Mesosagitta decipiens
Mesosagitta minima
Serratosagitta tasmanica
Serratosagitta serratodentata
Caecosagitta macrocephala
Sagitta bipunctata
Pterosagitta draco.

▲ Fig. 4: Overviews of all species that successfully showed immunoreactivity against tyrosinated tubulin (red), counterstained against nuclei (blue, HOECHST). The species is indicated in the images. All scale bars: 1000µm.

▶ Fig. 5: VNC of the species that successfully showed immunoreactivity against tyrosinated tubulin (red), counterstained against nuclei (blue, HOECHST). Species as indicated in the images. All scale bars: 100µm.

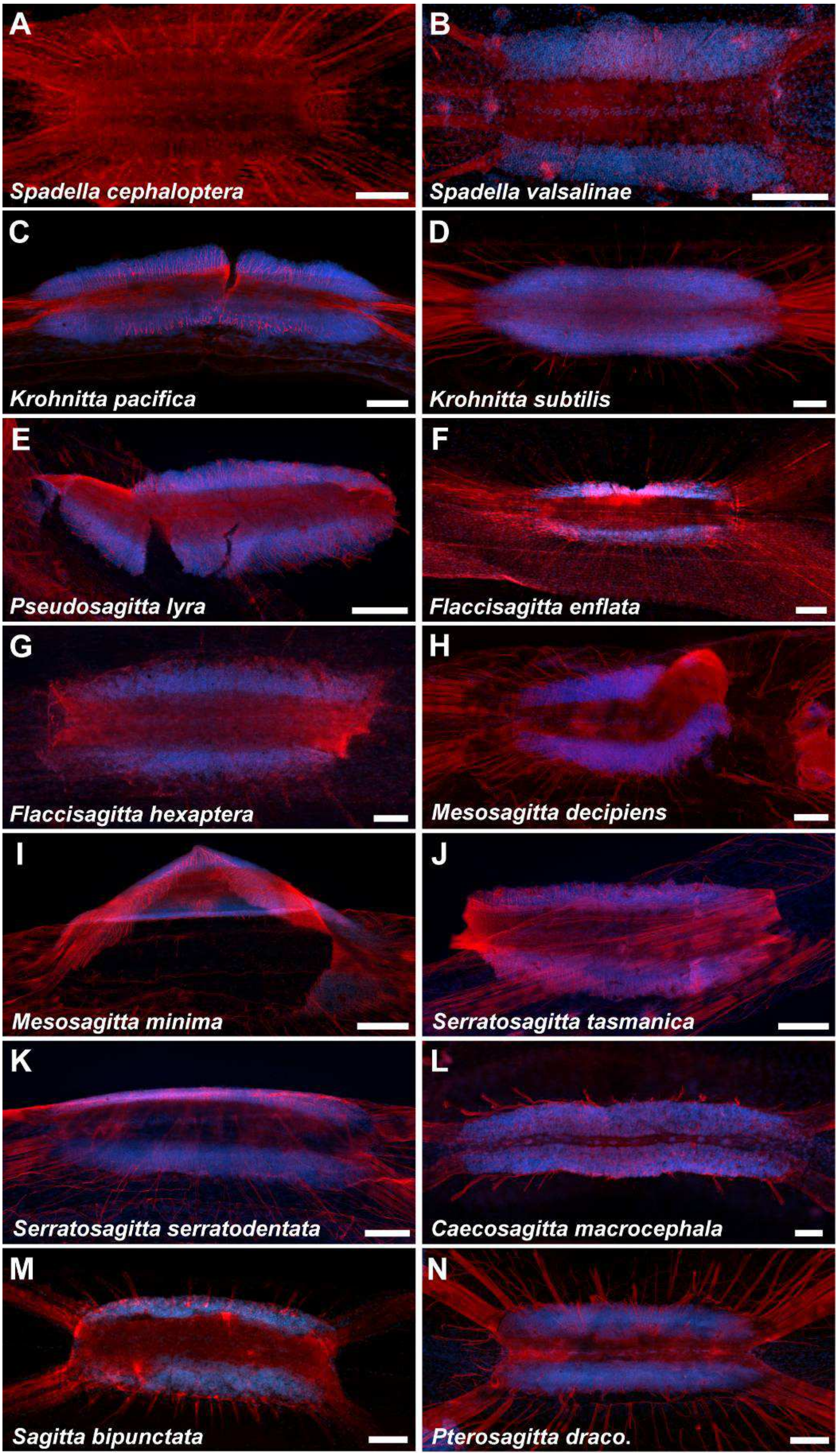
A
Spadella cephaloptera
B
Spadella valsalinae
C
Krohnitta pacifica
D
Krohnitta subtilis
E
Pseudosagitta lyra
F
Flaccisagitta enflata
G
Flaccisagitta hexaptera
H
Mesosagitta decipiens
I
Mesosagitta minima
J
Serratosagitta tasmanica
K
Serratosagitta serratodentata
L
Caecosagitta macrocephala
M
Sagitta bipunctata
N
Pterosagitta draco.

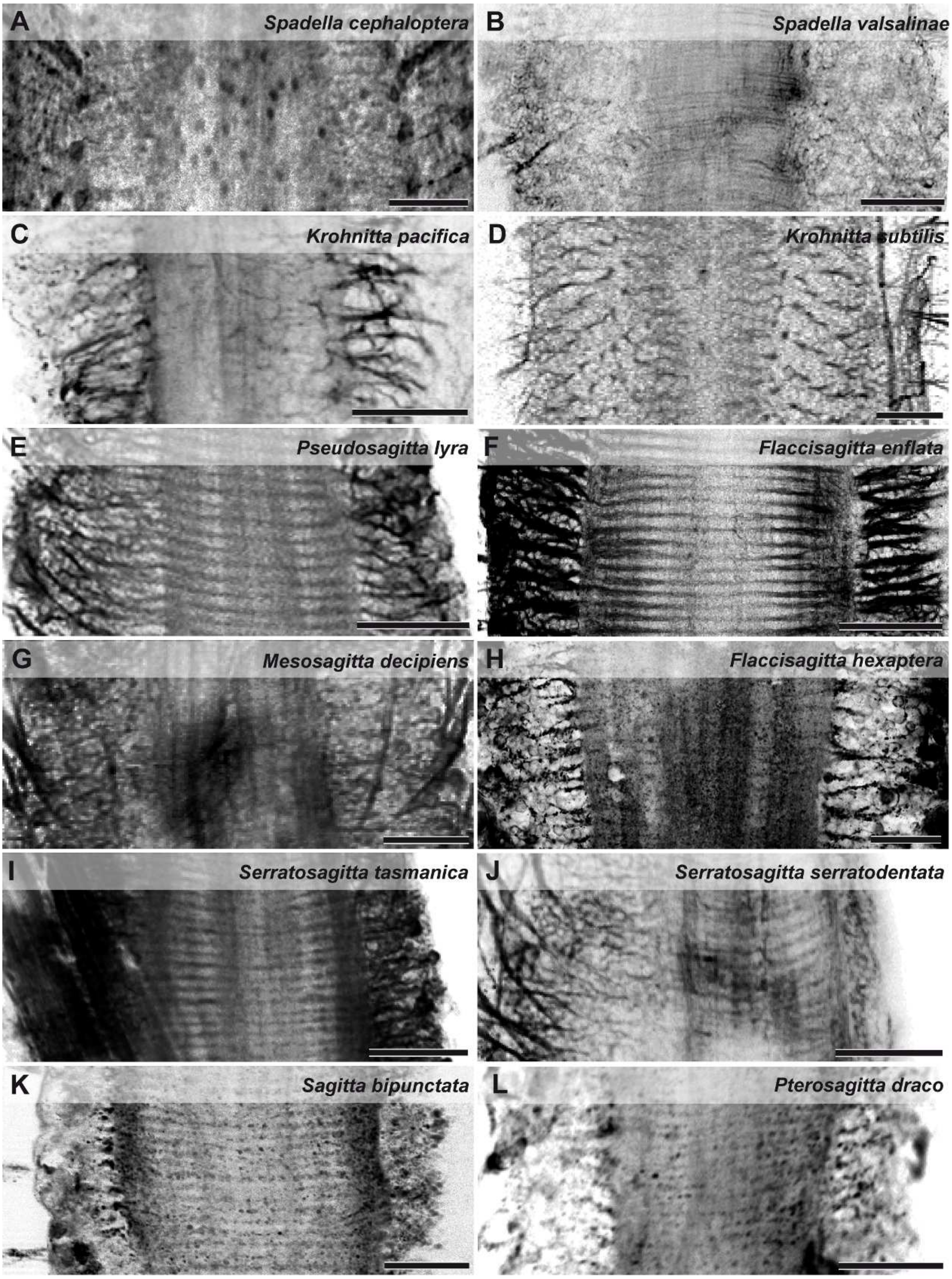
A
Spadella cephaloptera
B
Spadella valsalinae
C
Krohnitta pacifica
D
Krohnitta subtilis
E
Pseudosagitta lyra
F
Flaccisagitta enflata
G
Mesosagitta decipiens
H
Flaccisagitta hexaptera
I
Serratosagitta tasmanica
J
Serratosagitta serratodentata
K
Sagitta bipunctata
L
Pterosagitta draco

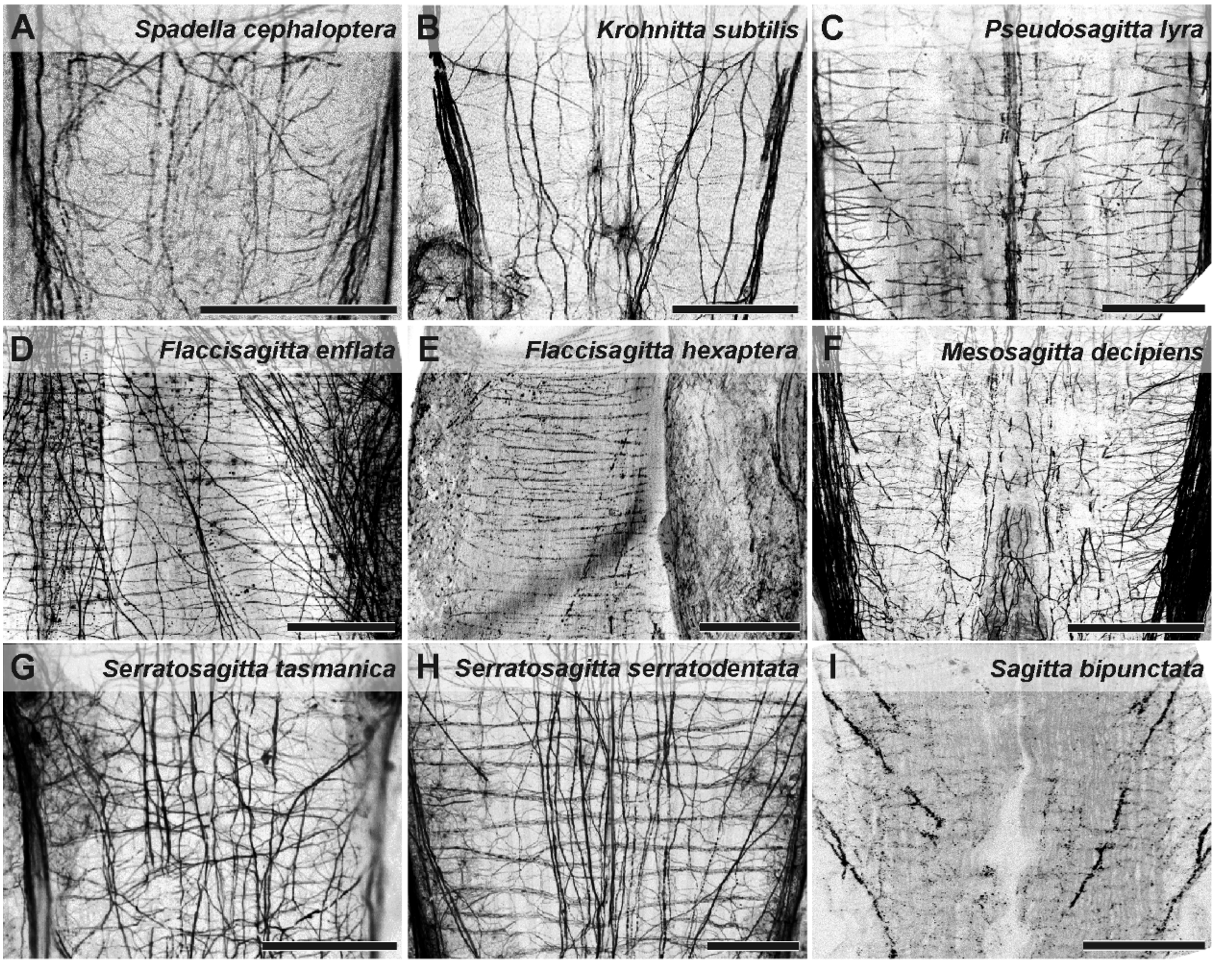
A
Spadella cephaloptera
B
Krohnitta subtilis
C
Pseudosagitta lyra
D
Flaccisagitta enflata
E
Flaccisagitta hexaptera
F
Mesosagitta decipiens
G
Serratosagitta tasmanica
H
Serratosagitta serratodentata
I
Sagitta bipunctata

▲ Fig. 7: Nerve net of some species with immunoreactivity against tyrosinated tubulin. The species is indicated in the images. Scale bars: A, C, G-I: 100µm; B, D-F: 200µm.

◀ Fig. 6: Details of the VNC structure in some species with immunoreactivity against tyrosinated tubulin. The species is indicated in the images. All scale bars: 50µm.

Tab. 1: Neuronal characters of the chaetognath VNC.

Species		Nuclei lateral bands (Fig. 5)	Nuclei midline (Fig. 5)	horizontal striation (Fig. 6)	vertical stripes (Fig. 6)
Eukrohnia sp.		presumably continuous layer	—	—	—
Spadella cephaloptera		2 separate bands	few, slightly clustered	no visible striation	no visible stripes
Spadella valsalinae		2 separate bands	few, slightly clustered nuclei	slight striation	no visible stripes
Krohnitta pacifica		continuous layer, majority of nuclei positioned lateral	—	no visible striation	no visible stripes
Krohnitta subtilis		continuous layer, majority of nuclei positioned lateral, fine gap along the midline	—	no visible striation	no visible stripes
Pseudosagitta gazellae		—	—	—	—
Pseudosagitta lyra		2 separate bands, narrow gap in between	several tight clusters	clear striation present	stripes present
Flaccisagitta enflata		2 separate bands	few scattered nuclei	clear striation present	no visible stripes
Flaccisagitta hexaptera		2 separate bands	several clusters	striation present	slight stripes present
Mesosagitta decipiens		2 separate bands	few scattered nuclei	faint striation present	stripes present
Mesosagitta minima		2 separate bands	continuous row of nuclei, 1-2 nuclei wide	clear striation present	stripes present

Serratosagitta tasmanica		2 separate bands	some scattered nuclei	clear striation present	stripes present
Serratosagitta serratodentata		2 separate bands	several clusters	faint striation present	no visible stripes
Caecosagitta macrocephala		2 separate bands, narrow gap in between	several clusters	faint striation present	no visible stripes
Pterosagitta draco		2 separate bands	several small clusters	faint striation present	no visible stripes
Sagitta bipunctata		2 separate bands	few, slightly clustered nuclei	striation present	no visible stripes

Tab. 2: Further neuronal characters of the chaetognath nervous system.

Species		Main connectives, width [µm] (Fig. 4, 5)	Lateral nerves, width [µm] (Fig. 5)	Caudal nerves, width [µm] (Fig. 4, 5)	Nerve Net (Fig. 7)
Eukrohnia sp.		join behind head, run along the midline almost as a single bundle	___	___	mostly 90° from caudal nerves, diagonal neurites
Spadella cephaloptera		run lateral, about 20µm	several, not clearly separated, about 3-6µm	about 20µm	unordered
Spadella valsalinae		split behind head, one bigger part runs lateral, one smaller part runs closer to the midline, about 15µm	long, hard to distinguish, about 2µm	about 20µm	___
Krohnitta pacifica		run lateral, about 25µm	short and numerous , about 2µm	about 15-20µm	one ventral neurite bundle runs along the midline, two finer ones run parallel, horizontal neurites in their vicinity, less order in the tail region, specimen heavily damaged
Krohnitta subtilis		run lateral, broader and less condensed near the VNC, about 90µm	short and fast branching, about 2-6µm	less condensed near the VNC, about 80-90µm	unordered, with many longitudinal neurite bundles
Pseudosagitta gazellae		___	___	___	___
Pseudosagitta lyra		join behind head, run along the midline almost as a single bundle, about 30µm	long, about 1,5-3µm	broader near the VNC, get more condensed fast, about 40µm	prominent horizontal neurites, several longitudinal neurite bundles

Flaccisagitta enflata		run lateral, barely condensed, about 100µm	many nerves, long, smooth transition to the main connectives and caudal nerves, about 3µm	barely condensed, about 160µm	ordered, longitudinal neurite bundles, horizontal neurites
Flaccisagitta hexaptera		run lateral, about 40µm	___	___	ordered, longitudinal and horizontal neurites
Mesosagitta decipiens		run lateral, frayed edges, about 100µm	about 3-5µm	frayed edges, about 160µm	slightly ordered longitudinal and horizontal neurites
Mesosagitta minima		run lateral, about 50µm	about 3µm	about 35µm	___
Serratosagitta tasmanica		run lateral, about 60µm	long, about 2µm	about 70µm	few, ordered longitudinal neurite bundles, chaotic horizontal and diagonal neurites
Serratosagitta serratodentata		run lateral, about 90µm	long, about 1-4µm	about 80µm	ordered, longitudinal and horizontal neurite bundles
Caecosagitta macrocephala		run lateral, about 70µm	about 6-15µm	about 90-100µm	almost only longitudinal, possibly due to damage
Pterosagitta draco		run lateral, about 60µm	about 3-13µm	about 80µm	behind head: unordered, too damaged in other places
Sagitta bipunctata		run lateral , about 80µm	about 5-15µm	about 80µm	___

The largest chaetognath within the present sample was a specimen of *F. hexaptera* (about 2,3cm long) the smallest one was of the newly discovered species of *Spadella valsalinae* (about 2,4mm long). These two species are shown in figure 8A at the same scale. Figure 8B shows *Spadella valsalinae* in relation to a gnathostomulid, which was also studied as described below (Chapter 5.1 New data of the Gnathostomulid nervous system).

4.2 Discussion

Characters of the nervous system

The attempted RFamide staining failed in most species. This was most likely caused by problems with the fixation process. Either the fixative, which had to be freshly prepared aboard the research vessels, was of insufficient quality or the prolonged storage in the chemical that occurred during transportation at unfavorable temperatures was responsible. Comparisons of RFamide-like ir will therefore be restricted to the results of only a few studies (Harzsch & Müller 2007; Harzsch et al. 2009; Rieger et al. 2011; Goto et al. 1992) on the topic. Another important factor that has to be addressed is tissue damage. During their capture chaetognaths are subjected to mechanical forces and the most delicate parts of the body may suffer. Especially the VNC often detaches partially or completely from the body, also severing the lateral nerves and sometimes the main connectives and caudal nerves. In addition, the outer layer of the epidermis along of body is often slightly damaged as well, which impacts the data on the nerve net.

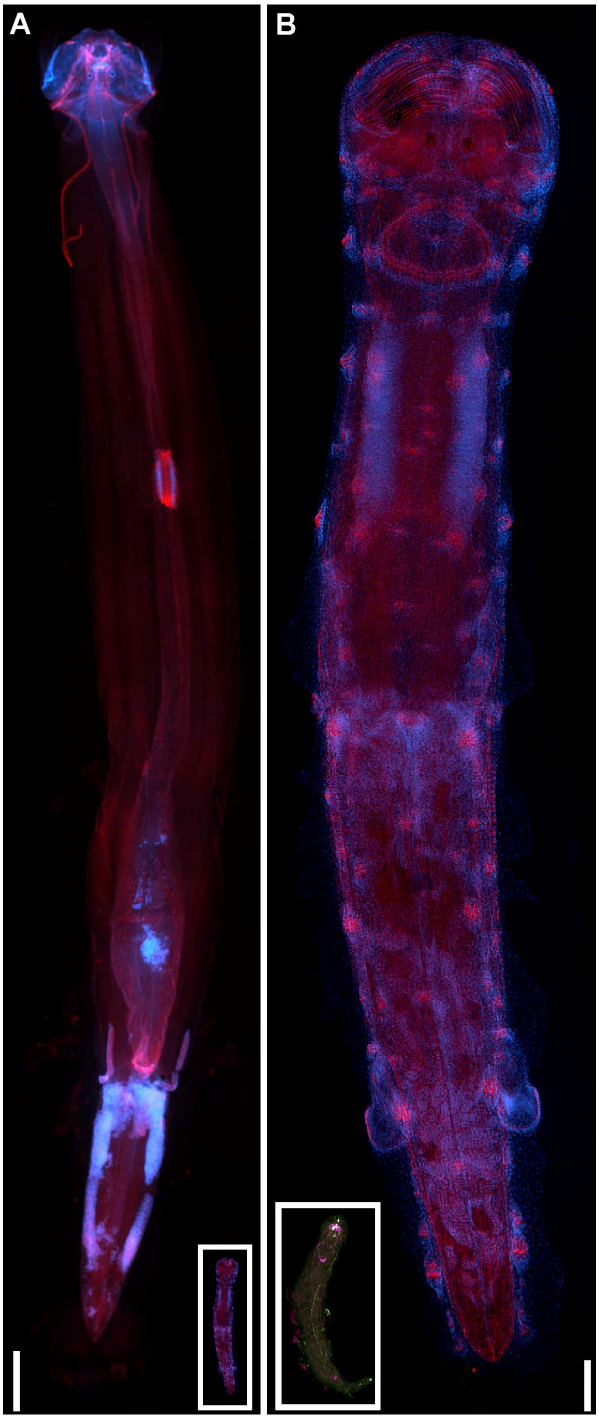

Fig. 8: Comparison of the sizes of the largest, (A) *Flaccisagitta hexaptera*, and smallest, (inset in A,B) *Spadella valsalinae* , chaetognath studied and a gnathostomulid, (inset in B) *Gnathostomula* sp. (red: tyrosinated tubulin, blue: nuclei, magenta: synapsin, green: RFamide). Scale bars: A: 1000µm; B: 100µm.

Main connectives

The appearance of the main connectives has some unique features in a few species: *Spadella valsalinae* is the only species in this analysis that has split main connectives, most likely an autapomorphy of this species. *Eukrohnia* sp. and *Pseudosagitta lyra* share a very interesting feature with main connectives that converge behind the head. *P. lyra* was described by Papillon et al. (2006) as having '[w]ithin the Sagittidae, the most obscure affinities' of the species included in the study. This morphological detail might hint to a position of *P. lyra* close to the Phragmophora/Aphragmophora split. However, no other species showed a similar arrangement and it might be wise to verify this result when more individuals are available for testing. The nervous system of the body is vulnerable to mechanical damage due to its exposed position, which often results in damage to the VNC but also might apply to the main connectives. *Flaccisagitta enflata* has the least condensed main connectives, and lateral nerves, of all species studied. This might be explained by its shape. *F. enflata*, as indicated by its name, has a very bloated trunk in comparison to other species. Maybe the main connectives have to spread out wider than normal to be able to innervate the entire body.

VNC

The VNC is about the same size in all examined species, with means that it takes up a bigger proportion of the trunk in small species and seems rather small in large species. The degree of condensation of the lateral neurites into lateral nerves varies.

The extent of condensation in the lateral nerves corresponds with the main connectives. *Sagitta bipunctata* (QUOY & GAIMARD, 1828) for example possesses condensed main connectives and lateral nerves, whereas in *Flaccisagitta enflata* both structures are spread out to the point that the main connectives, lateral nerves and caudal nerves almost merge. The length of the lateral nerves varies, but this is a very weak character state, since, as mentioned above, quite often the lateral nerves are damaged and might appear much shorter than they actually are.

Nuclei

Rather surprising was the lack of a distinct division of the nuclei in the VNC into two clusters in the krohnittid species and possibly Eukrohnia. The continuous layer is less massive in the middle and a narrow gap exists between the two sides. There are two possible explanations for this phenomenon: Either the lateral cell clusters extended ventrally to fully enclose the neuropil core, or the last common chaetognath ancestor was equipped with a continuous layer of neuronal somata, which became separated in most following subtaxa. The latter hypothesis might also explain why all species with distinct lateral clusters also have a small number of relatively isolated somata spread ventrally along the midline. These cells along the midline, clustered or not, are present in all other species and seem to be of little use in determining phylogenetic relationships.

Serial arrangement of the VNC

A distinct striation of the VNC was first described by Harzsch and Müller (2007) for *Sagitta setosa* with synapsin-ir. Anti-tyrosine tubulin produces a similar pattern, which is found almost exclusively in the sagittid species. The differences in striation, horizontally as well as vertically, can appear rather different in closely related species: the horizontal striation ranges from well pronounced bundles (e.g. *F. enflata*), to neurite bundles, that are not continuously stained, but still clearly discernible (e.g. *S. bipunctata*). The vertical stripes are defined by the intensity of the staining in the gaps between the horizontal bundles and range from clear light and darker bands (e.g. *P. lyra*) to an almost uniform coloration (e.g. *S. bipunctata*). *Spadella valsalinae* shows a slight horizontal striation, but it is much less condensed than the thick bundles observed in some of the sagittids. No striation is visible in the *Krohnitta* species or *S. cephaloptera*. Yet, BrdU experiments on hatchlings of S. cephaloptera, demonstrate that there is a serial arrangement of sorts in place (Fig. 2C,E, 3A). This is further underpinned by the serial arrangement of cells that express RFamide-like and perisulfakinin-like ir. So the absence of striation in the tyrosine-tubulin experiments does not mean that there is no serial component to the VNC itself. *Pterosagitta draco* (KROHN, 1853) exhibits a striation that most closely resembles *S. bipunctata*. However, more experiments, especially on the sagittid and krohnittid species are necessary to verify these results, since many are based on only one or two specimens and, as mentioned above, the VNC is prone to be damaged.

Nerve nets

In krohnittids and spadellids the nerve net does not follow any obvious order, whereas in some of the sagittid species display a varying degree of order. Especially the transversal neurites run at a 90° angle to the longitudinal axis.

This might be at least partially a result of the increased size of the animal like for example *F. enflata*. The body is relatively big, compared to the VNC, so an organized nerve net would be more cost and energy efficient.

Phylogenetic impact

The phylogenetic position of the Chaetognatha within the bilaterians is still unclear. This problem is complicated further by the fact that the phylogeny within the chaetognaths is also still up for debate. The neuroanatomy of the species studied might be a useful tool to further the understanding of both issues.

Internal chaetognath phylogeny

The earliest hypothesis in the discussion on the internal chaetognath phylogeny proposed a split into Phragmophora and Aphragmophora (Tokioka 1965), a theory that is still valid (Papillon et al. 2006), but faces a problem with *P. draco* as discussed below. The data presented here supports the spadellids, krohnittids and sagittids as monophyla, however it does not reveal the relationship between these taxa: the krohnittids share a lack of visible segmentation and an unordered nerve net with the spadellids, but are set apart by their rather unusual distribution of cells in the VNC, which would favor the hypotheses that Papillon et al. (2006) referred to as 'Tokioka'. However, the evidence is by no means strong enough to state this as a definite result. Regarding this topic, it would be necessary to include specimens of *Eukrohnia* into the analysis, which was not possible yet. The nervous systems of sagittids are set apart from the other species by being more organized (Bieri 1991).

The position of *P. draco*

Most recently, Papillon et al. (2006) reviewed prior theories and presented their own phylogeny based on ribosomal 18S DNA sequences. According to their analysis the spadellids are paraphyletic as are the Phragmophora/Aphragmophora since the aphragmophore *Pterosagitta draco* groups with the Phragmophora. A comparison of the neuronal architecture among the various species provides some new insights on *P. dracos* relations. As demonstrated in Rieger et al. (2010), the brain architecture of *P. draco* has some unique characteristics, but it is closer to the sagittid pattern, with a clearly separate core neuropil. The same goes for the RFamide-like ir in the brain. Unfortunately, the RFamide-like ir in the VNC could not be examined, but it is possible to compare the tyrosine tubulin-ir. Here the similarities are clearly with the sagittids, as discussed above. In conclusion, the neuronal characters of *P. draco* clearly group this species with the sagittids, rather than the spadellids. Further studies into other organ systems, as well as a more extensive molecular analysis in addition to the one by Papillon et al. (2006) are warranted to resolve the position of *P. draco.*

5. Outgroup comparisons with an emphasis on Gnathostomulida

5.1 New data of the Gnathostomulid nervous system

Since one of the various hypotheses on chaetognath phylogenetic relationships groups them with the Gnathostomulida (Fig. 1D), the main markers used on chaetognaths were also applied to gnathostomulids.

Results Gnathostomulida

The species found in samples from Sylt (see Material & Methods) were determined to be members of the genus *Gnathostomula* by the form of jaw and teeth, their size, and their body index (length of animal/max. body width, compare Sterrer 1972), most likely *Gnathostomula paradoxa* (AX, 1956), since this is the only species of this genus described for the region (Reise 1981).

Tyrosinated tubulin, RFamide-like peptides and synapsins are present in the examined specimens(Fig. 9A,D). Gnathostomulids have a brain in the anterior part of the body (Fig. 9A-C,F), from which several longitudinal neurite bundles extend along the animal (Fig. 9A,B) and recombine posterior in a much smaller neuronal center (Fig. 9A, 12). The stomatogastric innervation of the jaws also derives from the brain (Fig. 9B,C,F).

Synapsin and tyrosinated tubulin highlight the main centralized structures (Fig. 9A,D). However tyrosinated tubulin stains not only the nervous system, but also the ciliary structures of the epidermis, which obscure some of the finer nervous structures from observation (Fig. 9D). In addition the borders of the neuropil are not clearly visible, which is why the description of the general nervous system architecture is mainly based on synapsin-ir (Fig. 9B, 10).

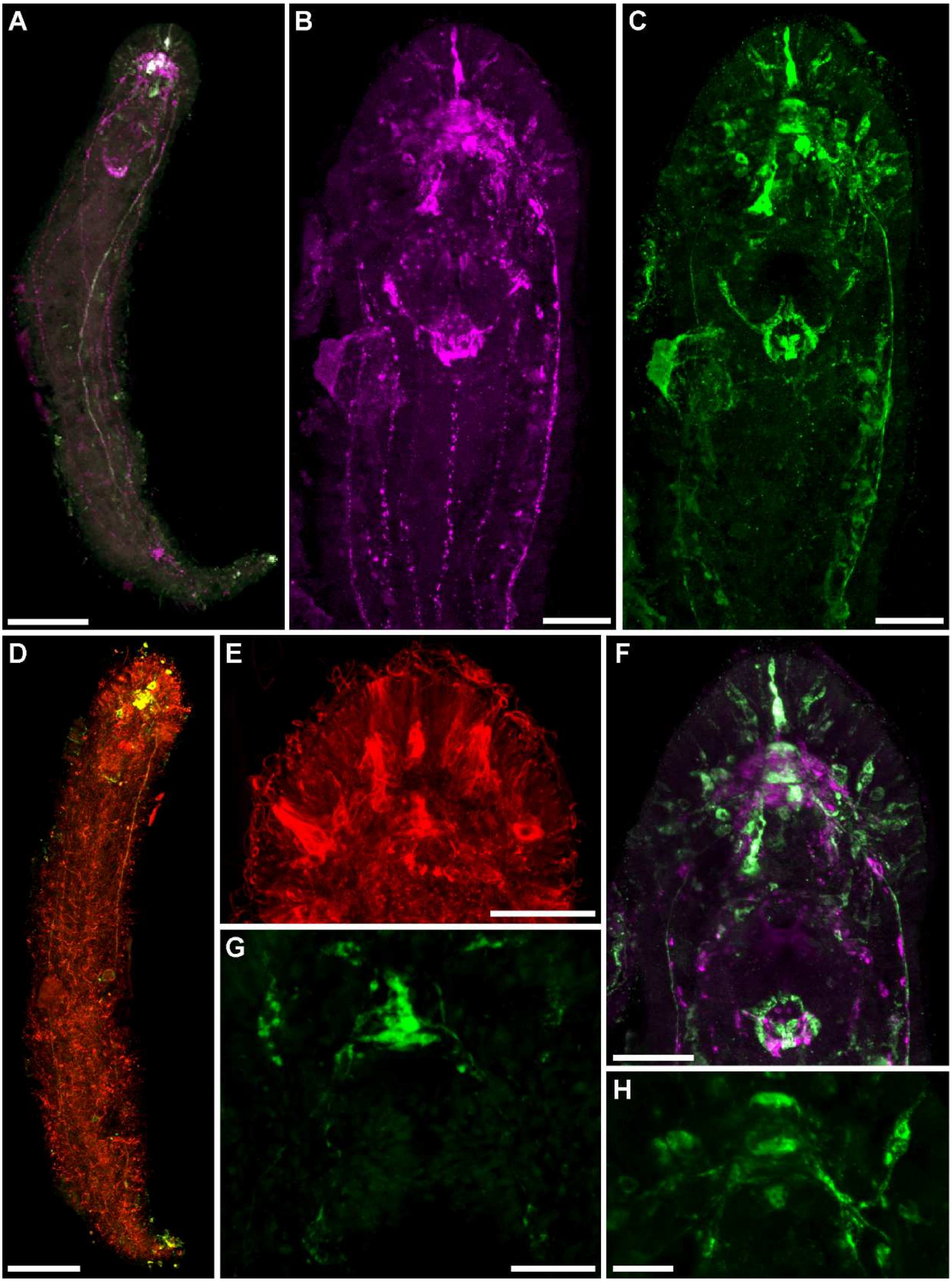

Fig. 9: Gnathostomulid immunoreactivity against several antigenes (magenta: synapsin, green: RFamide, red: tyrosinated tubulin). Scale bars: A,D: 50µm; B,C,E,F: 20µm; G,H: 10µm.

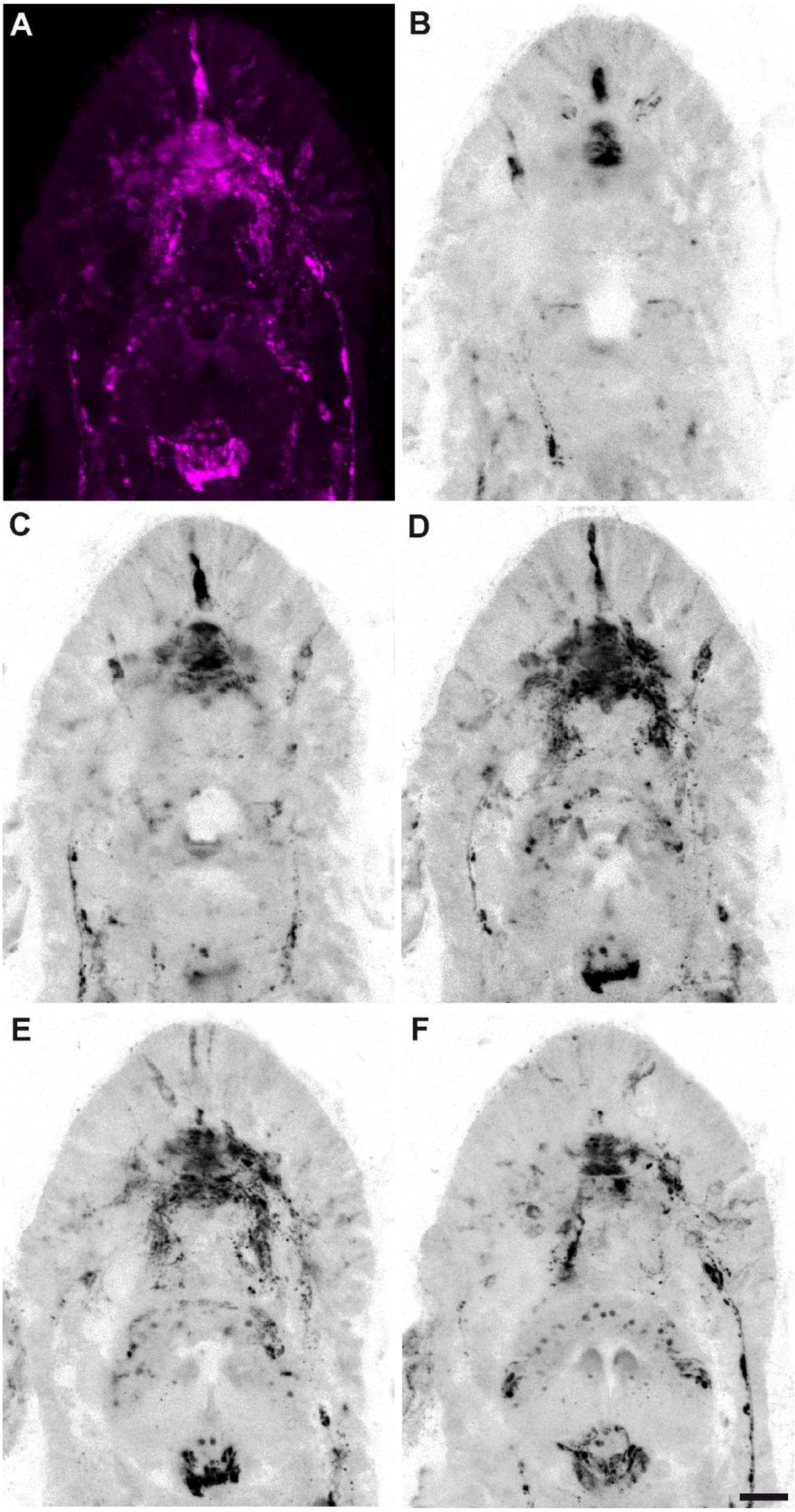

Fig. 10: Brain of a gnathostomulid, immunoreactivity against synapsin. (A) Maximum projection of a cLSM Z-stack, (B-F) Maximum projections of parts of the stack from (A) from dorsal (B) to ventral (F). Scale bar: 10µm.

Anti-Synapsin

Synapsin-ir is present in most centralized structures, namely in the brain, the longitudinal neurite bundles, and the penial 'connective' (Lammert 1986) also known as terminal 'commissure' (Müller & Sterrer 2004). Neither of these names is in accordance to the nomenclature suggested by Richter et al. (2010) but some terms from these publications will nevertheless be used here to avoid confusion.

The brain exhibits intensive synapsin-ir, and appears to consist of several connected neuropil regions (Fig. 10). However, the structure of the brain as described below could only be properly observed for a single specimen and may vary in other individuals. Most dorsal, two dense unpaired midline neuropils are visible (Fig. 10B). One is located at the anterior margin of the brain, the other is slightly more posterior. Between the two extends less dense neuropil (Fig. 10C). More ventrally they form the anterior neuropil part of the brain (Fig. 10D). Lateral they are flanked by bands of neuropil, which extend posterio-lateral and give rise to one part of the main longitudinal neurite bundles (termed by Lammert 1986 the 'lateral nerves'). Posterior, a larger mass of neuropil branches lateral in an even more posterior direction (Fig. 10D,E). These branches are connected to the unpaired buccal ganglion as well as the main longitudinal neurite bundles. This main longitudinal neurite bundles are two of six longitudinal neurite bundles that exhibit synapsin-ir (Fig. 9B), but are stained more intensely than all other bundles. The origin of the other four neurite bundles is less clear, but lies within the head (Fig. 9B). Two of them run along the midline, one of them dorsal, one ventral. They both seem to originate from the stomatogastric nervous system (Fig. 9B). The main neurite bundles, as well as the additional pairs of longitudinal neurite bundles, that emerge in the head region, extend more posterior than the penial connective and converge at the tip of the tail in what Lammert (1986) termed the caudal connective. The penial connective contains a band of neuropil unlike the caudal connective (Fig. 12A,B).

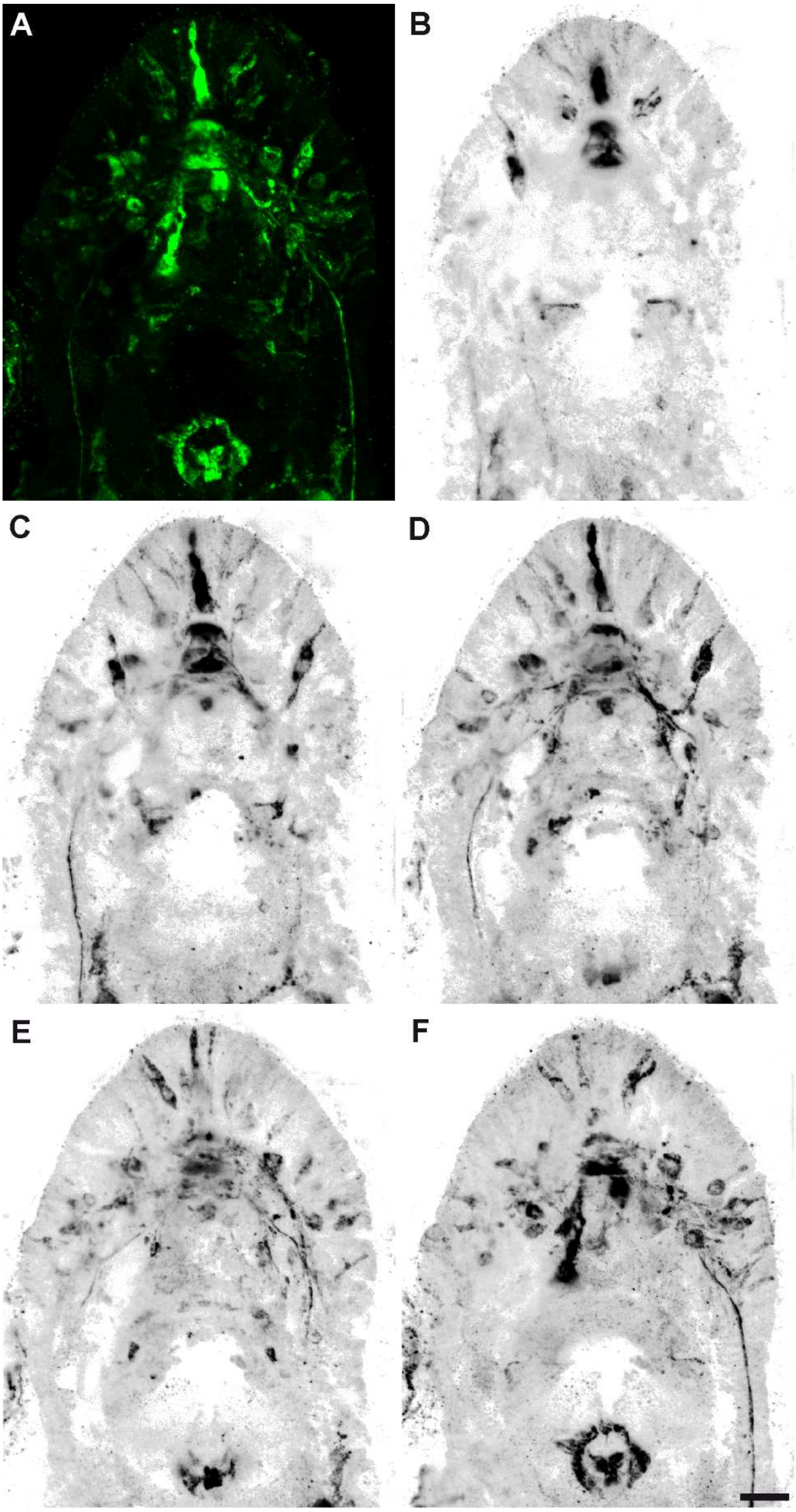

Fig. 11: Brain of a gnathostomulid, immunoreactivity against RFamide. (A) Maximum projection of a cLSM Z-stack, (B-F) Maximum projections of parts of the stack from (A) from dorsal (B) to ventral (F). Scale bar: 10µm.

Anti- RFamide

RFamide-like ir is present in the brain, the stomatogastric innervation and in a varying number of the longitudinal neurite bundles (Fig. 9A,C, 11). Mostly four of the longitudinal neurite bundles exhibit RFamide-like ir although in some specimens the more lateral neurite bundles were labeled much stronger than the other two and in a single specimen only two bundles with RFamide-like ir could be observed. Several large somata, that Müller and Sterrer (2004) referred to as 'bipolar perikarya', are located in the periphery of the head (Fig. 9E,H 11C,D). About 12-14 of them exhibit RFamide-like ir. Consistently, the most anterior one was particularly strongly labeled. The bipolar perikarya send neurites towards the anterior part of the brain. Two smaller RFamide-like ir somata are located posterior to the neuropil and project anteriorly (Fig. 9G). The brain neuropil contains RFamide-like ir processes in the anterior part. Two bands of RFamide-like ir neuropil transverse the brain (Fig. 9H, 11B,C). There are lateral connections between those two bands and to the main longitudinal neurite bundles (Fig. 11C,D). These bundles run along the body to the posterior end, where an interconnection exists at the penial connective (Fig. 12A,B) and where two RFamide-like ir somata and very little neuropil are also labeled (Fig. 12A). In some specimens, a pair of lateral somata is visible at the posterior end, which is connected to one of the additional longitudinal neurite bundles (Fig. 12C) as described by Müller and Sterrer (2004) for *Gnathostomula peregrina*.

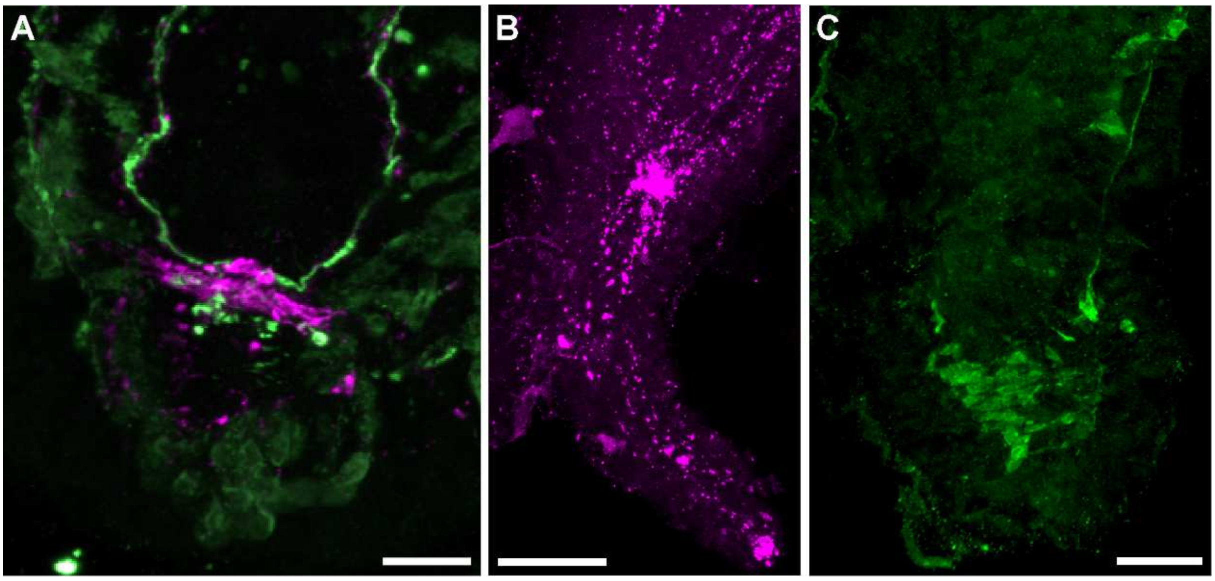

Fig. 12: Posterior end of a gnathostomulid, immunoreactivity against RFamide (green) and (magenta). Scale bars: B, C: 20µm; A: 10µm.

5.2 Discussion

Outgroup comparison

The chaetognath nervous system provides a wealth of characters that can be used for a comparison with other metazoan taxa. These include e.g. the nerve net, the arrangement of the brain and components of the cephalic nervous system, the ventral nerve centre with its connections to the brain and its posterior extension as well as individually identified RFamide-like ir neurons in the VNC. However, this comparison is complicated by the fact that Chaetognatha appear to be rather far removed from other bilaterian species. Given the data presented above, the most promising approach of the topic is to take a look at the general nervous system architecture and the distribution of RFamides in several major phyla. The focus is on the Gnathifera and Platyhelminthes, since one part of this project consisted of testing the hypothesis of a chaetognath/gnathostomulid relationship by analyzing the gnathostomulid nervous system.

Cnidaria

The nervous system of the various cnidarians is diverse in architectural aspects as pointed out in recent reviews by Schmidt-Rhaesa (2007), Watanabe et al. (2009) or Galliot and Quiquand (2011). The nervous system architecture in cnidarians consists of a nerve net, sometimes in combination with nerve rings or neurite bundles. Galliot and Quiquand (2011) speculate that the first common cnidarian ancestor likely had a nerve net and nerve rings. Like the rest of the cnidarian body, the nerve ring is circular and may be divided into functional subsystems (Watanabe et al. 2009). The nerve rings are the main condensation in the cnidarian nervous system. There is speculation about whether these nerve rings are an evolutionary precursor to the bilaterian central nervous system (Koizumi 2007). Koizumi (2007) describes the nerve ring of hydra as a concentration of neurons that show static developmental dynamics and are arranged around the pharynx, traits similar to the nerve rings in starfish and nematodes. In contrast, Schmidt-Rhaesa (2007) concludes that the many different types of nervous system, with or without condensed structures, only constitute a 'broad trend towards a diversification' instead of an evolutionary sequence. RFamides are present in Cnidarians and are found in all or at least many parts of their body in the ectodermal part of the nerve net, depending on the species (Watanabe et al. 2009).

Gnathifera

Recent molecular studies on the phylogenetic relationships of gnathostomulids supports grouping them together with Rotifera and Micrognathozoa, a group that is referred to as Gnathifera (Witek et al. 2009; Edgecombe et al. 2011; Nielsen 2012). A relation of chaetognaths and gnathostomulids was proposed based on molecular (Littlewood et al.

1998) and morphological data (Nielsen 2001), although Nielsen revised his opinion in the latest edition of his book (Nielsen 2012). Nonetheless, this hypothesis warrants a closer comparison between the nervous systems of these taxa, even though in some groups knowledge is limited.

Micrognathozoa is a taxon only recently described by Kristensen et al. (2000). According to the authors the nervous system consists of a slightly bilobate brain connected to the paired ventral nerve cords. They also found a stomatogastric innervation, a thoracal double ganglion and a caudal ganglion. However, it is unclear whether this stomatogastric nervous system is connected to the brain and whether the thoracal double ganglion and the caudal ganglion are associated with the nerve cords. There is no mention of a nerve net or plexus. Whether the nervous system is intra- or subepithelial could not be determined with certainty. Developmental or immunohistochemical data on the nervous system has not been presented so far.

The **Rotifera** (Syndermata) consist of acanthocephalans and the ‘classic’ rotifers. There is an ongoing debate about the relationships between these taxa. The originally proposed sistergroup relationship resulted in the name Syndermata for the combined taxa, however many recent studies conclude that the ‘classic’ rotifers are paraphyletic and should include acanthocephalans, although their exact position within the taxon is still unclear. Therefore, the term Syndermata became redundant (Witek et al. 2008; Fussmann 2011). The nervous system consists of a dorsal brain and a pair of longitudinal nerve cords in a ventro-lateral or lateral (in acanthocephalans) position. In addition several peripheral nerves and a varying number of smaller ganglia are described, including the stomatogastric mastax ganglion and the posterior pedal ganglion, (Sievert 2004a; Sievert 2004b; Nielsen 2012). Only one pair of ganglia is present in the posterior region of male acanthocephalans, which is missing in females (Sievert 2004a). Immunohistochemical studies have been conducted for several ‘classic’ rotifers, especially for RFamides and serotonin (Kotikova et al. 2005; Hochberg 2006; Hochberg 2007). RFamides are found in most parts of the central nervous system including the brain, nerve cords, penal ganglion and stomatogastric innervation. The few neurons are individual identifiable and in most cases paired (Kotikova et al. 2005; Hochberg 2007). The distribution of serotonin is similar, but a little less extensive, mainly missing in the penal ganglion (Kotikova et al. 2005; Hochberg 2006; Hochberg 2007).

Gnathostomulida have a brain and several longitudinal neurite bundles as described by Lammert (1986). The longitudinal bundles converge at the posterior end of the body and form what Lammert (1986) termed penial connective and caudal connective. The stomatogastric innervation mainly consists of the unpaired buccal ganglion that is connected to the brain via a pair of connectives. For *Gnathostomula paradoxa*, the author also shortly describes a subepithelial nerve net, which is formed by subepithelial neurons which seem to have no connection to the intraepidermal central nervous system. The ganglia are positioned intraepidermal, as are most sensory cells. The longitudinal neurite bundles are partly subepithelial (Lammert 1986). So far, very few immunohistochemical studies have been conducted. Next to the present study on *G. paradoxa*, only one other study exists. Müller and Sterrer (2004) used immunohistochemistry on Gnathostomula peregrina. Both species are members of the Bursovaginoidea. No immunohistochemical experiments have been performed on representatives of the Filospermoidea yet. Although Müller and Sterrer (2004) used antibodies against serotonin and RFamides they only got clear results for RFamides. They report eight longitudinal fiber bundles, two of them described as the main ones, which fuse at the posterior end of the animal in a 'terminal commissure'. One is called the ventro-median nerve that ends blind.

Platyzoa

In order to determine possible autapomorphies of the nervous system shared by chaetognaths and gnathifers it is necessary to include outgroups into the analysis. Two groups often associated with the Gnathifera are the Gastrotricha and Platyhelminthes. This group is referred to as Platyzoa. The Platyzoa were supported by recent molecular studies (Dunn et al. 2008; Edgecombe et al. 2011).

Gastrotricha are the topic of a recent paper by Rothe et al. (2011) that reviews the available data on the nervous system of several gastrotrich species. The authors attempted to reconstruct the nervous system of the Gastrotrich ancestor by comparing 40 different neuronal characters of both gastrotrichs and related outgroup species. Based on these characters, they propose a possible nervous system architecture of the gastrotrich ancestor that incorporates features found in recent species: Gastrotrichs have a dumb-bell shaped brain with lateral clusters of somata, a "belt-like" neuropil, also referred to as dorsal commissure, and a ventral commissure. Together, the dorsal and ventral commissures form a ring around the foregut. The nervous system also comprises an unknown number of pairs of anterior projections, but only one pair of ventro-lateral neurite bundles that fuses at the posterior end. The central nervous system is located basiepithelial. Several pairs of serotonin-ir and RFamide-like ir somata were detected in the brains of several species. The inference for the proposed ancestral pattern only considers five pairs of serotonin-ir somata, which may be individual identifiable. Part of the proposed ancestral pattern might also be a number of cells with RFamide-like ir, which are arranged serially and connect to the longitudinal nerve cords. However, the authors expressed some doubt about the initial experiment that prompted this hypothesis, suggesting it might be a case of pseudofluorescence.

Platyhelminthes have an orthogonal nervous system. It consists of an anterior, bilobed brain, two main longitudinal nerve cords, a varying number of minor longitudinal nerve cords, and transverse commissures along the body connecting the longitudinal nerve cords. The peripheral nervous system can consist of several nerve plexuses (subepidermal, submuscular, stomatogastric and genital; Halton & Gustafsson 1996; Reuter et al. 1998; Schmidt-Rhaesa 2007). The platyhelminthes are a well studied group. There is ample data on transmitter systems and this data was reviewed several times (Fairweather & Halton 1991; Halton & Gustafsson 1996; Gustafsson et al. 2002). RFamide is very abundant in all parts of the nervous system. Serotonin is also very abundant primarily in the brain, nerve cords and commissures, but also in parts of the nerve net and sensory structures.

Centralized structures of the nervous system - a comparison

The differences between the cnidarian nervous system and that of the bilaterian species mentioned here is obvious. The cnidarian nerve ring, structurally closest to what can be considered a brain, is not bilateral symmetrical and less condensed than the brains mentioned above, and while cnidarian neurite bundles may be similar to the longitudinal cords of the other species, neither they nor the nerve rings are a consistent part of the cnidarian nervous system architecture.

A first glance some similarities between the various bilaterian nervous systems mentioned above are apparent. Chaetognaths share the basic design consisting of a bilateral symmetrical brain, stomatogastric innervation, and longitudinal neurite bundles along the body with most other taxa that were analyzed here. However, that is also where comparisons begin to fall short.

Overall, the gnathiferan nervous systems have more features in common with the platyhelminth than with the chaetognath nervous system. When comparing the chaetognath and gnathostomulid brain, both have several neuropil domains, but while chaetognaths have two clearly separate neuropils, the neuropils of gnathostomulids do not have clearly distinguishable borders. The stomatogastric ganglia in chaetognaths are connected to the anterior brain domain versus a single buccal ganglion in gnathostomulids which links it to the posterior domain of the brain.

Both have a rather simple brain and several longitudinal neurite bundles. The presence of transversal commissures as found in platyhelminthes could not be demonstrated in gnathostomulids with the current set of methods. Neither of them has any ganglionic structure that resembles the Chaetognath ventral nerve center (VNC) in position or size. And, although “main connectives” were identified in all three taxa, the main connectives in chaetognaths do not extend to the end of the body unless one might consider they are continued in the caudal nerves. The main connectives in chaetognaths are broader and more prominent than the ones in either platyhelminthes or gnathostomulids. Also, the position of the chaetognath main connectives is somewhat different, since they unlike in the other taxa, do not remain in one dorsal or ventral plane, since they link the dorsal brain and the ventral VNC. Most chaetognaths lack any further longitudinal neurite bundles, although the nerve net may include single longitudinally positioned neurites or even small neurite bundles. In contrast platyhelminthes and gnathostomulids have additional, minor nerve cords. The transversal commissures of the platyhelminth orthogon somewhat resemble the transversal arrangement of single neurites in the nerve net of some sagittid species.

One can speculate, that the serial arrangement of the neurites within the VNC as observed for the sagittid species is a condensation of many single transversal commissures. This is certainly a valid assumption. However, it still does not increase the similarity to either of the species discussed above: it is also not very similar to the platyhelminth orthogon, since the neurite bundles do not form a ring, and transversal commissures in gnathostomulids likely do not exist. Most of the lateral nerves in chaetognaths, that are a prolongation of the VNC's neurite bundles, are not positioned at a 90° angle to the longitudinal axis, but rather spread at varying degrees.

When comparing immunohistochemical results, it is very apparent that serotonin is an unsuited marker for this specific phylogenetic discussion, since only one soma and few neurites were observed in chaetognaths. Of greater interest is the distribution of RFamides. In chaetognaths, RFamides are expressed only in the main central nervous system structures, the brain and VNC and, connecting the two, also the main connectives. Also, in *S. cephaloptera* (Harzsch et al. 2009) a postanal loop and a single neurite along the tail were detected. There is no known direct connection to sensory organs or any other organ system, although it is possible that the aforementioned loop and neurite, that are outside of the ganglionic parts, are part of a direct innervation. In gnathostomulids, RFamides are expressed mainly in the brain, the nerve cords and the stomatogastric innervation, but it is also present in the large bipolar somata, that are presumed to be associated with the sensory bristles of the head. In platyhelminthes however, RFamides are found in all components of the NS, even including the nerve net.

In platyhelminthes and gnathostomulids RFamide is abundant in the stomatogastric system, while adult chaetognaths have no RFamidergic structures visible within the stomatogastric ganglia. However, in developmental stages, neurites with RFamide-like ir are present in the vestibular ganglia and while they might still be present in adults they certainly are not as heavily involved in regulating stomatogastric processes as in other species. In conclusion, RFamidergic neurons seem to serve mostly as interneurons in chaetognaths and are almost exclusively restricted to the two main neural centers as opposed to other species, where they are used more widely and appear to serve a broader array of functions. However, it should be noted, that there are a wide variety of RFamides (Walker et al., 2010) and their identity cannot be determined by immunohistochemistry. It is likely, that the labeled neurons on the various taxa do not express the same type of RFamide which is an additional obstacle in finding homologies.

The chaetognath nerve net and the platyhelminth orthogon

Since some chaetognath species have an unexpectedly well organized nerve net, a comparison with one of the more ordered types of nerve net, the orthogon of the platyhelminthes, appears promising. An orthogon is defined by Richter et al. (2010) as "... [A] cluster of neurons. It is part of a nervous system and consists of at least two pairs of longitudinal neurite bundles, which are connected at regular intervals by transverse neurite bundles running at right angles to them (i.e., orthogonally). The transverse bundles may form a closed circle (circular bundles or ring commissures), or at least connect all the longitudinal bundles present. The thickness of the longitudinal neurite bundles can vary, usually with the ventral one being thicker than the others. An orthogon is not differentiated into ganglia linked by connectives." The central nervous system of the chaetognaths is vastly different to an orthogon, but the nerve net calls for a closer comparison. At least some of the sagittid species have a rather orthogon-like arrangement with prominent longitudinal and horizontal components. The longitudinal neurites are only loosely arranged in condensed bundles. However, it is unclear, if the horizontal neurites are in contact with all longitudinal bundles present. There are also frequent diagonal neurites in every species that link the nerve net to the main connectives or caudal nerves, a feature that naturally is not present in the orthogon. Also, many chaetognath species do not have as clear a pattern. Though it is possible to distinguish roughly horizontal and vertical neurites they tend to branch and curve at random places and angles. Without a definitive internal phylogeny of the chaetognaths it is difficult to tell which of these two configurations might be the original one. Another important question is, if the nerve net can be singled out for comparison at all, since it is not independent from the central structures, most notably the VNC. It is possible that the positive effects of an ordered nerve net are a sufficient driving force, to produce a somewhat similar architecture in only distantly related species.

The chaetognath VNC and the platyhelminth orthogon

The striation of the VNC is another character that merits a closer look in this discussion. The organization of the nervous system of the last common bilaterian ancestor is relevant for any hypothesis on the origin of the VNC. This topic has been discussed extensively by Harzsch and Wanninger (2010). Is the VNC an apomorphy of the Chaetognatha, possibly by a condensation of an orthogon-like plexus? It might explain the highly ordered configuration of neurites within the VNC as demonstrated by the vertical striation visible in many species. However, the number of somata and neurites associated with the VNC are much higher that the corresponding cells in platyhelminthes, but the number of cells, that contribute to a single transmitter system, in this case RFamide might not be that different. It would be very interesting to revisit this particular aspect once more data is available for the vast majority of cells in the VNC, which could not be linked to any transmitter system yet.

A comparison with additional taxa

Other hypotheses, like a close relation to the Arthropoda, Nematoda or somewhere else within the Ecdysozoa is already unlikely, since chaetognaths do not share defining morphological features with this group, like the fact that they are not molting. This led Mallatt et al. (2012) to the conclusion that their results, which placed a chaetognath species within the ecdysozoans, were not reliable. The architecture of the arthropod nervous system comprises a dorsal brain and paired ventral structures (see e.g. Schmidt-Rhaesa 2007). The best known example is the rope-ladder-like nervous system of insects and crustaceans. It may appear similar to the chaetognath nervous system, but there are some differences. The brain in these groups is a fusion of several segments, which correspond to a respective sensory structure. In chaetognaths the posterior domain receives input from several sensory organs, while the anterior domain is the connection to the stomatogastric innervation, which is connected anteriorly and loops around the esophagus, wholly unlike the stomatogastric innervation in arthropods (Harzsch 2006). The VNC, however, seems to have some similarities to the serially build nervous system of arthropods. It is a structure with a somewhat serial arrangement within the central neuropil, visible both in the distribution of neurons with RFamide-like immunoreactivity and sometimes in its striation pattern. But since a chaetognath's body does not show signs of segmentation beyond the split between trunk and tail, it is not possible to know whether the VNC has undergone a fusion, which can occur in some arthropod taxa. And while in arthropods single nerves innervate specific structures, all lateral nerves of the VNC only feed into the diffuse nerve net.

A close relation with the Nematoda seems just as unlikely. Nematodes have a rather simple nervous system. It consists of a brain that forms a ring around the pharynx, an unpaired nerve cord and 5 or more additional longitudinal neurite bundles that are connected by commissures, which are not distributed in a bilateral symmetrical fashion (Schmidt-Rhaesa 2007). The differences to the chaetognath system are evident: Chaetognaths have a dorsal brain which is part of two 'rings' around the esophagus: a chain of associated ganglia that is connected to the frontal part of the brain and forms the first, loose 'ring' around the esophagus while the main connectives, that leave the brain laterally and connect to the VNC, form a second, much more drawn out 'ring' around the gut. Both chaetognath 'rings' are structurally different from what is found in nematodes. Unlike the single nematode nerve cord, chaetognaths possess paired main connectives and nematodes also miss a ventral ganglionic structure like the VNC. In addition the chaetognath nervous system has a rather symmetrical build, especially in the central structures, which does not compare well to the nematode system of commissures.

Conclusion

Chaetognath phylogenetic relationships remain a mystery, with no proof for any closer affiliation to the taxa that were discussed. Although certain similarities are present, they are of no help to pin down the phylogenetic position beyond what was already presented in previous papers, but some interesting questions were raised that might profit from further investigation, like the presence of neuronal precursors or similarities that might be found in other transmitter systems. However, one conclusion, that seems justified from a neuro-anatomical point of view, is to discourage the hypothesis of a close affiliation or even inclusion of the chaetognaths within the Gnathifera. This might also be true for all Lophotrochozoa, since they all share a somewhat similar neuronal architecture that may have derived from an ancestral orthogonal nervous system (Schmidt-Rhaesa 2007). A close connection to the Ecdysozoa, especially to the Nematoda and Arthropoda as discussed above, is also unlikely. The conclusion drawn in the most recent previous publications, that chaetognaths are most likely a rather early bilaterian offshoot which diverged either at around the same time as the protostome/deuterostome split or early within the protostome line, is still the most likely hypothesis. Maybe in the future, the present results will help in furthering the understanding of chaetognath relationships, like, for example, through an ongoing joint effort of several groups of the Deep Metazoan Phylogeny network to assemble a phylogenetic tree based on neuronal character states.

6. Literature

Bieri R (1991) Systematics of the Chaetognatha. In Q. Bone, H. Kapp, & A. C. Pierrot-Bults, eds. *The Biology of Chaetognaths*. New York: Oxford University Press, pp.122-136.

Bone Q & Goto T (1991) Nervous System. In Q. Bone, H. Kapp, & A. C. Pierrot-Bults, eds. *The Biology of Chaetognaths*. New York: Oxford University Press, pp.18-31.

Chen J-Y & Huang D-Y (2002) A possible Lower Cambrian chaetognath (arrow worm). *Science* 298, 187.

Dunn CW, Hejnol A, Matus DQ, Pang K, Browne WE, Smith SA, Seaver E, Rouse GW, Obst M, Edgecombe GD, Sørensen MV, Haddock SHD, Schmidt-Rhaesa A, Okusu A, Kristensen RM, Wheeler WC, Martindale MQ & Giribet G (2008) Broad phylogenomic sampling improves resolution of the animal tree of life. *Nature* 452, 745-749.

Edgecombe GD, Giribet G, Dunn CW, Hejnol A, Kristensen RM, Neves RC, Rouse GW, Worsaae K & Sørensen MV (2011) Higher-level metazoan relationships: recent progress and remaining questions. *Org. Divers. Evol.* 11, 151-172.

Erber A, Riemer D, Bovenschulte M & Weber K (1998) Molecular phylogeny of metazoan intermediate filament proteins*. J. Mol. Evol.* 47, 751-762.

Fairweather I & Halton DW (1991) Neuropeptides in platyhelminths. *Parasitology* 102, 77-92.

Feigenbaum D (1991) Food and feeding behaviour. In Q. Bone, H. Kapp, & A. C. Pierrot-Bults, eds. *The Biology of Chaetognaths*. New York: Oxford University Press, pp.45-54.

Feigenbaum D & Reeve MR (1977) Prey detection in the Chaetognatha: Response to a vibrating probe and experimental determination of attack distance in large aquaria. *Limnol. Oceanogr.* 22, 1052-1058.

Fussmann GF (2011) Rotifers: Excellent subjects for the study of macro- and microevolutionary change. *Hydrobiologia* 662, 11-18.

Galliot B & Quiquand M (2011) A two-step process in the emergence of neurogenesis. *Eur. J. Neurosci.* 34, 847-862.

Ghirardelli E (1968) Some aspects of the biology of the chaetognaths. *Adv. Mar. Biol.* 6, 271-375.

Glück F (2011) Taxonomy, vertical distribution, biogeography and comparative sensory organ morphology of Chaetognaths in epi-, meso- and bathypelagic zones of the Atlantic Ocean and the Mediterranean Sea. Diplomarbeit. Rostock: Universität Rostock.

Goto T, Katayama-Kumoi Y, Tohyama M & Yoshida M (1992) Distribution and development of the serotonin-and RFamide-like immunoreactive neurons in the arrowworm, *Paraspadella gotoi* (Chaetognatha). *Cell. Tissue Res.* 267, 215-222.

Goto T & Yoshida M (1985) The mating sequence of the benthic arrowworm *Spadella schizoptera*. *Biol. Bull.* 169, 328-333.

Goto T & Yoshida M (1987) Nervous System in Chaetognatha. In M. A. Ali, ed. *Nervous Systems in Invertebrates.* Plenum Publishing Corporation, pp.461-481.

Gustafsson M, Halton D, Kreshchenko N, Movsessian S, Raikova O, Reuter M & Terenina N (2002) Neuropeptides in flatworms. *Peptides* 23, 2053-2061.

Halton DW & Gustafsson MKS (1996) Functional morphology of the platyhelminth nervous system. *Parasitology* 113, S47-S72.

Harzsch S (2006) Neurophylogeny: Architecture of the nervous system and a fresh view on arthropod phyologeny. *Comp. Integr. Biol.* 46, 162-194.

Harzsch S & Müller CHG (2007) A new look at the ventral nerve centre of *Sagitta*: implications for the phylogenetic position of Chaetognatha (arrow worms) and the evolution of the bilaterian nervous system. *Front. Zool.* 4, 14.

Harzsch S, Müller CHG, Rieger V, Perez Y, Sintoni S, Sardet C & Hansson B (2009) Fine structure of the ventral nerve centre and interspecific identification of individual neurons in the enigmatic Chaetognatha. *Zoomorphology* 128, 53-73.

Harzsch S & Wanninger A (2010) Evolution of invertebrate nervous systems: the Chaetognatha as a case study. *Acta Zool.* 91, 35-43.

Helfenbein KG, Fourcade HM, Vanjani RG & Boore JL (2004) The mitochondrial genome *of Paraspadella gotoi* is highly reduced and reveals that chaetognaths are a sister group to protostomes. *Proc. Nat. Acad. Sci. USA* 101, 10639-10643.

Hochberg R (2006) On the serotonergic nervous system of two planktonic rotifers, *Conochilus coenobasis* and *C. dossuarius* (Monogononta, Flosculariacea, Conochilidae). *Zool. Anz.* 245, 53-62.

Hochberg R (2007) Topology of the nervous system of *Notommata copeus* (Rotifera: Monogononta) revealed with anti-FMRFamide, -SCPb, and -serotonin (5-HT) immunohistochemistry. *Invertebrate Biol.* 126, 247-256.

Kapp H (1991) Morphology and anatomy. In Q. Bone, H. Kapp, & A. C. Pierrot-Bults, eds. *The Biology of Chaetognaths*. New York: Oxford University Press, pp.5-17.

Kapp H (2000) The unique embryology of Chaetognatha. *Zool. Anz.* 239, 263-266.

Kapp H (2004) Chaetognatha, Pfeilwürmer. In W. Westheide & R. Rieger, eds. *Einzeller und Wirbellose Tiere*. Spezielle Zoologie. Heidelberg, Berlin: Spektrum Akademischer Verlag, pp.757-762.

Kapp H & Giere O (2005) *Spadella interstitialis* sp. nov., a meiobenthic chaetognath from Mediterranean calcareous sands. *Meiofauna Marina* 14, 109-114.

Koizumi O (2007) Nerve ring of the hypostome in Hydra: Is it an origin of the central nervous system of bilaterian animals? *Brain Behav. Evol.* 69, 151-159.

Kotikova EA, Raikova OI, Reuter M & Gustafsson MKS (2005) Rotifer nervous system visualized by FMRFamide and 5-HT immunocytochemistry and confocal laser scanning microscopy. *Hydrobiologia* 546, 239-248.

Kristensen, Reinhardt Møberg & Funch P (2000) Micrognathozoa: a new class with complicated jaws like those of Rotifera and Gnathostomulida. *J. Morphol.* 246, 1-49.

Lammert V (1986) V*ergleichende Ultrastruktur-Untersuchungen an Gnathostomuliden und die phylogenetische Bewertung ihrer Merkmale*. Dissertation. Göttingen: Georg-August-Universität zu Göttingen.

Littlewood DTJ, Telford MJ, Clough KA & Rohde K (1998) Gnathostomulida - an enigmatic metazoan phylum from both morphological and molecular perspectives. *Mol. Phylogenet. Evol.* 9, 72-79.

Marletaz F, Gilles A, Caubit X, Perez Y, Dossat C, Samain S, Gyapay G, Wincker P & Le Parco Y (2008) Chaetognath transcriptome reveals ancestral and unique features among bilaterians. *Genome Biol.* 9: R94.

Marletaz F & Le Parco Y (2008) Careful with understudied phyla: the case of Chaetognath. *BMC Evol. Biol.* 8, 251.

Matus DQ, Copley RR, Dunn CW, Hejnol A, Eccleston H, Halanych KM, Martindale MQ & Telford MJ (2006) Broad taxon and gene sampling indicate that chaetognaths are protostomes. *Curr. Biology* 16, R575-R576.

Miyamoto H, Machida RJ & Nishida S (2010) Complete mitochondrial genome sequences of the three pelagic chaetognaths *Sagitta nagae*, *Sagitta decipiens* and *Sagitta enflata*. *Comp. Biochem. Physiol. Part D Genomics Proteomics* 5, 65-72.

Mallatt J, Waggoner Craig C & Yoder MJ (2012) Nearly complete rRNAgenes from 371 Animalia: Updated structure-based alignment and detailed phylogenetic analysis. *Mol. Phylogenet. Evol.* 64, 603-617.

Müller MCM & Sterrer W (2004) Musculature and nervous system of *Gnathostomula peregrina* (Gnathostomulida) shown by phalloidin labeling, immunohistochemistry, and cLSM, and their phylogenetic significance. *Zoomorphology* 123, 169-177.

Müller CHG, Rieger V, Perez Y, Harzsch S (submitted) Multicellular ciliary sense organs of arrow worms (Chaetognatha): a comparative immunohistochemical and ultrastructural study. Zoomorphology.

Nielsen C (2001) *Animal Evolution Interrelationships of the living phyla* 2nd ed., Oxford: Oxford University Press.

Nielsen C (2012) *Animal Evolution Interrelationships of the living phyla* 3rd ed., Oxford: Oxford University Press.

Papillon D, Perez Y, Caubit X & Le Parco Y (2004) Identification of chaetognaths as protostomes is supported by the analysis of their mitochondrial genome*. Mol. Biol. Evol.* 21, 2122-2129.

Papillon D, Perez Y, Caubit X & Parco YL (2006) Systematics of Chaetognatha under the light of molecular data, using duplicated ribosomal 18S DNA sequences. *Mol. Phylogenet. Evol.* 38, 621-634.

Pearre Jr S (1991) Growth and reproduction. In Q. Bone, H. Kapp, & A. C. Pierrot-Bults, eds. *The Biology of Chaetognaths*. New York: Oxford University Press, pp.61-75.

Perez Y, Müller CHG & Harzsch S (submitted) The Chaetognatha: an anarchistic taxon between Protostomia and Deuterostomia.

Perez Y, Rieger V, Martin E, Müller CHG & Harzsch S (2013) Neurogenesis in an early protostome relative: stem cells in the ventral nerve centre of chaetognath hatchlings are arranged in a highly organized geometrical pattern. *J. Exp. Zool. (Mol. Dev. Evol.)* 9999B: 1-15.

Philippe H, Brinkmann H, Copley RR, Moroz LL, Nakano H, Poustka AJ, Wallberg A, Peterson KJ & Telford MJ (2011) Acoelomorph flatworms are deuterostomes related to *Xenoturbella*. *Nature* 470, 255-258.

Pierrot-Bults AC & Nair VR (1991) Distribution patterns in Chaetognatha. In Q. Bone, H. Kapp, & A. C. Pierrot-Bults, eds. *The Biology of Chaetognaths*. New York: Oxford University Press, pp.86-116.

Reise K (1981) Gnathostomulida abundant alongside polychaete burrows. *Mar. Ecol. Prog. Ser.* 6, 329-333.

Reuter M, Mäntylä K & Gustafsson MKS (1998) Organization of the orthogon - main and minor nerve cords. *Hydrobiologia* 383, 175-182.

Richter S, Loesel R, Purschke G, Schmidt-Rhaesa A, Scholtz G, Stach T, Vogt L, Wanninger A, Brenneis G, Döring C, Faller S, Fritsch M, Grobe P, Heuer CM, Kaul S, Møller OS, Müller CHG, Rieger V, Rothe BH, Stegner ME & Harzsch S (2010) Invertebrate neurophylogeny: suggested terms and definitions for a neuroanatomical glossary. *Front. Zool.* 7, 29.

Rieger V, Perez Y, Müller CHG, Lipke E, Sombke A, Hansson BS & Harzsch S (2010) Immunohistochemical analysis and 3D reconstruction of the cephalic nervous system in Chaetognatha: insights into the evolution of an early bilaterian brain? *Invertebrate Biol.* 129, 77-104.

Rieger V, Perez Y, Müller CHG, Lacalli T, Hansson BS & Harzsch S (2011) Development of the nervous system in hatchlings of *Spadella cephaloptera* (Chaetognatha), and implications for nervous system evolution in Bilateria. *Dev. Growth Differ.* 53, 740-759.

Rothe BH, Schmidt-Rhaesa A & Kieneke A (2011) The nervous system of *Neodasys chaetonotoideus* (Gastrotricha: Neodasys) revealed by combining confocal laserscanning and transmission electron microscopy: evolutionary comparison of neuroanatomy within the Gastrotricha and basal Protostomia. *Zoomorphology* 130, 51-84.

Schmidt-Rhaesa A (2007) Nervous system. In *The Evolution of Organ Systems*, Oxford: Oxford University Press, pp. 95-117.

Shinn GL (1997) Chapter 3: Chaetognatha. In F. W. Harrison & E. E. Ruppert, eds. *Microscopic Anatomy of Invertebrates. Hemichordata, chaetognatha, and the Invertebrate Chordates*. New York: Wiley-Liss.

Sievert L (2004a) Acanthocephala, Kratzer. In W. Westheide & R. Rieger, eds. *Einzeller und Wirbellose Tiere*. Spezielle Zoologie. Heidelberg, Berlin: Spektrum Akademischer Verlag, pp.723-728.

Sievert L (2004b) “Rotatoria” (“Rotifera”), Rädertierchen. In W. Westheide & R. Rieger, eds. *Einzeller und Wirbellose Tiere*. Spezielle Zoologie. Heidelberg, Berlin: Spektrum Akademischer Verlag, pp.714-722.

Slabber M (1778) *Natuurkundige Verlustigingen Behelzende Microscopise Waarnemingen Van in- En Uitlandse Water- En Land-dieren*. Haarlem: J. Bosch.

Sterrer W (1972) Systematics and evolution within the Gnathostomulida. *Syst. Biol.* 21, 151.

Szaniawski H (2005) Cambrian chaetognaths recognized in Burgess Shale fossils. *Acta Palaeontol. Pol.* 50, 1-8.

Szaniawski H (2002) New evidence for the protoconodont origin of chaetognaths. *Acta Palaeontol. Pol.* 47, 405-419.

Tazaki A, Gaudieri S, Ikeo K, Gojobori T, Watanabe K & Agata K (1999) Neural network in planarian revealed by an antibody against planarian synaptotagmin homologue. *Biochem. Biophys. Res. Commun.* 260, 426-432.

Thuesen EV (1991) The tetrodotoxin venom of chaetognaths. In Q. Bone, H. Kapp, & A. C. Pierrot-Bults, eds. *The Biology of Chaetognaths*. New York: Oxford University Press, pp.55-60.

Tokioka T (1965) The taxonomical outline of chaetognaths. *Publ. Seto Mar. Biol. Lab.* 12, 335-357.

Walker RJ, Papaioannou S & Holden-Dye L (2010) A review of FMRFamide- and RFamide-like peptides in metazoa. *Invertebr. Neurosci.* 9, 111-153.

Watanabe H, Fujisawa T & Holstein TW (2009) Cnidarians and the evolutionary origin of the nervous system. *Dev. Growth Differ.* 51, 167-183.

Winkelmann C, Gasmi S, Gretschel G, Müller CHG & Perez Y (2012) Description of *Spadella valsalinae* sp. nov., a neo-endemic benthic chaetognath from Northern Adriatic Sea (Croatia) with remarks on its morphology, phylogeny and biogeography. *Org. Divers. Evol.* DOI 10.1007/s13127-012-0108-0.

Witek A, Herlyn H, Meyer A, Boell L, Bucher G & Hankeln T (2008) EST based phylogenomics of Syndermata questions monophyly of Eurotatoria. *BMC Evol. Biol.* 8, 345.

Witek A, Herlyn H, Ebersberger I, Mark Welch DB & Hankeln T (2009) Support for the monophyletic origin of Gnathifera from phylogenomics. *Mol. Phylogenet. Evol.* 53, 1037-1041.

7. Authors contributions/ Anteil der Eigenleistung

I contributed to the following papers to the extent mentioned below:
Ich habe folgenden Anteil der Arbeit an den untenstehenden Papern geleistet:

Harzsch et al. (2009) Fine structure of the ventral nerve centre and interspecific identification of individual neurons in the enigmatic Chaetognatha.

Original research/eigene Daten	10%
Figures and Illustrations/ Bildtafeln und Illustrationen	10%
Text	5%

Rieger et al. (2010). Immunohistochemical analysis and 3D reconstruction of the cephalic nervous system in Chaetognatha: insights into the evolution of an early bilaterian brain?

Original research/eigene Daten	60%
Figures and Illustrations/ Bildtafeln und Illustrationen	100%
Text	50%

Rieger et al. (2011) Development of the nervous system in hatchlings of *Spadella cephaloptera* (Chaetognatha), and implications for nervous system evolution in Bilateria.

Original research/eigene Daten	90%
Figures and Illustrations/ Bildtafeln und Illustrationen	100%
Text	60%

Perez et al. (2013) Neurogenesis in an early protostome relative: stem cells in the ventral nerve centre of chaetognath hatchlings are arranged in a highly organized geometrical pattern.

Original research/eigene Daten	90%
Figures and Illustrations/ Bildtafeln und Illustrationen	85%
Text	45%

Müller et al. (submitted) Multicellular ciliary sense organs of arrow worms (Chaetognatha): a comparative immunohistochemical and ultrastructural study.

Original research/eigene Daten	35%
Figures and Illustrations/ Bildtafeln und Illustrationen	55%
Text	35%

Steffen Harzsch

Signature of advisor/Unterschrift des Betreuers

Prof. Dr. Steffen Harzsch
Universität Greifswald
Zoologisches Institut und Museum
Cytologie und Evolutionsbiologie
Soldmannstraße 23
D - 17487 Greifswald

8. Publications

8.1 Fine structure of the ventral nerve centre and interspecific identification of individual neurons in the enigmatic Chaetognatha.

Harzsch S, Müller CHG, **Rieger** V, Perez Y, Sintoni S, Sardet C, Hansson B (2009)

Zoomorphology 128: 53-73

Zoomorphology (2009) 128:53–73
DOI 10.1007/s00435-008-0074-4

ORIGINAL PAPER

Fine structure of the ventral nerve centre and interspecific identification of individual neurons in the enigmatic Chaetognatha

**Steffen Harzsch · Carsten H. G. Müller · Verena Rieger ·
Yvan Perez · Silvia Sintoni · Christian Sardet ·
Bill Hansson**

Received: 5 April 2008 / Accepted: 7 October 2008 / Published online: 21 November 2008
© The Author(s) 2008. This article is published with open access at Springerlink.com

Abstract The enigmatic arrow worms (Chaetognatha) are marine carnivores and among the most abundant planktonic organisms. Their phylogenetic position has been heavily debated for a long time. Most recent molecular studies still provide a diverging picture and suggest arrow worms to be some kind of basal protostomes. In an effort to understand the organization of the nervous system in this clade for a broad comparison with other Metazoa we analysed the ultrastructure of the ventral nerve centre in *Spadella cephaloptera* by transmission electron microscopy. We were able to identify six different types of neurons in the bilateral somata clusters by means of the cytoplasmic composition (regarding the structure of the neurite and soma including the shape and eu-/heterochromatin ratio within the nucleus) as well as the size and position of these neurons. Furthermore, our study provides new insights into the neuropil composition of the ventral nerve centre and several other fine structural features. Our second goal was to examine if individually identifiable neurons are present in the ventral nerve centres of four chaetognath species, *Sagitta setosa, Sagitta enflata, Pterosagitta draco*, and *Spadella cephaloptera.* For that purpose, we processed whole mount specimens of these species for immunolocalization of RFamide-related neuropeptides and analysed them with confocal laser-scanning microscopy. Our experiments provide evidence for the interspecific homology of individual neurons in the ventral nerve centres of these four chaetognath species suggesting that the potential to generate serially arranged neurons with individual identities is part of their ground pattern.

Keywords Ventral nerve centre · *Spadella cephaloptera* · *Pterosagitta draco* · *Sagitta* spp. · Ultrastructure · Immunolocalization · Seriality · Neurophylogeny · Metazoa

Introduction

The Chaetognatha (arrow worms) are transparent marine carnivores that range in length from 1 to 120 mm and are among the most abundant planktonic organisms. The taxon comprises more than 120 species from all geographical and vertical ranges of the ocean (Shinn 1997; Nielsen 2001; Kapp 2007). Palaeontological evidence recently showed chaetognaths to be present in the Early Cambrian (approx.

S. Harzsch (✉) · C. H. G. Müller · V. Rieger · S. Sintoni ·
B. Hansson
Department of Evolutionary Neuroethology,
Max Planck Institute for Chemical Ecology, Beutenberg Campus,
Hans-Knöll-Street 8, 07745 Jena, Germany
e-mail: sharzsch@ice.mpg.de

C. H. G. Müller
Institut für Biowissenschaften,
Allgemeine und Spezielle Zoologie, Universität Rostock,
Universitätsplatz 2, 18051 Rostock, Germany

Y. Perez
Institut Méditerranéen d'Ecologie et de Paléoécologie,
UMR 6116 CNRS, "Persistence and Evolution
of the Biodiversity", Université de Provence,
3 Place Victor Hugo Case 36,
13331 Marseille Cedex 3, France

S. Sintoni
Fakultät für Naturwissenschaften,
Institut für Neurobiologie und Sektion Biosystematische
Dokumentation, Universität Ulm, 89081 Ulm, Germany

C. Sardet
Bio Mar Cell, Laboratoire de Biologie du Développement,
UMR7009 CNRS/UPMC, Station Zoologique,
Observatoire Océanologique,
06234 Villefranche-sur-Mer Cedex, France

540–520 Myr ago) Chengjang biota (Vannier et al. 2007). These authors suggest placing them among the earliest active predators and conclude that the ancestral chaetognaths were planktonic with possible ecological preferences for hyperbenthic niches close to the sea bottom. The phylogenetic position of the chaetognaths within the Bilateria is heavily debated (review Harzsch and Müller 2007) and the most recent molecular studies provide a diverging picture. By using Bayesian inference and maximum likelihood method to analyse two broad phylogenomic datasets, Dunn et al. (2008) suggest a sister-group relationship of Chaetognatha to the Lophotrochozoa whereas Marlétaz et al. (2008) propose a most likely position of the Chaetognatha as a sister-group to all Protostomia.

The ventral nerve centre of Chaetognatha is an elongate structure lying between the epidermis and its basement membrane (reviewed in Harzsch and Müller 2007). This neuronal centre controls swimming by initiating contractions of the body wall musculature (Duvert et al. 1980; Duvert and Barets 1983; Duvert and Savineau 1986) and integrates mechanosensory input from the numerous ciliary fence receptors in the epidermis (Bone and Pulsford 1984; Bone and Goto 1991; Shinn 1997; Malakhov et al. 2005). It consists of a central fibrillar neuropil core, flanked by lateral clusters of cell bodies and it is anteriorly connected to the brain by two main connectives (Bone and Pulsford 1984; Goto and Yoshida 1987; Shinn 1997). The ventral nerve centre gives rise to a densely ramifying nervous plexus that provides motor innervation to the body musculature and innervates the ciliary fence receptors (Bone and Pulsford 1984). Some aspects of the fine structure of the ventral nerve centre have been analysed in several species belonging to the genus *Sagitta* (Ahnelt 1980; Bone and Pulsford 1984; Goto and Yoshida 1987; Bone and Goto 1991). One goal of the present report is to provide further insights into the ultrastructural characteristics of the ventral nerve centre and to compare these between representatives of *Spadella* and *Sagitta*. Furthermore, this fine structural analysis will serve as a background for a meaningful analysis of the immunolocalization studies described below.

Studies on the immunolocalization of RFamide-related neuropeptides emphasized serially arranged neurons in the ventral nerve centres of two arrow worm species, *Sagitta setosa* (Müller, 1947) and *Paraspadella gotoi* (Casanova, 1990) and suggested the presence of individually identifiable neurons (Bone et al. 1987; Harzsch and Müller 2007; Goto et al. 1992). The concept of individually identifiable neurons is valid for the nervous systems of many protostome taxa. This means that neurons within the central nervous system can be treated as individuals that can be recognized from animal to animal of one species or even in individuals belonging to different species that are more or less closely related (see Burrows 1996 for a review of this concept in Arthropoda). Kutsch and Breidbach (1994) presented a catalogue of features for examining cellular characteristics of individually identifiable neurons in order to explore whether they may be homologous between different arthropod taxa. Their catalogue includes features such as the common ontogenetic origin of neurons, physiological criteria such as the characterization of a neuron as inhibitory or excitatory, biochemical criteria such as the expression of specific neurotransmitters or neuron-specific markers, and morphological criteria such as the position of the neuronal somata in relation to the ganglion framework as well as the course of the neurites and the targets that they innervate. Within the Protostomia, individually identifiable neurons have been shown to be present in the nervous systems of, e.g. Arthropoda (Burrows 1996; Harzsch et al. 2005; Harzsch 2006), Annelida (Stuart et al. 1987; Huang et al. 1998, Gilchrist et al. 1995; Brodfuehrer and Thorogood 2001; Orrhage and Müller 2005; Müller 2006), Nemathelminthes/Cycloneuralia (White et al. 1986; Walthall 1995), basal Mollusca (Friedrich et al. 2002; Voronezhskaya et al. 2002), Plathelminthes (Halton and Gustafsson 1996; Reuter et al. 1998; Reuter and Halton 2001), and Gnathifera (Müller and Sterrer 2004). The presence of at least some individually identifiable neurons in basal deuterostomes such as tunicates (Meinertzhagen 2004; Stach 2005; Meinertzhagen et al. 2004; Imai and Meinertzhagen 2007; Soviknes et al. 2007), and the lancelet (Wicht and Lacalli 2005) indicates that the potential to establish individual identities may not only be present in the ground pattern of Protostomia; but may even date back to the ground pattern of Bilateria. Our previous study on representatives of *Sagitta* had indicated the possibility that individually identifiable neurons may also be present in Chaetognatha (Harzsch and Müller 2007). The present contribution sets out to explore this question in more detail.

The tetrapeptide FMRFamide (Phe-Met-Arg-Phe-NH2) and FMRFamide-related peptides (FaRPs) form a large neuropeptide family with more than 50 members, all of which share the RFamide motif (reviews: Price and Greenberg 1989; Greenberg and Price 1992; Walker 1992; Dockray 2004; Kriegsfeld 2006; Zajac and Mollereau 2006). This neuropeptide family is widely distributed among invertebrates and vertebrates and an increasing amount of literature on the structural diversity and neurohormonal action of invertebrate FaRPs and other peptides, e.g. in Coelenterata (review Grimmelikhuijzen et al. 1992), Plathelminthes (review Fairweather and Halton 1991; Choi et al. 1996), Mollusca (review Muneoka and Kobayashi 1992), and Arthropoda (Keller 1992; Gaus et al. 1993; Groome 1993; Nässel 1993; Homberg 1994; Nässel and Homberg 2006) highlights a growing appreciation of the importance of these substances. So far, the evidence for the presence of FaRPs in Chaetognatha stems from immunocytochemical experiments only (Bone et al. 1987; Goto et al. 1992; Harzsch and Müller 2007) but the sequences of the FaRPs present in this clade are still unknown. The cell bodies of the RFamide-like immunoreactive neurons in arrow worms are located in the lateral cell soma clusters that flank the central neuropil. The previous studies have shown that the RFamide-like immunoreactive neurons are individually identifiable and can be homologized between different specimens within single arrow worm species (intraspecific homology; Kutsch and Breidbach 1994). However, so far it was not known if certain individually identified neurons can also be identified across different species of the Chaetognatha (interspecific homology; Kutsch and Breidbach 1994). Therefore, the second goal of this study was to answer the question if RFamide-like immunoreactive neurons can be individually identified and homologized between four arrow worm species, *S. setosa*, *Sagitta enflata* (Grassi 1881), *Pterosagitta draco* Krohn 1853, and *Spadella cephaloptera* (Busch 1851) based on biochemical and morphological features as laid out by Kutsch and Breidbach (1994).

Materials and methods

Experimental animals

For histological, immunohistochemical, and electron microscopical studies, adult specimens of *Sagitta setosa* (Müller, 1947) (Aphragmophora, Sagittidae) were obtained off Helgoland (North Sea) in August 2006 by horizontal (surface water samples) as well as by vertical (down to 20 m depth) plankton hauls on Helgoland Roads with the research vessel "MS Aade". Adult specimens of *Sagitta enflata* (Grassi, 1881) (Aphragmophora, Sagittidae) were obtained in November 2006 by horizontal plankton hauls (surface water samples) ca. 1 nautical mile off the coast of Villefranche-sur-mer (France). Adult specimens of *Spadella cephaloptera* (Busch, 1851) (Phragmophora, Spalleidae) were collected in Sormiou (Marseille, France) in June 2006 and August 2007. A plankton net was grazed over the sea grass beds by snorkelling. Animals were kept in aquaria containing natural seawater (21 ± 1°C) at the Université de Provence, Marseille. Specimens of *Sagitta bipunctata* (Quoy and Gaimard, 1827) (Aphragmophora, Sagittidae) were collected near Cassidaigne (Marseille, France) in October 1997 during a planktonic survey carried out on mesopelagic communities at depth levels of approximately 500 m. Specimens of *Sagitta hispida* (Conant, 1895) (Aphragmophora, Sagittidae) were collected from the Indian River Lagoon (27°14′N, 80°90′W) in surface water near Fort Pierce (FL, USA) with a plankton net suitable for capturing macrofauna organisms (300 μm mesh size). *Pterosagitta draco* Krohn, 1853 (Aphragmophora, Pterosagittidae) was provided by Gisèle Champalbert and Marc Pagano from the Institut pour la Recherche et le Développement (IRD UR 167 SyRoCo) who collected samples during a mission in the Indian Ocean (Tulear). The immunohistochemical observations reported in this paper are based on the analysis of at least ten specimens for each species except *P. draco*, of which unfortunately only one specimen was available.

Preparation for bright field microscopy and transmission electron microscopy

Adult specimens of *S. cephaloptera*, 3–4 mm in length, were starved for 2 days in order to fix them in an unfed condition. Adult individuals of the species *S. bipunctata* and *S. hispida* (Aphragmophora, Sagittidae) were immediately fixed from fresh plankton samples. A total of ten individuals of *S. cephaloptera* was fixed either by immersing the entire specimen or by cutting the body into three pieces (head, trunk, and tail). The tissues were immersed for 12 h in a cold solution of Karnovsky's prefixative (Karnovsky 1965), consisting of 2% glutaraldehyde, 2% paraformaldehyde, 1.52% NaOH, and 1.2 g D-glucose, dissolved in 2.25% Na-hydrogenphosphate buffer (pH 7.4). After washing in the same buffer (12 h), the specimens were postfixed for 4 h in 1% OsO_4 solution (same buffer) at room temperature and, following dehydration in a graded series of acetone, embedded in epoxide resin (Araldit, FLUKA).

Several adult individuals of *S. bipunctata* were fixed without any dissection according to the method developed by Arnaud et al. (1978), including a prefixation for 4–8 h in a cold solution of 2% glutaraldehyde, 1% paraformaldehyde, 30% filtered seawater in 0.2 M Sodium-cacodylate buffer (pH 7.3; final osmolarity of the fixative was around 1,240 mosm), followed by a 12-h rinse in the same buffer with glucose added. The specimens were postfixed was in 1% OsO_4 (in cacodylate buffer with NaCl) at 4°C for 1 h. The specimens were dehydrated in a graded series of ethanol and propylene oxide and finally embedded in Epon resin.

About 20 adult individuals of *S. hispida* were fixed by Dr George Shinn (Northeast Missouri State University) in a modified solution after Karnovsky (1965), consisting of the same concentration of chemicals used for fixing *S. cephaloptera*. The head and the tail were separated from the trunk with a razor blade (1–2 min after immersion into the primary fixative). However, for postfixation a higher concentrated OsO_4 solution (2% in 0.2 M phosphate buffer) was used. The trunk of *S. hispida* was then dehydrated in a graded series of ethanol, transferred through three changes of propylene oxide solutions, and embedded in Epon 812.

Serial semithin sections (1 μm) were prepared and stained using 1% toluidine blue in a solution of 1% Na-tetraborate (borax). Serial ultrathin sections were stained with uranyl acetate and lead citrate for 5 min each and then examined under a Zeiss 902A Transmission Electron Microscope, operated at 80 kV. Some of the TEM-images shown in this paper (e.g. Figs. 3a, e, 4h) are photomontages compiled with the ITEM software, from up to 30 single digital micrographs.

Immunohistochemistry

Specimens were fixed overnight at 4°C (or for 4 h, room temperature) in 4% paraformaldehyde (PFA) in phosphate buffer (PB; 0.1 M, pH 7.4). Immunohistochemistry was carried out on free-floating whole mounts of adult specimens with fluorochrome-conjugated secondary antibodies using standard protocols (Harzsch and Müller 2007). After fixation the tissues were washed in several changes of phosphate buffered saline (PBS) for at least 4 h, preincubated in PBS-TX (1% normal goat serum, 0.3% Triton X-100, 0.05% Na-acide) for 1 h and then incubated overnight in the primary anti-FMRFamide antibody (from rabbit; Diasorin) diluted 1:1,000 in PBS-TX at room temperature. Specimens were then washed for at least 2 h in several changes of PBS and subsequently incubated in secondary antibodies against rabbit proteins conjugated to the fluorochrome Alexa Fluor 488 (Molecular Probes, obtained by MoBiTec, Göttingen, Germany) for 4 h. Some specimens of *S. cephaloptera* were processed with a histochemical counter stain, a high-affinity probe for actin, by adding Phallotoxins conjugated to Alexa Fluor 546 (Molecular Probes; concentration 200 units/ml) to the secondary antibody in a dilution 1:50. Other samples were counterstained with the nuclear dye bisbenzimide (0.1%, Hoechst H 33258) for 15 min at room temperature. Finally, the tissues were washed for at least 2 h in several changes of PBS and mounted in GelMount (Sigma).

The antiserum we used was generated in rabbit against synthetic FMRFamide (Phe-Met-Arg-Phe-NH_2) conjugated to bovine thyroglobulin (DiaSorin, Cat. No. 20091, Lot No. 923602). According to the manufacturer, staining with this antiserum is completely eliminated by pre-treatment of the diluted antibody with 100 µg/ml of FMRFamide. We repeated this experiment and preincubated the antiserum with 10^{-4} M FMRFamide (16 h, 4°C). In this control, neuronal structures were not labelled. In an additional control experiment for possible non-specific binding of the secondary antiserum, we omitted the primary antiserum, replaced it with blocking solution, and followed the labelling protocol as above. In this control, staining was absent.

We compared the labelling pattern obtained in our specimens with that in a previous study, in which a polyclonal antiserum to the sequence Arg-Phe-amide was used in *S. setosa* (Bone et al. 1987). This latter antiserum was obtained by immunizing rabbits with synthetic FMRFamide which was coupled via glutaraldehyde to bovine thyroglobulin (Grimmelikhuijzen and Spencer 1984). Incubation of this antiserum with sepharose-bound FMRFamide, FLRFamide, or RFamide abolished all staining and this antiserum has been shown to be most sensitive to the C-terminal sequence-RFamide (-Arg-Phe-NH2; Grimmelikhuijzen 1985). It has been used to label RFamide-like immunoreactive structures, e.g. in a medusa (Grimmelikhuijzen and Spencer 1984) and in several *Hydra* species (Grimmelikhuijzen 1985). Bone et al. (1987), using the antiserum generated by Grimmelikhuijzen and Spencer (1984) in *S. setosa,* concluded that the chaetognath peptide might be related to any peptide terminating with the sequence RFamide. Because the labelling pattern obtained by Bone et al. (1987) closely corresponds to that of *S. setosa* as found in the present report we conclude that the DiaSorin antiserum that we used most likely also labels any peptide terminating with the sequence RFamide. Therefore, we will refer to the labelled structures in our specimens as "RFamide-like immunoreactive (RFir) neurons" throughout the paper.

Light-microscopic analysis and 3D reconstruction

Digital images of *S. setosa* (Fig. 5a) were obtained with a Zeiss Axioskop fitted with a CCD-1300B digital camera (Vosskühler GmbH) and processed with the Lucia Measurement 5.0 software package (Laboratory Imaging Ltd). The specimens of *S. enflata*, *P. draco*, and *S. cephaloptera* were scanned with a Zeiss LSM 510 Meta Confocal Laser-Scanning Microscope. Those images are based on stacks of between 5 and 10 optical sections (single images are averages of four laser sweeps) of a *z*-series taken at intervals of 1 µm. Images were black–white inverted and processed in Adobe Photoshop by using the global contrast and brightness adjustment features. The colour coded 3D images in Fig. 4 were generated using the Zeiss LSM viewer software (use red–green glasses to view). Image stacks obtained from *z*-series by the Zeiss LSM 510 Meta were directly loaded into the 3D reconstruction software Amira (Mercury Systems) operated on a Fujitsu Siemens Celsius 560 workstation. The reconstructions in Fig. 7 were generated by using Amira's "create isosurface" module.

Results

Comparative histology

In adult specimens of *Spadella cephaloptera*, the ventral nerve centre is located in the anterior third of the animal and extends across ca. two-thirds of the trunk width as visualized by whole-mount histochemical and immunohistochemical labelling of nuclei (Fig. 1). These preparations

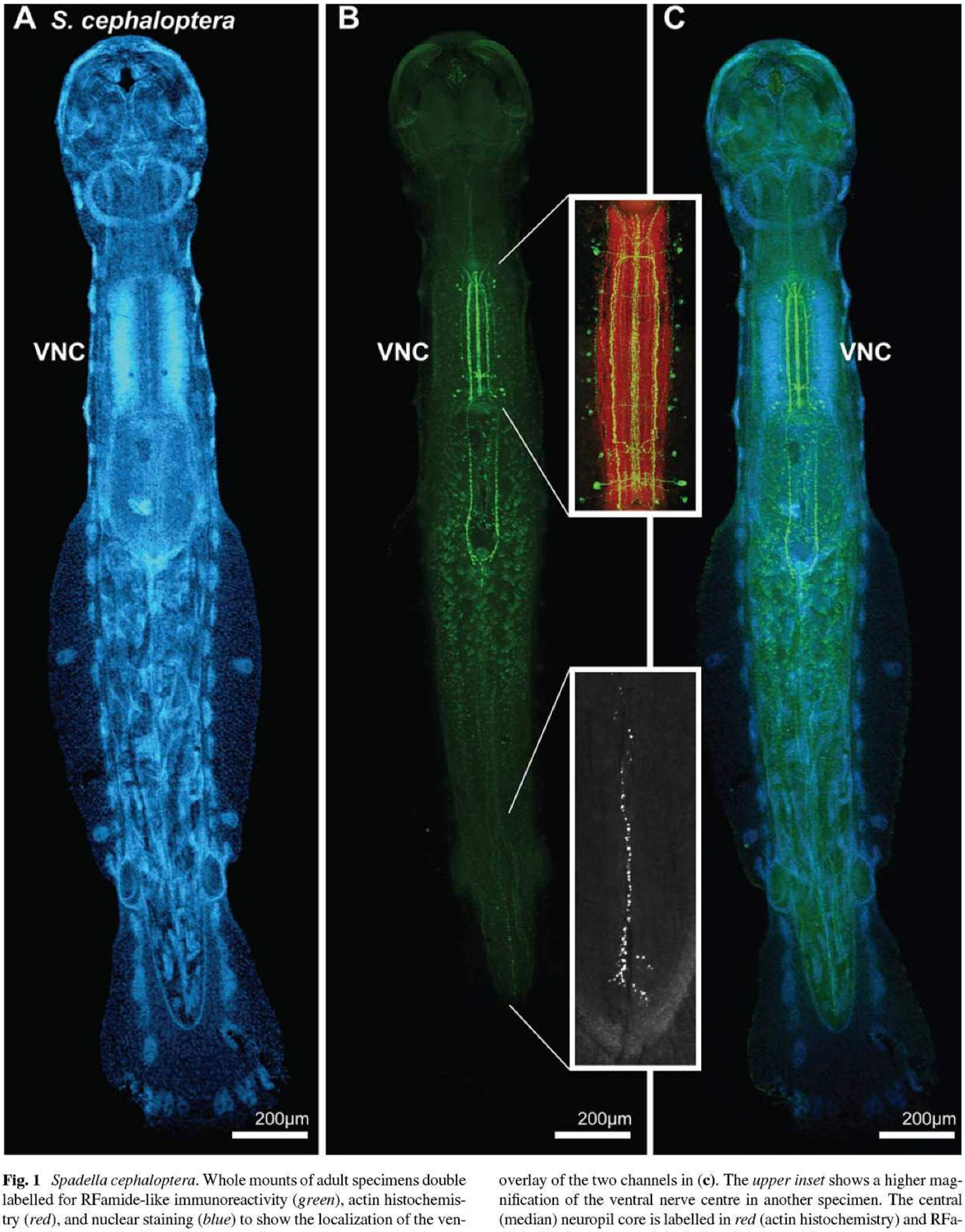

Fig. 1 *Spadella cephaloptera*. Whole mounts of adult specimens double labelled for RFamide-like immunoreactivity (*green*), actin histochemistry (*red*), and nuclear staining (*blue*) to show the localization of the ventral nerve centre (confocal laser-scan microscopy). **a–c** show the same specimen with the *green* channel in **(a)** (RFamide-like immunoreactivity), the *blue* channel in **(b)** (nuclear staining with HOECHST), and the overlay of the two channels in **(c)**. The *upper inset* shows a higher magnification of the ventral nerve centre in another specimen. The central (median) neuropil core is labelled in *red* (actin histochemistry) and RFamide-like immunoreactivity is labelled *green*. The *lower inset* shows a higher magnification of the posteriorly directed fibre that extends from the posterior loop to terminate within the tail. *VNC* ventral nerve centre

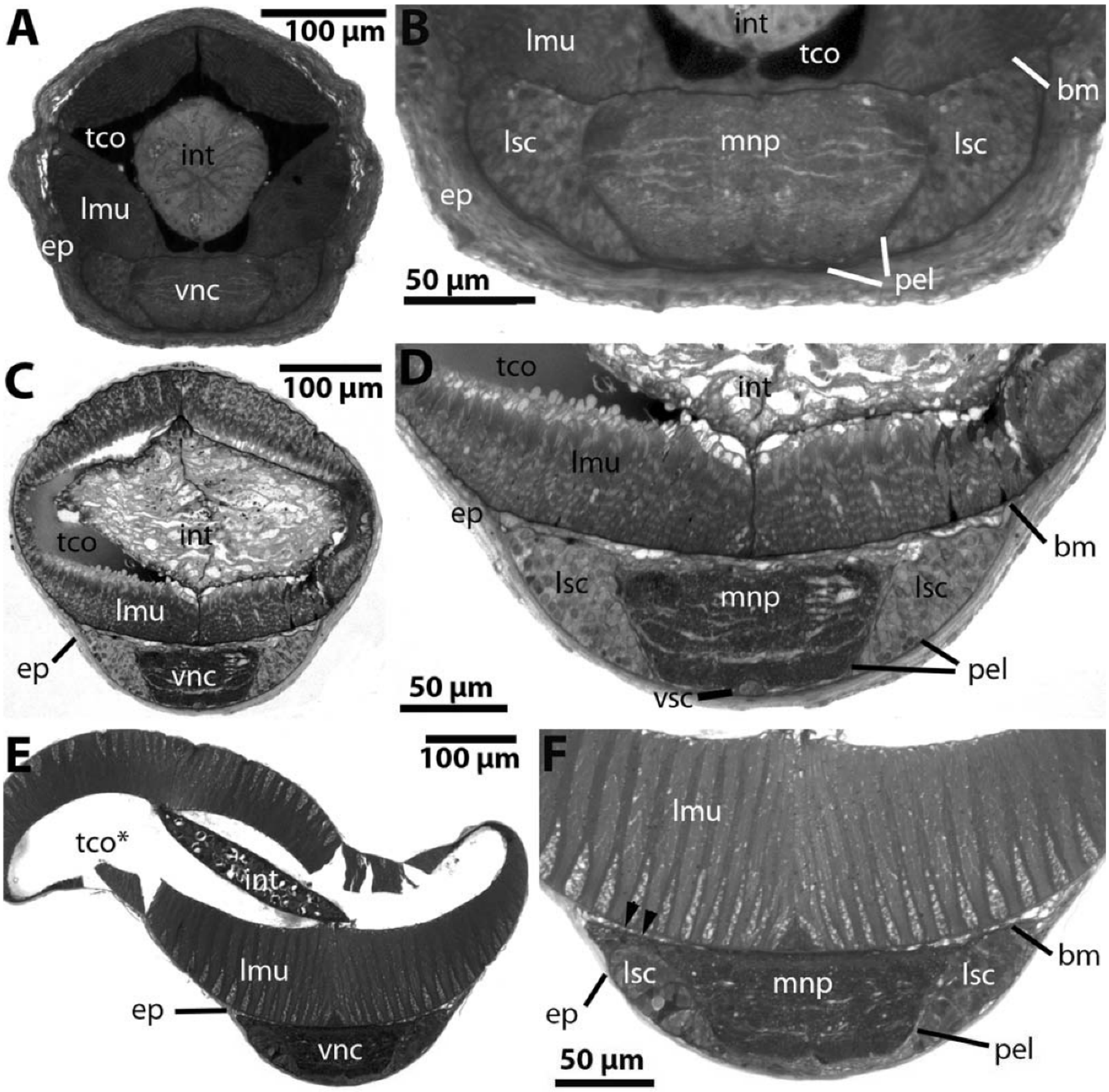

Fig. 2 *Spadella cephaloptera* (**a**, **b**), *Sagitta hispida* (**c**, **d**), *Sagitta bipunctata* (**e**, **f**). Light microscopy to show the comparative anatomy of the ventral nerve centres. **a**, **c**, **e** Cross-sections at the anterior or mid-level of the trunk. **b, d, f** Higher magnification of the ventral half of the cross-sections. The cross-section in **e** is deformed because of the trunk coelomatic space (*tco**) being collapsed during the fixation process. The *double arrowheads* in **f** indicate one lateral nerve leaving the lateral cluster of neuron somata along its dorsal margin. *bm* basal matrix (epidermis), *ep* multilayered epidermis, *int* intestine, *lmu* longitudinal trunk musculature, *lsc* lateral cluster of neuron somata, *mnp* central (median) neuropil, *pel* sheath of specialized proximal epidermal cells, *tco* trunk coelom, *vsc* ventromedian cluster of neuron somata, *vnc* ventral nerve centre

and methylene blue-stained cross-sections (1 µm, plastic embedded material) show that the ventral nerve centre consists of a central (median) neuropil (mnp; with a multitude of large- and small-diameter profiles of neurites) that is flanked by two lateral clusters of neuronal somata (lsc) and unpaired clusters of neuronal somata (vsc) at the ventral midline of the central (or median) neuropil (*Spadella cephaloptera*: Fig. 2a, b; *Sagitta hispida*: Fig. 2c, d; *Sagitta bipunctata*: Fig. 2e, f). The lateral clusters of neuron somata appear shark teeth-like in *S. cephaloptera* (Fig. 2b), whereas they look triangular or ellipsoidal in *S. hispida* and *S. bipunctata* (Fig. 2d, f). The ventral nerve centre rests on the basal matrix so that it has a basiepithelial position with respect to the multilayered epidermis (see entire Fig. 2). The anterior part of the paired main connectives, which join the cerebral ganglion and the ventral nerve centre, changes from a subepithelial into a basiepithelial position by abrupt disappearance of the basal matrix between the connective neurite bundles and the proximal epidermal layers whereas the paired caudal nerves always remain in a basiepithelial position (data not shown). The neuropil has an elongate-hexagonal form in the benthic *S. cephaloptera* (Fig. 2a, b) and a more trapezoidal or rectangular outline in pelagic sagittid chaetognaths (Fig. 2c, f). Bundles of neurites pass out radially from the dorsolateral edges of the neuropil (*arrowheads* in Fig. 2f). Over the entire length of the nerve centre, the profiles of large neurites (presumably axons) can be observed that emerge from neurons within the lateral clusters, to enter the neuropil and to transverse the neuropil core where fibres from both sides either seem to make contact or cannot be followed anymore because they take a longitudinal course, respectively (Fig. 2b, d).

The ventral nerve centres of benthic and pelagic species slightly differ in size and proportion to other tissue types in the trunk. In all three species it is slightly over 200 µm wide. In *S. cephaloptera,* it is about 75 µm high, and in both *S. hispida* and *S. bipunctata*, it is about 60 µm high. In *S. cephaloptera*, it occupies approximately one-fourth of a semithin cross-section (dorsoventral extension of the ventral nerve centre in relation to the maximum trunk diameter) whereas in *S. hispida* and *S. bipunctata*, the ventral nerve centre has a dorsoventral extension not higher than one-fifth of the maximal dorsoventral diameter of the trunk. One striking difference is the higher width and complexity of the ventral epidermis of *S. cephaloptera* compared to the other two species. While the distal (also called "outer" or "vacuolated") epidermal cells are constantly arranged in a single-layer pattern, the number of layers made up by the proximal ("inner"), tonofilament-rich epidermal cells is especially high, ranging up to 30 layers (Fig. 3a, e), thus exceeding the number of layers counted in the pelagic taxa *S. hispida* and *S. bipunctata* (compare Fig. 2b with Fig. 2d, f). In *S. cephaloptera*, the ventral nerve centre appears to be integrated into the pentagonal cross-profile of the trunk, perhaps as an adaptation to the attachment to sea grass leaves with the ventral surface of the trunk that is equipped with adhesive cells (Fig. 2a).

Ventral nerve centre ultrastructure in *Spadella cephaloptera*

General

The basiepithelial or, more precisely, the basiepidermal location of the ventral nerve centre of *S. cephaloptera* is reliably revealed by transmission electron microscopy. The dorsal margin of the central neuropil as well as of the lateral soma clusters is bordered by extracellular matrix lined by two basal laminae (Fig. 4a, h). Ultrastructural characteristics of the extracellular matrix have been described in great detail by Duvert and Salat (1990). The ventral and lateral margins of the lateral somata clusters and the neuropil are limited by specialized epidermal cells of the proximal type (Figs. 3a, e, 4g–i). The proximal epidermal cells are characterized by a broad, compact, and moderately electron-dense cytoplasmic layer that contains numerous intermediate filaments and surrounds the inconspicuous, granular cytoplasm which is poor in cytoplasmic organelles (Fig. 3a, e). The innermost proximal epidermal cells, however, seem to be transformed into layers that are much more compressed and elongated. Intermediate filaments are only concentrated at the distal margin of these cells. The packing of the intermediate filaments appears much denser, so that the layer electron optically looks darker (Figs. 3a, b, e, 4d, g, h, l). Along the contact zone between the lateral soma clusters and the neuropil the epidermal wrapping layer resembles a meshwork of strongly ramified cytoplasmic processes which also contain microtubules (Fig. 4h–i). Tangential sections through that transition zone show the presence of gaps through which neurite bundles can pass from the lateral somata clusters (Fig. 3a, 4k; see also below).

The neuropil comprises an elaborated system of neuronal processes. Along the mediosagittal plane, a majority of thin longitudinal neurites (most of them assumed to be axonal strands) can be observed. Synapses are observed in most parts of the neuropil, but are particularly abundant along or near the mediosagittal plane as well as parallel to the dorsal margin close to the basal matrix. A considerable variety of synaptic vesicles confirms the assumed diversity of neuron types (data not shown). At irregular intervals, bilateral pairs of neurite bundles emerge radially from the dorsolateral edge of the neuropil (Fig. 5l) and then turn into the intraepidermal nerve plexus or make contact to the ciliary fence organs (data not shown).

Individual neuron types

In addition to the individual identification of certain neuron types with the aid of immunohistochemical markers (see below), we were also able to distinguish some conspicuous neurons on the ultrastructural level by means of their cytoplasmic composition and structure of the nucleus, as well as size and position.

In all regions of the lateral somata clusters, we detected characteristic neurons with a large, spacious soma containing numerous small and rounded mitochondria of the tubular type, a large, polymorphous, often pierced-looking

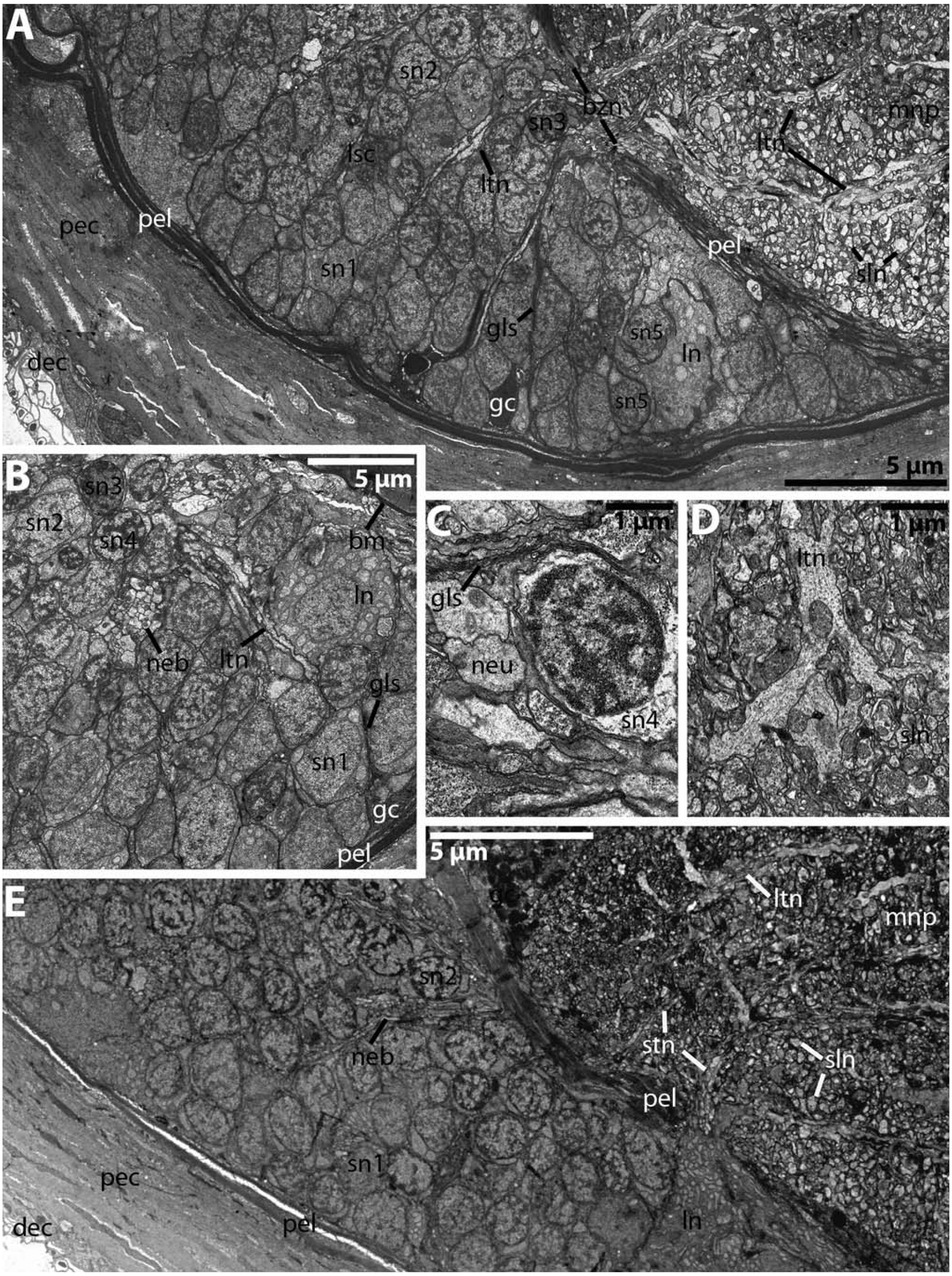
A
sn2
bzn
sn3
lsc
ltn
mnp
ltn
pec
pel
sn1
pel
sln
gls
sn5
ln
dec
gc
sn5
5 µm
B
sn3
5 µm
sn2
sn4
bm
ln
neb
ltn
gls
sn1
gc
pel
C
1 µm
gls
neu
sn4
D
1 µm
ltn
sln
5 µm
E
gc
ltn
mnp
sn2
neb
stn
sln
pel
pec
sn1
dec
pel
ln

Fig. 3 *Spadella cephaloptera*. Transmission electron microscopy; structure and neuron typology within the ventral nerve centre. **a** Cross-section of the anterior portion of the ventral nerve centre (*left half*) showing from *left* to *right* the multilayered epidermis, the lateral cluster of neuron somata (*lsc*) and the central (median) neuropil (*mnp*). **b** Higher magnified transverse view of the median region of one lateral cluster of neuron somata comprising various types of neurons. **c** Cross-profile of a type four neuron in a lateral neuron cluster (*sn4*). **d** Highly magnified transverse view of a mediolateral sector within the median neuropil displaying one large and branched fibre probably emitted from a type four neuron. **e** Cross-section of the median portion of the ventral nerve centre (*left half*). *bm* basal matrix (epidermis), *bzn* zone of neurite bundles (mostly axons) breaking through the proximalmost epidermal sheath, *dec* distal epidermal cells, *gls* glial sheath, *gc* glia-like cells, *ln* large neuron type rich in small mitochondria, *ltn* large transverse fibre profiles, *neb* bundle of neurites heading towards the breakthrough zone, *neu* neurite, *pec* proximal epidermis cells, *pel* sheath of specialized proximal epidermal cells, *sln* longitudinal fibres with small diameters, *sn1-5* various neurons of small diameters (types 1–5), *stn* bundle of small and electron lucent transverse fibres

nucleus, many Golgi stacks, opaque vacuoles, and a strongly developed rough endoplasmic reticulum (neurons labelled “ln” in Fig. 3a, b, e; see also Figs. 4b, d). These “large neurons” may stand alone or are grouped together to units of up to three cells and are mostly located close to the ventromedian margin of the somata cluster (Figs. 3a, e). They taper at their inner margin and send out long neurites, 1–3 μm in diameter. These neurites possess neurotubules and many mitochondria, their processes pierce the sheath of specialized proximal epidermal cells, and extend into the neuropil which they transverse (Figs. 3e, 4c). The size of these neurons and their unique cytoplasmic composition indicates a high metabolic activity as is the case, e.g. in neurosecretory cells or cells that have to maintain a large dendritic/axonal investment such as motorneurons or command neurons.

In the anterior and median region of the lateral somata clusters, there are other fibres of similarly large diameters, the origin of which we could not trace (*ltn* in Fig. 3a, b, d). These profiles show a high abundance of neurotubules, have a weakly osmiophilic cytoplasm and include only a few mitochondria. On their way to the neuropil core, these neurites may branch and extend towards dorsal and ventral directions (Fig. 8d). The fibres were not seen to make synaptic contacts with smaller neurites regardless of whether they run longitudinal or transversal through the neuropil.

Apart from the large neurons, several types of smaller neurons can be distinguished mainly based on differences in the structure and shape of the nucleus and of the cytoplasm. For example, the small “type four neurons” have ovoid somata, approximately 3 μm in diameter. They seem to be restricted to regions near the main breakthrough zones for neurite bundles (*sn4* in Fig. 3b, c). Their nucleus is always circular and displays a voluminous portion of extremely osmiophilic heterochromatin, well contrasting with the weakly osmiophilic euchromatin (Fig. 3c). All other unambiguously identifiable neuron types (*sn1*, *sn2*, *sn3*, *sn5*) have the same dimensions as sn4 (Fig. 3a, b, e), but are more frequent and widespread in the lateral somata clusters (e.g. Fig. 3a, b). They possess nuclei with a different eu-/heterochromatin ratio and produce much thinner neurites that fasciculate and enter the neuropil bundles. “Type one neurons” (*sn1*) are mostly concentrated along the lateral (outer) margins of the lateral somata clusters (Fig. 3a, e). Their cytoplasm is endowed with many medium-sized, elongated mitochondria (tubular type). The nucleus has a sac-like or ovoid shape; the caryoplasm displays only diffuse portions of heterochromatin. The nucleus itself barely contrasts with the surrounding cytoplasm (e.g. Fig. 4h, i, k). In contrast, “type two neurons” (*sn2*) are characterized by a moderately electron-dense cytoplasm, poorly supplied with organelles, polymorphous nuclei with only little, but well contrasted heterochromatin (Figs. 3a, b, 4e, h). This cell type is also found to be common in small aggregations of neuron somata oriented medioventrally subjacent to the neuropil and aligned in a string-of-pearls pattern when examined in sagittal sections (Fig. 4g). “Type three neurons” (*sn3*) seem to be predominant along the inner half of the lateral somata cluster. On the level of the nucleus, the moderately osmiophilic cytoplasm is quite spacious and equipped with many medium-sized, partly branched mitochondria (tubular type), smooth and rough ER cisternae, free ribosomes, and occasionally also Golgi stacks. The circular nucleus has a considerable portion of heterochromatin whereas the euchromatin portion does not contrast as clear as observed in the other neuron types described (Figs. 3a, b, 4f, h). Neurons herewith labelled as “type five neurons” (*sn5*) very much resemble those of type four (cytoplasmic composition, shape, and ultrastructural appearance of nuclei), but can be clearly differentiated from them by their location, being either in the direct vicinity of the large neurons or penetrating their somata, and being wrapped by layers with glia-like characteristics (Figs. 3a, 4d). The sheath layer of the soma is continued down to the region where the primary neurite originates (Fig. 4j). On approaching the inner border of the lateral somata zone, the small neurites of the neuron types 1–4 fasciculate into distinct bundles (see Fig. 4h, j and further description below). All neurites seem to converge at the inner midlateral region of the lateral soma clusters (Fig. 9h). At the lateral tips of the neuropil the epidermal sheath layer(s) is/are pierced and let through the joint neurite bundles. Above and below this main break-through zone there are smaller perforations of the epidermal sheath layer(s) which are traversed by smaller neurite bundles (Fig. 4k).

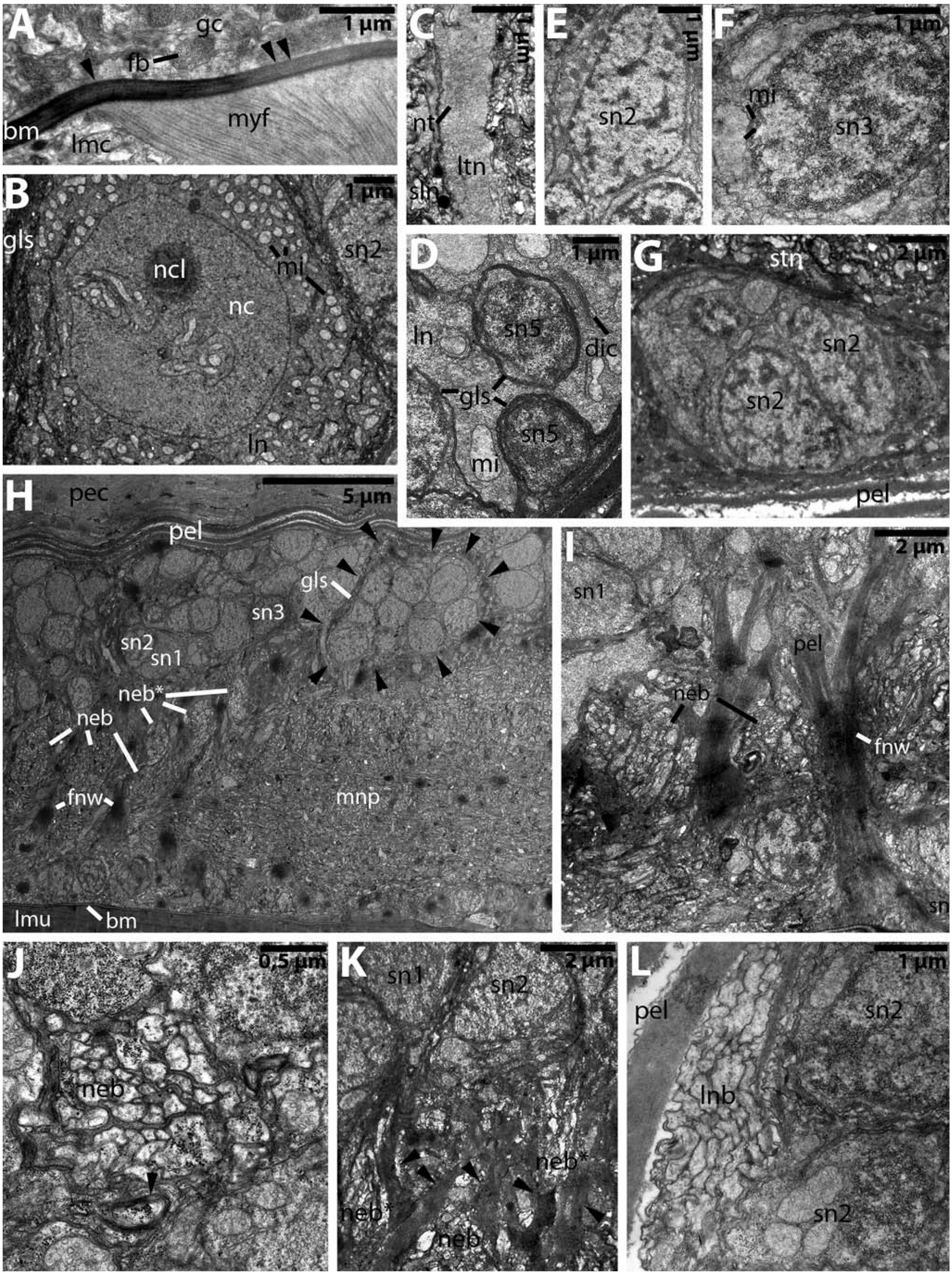
A
gc
1 µm
fb
bm
lmc
myf
B
1 µm
gls
ncl
nc
mi
sn2
ln
C
1 µm
nt
ltn
sln
D
1 µm
ln
sn5
dic
gls
sn5
mi
E
1 µm
sn2
F
1 µm
mi
sn3
G
2 µm
stn
sn2
sn2
pel
H
pec
5 µm
pel
gls
sn3
sn2
sn1
neb*
neb
fnw
mnp
lmu
bm
I
2 µm
sn1
pel
neb
fnw
sn
J
0,5 µm
neb
K
2 µm
sn1
sn2
neb*
neb*
neb
L
1 µm
pel
sn2
lnb
sn2

Fig. 4 *Spadella cephaloptera*. Transmission electron microscopy; structure and neuron typology within the ventral nerve centre. **a** Longitudinal section through the dorsal margin zone of the ventral nerve centre showing peripheral glia-like cells (*gc*) enriched with compartments of fibrillous material (*fb*) and associated with the basal matrix (*bm*). Note the inhomogeneity of the basal matrix changing from high osmiophilic, fibril-rich (*single arrowhead*) to moderate osmiophilic, lesser fibrillous (*double arrowheads*) areas. **b** Transverse portrait of the nuclear region of a large neuron (*ln*) containing a frayed-looking nucleus (*nc*) and high numbers of small rounded mitochondria (*mi*). **c** Highly magnified cross-section through a large fibre running transversally towards the centre of the central (median) neuropil. **d–g** Profiles of clearly identifiable neuron types (**d–f** cross-sections, **g** longitudinal section): **d** Strongly myelinized single type five neuron (*sn5*) running through one large neuron (*ln*), **e** type two neuron (*sn2*), **f** type three neuron (*sn3*), **g** aggregated type two neurons (*sn2*) placed medioventrally subjacent to the central (median) neuropil. **h** Slightly oblique longitudinal section through the transition zone between one lateral cluster of neuron somata and the periphery of the central (median) neuropil (*mnp*). Note the iterated arrangement of different neurite bundles (*neb, neb**) in the breakthrough area heading towards the centre and of the package-like pattern of somata within the lateral cluster (one package marked by *arrowheads*). **i** Longitudinal view of the transition zone described for H. Transverse neurite bundles (*neb*) are separated by ramified, microtubule-rich processes (*fnw*) of specialized proximal epidermal cells enveloping the entire ventral nerve centre (*pel*). **j** Section through one transverse neurite bundle running towards the sheath of specialized proximal epidermal cells (*pel*). Note the single neurite ensheathed by glial processes (*arrowhead*). **k** Longitudinal section through the breakthrough region demonstrating two different types of bundles of small neuritis. One is cut transversally and emerged from neurons oriented medially within the lateral cluster (*neb*), the other comes from neurons located more dorsally and having an electron-lucent cytoplasm (*neb**). **l** Bundle of lateral neurites (*lnb*) leaving the lateral cluster of neuron somata at its dorsolateral margin and piercing the sheath of specialized proximal epidermal cells (*pel*). *dic* Golgi stack, *gls* glial sheath, *lmc* longitudinal trunk musculature cell, *lmu* longitudinal trunk musculature, *ltn* large transverse fibre profiles, mi mitochondrion, *myf* myofilament structure, *ncl* nucleolus, *pec* proximal epidermis cells, *sln* longitudinal fibres with small diameters, *sn1-5* various neurons of small diameters (types 1-5), *stn* small and electron lucent longitudinal fibres

Glia-like cells and grouping of neurons

Cells with glial characteristics such as extremely osmiophilic cyto- and caryoplasm are often arranged around the lateral periphery of the lateral somata clusters (gc in Fig. 3a, b) and the entire neuropil (Fig. 4a). From various regions of the soma, the glia-like cells emanate thin cytoplasmic processes that extend between the interneuronal spaces and give rise to a multilayered sheath around groups of 10–20 neurons as seen in both cross- and longitudinal-sections (Fig. 4h). Within such an assembly neuronal somata, glia-like sheaths are much less clear and, if present, are composed of one single layer (Figs. 3a, b, e, 4e, h). The clearly separated packages of somata seem to be aligned in a serially repeated pattern, but this issue needs further analysis. Glia-like wrapping of single somata (Fig. 4d) or neurites (Fig. 4j) is only occasionally seen in the lateral clusters, but is considered typical for "type five neurons" (see above).

RFamide-like immunoreactivity

Previous studies in Sagitta setosa

RFamide-like immunoreactive (*RFir*) neurons have previously been reported to be present in *S. setosa* (Bone et al. 1987) and *Paraspadella gotoi* (Goto et al. 1992), yet these authors did not describe the labelling pattern in greater detail. Harzsch and Müller (2007) also studied *S. setosa* and provided a detailed analysis of RFir elements in the ventral nerve centre of this species. We will briefly summarize this labelling pattern here to serve as a basis for the comparison with *S. enflata* and *S. cephaloptera.*

In the ventral nerve centre of *S. setosa*, the cell bodies of the *RFir* neurons are located within the lateral soma zones, mostly close to the interface between the neuropil core and the soma clusters, whereas longitudinal *RFir* fibre tracts are restricted to the ganglion core (Fig. 5a; reprinted from Harzsch and Müller 2007; copyright for this figure is held by Harzsch and Müller). Three main longitudinal tracts of *RFir* fibres can be distinguished: the medial bundle (MB), the bilaterally paired intermediate bundles (IB), and the paired lateral bundles (LB; Fig. 5a) that run along the lateral borders of the neuropil core. The *RFir* neurons, all of which are unipolar, can be subdivided into two different populations: a first series of neurons with lateral somata (*L1-4*; small circles in Fig. 5a) in the anterior third of the nerve centre and a second series of slightly larger dorsal neurons (*D1-5*; large circles in Fig. 5a; and see Fig. 6a) in the posterior two-thirds of the nerve centre. The somata of these are located slightly more dorsally than those of the lateral neurons. The arrangement of the most anterior lateral neurons displayed some variation between individual specimens of *S. setosa* and in addition to the neurons *L1* and *L2* that were identified consistently in all analysed specimens; additional neurons were present in some specimens (small circles labelled with a question mark in Fig. 5a; see Harzsch and Müller 2007). Contrary to *L1* and *L2*, the neurons *L3*, *L4*, and *D1–D6* (*D6* is *D7* in the new nomenclature used in this paper as will be explained below, page [20]) were reliably present in all analysed specimens of *S. setosa* and hence represent typical examples for individually identifiable, bilaterally symmetrical arranged neurons. The neurons *D1–D5* have an identical morphology and appear to be serially repeated clones (Fig. 6a). Their neurites exit the soma in a medial direction to enter the neuropil core at a right angle to the anterior–posterior axis. The neurites of cells *D1–D5* all cross-over the lateral longitudinal bundle to join the intermediate bundle (Fig. 6a; Harzsch and Müller 2007).

Sagitta enflata

Concurrent with the much larger size of *S. enflata* compared to *S. setosa*, the ventral nerve centre in the former

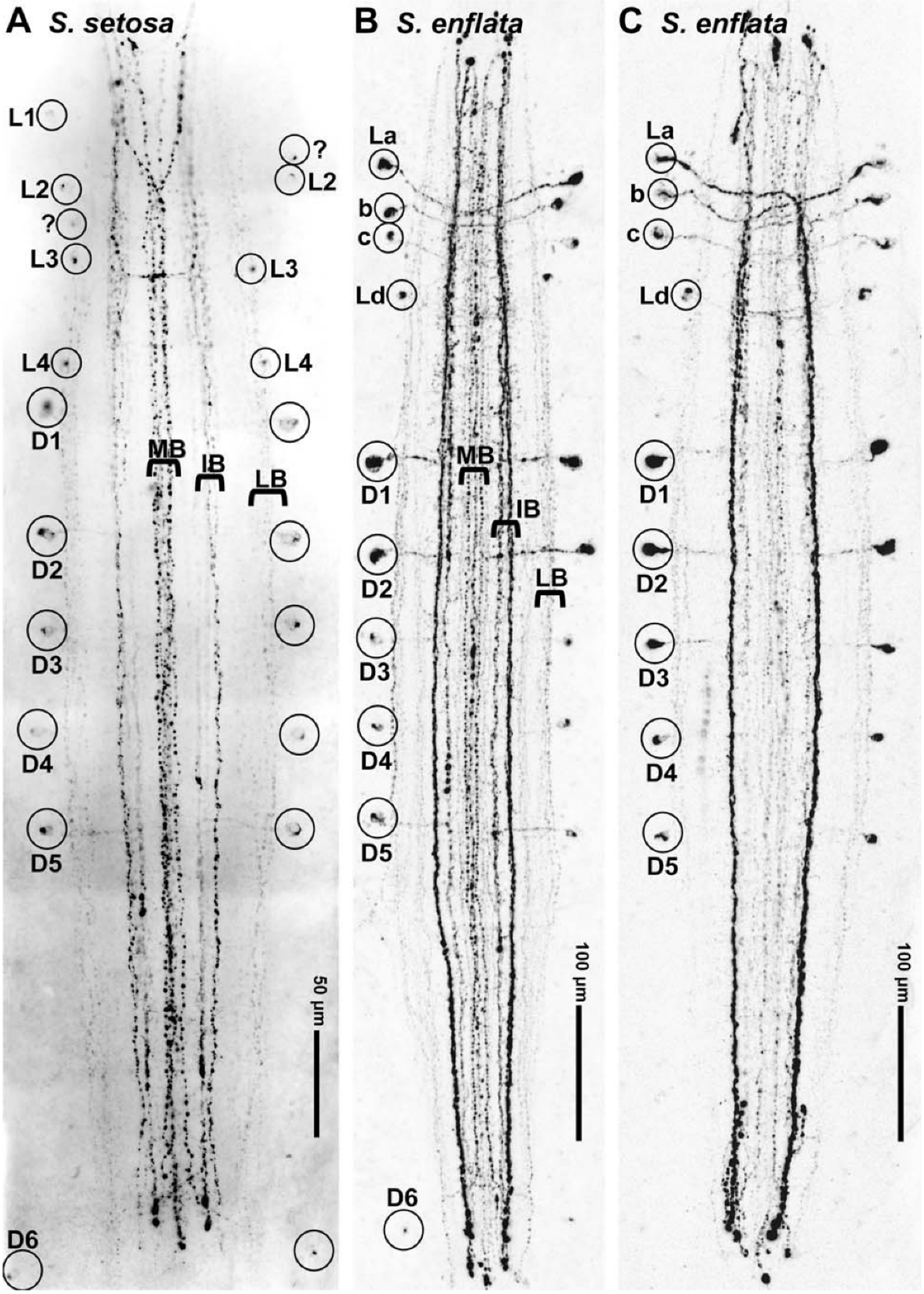
A S. setosa
L1
L2
?
L3
L4
D1
D2
D3
D4
D5
D6
?
L2
L3
L4
MB
IB
LB
50 µm
B S. enflata
La
b
c
Ld
D1
D2
D3
D4
D5
D6
MB
IB
LB
100 µm
C S. enflata
La
b
c
Ld
D1
D2
D3
D4
D5
100 µm

Fig. 5 *Sagitta setosa* (**a**) and *Sagitta enflata* (**b**, **c**). Ventral views of whole mount specimens, confocal laser-scan microscopy. Localization of RFamide-like immunoreactivity in the ventral nerve centres of different specimens. Figure 1 **a** is reprinted from Harzsch and Müller (2007: BMC Frontiers in Zoology, copyright held by S. Harzsch and C.H.G. Müller). **a** Is a photomontage of black–white inverted fluorescence micrographs, **b** and **c** are confocal laser-scan images. Individually identifiable neurons are encircled and labelled with *letters* (for details see text). Abbreviations identify the longitudinal bundles: *IB* intermediate bundle, *LB* lateral bundle, *MB* medial bundle

species is about twice as long and as broad as that of *S. setosa*. The three main longitudinal tracts of RFamide-like immunolabelled (*RFir*) fibres that are present in *S. setosa* are also apparent in *S. enflata*: the medial bundle (MB), the bilaterally paired intermediate bundles (IB), and the paired lateral bundles (LB; Figs. 5b, c, 7a, b). The medial bundle is composed of an unpaired median fibre that is to the left and right flanked by paired fibres (Fig. 7b). The intermediate longitudinal bundle is composed of an inner and an outer portion (Fig.7a) similar to the pattern in *S. setosa* (Harzsch and Müller 2007). The fibres in the more diffuse lateral bundle are weakly labelled compared to the median and intermediate bundles (Fig. 7a). Anteriorly and posteriorly, most fibres within the medial and intermediate bundles terminate in heavily labelled spherical structures and do not appear to proceed further anteriorly or posteriorly (Figs. 5b, c, 8b). Three-dimensional reconstructions of confocal image stacks using Amira software showed that all fibres within the *RFir* fibre network are arranged in roughly the same horizontal dorsoventral level. The labelling pattern of *RFir* somata was identical in all specimens that we analysed as exemplified by the two specimens shown in Figs. 5b, c, 6b, c, 8a, B, suggesting intraspecific homology of the neurons. As in *S. setosa,* two different populations of *RFir* neurons are present in the ventral nerve centre of *S. enflata*: the series of lateral neurons (*La–d*; small circles in Fig. 5b, c; and see Fig. 8a, b) in the anterior part of the nerve centre and the second series of slightly larger dorsal neurons (*D1–7*; large circles in Figs. 5b, c, 6b, c,7a, 8c). The arrangement of the four anterior lateral neurons was consistent between individual specimens of *S. enflata.* These neurons hence represent typical examples of individually identifiable, bilateral symmetrically arranged neurons (Fig. 8a, b). However, we could not determine unambiguously, which of the La–d neurons in *S. enflata* may be equivalent to the *L1–4* neurons in *S. setosa*, because in the latter species the course of the neurites of these cells could not be followed over any reasonable distance (Harzsch and Müller 2007). In *S. enflata,* the neurites of all four *L* neurons seem to cross the nerve centre contralaterally to target the intermediate bundle (Fig. 8a, b). As in *S. setosa,* the *D1–D6* neurons did reliably label in all analysed specimens

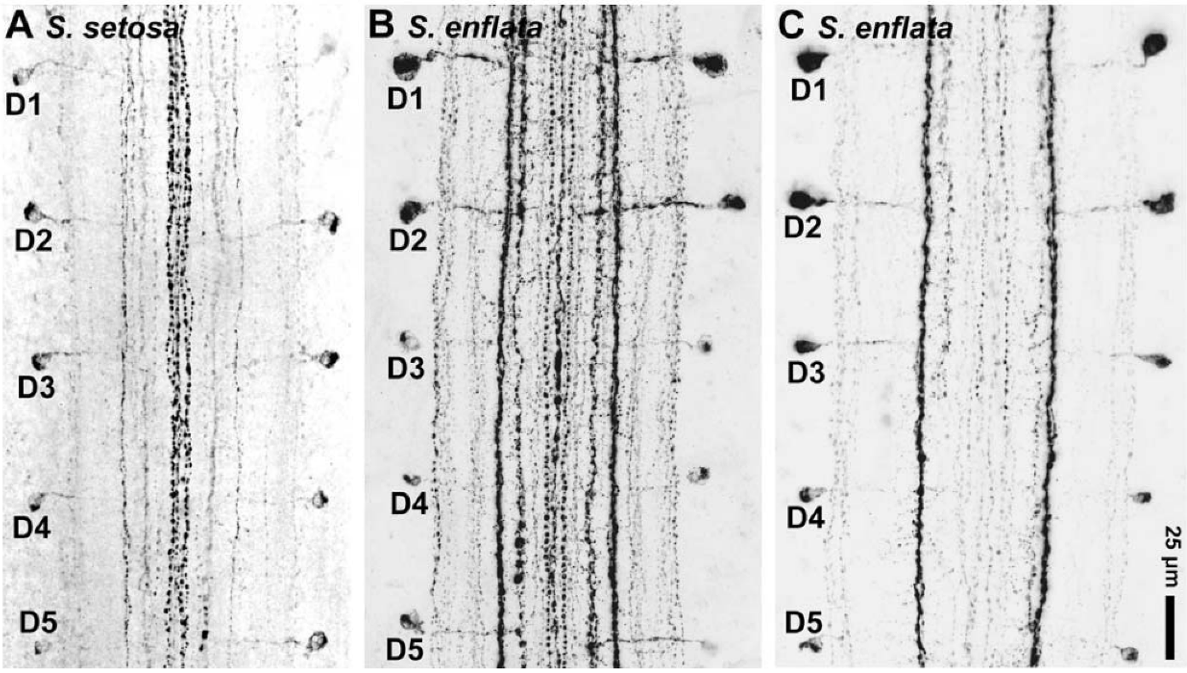

Fig. 6 *Sagitta setosa* (**a**) and *Sagitta enflata* (**b**, **c**). Ventral views of whole mount specimens, confocal laser-scan microscopy (black–white inverted images). Localization of RFamide-like immunoreactivity in the ventral nerve centres of different specimens. The individually identified *D* neurons that can be homologized between the two species are labelled with letters *D1–D5* (for details see text)

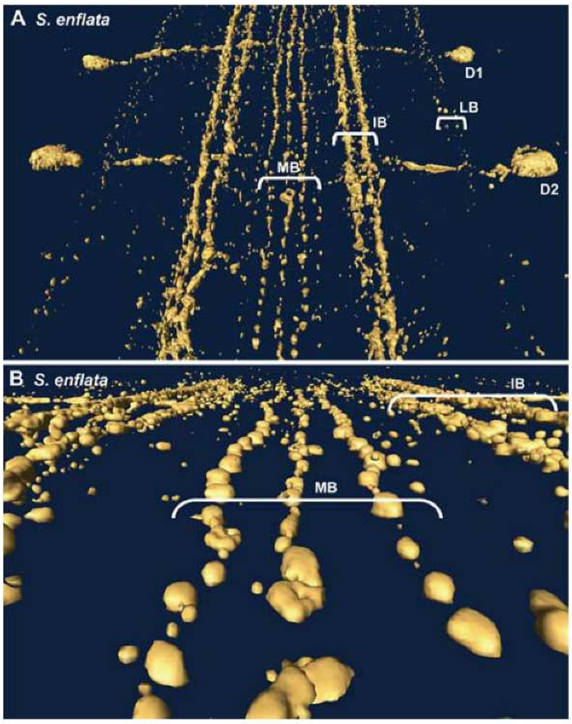

Fig. 7 *Sagitta enflata*. Computer-based 3D surface reconstruction (Amira) of RFamide-like immunoreactive material in the ventral nerve centre viewed from a posterior/ventral perspective. **a** Shows the *D1* and *D2* neurons and **b** is a higher magnification of the median fibre bundle (for details see text). Abbreviations identify the longitudinal bundles: *IB* intermediate bundle, *LB* lateral bundle, *MB* medial bundle

of *S. enflata* and have a similar morphology in both species. One exception is that in *S. enflata*, *D1* and *D2* were slightly larger than the other *D* neurons (Figs. 6b, c). Nevertheless, *D1–D5* can be homologized between the two *Sagitta* species examined here ("interspecific homology" according to the nomenclature established by Kutsch and Breidbach, 1994) because in all specimens their neurites exit the soma in a medial direction and enter the neuropil core at a right angle to cross-over the lateral longitudinal bundle (LB) and target the inner fibres of the intermediate bundle (IB; Figs. 6b, c, 7a, 8c). However, in some specimens tiny branches of *D1* and *D2* were present that appeared to proceed further medially from the contact point with the intermediate bundle (Figs. 7a, 8c). A similar observation has already been reported from *S. setosa* (Harzsch and Müller 2007: Figs. 8c, d).

Pterosagitta draco

Unfortunately, we were able to process only one specimen of *P. draco*. The labelling pattern was virtually identical to that in the two *Sagitta* species studied. These similarities includes the three main longitudinal tracts of RFamide-like immunolabelled (*RFir*) fibres, the medial bundle (MB), the bilaterally paired intermediate bundles (IB), and the paired lateral bundles (LB; Fig. 9a, b). Furthermore, the series of lateral (*L*) neurons and the second series of slightly larger dorsal neurons (*D1–7*) is also present in *P. draco* (Fig. 9a, c, d). Although the quality of the stain did not match that of both *Sagitta* species, we were nevertheless able to follow the course of primary neurites of D1–5 (Fig. 9c) and D7 (Fig. 9d). They most closely resemble those in the two *Sagitta* species.

Fig. 8 *Sagitta enflata*. Ventral views of whole mount specimens, confocal laser-scan microscopy. Details of the RFamide-like immunoreactive system in the ventral nerve centre. Images are colour coded 3D; use red–green glasses to view. **a**, **b** The series of L neurons in two different individuals. **c** Higher magnification of the *D1* and *D2* neurons. Abbreviations identify the longitudinal bundles: *IB* intermediate bundle, *LB* lateral bundle, *MB* medial bundle

Spadella cephaloptera

As in both species of *Sagitta* and in *P. draco*, three main longitudinal tracts of RFamide-like immunolabelled (*RFir*) fibres are present in *S. cephaloptera*, the medial bundle (MB), the bilaterally paired intermediate bundles (IB), and the paired lateral bundles (LB; Fig. 10; and upper inset in Fig. 1b). The fibres in the medial and intermediate bundles are more strongly labelled than the lateral bundles. As in *Sagitta* species, most fibres within all three bundles are confined to the ventral nerve centre and only few labelled fibres proceed further anteriorly into the main connectives (CO; Fig. 10b) or posteriorly into the caudal tracts (CT). Concurrent with the observations by Goto et al. (1992) on *Paraspadella gotoi*, we recorded that the *RFir* fibres that leave the ventral nerve centre posteriorly in *S. cephaloptera* form a caudal loop (CL; Figs. 1b, 10a). In some specimens, fine fibres branched off from the posterior end of the caudal loop (inset in Fig. 1a) to proceed further caudally (lower inset in Fig. 1b). These branches give rise to what appears to be a single labelled fibre that extends medially downwards to the tail of the animal where it terminates in varicose endings (lower inset in Fig. 1b). The labelling pattern of *RFir* somata was identical in all specimens that we analysed as exemplified by the two specimens shown in Figs. 10b, c suggesting, as in *Sagitta* species, intraspecific homology of the neurons. Once again, two different populations of *RFir* neurons seem to be present in the ventral nerve centre of *S. cephaloptera*, the anterior series of *L* neurons (*La–d*; small circles in Fig. 10b, c) and the second series of *D* neurons (*D1–7*; large circles in Fig. 10b, c). The distinction between the *L* and *D* series could be made because, as in *S. enflata*, the soma of *Ld* is clearly located more medially than that of

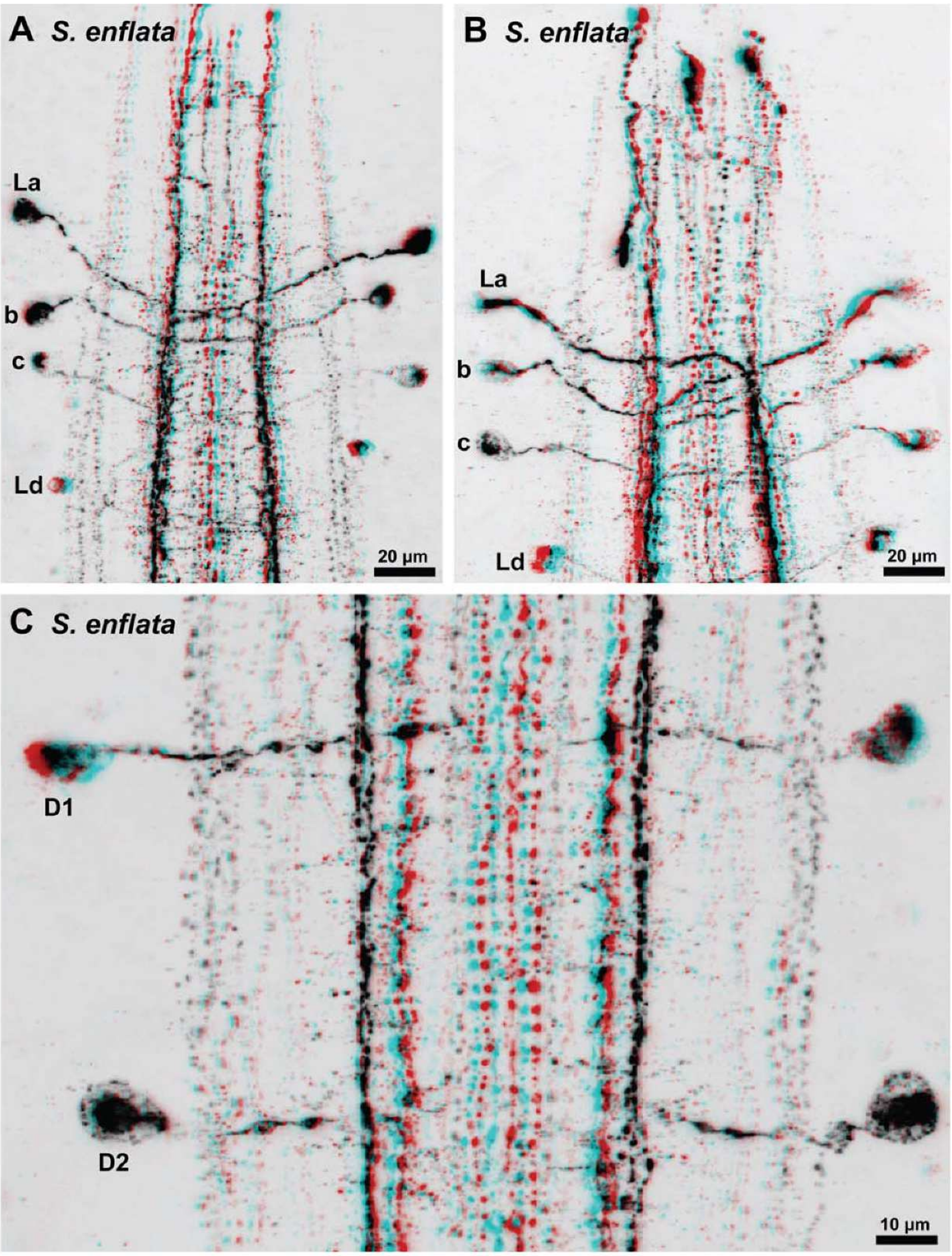
A S. enflata
La
b
c
Ld
20 µm
B S. enflata
La
b
c
Ld
20 µm
C S. enflata
D1
D2
10 µm

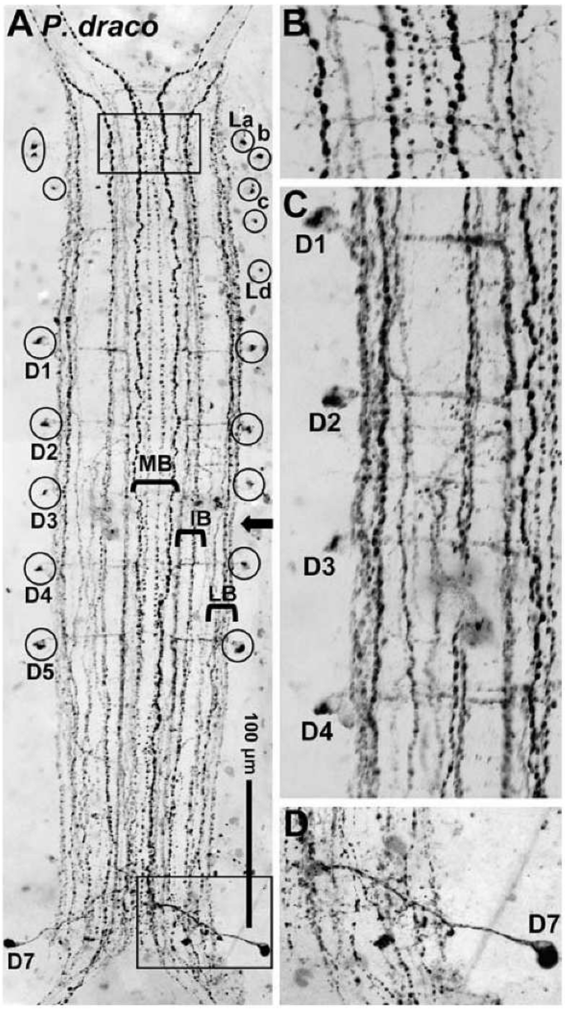

Fig. 9 *Paraspadella draco*. Ventral views of a wholemount specimen, confocal laser-scan microscopy (black–white inverted images). Localization of RFamide-like immunoreactivity in the ventral nerve centre of a single specimen. **a** Low power view; individually identifiable neurons are encircled and labelled with *letters* (for details see text). Abbreviations identify the longitudinal bundles: *IB* intermediate bundle, *LB* lateral bundle, *MB* medial bundle. **b** Higher magnification of the anterior *boxed area* in **a**. **c** Higher magnification of the series of *D* neurons (*D1–D4*). **d** Higher magnification of the *lower boxed area* in **a** to show cell *D7*

the previous *Lc* neuron and the following D1 cell (Figs. 5b, c, 10b, c). The arrangement of the *La–d* neurons was consistent between individual specimens of *S. cephaloptera* ("intraspecific homology" in the nomenclature established by Kutsch and Breidbach 1994) and their moNSrphology was very similar to that of the *L* neurons in *S. enflata,* including the contralaterally crossing neurites that target the intermediate bundle. This architecture suggests a homology of the *S. enflata* and the *S. cephaloptera L* neurons. Contrary to representatives of the genera *Sagitta* and *Pterosagitta,* the series of *D* neurons comprised seven and not only six cells as in *S. cephaloptera*. In addition, a conspicuous giant neuron, termed the *X* neuron, was present between the *D6* and *D7* cells (Fig. 10b, c). In some specimens, additional unidentified neurons were labelled (arrows in Fig. 10b). The course of the fibres that the *D* neurons extend could only be analysed for *D5–D7* and *X*. Their neurites exit the somata in a medial direction to cross-over the lateral and intermediate bundles. We could not determine if the neurites then cross-over to the contralateral side or if they target the medial fibre bundle (Fig. 10b, c).

Discussion

Ultrastructure of the ventral nerve centre: evidence for serially arranged elements?

Our electron microscopical observations in *Spadella cephaloptera* add new insights into the fine structural organization of a chaetognath ventral nerve centre. In addition to those studies addressing the general anatomy of the chaetognath nervous system (e.g. Hertwig 1880; Grassi 1883; von Ritter-Zahony 1908; Burfield 1927; John 1933; Kuhl 1938; Hyman 1959) a considerable amount of work has been dedicated to understanding the fine structural architecture of the brain including the retrocerebral organ (Scharrer 1965; Rehkämper and Welsch 1985; Goto and Yoshida 1987; Bone and Goto 1991; Shinn 1997), of the cephalic or trunk sense organs connected to the central nervous system (eyes: e.g. Eakin and Westfall 1964; Ducret 1975; Goto et al. 1984, 1989; Goto and Yoshida 1985; ciliary fence organs: e.g. Welsch and Storch 1983; Malakhov et al. 2005; corona ciliata: e.g. Giulianini et al. 1999; Malakhov et al. 2005; solitary head sensilla: Bone and Pulsford 1978, 1984), of the intraepidermal nerve plexus (Ahnelt 1980, 1984), and of the neuromuscular junctions in visceral and skeletal musculature (Duvert and Barets 1983). However, the majority of these contributions are based on the examination of pelagic chaetognaths with most of them dedicated to species of the genus *Sagitta*. When not considering those papers dealing with the cephalic nervous system and herewith associated sense organs, there remain few studies comprehensively dealing with the ventral nerve centre fine structure. Only the works of Ahnelt (1980: Fig. 159), Bone and Pulsford (1984: Figs. 25, 26, 27, 28, 29), Goto and Yoshida (1987: Fig. 17a–c), and Bone and Goto (1991: Fig. 3.9) provided some TEM images showing components of the ventral nerve centre of five species of *Sagitta*, which are useful for a comparison with our data. The fine structure of the ventral nerve centre in benthic Chaetognatha are even less well documented. Only Ahnelt (1980) published a

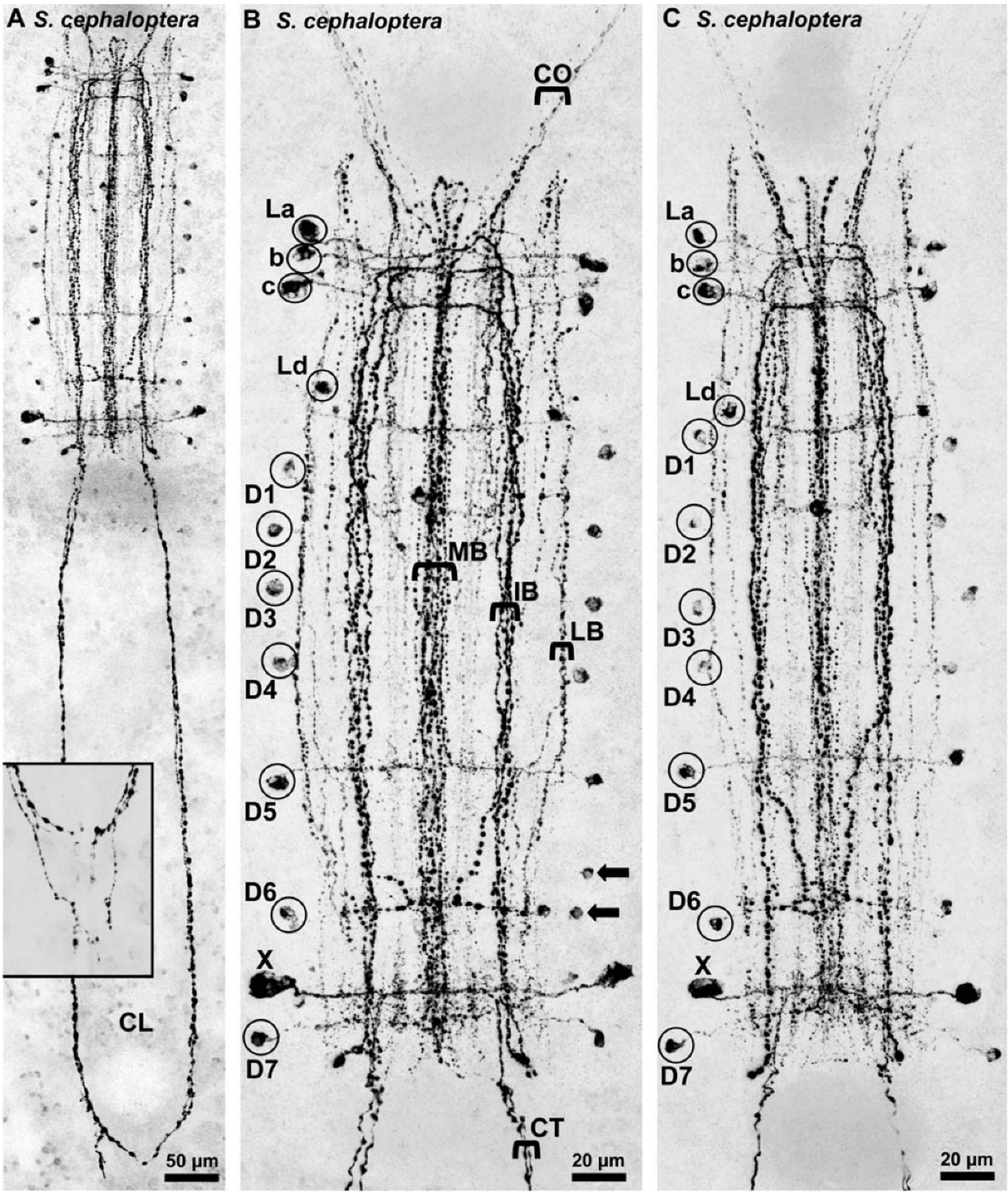
A S. cephaloptera
CL
50 µm
B S. cephaloptera
CO
La
b
c
Ld
D1
D2
D3
D4
D5
D6
X
D7
MB
IB
LB
CT
20 µm
C S. cephaloptera
La
b
c
Ld
D1
D2
D3
D4
D5
D6
X
D7
20 µm

Fig. 10 *Spadella cephaloptera*. Ventral views of whole mount specimens, confocal laser-scan microscopy (black–white inverted images). Localization of RFamide-like immunoreactivity in the ventral nerve centre. The inset in **a** shows the posterior part of the caudal loop in a different specimen to show the fibre branches that come off the posterior part of the caudal loop. **b** Higher magnification of the specimen shown in **a**. **c** Shows a second specimen to illustrate that the labelling pattern is almost identical between different specimens. Individually identifiable neurons are encircled and labelled with *letters* (for details see text). *Arrows* in **b** label additional unidentified neurons. *CL* caudal loop, *CO* main connective, *CT* caudal tract, *IB* intermediate bundle, *LB* lateral bundle, *MB* medial bundle

transverse section through the dorsolateral periphery of the ventral nerve centre of *S. cephaloptera* showing the transition zone between one lateral somata cluster and the neuropil core. This author (Ahnelt 1984) already noted the intense coating of the ventral nervous centre with functionally transformed proximal epidermal cells in *S. cephaloptera*. Our report of the epidermal sheath confirms his observations and also adds more details on the serially fenestrated complex of proximal epidermal cells that extends between the lateral somata clusters and the central (median) neuropil.

Bone and Pulsford (1984) mentioned the presence of "two pairs of large neuron somata" (p. 218) in the ventral nerve centre of *Sagitta* spp. but did not provide a more detailed description of these neurons. We suggest that these large neurons at the ventromedian margin of the lateral somata clusters in the ventral nerve centres of *S. setosa* (see Harzsch and Müller 2007, Fig. 6c, d) and *S. cephaloptera* (this study, e.g. Fig. 9b) may be comparable. However, any comparison of neuron types based on fine structural features between different taxa should be conducted with care, because different physiological conditions may be "frozen" in certain neurons at the time of fixation, even though they might belong to the same type. A comprehensive comparative fine structural study of the ventral nerve centres of a variety of pelagic and benthic chaetognath taxa may reveal new or support already presumed neuronal identities.

The glial packing of ventral nerve centre neurons depicted here in *S. cephaloptera* appears to reflect a common principle of a functional assembly of neurons in the nervous system of chaetognaths. Described for the ventral nerve centre of *S. crassa* (Bone and Pulsford 1984), the grouping of somata has also been documented to occur in the cerebral ganglion (*S. setosa*: Rehkämper and Welsch 1985: Fig. 3b; *S. hexaptera*: Goto and Yoshida 1987: Fig. 6a) and the vestibular ganglia (*S. hexaptera*: Goto and Yoshida 1987: Fig. 11a). Future studies with immunohistochemical markers in combination with TEM and neuronal tract tracing methods may shed light on the questions whether the neurons in those packages are morphologically similar, share corresponding projection patterns and may also be functionally related.

In addition to the individually identified RFamidergic neurons, e.g. of the D series that will be discussed below, there is more evidence for serialities in the ventral nerve centre. Harzsch and Müller (2007), using an immunohistochemical marker for synaptic proteins reported an array of microcompartments in the neuropil of the ventral nerve centre of *S. setosa*. Also in *S. setosa*, Bone and Pulsford (1984) mentioned "constant arrangements" of large transverse fibres, paired large somata, and ciliary fence organs along the body surface as being serially arranged and in reproducibly identifiable positions. Bone and Pulsford (1984) furthermore assumed that constant patterns might also be expected for all other, "smaller neurons." We tentatively suggest the repeated arrangement of packages of neurons and the iterated passages of neurite bundles through gaps in the proximal epidermal layer as additional structures with a serial arrangement in the chaetognathan ground pattern.

Interspecific identification of individual neurons in Chaetognatha: a new character to explore chaetognath intraphyletic relationships?

The presence of individually identified RFamide-like immunoreactive (*RFir*) neurons that can be recognized from animal to animal of one species previously has been reported for *S. setosa* (Bone et al. 1987; Harzsch and Müller 2007). More specifically, these are the series of L and D neurons and these neurons, according to the terminology suggested by Kutsch and Breidbach (1994), can be designated as displaying intraspecific homology. In the present report, we provide examples for individually identifiably neurons with intraspecific homology for three more chaetognath species, *Sagitta enflata, Pterosagitta draco*, and *S. cephaloptera*, so that, together with the data on *Paraspadella gotoi* by Goto et al. (1992) it seems likely that the potential to generate neurons with individual identities is part of the ground pattern of Chaetognatha. More importantly, our study for the first time provides evidence that specific neurons can be homologized between different species of Chaetognatha ("interspecific homology" according to Kutsch and Breidbach 1994). Based on a biochemical criterion, the common expression of RFamide-related neuropeptides, and based on morphological criteria such as the position of the neuronal somata in relation to the architectural framework of the ventral nerve centre as well as the course of their neurites we suggest that the neurons *D1–D5* and *D7* can be homologized between all the species studied here. The correspondence of the *L* neurons in these taxa is not so clear, because their axonal morphology is poorly resolved in *S. setosa* (Harzsch and Müller 2007). However, there is a striking similarity between the *L* neurons of *S. enflata* and *S. cephaloptera* suggesting that these neurons can be homologized even between the members of two different chaetognath genera. Yet, the course of the neurites of the *D* neurons is slightly different between the representatives of *Sagitta* and *Spadella*: whereas in *S. cephaloptera* the *D* neurites course medially as far as the medial longitudinal fibre bundle, in the two *Sagitta* species studied these neurites target the intermediate bundle and only in some cases small branches extend more medially towards the medial bundle. In addition, our immunolocalizations provide evidence for the presence of more *RFir* neurons in *Spadella* than in *Sagitta*.

This finding extends a previous report by Goto et al. (1992) on representatives of the genus *Paraspadella*. Although the authors did not describe the course of the neurites in great detail, they identified two pairs of *RFir* neurons in the posterior part of the ventral nerve centre named "posterior somata." Considering their position in the ventral nerve centre, it is likely that these somata correspond to the *D6* and *X* neurons found in the present study which implies that these neurons can be recognized as two apomorphies of the Spadellidae. In *Paraspadella gotoi*, Goto et al. (1992: Fig. 1f) described a single *RFir* bipolar neuron located outside of the ventral nerve centre close to the tail. This neuron extends a posterior neurite that branches in the tail region as well as an anteriorly directed neurite that connects to the caudal loop. Although *S. cephaloptera* has a similarly unpaired fibre that innervates the tail region we did not trace a neuronal cell soma associated with this fibre but assume that it originates in the caudal loop in this species.

Conclusion

In Arthropoda, the morphology of individually identified serotonin-immunoreactive neurons in the ventral nerve cord has been used to contribute new characters to the discussion on arthropod phylogeny (review Harzsch et al. 2005; Harzsch 2006). In species of the Insecta, there are many examples for identified neurons the architecture of which is surprisingly similar across all taxa that have been examined, e.g. a serotonergic olfactory interneuron that innervates the antennal lobe (see review by Schachtner et al. 2005) or dorsal unpaired octopaminergic neurons in the ventral nerve cord (see review by Pflüger and Stevenson 2005). Along these lines, our current report raises the possibility that analysing the morphology of individual neurons in additional chaetognath species may also contribute useful characters for reconstructing chaetognath phylogeny. That way, it may for example be possible to gain new insights into the disputed phylogenetic relationship of *Pterosagitta draco* (Papillon et al. 2006), in which the pattern of RFamidergic neurons shows conspicuous similarities to *Sagitta* spp. rather than to *Spadella* spp. However, for such an effort a much broader taxon sampling will be needed. More specifically, bentho-planktonic representatives such as the presumably basally branching taxon Heterokrohniidae (Papillon et al. 2006) need to be studied for a broad coverage of Chaetognatha. With such an expanded data set it may also be possible to discuss, e.g. the evolutionary relationship between the *D* neuron architecture in *Sagitta* versus *Spadella*. The *Spadella D* neurons could for example be derived from the *Sagitta D* neurons by a medial extension of the main neurite. Alternatively, the *Sagitta D* neurons could have originated from the *Spadella* type by a restriction of the primary neurite.

However, more data will be necessary to decide what the primary architecture may be here. Another intriguing observation is that in *Spadella* species, the morphology of the *L* and *D* neurons is more similar to each other than in *Sagitta* species. One possible explanation may be that initially, Chaetognatha had a series of serially iterated neurons with an identical morphology which during subsequent evolution differentiated into morphologically distinct subsets. Once again, the ancestral architecture of the arrow worm nervous system will be reconstructed when a broader taxon sampling will be available.

The species studied in the present report belong to the Aphragmophora (Sagittidae) and Phragmophora (Spadellidae), which constitute the two main taxonomic groups of the Chaetognatha. These two taxa were characterized by Tokioka (1965) based on the presence (Phragmophora) and absence (Aphragmophora) of transverse muscles (phragms). A recent molecular analysis of the intraphyletic relationships has revealed the variability of this character (homoplasy) and highlighted the influence of the life style on chaetognath morphology, particularly for benthic species that adapt to a planktonic lifestyle (Papillon et al. 2006). The functional significance of RFamide peptides in metazoans is an intense field of research and one of the emerging themes is the remarkable conservation in control of feeding (Dockray 2004) and mating (Kriegsfeld 2006) behaviours both in Protostomia and Deuterostomia as well as in cnidarians (Pernet et al. 2004). A thorough interspecific comparative analysis of *RFir* neurons is likely to provide more insights into how the variations in the organization of the muscular and nervous systems in Chaetognatha correlate with their diverging life styles as well as their feeding and mating behaviours.

Acknowledgments We would like to thank the team of the "Gastforschung" at the Biologische Anstalt Helgoland for assistance in collecting *Sagitta setosa*. Planktonic samples collected in the Indian Ocean were kindly provided by Gisèle Champalbert and Marc Pagano from the Institut pour la Recherche et le Développement (IRD UR 167 SyRoCo). We gratefully acknowledge the assistance by Prof. Dr Ludwig Jonas and his technician team from the Electron Microscopic Centre of the University of Rostock, by Dr Walter Richter and colleagues of the Electron Microscopic Centre of the Friedrich-Schiller-University Jena, and by Christa Ladwig from the Electron Microscopic Unit of the University Hospital Essen. Our special thanks go to Dr George Shinn for providing fixed specimens of *S. hispida*. This study was supported by grant HA 2540/7-1 in the DFG focus programme „Metazoan Deep Phylogeny" and by the Max Planck Society.

Open Access This article is distributed under the terms of the Creative Commons Attribution Noncommercial License which permits any noncommercial use, distribution, and reproduction in any medium, provided the original author(s) and source are credited.

References

Ahnelt P (1980) Das Coelom der Chaetognathen. Thesis, University of Vienna, 209 pp + 178 figs

Ahnelt P (1984) Chaetognatha, chapter 40. In: Bereiter-Hahn J, Matoltsy AG, Richards KS (eds) Biology of the integument. vol 1. Invertebrates. Springer, New York, pp 746–755

Arnaud J, Brunet M, Mazza J (1978) Studies on the midgut of *Centropages typicus* (Copepoda, Calanoida). I. Structural and ultrastructural data. Cell Tissue Res 187:333–353. doi:10.1007/BF00224375

Bone Q, Goto T (1991) The nervous system. In: Bone Q, Kapp H, Pierrot-Bults AC (eds) The biology of Chaetognaths. Oxford University Press, Oxford, pp 18–31

Bone Q, Pulsford A (1978) The arrangement of ciliated sensory cells in *Spadella* (Chaetognatha). J Mar Biol Assoc UK 58:565–570

Bone Q, Pulsford A (1984) The sense organs and ventral ganglion of *Sagitta* (Chaetognatha). Acta Zool Stockh 65:209–220

Bone Q, Grimmelikhuijzen CLP, Pulsford A, Ryan KP (1987) Possible transmitter functions of acetylcholine an an RFamide-like substance in *Sagitta* (Chaetognatha). Proc R Soc Lond B Biol Sci 230:1–14

Brodfuehrer PD, Thorogood MSE (2001) Identified neurons and leech swimming behavior. Prog Neurobiol 63:371–381. doi:10.1016/S0301-0082(00)00048-4

Burfield ST (1927) *Sagitta*. LMBC Proc Trans Liverp Biol Soc 41:1–104

Burrows M (1996) The neurobiology of an insect brain. Oxford University Press, Oxford, pp 1–704

Choi JC, Choi Y, Hur KD, Kim CH, Shaw C, Maule AG et al (1996) Platyhelminth FMRFamide-related peptides. Int J Parasitol 26:335–345. doi:10.1016/0020-7519(96)00012-4

Dockray GJ (2004) The expanding family of -RFamide peptides and their effects on feeding behaviour. Exp Physiol 89:229–235. doi:10.1113/expphysiol.2004.027169

Ducret F (1975) Structure et ultrastructure de l'oeil chez les chaetognathes (gères *Sagitta* et *Eukrohnia*). Cah Biol Mar 16:287–300

Dunn CW, Hejnol A, Matus DQ et al (2008) Broad phylogenomic sampling improves resolution of the animal tree of life. Nature 452(7188):745–749. doi:10.1038/nature06614

Duvert M, Barets AL (1983) Ultrastructural studies of neuromuscular junctions in visceral and skeletal muscles of the chaetognath *Sagitta setosa*. Cell Tissue Res 233:657–669. doi:10.1007/BF00212233

Duvert M, Salat C (1990) Ultrastructural and cytochemical studies on the connective tissue of chaetognaths. Tissue Cell 22:865–878. doi:10.1016/0040-8166(90)90049-F

Duvert M, Savineau JP (1986) Ultrastructural and physiological studies of the contraction of the trunk musculature of *Sagitta setosa* (chaetognath). Tissue Cell 18:937–952. doi:10.1016/0040-8166(86)90048-0

Duvert M, Gros D, Salat C (1980) Ultrastructural studies of the junctional complex in the musculature of the arrow-worm (*Sagitta setosa*) (Chaetognatha). Tissue Cell 12:1–11. doi:10.1016/0040-8166(80)90048-8

Eakin RM, Westfall JA (1964) Fine structure of the eye of a chaetognath. J Cell Biol 21:115–132. doi:10.1083/jcb.21.1.115

Fairweather I, Halton DW (1991) Neuropeptides in plathyelminths. Parasitology 102(Suppl):77–92

Friedrich S, Wanninger A, Brückner M, Haszprunar G (2002) Neurogenesis in the mossy chiton, *Mopalia muscosa* (Gould) (Polyplacophora): evidence against molluscan metamerism. J Morphol 253:109–117. doi:10.1002/jmor.10010

Gaus G, Doble KE, Price DA, Greenberg MJ, Lee TD, Battelle BA (1993) The sequences of five neuropeptides isolated from Limulus using antisera to FMRFamide. Biol Bull 184:322–329. doi:10.2307/1542450

Gilchrist LS, Klukas KA, Jellies J, Rapus J, Eckert M, Mesce KA (1995) Distribution and developmental expression of octopamine-immunoreactive neurons in the central nervous system of the leech. J Comp Neurol 353:451–461. doi:10.1002/cne.903530312

Giulianini PG, Ghirardelli E, Ferrero EA (1999) Ultrastruttura comparativa della corona ciliate in *Spadella cephaloptera* e *Sagitta setosa* (Chaetognatha). Biol Mar Medit 6:666–669

Goto T, Yoshida M (1985) Photoreception in Chaetognatha. In: Ali MA (ed) Photoreception and vision in invertebrates. Plenum Publishing Corporation, New York, pp 727–742

Goto T, Yoshida M (1987) Nervous system in Chaetognatha. In: Ali MA (ed) Nervous systems in invertebrates. Plenum Publishing Corporation, New York, pp 461–481

Goto T, Takasu N, Yoshida M (1984) A unique photoreceptive structure in the arrowworms *Sagitta crassa* and *Spadella schizoptera* (Chaetognatha). Cell Tissue Res 235:471–478. doi:10.1007/BF00226941

Goto T, Terazaki M, Yoshida M (1989) Comparative motphology of the eyes of *Sagitta* (Chaetognatha) in relation to depth of habitat. Exp Biol 48:95–105

Goto T, Katayama-Kumoi Y, Tohyama M, Yoshida M (1992) Distribution and development of the serotonin-and RFamide-like immunoreactive neurons in the arrowworm, *Paraspadella gotoi* (Chaetognatha). Cell Tissue Res 267:215–222. doi:10.1007/BF00302958

Grassi E (1883) I Chetognathi. Fauna Flora Neapels 5:1–126

Greenberg MJ, Price DA (1992) Relationships among the FMRFamide-like peptides. Prog Brain Res 92:25–37. doi:10.1016/S0079-6123(08)61162-0

Grimmelikhuijzen CJP (1985) Antisera to the sequence Arg-Phe-amide visualize neuronal centralization in hydroid polyps. Cell Tissue Res 241:171–182. doi:10.1007/BF00214639

Grimmelikhuijzen CJP, Spencer AN (1984) FMRFamide immunoreactivity in the nervous system of the medusa *Polyorchis penicillatus*. J Comp Neurol 230:361–371. doi:10.1002/cne.902300305

Grimmelikhuijzen CJP, Cartensen K, Darmer D, Moosler A, Nothacker HP, Reinscheid RK et al (1992) Coelenterate neuropeptides: structure, action and biosynthesis. Am Zool 32:1–12

Groome JR (1993) Distribution and partial characterization of FMRFamide-like peptides in the horseshoe crab, *Limulus polyphemus*. Comp Biochem Physiol 104C:79–85

Halton DW, Gustafsson MKS (1996) Functional morphology of the plathyhelminth nervous system. Parasitology 113:47–72

Harzsch S (2006) Neurophylogeny: architecture of the nervous system and a fresh view on arthropod phylogeny. Integr Comp Biol 46:162–194. doi:10.1093/icb/icj011

Harzsch S, Müller CHG (2007) A new look at the ventral nerve centre of *Sagitta*: implications for the phylogenetic position of Chaetognatha (arrow worms) and the evolution of the bilaterian nervous system. Front Zool 4:14. doi:10.1186/1742-9994-4-14

Harzsch S, Müller CHG, Wolf H (2005) From variable to constant cell numbers: cellular characteristics of the arthropod nervous system argue against a sister-group relationship of Chelicerata and "Myriapoda" but favour the Mandibulata concept. Dev Genes Evol 215:53–68. doi:10.1007/s00427-004-0451-z

Hertwig O (1880) Die Chaetognathen. Mon Jena Z Med Naturw 14:196–311

Homberg U (1994) Distribution of neurotransmitters in the insect brain. Prog Zool 40:1–88

Huang Y, Jellies J, Johansen KM, Johansen J (1998) Development and pathway formation of peripheral neurons during leech embryogenesis. J Comp Neurol 397:394–402. doi:10.1002/(SICI)1096-9861(19980803)397:3<394::AID-CNE6>3.0.CO;2-Y

Hyman LH (1959) Chaetognatha. In: Hyman LH (ed) The invertebrates. Smaller coelomate groups, vol 5. McGraw-Hill, New York, pp 1–71

Imai JH, Meinertzhagen IA (2007) Neurons of the ascidean larval nervous system in *Ciona intestinalis*: I. Central nervous system. J Comp Neurol 501:316–334. doi:10.1002/cne.21246

John CC (1933) Habits, structure and development of *Spadella cephaloptera*. Q J Microsc Sci 75:625–696

Kapp H (2007) Chaetognatha, Pfeilwürmer. In: Westheide W, Rieger R (eds) Spezielle Zoologie Teil 1. Gustav Fischer Verlag, Stuttgart, pp 898–904

Karnovsky MJ (1965) A formaldehyde-glutaraldehyde fixative of high osmolality for use in electron microscopy. J Cell Biol 27:137–138

Keller R (1992) Crustacean neuropeptides: structures, functions and comparative aspects. Experientia 48:439–448. doi:10.1007/BF01928162

Kriegsfeld LJ (2006) Driving reproduction: RFamide peptides behind the wheel. Horm Behav 50:655–666. doi:10.1016/j.yhbeh.2006.06.004

Kuhl W (1938) Chaetognatha. In: Bronn HG (ed) Klassen und Ordnungen des Tierreichs. Band 4, Vermes Abteilung 4, Buch 2, Teil 1. Akademische Verlagsgesellschaft Goest & Portig KG, Leipzig, pp 1–226

Kutsch W, Breidbach O (1994) Homologous structures in the nervous system of Arthropoda. Adv Insect Physiol 24:1–113. doi:10.1016/S0065-2806(08)60082-X

Malakhov VV, Berezinskaya TL, Solovyev KA (2005) Fine structure of sensory organs in chaetognaths: ciliary fence receptors, ciliary tuft receptors and ciliary loop. Invert Zool 2:67–77 (in Russian)

Marlétaz F, Gilles A, Caubit X, Perez Y, Dossat C, Samain S et al (2008) Chaetognath transcriptome reveals ancestral and unique features among bilaterians. Genome Biol 9(6):R94. doi:10.1186/gb-2008-9-6-r94

Meinertzhagen IA (2004) Eutely, cell lineage, and fate within the ascidian larval nervous system: determinacy or to be determined? Can J Zool 83:1–12

Meinertzhagen IA, Lemaire P, Okamura Y (2004) The neurobiology of the ascidian tadpole larva: recent developments in an ancient chordate. Annu Rev Neurosci 27:453–485. doi:10.1146/annurev.neuro.27.070203.144255

Müller MCM (2006) Polychaete nervous systems: ground pattern and variations—cLS microscopy and the importance of novel characteristics in phylogenetic analysis. Integr Comp Biol 46:125–133. doi:10.1093/icb/icj017

Müller MCM, Sterrer W (2004) Musculature and nervous system of *Gnathostomula peregrina* (Gnathostomulida) shown by phalloidin labeling, immunohistochemistry, and cLSM, and their phylogenetic significance. Zoomorphology 123:169–177

Muneoka Y, Kobayashi M (1992) Comparatative aspects of structure and action of molluscan neuropeptides. Experientia 48:448–456. doi:10.1007/BF01928163

Nässel DR (1993) Neuropeptides in the insect brain: a review. Cell Tissue Res 273:1–29. doi:10.1007/BF00304608

Nässel DR, Homberg U (2006) Neuropeptides in interneurons of the insect brain. Cell Tissue Res 326:1–24. doi:10.1007/s00441-006-0210-8

Nielsen C (2001) Animal evolution. Oxford University Press, Oxford

Orrhage L, Müller MCM (2005) Morphology of the nervous system of Polychaeta (Annelida). Hydrobiologia 535(526):79–111

Papillon D, Perez Y, Caubit X, Le Parco Y (2006) Systematics of Chaetognatha under the light of molecular data, using duplicated ribosomal 18S DNA sequences. Mol Phylogenet Evol 38:621–634. doi:10.1016/j.ympev.2005.12.004

Pernet V, Anctil M, Grimmelikhuijzen CJ (2004) Antho-RFamide-containing neurons in the primitive nervous system of the anthozoan *Renilla koellikeri*. J Comp Neurol 472:208–220. doi:10.1002/cne.20108

Pflüger J, Stevenson PA (2005) Evolutionary aspects of octopaminergic systems with emphasis on arthropods. Arthropod Struct Dev 34:379–396. doi:10.1016/j.asd.2005.04.004

Price DA, Greenberg MJ (1989) The hunting of the FaRPs: the distribution of FMRFamide-related peptides. Biol Bull 177:198–205. doi:10.2307/1541933

Rehkämper G, Welsch U (1985) On the fine structure of the cerebral ganglion of *Sagitta* (Chaetognatha). Zoomorphology 105:83–89. doi:10.1007/BF00312142

Reuter M, Halton DW (2001) Comparative neurobiology of Plathelminthes. In: Littlewood DTJ, Bray RA (eds) Interrelationships of Plathyelminthes. Taylor & Francis, London, pp 239–249

Reuter M, Mäntylä K, Gustafsson KS (1998) Organization of the orthogon—main and minor nerve cords. Hydrobiologia 383:175–182. doi:10.1023/A:1003478030220

Schachtner J, Schmidt M, Homberg U (2005) Organization and evolutionary trends of primary olfactory brain centers in Tetraconata (Crustacea+Hexapoda). Arthropod Struct Dev 34:257–299. doi:10.1016/j.asd.2005.04.003

Scharrer E (1965) The fine structure of the retrocerebral organ of *Sagitta* (Chaetognatha). Life Sci 4:923–926. doi:10.1016/0024-3205(65)90191-8

Shinn GL (1997) Chaetognatha. In: Harrison FW, Ruppert EE (eds) Microscopic anatomy of invertebrates, vol 15: Hemichordata, Chaetognatha, and the invertebrate chordates. Wiley-Liss Inc, New York, pp 103–220

Soviknes AM, Chourrout D, Glover JC (2007) Development of the caudal nerve cord, motoneurons, and muscle innervation in the appendicularian urochordate *Oikopleura dioica*. J Comp Neurol 503:224–242. doi:10.1002/cne.21376

Stach T (2005) Comparison of the serotonergic nervous system among Tunicata: implications for its evolution within Chordata. Org Divers Evol 5:15–24. doi:10.1016/j.ode.2004.05.004

Stuart DK, Blair SS, Weisblat DA (1987) Cell lineage, cell death, and the developmental origin of identified serotonin- and dopamine-containing neurons of the leech. J Neurosci 7:1107–1122

Tokioka T (1965) The taxonomical outline of chaetognaths. Publ Seto Mar Biol Lab 12:335–357

Vannier J, Steiner M, Renvoise E, Hu S-X, Casanova J-P (2007) Early Cambrian origin of modern food webs: evidence from predator arrow worms. Proc R Soc Lond B Biol Sci 274:627–633. doi:10.1098/rspb.2006.3761

von Ritter-Zahony R (1908) Zur Anatomie des Chaetognathenkopfes. Denkschr Akad Wiss Wien 84:33–41

Voronezhskaya EE, Tyurin SA, Nezlin LP (2002) Neuronal development in larval chiton *Ischnochiton hakodadensis* (Mollusca: Polyplacophora). J Comp Neurol 444:25–38. doi:10.1002/cne.10130

Walker RJ (1992) Neuroactive peptides with an RFamide or Famide carboxyl terminal. Comp Biochem Physiol 102C:213–222

Walthall WW (1995) Repeating patterns of motoneurons in nematodes: the origin of segmentation? In: Breidbach O, Kutsch B (eds) The nervous systems of invertebrates: an evolutionary and comparative approach. Birkhäuser Verlag, Basel, pp 61–75

Welsch U, Storch V (1983) Fine structural and enzyme histochemical observations on the epidermis and the sensory cells of *Sagitta elegans* (Chaetognatha). Zool Anz 210:34–43

White JG, Southgate E, Thomson JN, Brenner S (1986) The structure of the nervous system of the nematode *Caenorhabditis elegans*. Philos Trans R Soc Lond B Biol Sci 314:1–340. doi:10.1098/rstb.1986.0056

Wicht H, Lacalli TC (2005) The nervous system of *Amphioxus*: structure, development, and evolutionary significance. Can J Zool 83:122–150. doi:10.1139/z04-163

Zajac J-M, Mollereau C (2006) Introduction: RFamide peptides. Peptides 27:941–942. doi:10.1016/j.peptides.2005.12.005

8.2 Immunohistochemical analysis and 3D reconstruction of the cephalic nervous system in Chaetognatha: insights into an early bilaterian brain?

Rieger V, Perez Y, Müller CHG, Lipke E, Sombke A, Hansson BS, Harzsch S (2010)

Invertebrate Biology 129: 77-104

Invertebrate Biology

Invertebrate Biology 129(1): 77–104.
© 2010, The Authors
Journal compilation © 2010, The American Microscopical Society, Inc.
DOI: 10.1111/j.1744-7410.2010.00189.x

Immunohistochemical analysis and 3D reconstruction of the cephalic nervous system in Chaetognatha: insights into the evolution of an early bilaterian brain?

Verena Rieger,[1,2] Yvan Perez,[3] Carsten H. G. Müller,[1,2] Elisabeth Lipke,[4] Andy Sombke,[1,2]
Bill S. Hansson,[2] and Steffen Harzsch[1,2,a]

[1] Department of Cytology and Evolutionary Biology, Zoological Institute, University of Greifswald, D-17489 Greifswald, Germany
[2] Department of Evolutionary Neuroethology, Max Planck Institute for Chemical Ecology, D-07745 Jena, Germany
[3] Mediterranean Institute of Ecology and Paleoecology, University of Provence, Marseille, France
[4] Department of General Zoology and Zoological Systematics, Zoological Institute, University of Greifswald, D-17489 Greifswald, Germany

Abstract. We examined the brain architecture in different species of Chaetognatha using immunofluorescence methods with a set of nervous system markers and confocal laser-scan microscopic analysis. These markers include antibodies against synaptic proteins, RFamide-related peptides, and tyrosinated tubulin, as well as a marker of cell nuclei. Furthermore, we present a 3D reconstruction based on histological section series. Our results expand the previous knowledge on neuroanatomy in Chaetognatha. We suggest a structural and functional subdivision of the rather complex chaetognath brain into two domains, a posterior domain that may be primarily involved in the integration of sensory input, and an anterior domain that may be involved in the control of the mouthparts and the anterior part of the digestive system. Immunolocalization of a neuropeptide suggests the presence of an identifiable group of neurons associated with the brain of all species examined here. However, our data also reveal a certain degree of interspecific variation and divergence within the Chaetognatha concerning, for example, the pattern of nerves branching off the brain and the proportional sizes of the various neuropil compartments. We compare our data to brain architecture in various other representatives of Protostomia and Deuterostomia. The chaetognath brain fits within the range of structural variation encountered in protostomian brains, and we cannot find any brain characteristics that would argue in favor of placing chaetognaths outside of the Protostomia. Rather, we see the circumoral arrangement of their cephalic nervous system as an argument that suggests protostome affinities.

Additional key words: neurophylogeny, immunohistochemistry, evolution, Bilateria, neurotransmitters

The Chaetognatha ("arrow worms") is a taxon of cosmopolitan marine predators with a distinct shape resembling an arrow (Fig. 1A). Since their first description in 1769 by Slabber, the Chaetognatha have resisted all attempts of pinning down their phylogenetic affinities, and the majority of theories on their position appear to be unstable (reviews: Harzsch & Müller 2007; Harzsch & Wanninger 2010). The most recent phylogenomic studies using Bayesian inference and maximum likelihood methods to analyze broad datasets either suggest a sister-group relationship with Lophotrochozoa (Matus et al. 2006; Dunn et al. 2008) or a position as sister-group to all Protostomia (Marlétaz et al. 2006, 2008; Philippe et al. 2007). In addition, a detailed survey of their transcriptomic and genomic features (Marlétaz & LeParco 2008; Marlétaz et al. 2008) reveals both shared ancestral and derived characteristics, promoting chaetognaths as a pivotal model for our understanding of the bilaterian evolutionary history. Considering that Chaetognatha may have branched off close to the

---

[a] Author for correspondence.
E-mail: sharzsch@ice.mpg.de

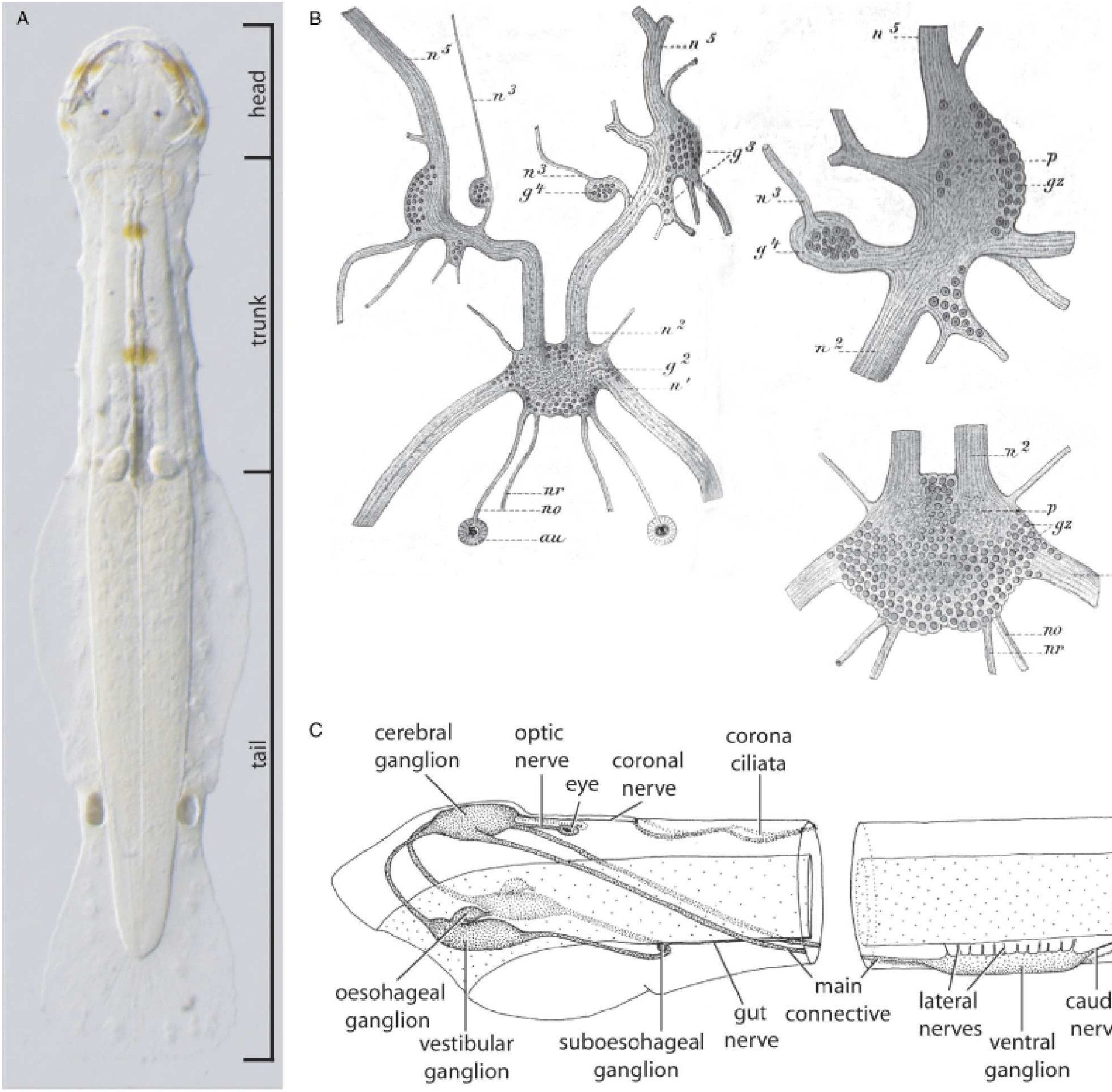
A
head
trunk
tail
B
n5
n3
n3
g4
g3
n2
g2
n1
nr
no
au
n5
p
gz
n3
g4
n2
n2
p
gz
n1
no
nr
C
cerebral ganglion
optic nerve
eye
coronal nerve
corona ciliata
oesohageal ganglion
vestibular ganglion
suboesohageal ganglion
gut nerve
main connective
lateral nerves
ventral ganglion
caudal nerve

Fig. 1. **A.** Live specimen of *Spadella cephaloptera*. **B.** *Sagitta bipuncata,* dissected nervous system of the head as drawn by Hertwig (1880); overview with × 50 magnification, details of the brain and vestibular ganglion with × 100 magnification. The illustrated ganglia and nerves were isolated by preparation and do not reflect the original anatomical arrangement in the head. au, Auge (eye); nr, Riechnerv (olfactory nerve); no, Sehnerv (optical nerve); gz, Ganglienzellen (ganglionic cells); g^2, Oberes Schlundganglion (upper esophageal ganglion); g^3, Seitenganglion des Kopfes (side ganglion of the head); g^4, Buccalganglion (buccal ganglion); n^1, Commissur zwischen Bauchganglion und Schlundganglion (commissure between abdominal ganglion and esophageal ganglion); n^2, Nerv zwischen Schlundganglion und Seitenganglion des Kopfes (nerve between esophageal ganglion and side ganglion of the head); n^3, Darmnerv (gut nerve); n^5, Hauptnerv des Seitenganglions vom Kopfe (main nerve of the side ganglion of the head); p, Nervöse Punktsubstanz (neuropil); **C.** Nervous system of chaetognaths (modified from Kapp 2007).

split between protostomes and deuterostomes, analyzing their brain may be revealing with regard to nervous system architecture in the last common bilaterian ancestor (Harzsch & Wanninger 2010).

There is a long-standing interest in the body organization of chaetognaths. General information on their morphology and anatomy has been summarized in the contributions by Goto & Yoshida

Table 1. Overview of relevant papers dealing with neuroanatomy of chaetognaths. This table lists, compares, or discriminates synonyms for obvious or assumed homologa in the cephalic nervous system of Chaetognatha based on a review of previous literature. EM, electron microscopy; Imhc, immunohistochemistry; LM^1, simple incident-light microscopy (with or without prior dissection of the nervous system); LM^2, simple incident- or advanced transmitted-light microscopy (based on the examination of histological sections); 3D-Reco, 3D reconstruction of nervous system based on entire histological section series.

Author(s)	Taxon	Study method	Cerebral ganglion	Posterior neuropil domain	Anterior neuropil domain
Krohn (1844)	*Sagitta bipunctata*	LM^1	"Kopfknoten"	Not distinguished	Not distinguished
Hertwig (1880)	*Flaccisagitta hexaptera*, *S. bipunctata*, *Spadella cephaloptera*	LM^{1,2}	"Oberes Schlundganglion"	Not distinguished	Not distinguished
Grassi (1883)	*F. hexaptera*, *S. bipunctata*, *Pseudosagitta lyra*	LM^{1,2}	"ganglio sopraesophageo"	"sostanza punteggiata o di Leydig"	"sostanza fibrosa — punteggiata"
Delage & Hérouard (1897)	*Spadella* sp.	LM^{1,2}	"ganglion cérébroide" (= "cervean")+ "ganglions lateraux"	Not distinguished	Not distinguished
von Ritter-Zàhony (1909, 1911)	*F. hexaptera*, *Parasagitta setosa*, *Parasagitta elegans*, *Flaccisagitta enflata*, *P. lyra*	LM^{1,2}	"Cerebral ganglion" (= "Gehirn")	Not distinguished	Not distinguished
Burfield (1927)	*S. bipunctata*	LM^2	"Brain"	Illustrated but not distinguished	"Punktsubstanz of the brain"
John (1933)	*S. cephaloptera*	LM^2	"Brain"	Illustrated but not distinguished	Illustrated but not distinguished
Kuhl (1938)	*P. setosa*, *F. hexaptera*, *P. lyra*	LM^{1,2}	"Cerebral ganglion"	"Punktsubstanz"	Illustrated but not distinguished
Bullock (1965)	*P. elegans*	LM^{1,2}	"Cerebral ganglion" (= "brain")	Not distinguished	Not distinguished
Goto & Yoshida (1987)	*Aidanosagitta crassa*	LM^2, EM	"Cerebral ganglion"	noticed, but not defined	noticed, but not defined
Rieger et al. (present paper)	*Ferosagitta hispida*+ other Sagittidae, *S. cephaloptera*	LM^2+3D-Reco, Imhc	"Cerebral ganglion"	Posterior neuropil domain (newly defined)	Anterior neuropil domain (newly defined)

Author(s)	Retrocerebral organ	Frontal connectives ($n = 2$)	Optic nerves ($n = 2$)	Eyes ($n = 2$)	Coronal nerves ($n = 2$)
Krohn (1844)	Not described	"vordere Kopfnerven"	"Sehnerven" (emitted from main connectives)	"Augen"	"hintere, eine Schlinge bildende Kopfnerven"
Hertwig (1880)	Not described	"Nerv zwischen Schlundganglion und Seitenganglion des Kopfes"	"Sehnerven" (= "Nervi optici")	"Augen"	"Riechnerven" (= "Nervi olfactorii")

Grassi (1883)	Described but not recognized ("fossetta"+"appandici")	"tronchi anteriori del cervello"	"nervi ottici"	"occhi"	"nervi coronali"
Delage & Hérouard (1897)	Not described	Illustrated but not specified	"nerfs optiques"	"taches oculiformes"	"fins filets pour la couronne ciliée cervicale"
von Ritter-Zàhony (1909, 1911)	"Gehirngrübchen"	"Frontalkommissuren" (= Stirnkommissuren")	"Optici"	"Augen"	"Coronalnerven"
Burfield (1927)	"Retrocerebral organ"	"Frontal commissures"	"Optic nerves"	"Eyes"	"Coronal nerves"
John (1933)	"Retrocerebral organ"	"Frontal commissures"	"Optic nerves"	"Eyes"	"Coronal nerves"
Kuhl (1938)	"Retrocerebraldrüsen"	"Frontalconnective"	"Augennerven" (= "Nervi optici")	"Augen"	"Coronalnerven"
Bullock (1965)	"Retrocerebral organ"	"Frontal connectives"	"Optic nerves"	"Eyes"	"Coronal nerves"
Goto & Yoshida (1987)	"Retrocerebral organ"	"Frontal connectives"	"Optic nerves"	"Eyes"	"Coronal nerves"
Rieger et al. (present paper)	"Retrocerebral organ"	"Frontal connectives"	"Optic nerves"	"Eyes"	"Coronal nerves"

Author(s)	Corona ciliata	Frontocerebral nerve ($n = 2$–4)	Laterocerebral nerves ($n = 2$)	Main connectives ($n = 2$)	Ventral nerve center
Krohn (1844)	"hintere, eine Schlinge bildende Kopfnerven"	Not described	Not described	"hintere Kopfnerven" (= "Schlundcommissuren")	"Bauchknoten" (= Rumpfknoten")
Hertwig (1880)	"Riechorgan"	Illustrated but not specified ($n = 2$)	Not described	"Commissuren"	"Bauchganglion"
Grassi (1883)	"Corona cigliata"	"nervi che si departano dai lati anteriori del cervello" ($n = 4$)	Not described	"commissura del cervello col ganglio addominale"	"ganglio addominale"
Delage & Hérouard (1897)	"couronne ciliaire cervicale"	"nerfs des crochets supérieurs" ($n = 4$)	"nerfs des crochets inférieurs"	"collier nerveux"	"Ganglion abdominal" (= "ganglion ventral")
von Ritter-Zàhony (1909, 1911)	"Corona" (= "Flimmerkrone")	Not described	Not described	"Hauptkommissuren"	"Bauchganglion"
Burfield (1927)	"Corona"	Not described	Not described	"Main commissures"	"Ventral ganglion"
John (1933)	"Corona ciliata"	Not described	Not described	"Main commissures"	"Visceral ganglion"
Kuhl (1938)	"Corona ciliata"	Not described	Not described	"Paarige Connective"	"Ventralganglion"
Bullock (1965)	"Corona" (= "ciliary loop")	Not described	Not described	"circumesophageal connectives"	"Ventral ganglion"
Goto & Yoshida (1987)	"corona ciliata"	Not described	Not described	"Main connectives"	"Ventral ganglion"
Rieger et al. (present paper)	"corona ciliata"	Not present	Not present	"Main connectives"	"Ventral nerve center"

Author(s)	Frontal ganglia ($n = 2$)	Vestibular ganglia ($n = 2$)	Frontal nerves ($n = 2$ or 4)	Mandibular nerves ($n = 2$)	Vestibular nerves ($n = 2$)
Krohn (1844)	Not described	"angeschwollene Knötchen"	Not specified ("Fädchen")	Not specified ("Fädchen")	Not specified ("Fädchen")
Hertwig (1880)	Not described	"Seitliche Kopfganglien"	Illustrated but not specified ($n = 2$)	Illustrated but not specified	Illustrated but not specified
Grassi (1883)	"lobetti accessorii del ganglio vestibulare"	"gangli vestibolari"	Illustrated but not specified ($n = 4$)	"nervi"	Illustrated but not specified
Delage & Hérouard (1897)	Not described	"ganglions céphaliques"	Not described	Not described	Not described
von Ritter-Zàhony (1909, 1911)	"Frontalganglian"	"Vestibularganglien"	"Frontalnerven" ($n = 2$)	Not specified ("Nerven")	Not specified ("Nerven")
Burfield (1927)	"Frontal ganglia"	"Vestibular ganglia"	"Frontal nerves" ($n = 2$)	"Mandibular nerves"	"Vestibular nerves"
John (1933)	Not described	"Vestibular ganglia"	"Frontal nerves" ($n = 2$)	"Mandibular nerves"? (originate posteriorly from vestibular ganglia)	"Vestibular nerves"
Kuhl (1938)	"Frontalganglien"	"Vestibularganglien"	"Frontalnerven" (= "Nervi coronales") ($n = 2$)	Illustrated but not specified	Illustrated but not specified
Bullock (1965)	"Frontal ganglia"	"Vestibular ganglia"	"Frontal nerves" (run to the posterior teeth)	"Mandibular nerves" (innervates muscles of grasping spines"	"Vestibular nerves" (goes to the borders of the vestibule")
Goto & Yoshida (1987)	Anterior portion of vestibular ganglia	"Vestibular ganglia"	Not described	"Mandibular nerves"	"Vestibular nerves"
Rieger et al. (present paper)	Anterior portion of vestibular ganglia	"Vestibular ganglia"	"Frontal nerves" ($n = 2$)	"Mandibular nerves"	"Vestibular nerves"

Author(s)	Dorsal nerves ($n = 2$)	Dorsovestibular nerves ($n = 2$)	Esophageal ganglia ($n = 2$)	Esophageal nerves ($n = 2$)
Krohn (1844)	Not specified ("Fädchen")	Not specified ("Fädchen")	Not described	Not specified ("Fädchen")
Hertwig (1880)	"Hauptnerv des Seitenganglions vom Kopfe"	Not described	"Buccalganglien"	"Darmnerven"
Grassi (1883)	"nervi lunghissimi (del ganglio vestibolare)"	Not described	"gangli periesofagei"	"nervi esofagei superiori (del ganglio periesophageo)"
Delage & Hérouard (1897)	"nerfs vestibulaires"?	Not described	"ganglions buccaux" (?)	"nerfs vestibulaires" (?)
von Ritter-Zàhony (1909, 1911)	"Dorsalnerven"	Not described	"Schlundganglien"	"Seitliche Schlundnerven"
Burfield (1927)	"Dorsal nerves"	Not described	"Esophageal ganglia"	"Lateral esophageal nerves"
John (1933)	"Dorsal nerves"? (branching off dorsolaterally of the vestibular ganglion)	"Nerves to *M. obliquus longus* and *M. retractor preputii*"	"Esophageal ganglia"	"Esophageal nerves"

Kuhl (1938)	"Dorsalnerven" (= "Nervi dorsales")	Not described	"Oesophagealganglien"	"Laterale Oesophagealnerven"
Bullock (1965)	"Dorsal nerves"	Not described	"Pharyngeal ganglia"	"Esophageal nerves"
Goto & Yoshida (1987)	"Dorsal nerves"	Not described	"Esophageal ganglia"	"Lateral esophageal nerve"
Rieger et al. (present paper)	"Dorsal nerves"	Not present?	Not present	Not present

Author(s)	Esophageal commissure	Labial ganglia ($n = 2$)	Labial nerves ($n = 2$)	Suboesophageal ganglion	Stomatogastric nerve
Krohn (1844)	Not described	Not described	Not described	Not described	Not described
Hertwig (1880)	Present but not specified (cut during preparation)	Not described	Illustrated but not specified	Not described	Not described
Grassi (1883)	"commissura retroboccale"	Not described	Illustrated but not specified	Not described	Not described
Delage & Hérouard (1897)	Not described	Not described	Not described	Not described	Not described
von Ritter-Zàhony (1909, 1911)	"Schlundkommissur"	"Labialganglien"	"Labialnerven"	Not described	"Ventraler Schlundnerv"
Burfield (1927)	"Esophageal commissure"	"Very minute ganglion"	"Labial nerves"	Not described	"Ventral esophageal nerve"
John (1933)	"Esophageal commissure"	Not described	"Labial nerves"	Not described	"Unpaired ventral esophageal nerve"
Kuhl (1938)	"Schlundkommissur"	Not described	Illustrated but not specified	Not described	"Unpaarer Ventraler Oesophagusnerv" (= "Ventraler Schlundnerv")
Bullock (1965)	"Ventral subpharyngeal commissure"	Mentioned but not illustrated	Mentioned but not illustrated	"Labial nerves"	"ventral pharyngeal nerve"
Goto & Yoshida (1987)	"Esophageal commissure"	Not described	Not described	"Subesophageal ganglion"	"Ventral esophageal nerve"
Rieger et al. (present paper)	"Esophageal commissure"	Not present	Not present?	Not clearly visible	"Stomatogastric nerve"

(1987), Bone & Goto (1991), Kapp (1991, 2007), Nielsen (2001), and Ax (2001); the most detailed review of their microscopic anatomy is that of Shinn (1997). Chaetognaths have a complex nervous system that comprises intra- and basiepidermal components (Ahnelt 1980, 1984; Salvini-Plawen 1988, reviews: Bone & Goto 1991; Shinn 1997). The earliest studies on their nervous system date back >160 years. Krohn (1844), Kowalevsky (1871), and Langerhans (1878) provided first observations on the basis of light microscopy of various sagittid species. Hertwig (1880) summarized and critically reviewed these pioneering studies, corrected mistakes with respect to terminology and previous interpretation of neuronal structures, and thereby gave the first comprehensive description of a chaetognath's cephalic nervous system (Fig. 1B,C). Later on, Grassi (1881, 1883), von Ritter-Záhony (1909, 1911), Burfield (1927), Hanström (1928), and Kuhl (1938) contributed to our knowledge of basic neuroanatomy in Chaetognatha, again based on representatives of the pelagic genus *Sagitta* (Table 1). To date, the studies by Bone & Pulsford (1984) and Goto & Yoshida (1984, 1987) are the most thorough on general nervous system organization and internal brain anatomy of chaetognaths. Furthermore, the fine structure of the brain has received much attention (Scharrer 1965; Ahnelt 1980, 1984; Rehkämper & Welsch 1985; Goto & Yoshida 1987; Salvini-Plawen 1988). Recent immunohistochemical studies have extended our knowledge of the architecture of the ventral nerve center and the nerve plexus in the trunk (Harzsch & Müller 2007; Harzsch et al. 2009).

In Chaetognatha, the cephalic nervous system consists of the unpaired cerebral complex (the brain or cerebral ganglion, and the retrocerebral organ, *sensu* Salvini-Plawen 1988), a pair of vestibular ganglia, a pair of esophageal ganglia, and a subesophageal ganglion from which the stomatogastric nerve emerges (Fig. 1A,C; Bone & Pulsford 1984; Goto & Yoshida 1984, 1987; reviews: Bone & Goto 1991; Shinn 1997). Except for the elaborate intraepidermal plexus, all components of the cephalic nervous system are deeply sunk into the musculature that moves the grasping spines and the esophagus. Connectives link the brain and the vestibular ganglia, as well as the vestibular ganglia and the esophageal ganglia. The antero-posteriorly extending bundles, which connect the brain and the ventral nerve center, are called the main connectives. Connectives also link the brain and the vestibular ganglia (frontal connectives), as well as the vestibular ganglia and the subesophageal ganglion (Goto & Yoshida 1987; Shinn 1997). The vestibular ganglia presumably control the operation of the grasping spines and receive sensory input from the vestibular ridge papillae surrounding the mouth via the frontal nerves (e.g., John 1933). The esophageal and subesophageal ganglia exclusively consist of nerve cell bodies (Goto & Yoshida 1987). The esophageal ganglion gives rise to the medially directed ventral esophageal nerve, which seems to target the esophageal muscles (Shinn 1997).

The brain is situated immediately below the multilayered epidermis of the head and consists of a neuropil core with numerous synapses surrounded by clusters of neuronal cell somata (Rehkämper & Welsch 1985; Goto & Yoshida 1987; Bone & Goto 1991). It is ensheathed by a broad capsule of extracellular matrix (ECM) produced by the epidermis (Salvini-Plawen 1988; Bone & Goto 1991; Shinn 1997). Owing to its complete encapsulation by ECM, Salvini-Plawen (1988) pointed out the basiepidermal nature of the brain. In the head, nerves emerging from the brain are embedded in supporting structures made of complex sheets of connective tissue. These nerves, which target esophageal and somatic head muscles, have conventional nerve endings and neuromuscular junctions that display ultrastructural features similar to classic motor end plates (Duvert & Barets 1983; Shinn 1997). The vestibular and esophageal ganglia, however, are clearly subepidermal and embedded between the head muscles. Peripheral organs associated with the brain are a pair of eyes (Goto & Yoshida 1984, 1988; Goto et al. 1984, 1989), a ciliated loop (the corona ciliata) which is localized in the dorsal part of the head (Bone & Goto 1991; Shinn 1997), and the retrocerebral organ, a structure with an unknown putative sensory function, possibly a baroreceptor (Shinn 1997). So far, four studies have used immunohistochemical techniques to examine the distribution of serotonin and RFamide-like immunoreactive neurons (Bone et al. 1987; Goto & Yoshida 1987; Goto et al. 1992), and aspartate immunoreactivity (Duvert et al. 1997), in the brain. However, no confocal laser-scan analysis of transmitter distribution in the brain has been carried out to date, so that the localization of the immunoreactive structures was analyzed at a relatively low level of resolution compared with the potential of modern confocal microscopy. The present study sets out to analyze the chemoarchitecture of the chaetognath brain in more detail and in a comparative context. Furthermore, we present a 3D reconstruction of the cephalic nervous system, thereby extending our knowledge on general brain anatomy in Chaetognatha.

Methods

Experimental animals

Adult specimens of *Spadella cephaloptera* (Busch, 1851) (Phragmophora, Spadellidae) were collected in Sormiou (Marseille, France) in June 2006 and August 2007. A plankton net was grazed over the sea grass beds by snorkeling. Animals were kept in aquaria containing natural seawater (21 ± 1°C) at the University of Provence, Marseille, before immunohistochemical processing.

Specimens of *Sagitta bipunctata* Quoy & Gaimard, 1827 (Aphragmophora, Sagittidae) were collected near the Cassidaigne canyon (Marseille, France) in October 1997 during a planktonic survey carried out on mesopelagic communities at depth levels of ~ 400 m.

Specimens of *Pterosagitta draco* (Krohn, 1853) (Aphragmophora, Pterosagittidae), *Flaccisagitta enflata* (Grassi, 1881), and *Flaccisagitta hexaptera* (d'Orbigny, 1936) (Aphragmophora, Sagittidae) were collected by Akihiro Shiroza at depth levels of ~ 0–100 m during a cruise in the West Atlantic in March 2008 (Ship: NOAA R/V Nancy Foster; Mission code: CRER2 Coral Reef Ecosystem Research). Specimens of *P. draco* were also provided by Gisèle Champalbert and Marc Pagano from the Institute for Research and Development (IRD UR 167 SyRoCo), who collected samples during a mission in the Indian Ocean (Tulear).

A presumably new species of the genus *Spadella* was discovered during a diving expedition near Valsalina (Pula, Croatia). Altogether, 20 living specimens were sieved out of a poorly assorted *Amphioxus*-sediment in 10-m depth.

For 3D reconstructions of the cephalic nervous system, we used one specimen of the tropical West Atlantic *Ferosagitta hispida* (Conant, 1895), in surface water of the Indian River Lagoon (27°14′N, 80°90′W) near Fort Pierce, FL, USA, with a plankton net suitable for capturing macrofauna organisms (300-μm mesh size).

Histochemistry and immunohistochemistry

Specimens were fixed overnight at 4°C (or alternatively for 4 h, room temperature) in 4% paraformaldehyde in phosphate buffer ($0.1\,\text{mol}\,\text{L}^{-1}$, pH 7.4). Histochemistry and immunohistochemistry were carried out on free-floating whole mounts of adult specimens with fluorochrome-conjugated secondary antibodies using standard protocols (Harzsch & Müller 2007). After fixation, the tissues were washed in several changes of phosphate-buffered saline (PBS) for ≥ 4 h, pre-incubated in PBS-TX (1% normal goat serum, 0.3% Triton X-100, 0.05% Na-acide) for 1 h, and then incubated overnight in the following histochemical reagents and primary antibodies diluted in PBS-TX (room temperature): (1) anti-tyrosine tubulin monoclonal from mouse (1:1000; Sigma, St. Louis, MO, USA), (2) anti-FMRFamide polyclonal from rabbit (1:2000; ImmunoStar, Hudson, WI, USA), (3) anti-synapsin SYNORF-1 monoclonal from mouse (1:10; antibody kindly provided by Prof. Dr. E. Buchner, Universität Würzburg).

For double labeling, combinations of these antisera were used. Specimens were then washed for ≥ 2 h in several changes of PBS, and subsequently incubated in secondary antibodies against rabbit proteins conjugated to the fluorochrome Alexa Fluor 488 (1:500; Molecular Probes, Eugene, OR, USA) and antibodies against mouse proteins conjugated to Cy3 (1:500; Jackson Immuno Research, West Grove, PA, USA) for 4 h. The specimens were stained with the nuclear dye bisbenzimide (0.5%, 4 h at room temperature; Hoechst H 33258), simultaneous to the secondary antibody incubations. Finally, the tissues were washed for ≥ 2 h in several changes of PBS and then mounted in MOWIOL (Calbiochem, Nottingham, UK). The immunohistochemical observations reported in this article are based on the analysis of at least six specimens for each species, except for *P. draco,* for which only one specimen could be processed successfully for RFamide immunoreactivity.

Specificity of the antisera

The tetrapeptide FMRFamide (Phe–Met–Arg–Phe–NH$_2$) and FMRFamide-related peptides form a large neuropeptide family with >50 members, all of which share the RFamide motif (reviews: Price & Greenberg 1989; Greenberg & Price 1992; Walker 1992; Dockray 2004; Kriegsfeld 2006; Zajac & Mollereau 2006) and which are widely distributed among invertebrates and vertebrates. The antiserum we used was generated in rabbit against synthetic FMRFamide (Phe–Met–Arg–Phe–NH$_2$) conjugated to bovine thyroglobulin (DiaSorin, Saluggia, Italy, Cat. No. 20091, Lot No. 923602). According to the manufacturer, staining with this antiserum is completely eliminated by pre-treatment of the diluted antibody with $100\,\mu\text{g}\,\text{mL}^{-1}$ of FMRFamide. We repeated this experiment and pre-incubated the antiserum with $10^{-4}\,\text{mol}\,\text{L}^{-1}$ FMRFamide (16 h, 4°C). In this control, neuronal structures were not labeled. In an additional control experiment for possible non-specific binding of the secondary antiserum, we omitted the primary antiserum, replaced it with blocking solution, and followed the labeling protocol as above. In this control, staining was absent.

We compared the labeling pattern obtained in our specimens with that in a previous study, in which a polyclonal antiserum to the sequence Arg–Phe-amide was used in *Parasagitta setosa* (Bone et al. 1987). This latter antiserum was obtained by immunizing rabbits with synthetic FMRFamide, which was coupled via glutaraldehyde to bovine thyroglobulin (Grimmelikhuijzen & Spencer 1984). Incubation of this antiserum with sepharose-bound FMRFamide, FLRFamide, or RFamide abolished all staining, and this antiserum has been shown to be most sensitive to the C-terminal sequence –RFamide (–Arg–Phe–NH_2; Grimmelikhuijzen 1985). It has been used to label RFamide-like immunoreactive structures, e.g., in a medusa (Grimmelikhuijzen & Spencer 1984) and in several *Hydra* species (Grimmelikhuijzen 1985). Bone et al. (1987), using the antiserum generated by Grimmelikhuijzen & Spencer (1984) in *P. setosa,* concluded that the chaetognath peptide might be related to any peptide terminating with the sequence RFamide. Because the labeling pattern obtained by Bone et al. (1987) closely corresponds to that found in the present report, we conclude that the DiaSorin antiserum that we used most likely also labels any peptide terminating with the sequence RFamide. Therefore, we will refer to the labeled structures in our specimens as "RFamide-like immunoreactive (RFir) neurons" throughout this article.

The monoclonal mouse anti-*Drosophila* synapsin "SYNORF-1" was raised against a *Drosophila* GST–synapsin fusion protein and recognizes at least four synapsin isoforms (~70, 74, 80, and 143 kDa) in western blots of head homogenates of *Drosophila* (Klagges et al. 1996). Western blot analysis of brain homogenates of the anomuran crab *Coenobita clypeatus* showed that the epitope which SYNORF-1 recognizes is strongly conserved between the fruit fly and the crustacean (Harzsch & Hansson 2008). The antibody also labels neuromuscular synapses both in *Drosophila* and in Crustacea (Harzsch et al. 1997), as well as central synapses in Platyhelminthes (Cebià 2008), suggesting that the epitope to which this antiserum binds is conserved over wide evolutionary distances. Our previous analysis on the ventral nerve center strongly suggested that this antibody also labels synaptic neuropil in the Chaetognatha (Harzsch & Müller 2007).

The monoclonal anti-tyrosine tubulin (mouse IgG3; Sigma Product Number T 9028, Clone TUB-1A2) was raised against a peptide containing the carboxy terminal amino acids of α-tubulin. According to the manufacturer, this antibody reacts with tyrosine tubulin from bovine brain, African monkey green kidney cells, dog kidney, marsupial kidney, mouse pituitary tumor (AtT-20), yeast, and *Xenopus,* indicating that the antigen which this antibody recognizes is evolutionarily conserved across a broad range of species. Tubulin is the major building block of microtubules and represents a heterodimer of α-tubulin and β-tubulin. Microtubules grow and turn over rapidly, but some populations of interphase microtubules are more stable, such as acetylated α-tubulin (Kreis 1987). Tubulin tyrosinylation is involved in the assembly status of tubulin. Tyrosinated tubulin (tyr-tubulin) represents a relatively dynamic subclass of interphase microtubules (Kreis 1987).

Microscopic analysis

Digital images were obtained using a Zeiss Axioimager Z1 fluorescence microscope equipped with a structured illumination device (ApoTome) and a digital camera AxioCamMRm (Zeiss, Jena, Germany) controlled by the AxioVision V 4.6.3-SP1 software package (Zeiss). In addition, samples were scanned with a Zeiss LSM 510 Meta Confocal Laser-Scanning Microscope. Those images are based on Z-stacks of several optical sections and were obtained using the LSM 510 V.4.0. SP2 software (Zeiss). Images were black–white inverted and processed in Adobe Photoshop by using the global contrast and brightness adjustment features. Identification of head musculature is based on the descriptions and drawings of von Ritter-Záhony (1909), Burfield (1927), and John (1933).

3D reconstruction

A head of *F. hispida* embedded in an epoxy resin (Araldit, Agar Scientific, Stansted, UK) was cut transversally in a series of ~400 sections, each measuring 1.5 µm in thickness. The series was then stained in a toluidine blue solution and afterwards digitalized with Zeiss Axioimager Z1 fluorescence microscope (type of camera and used software was the same as listed up in paragraph above). Alignment of sections, marking of target structures and 3-D-modeling was conducted by using Mercury AMIRA software (Chelmsford, MA, USA, version 4.1.0).

Results

Cephalic nervous system

The 3D reconstruction of the cephalic nervous system in *F. hispida* (Fig. 2) is based on a histological section series (Figs. 3, 4). Most parts of the cephalic nervous system are deeply sunk into mesodermal

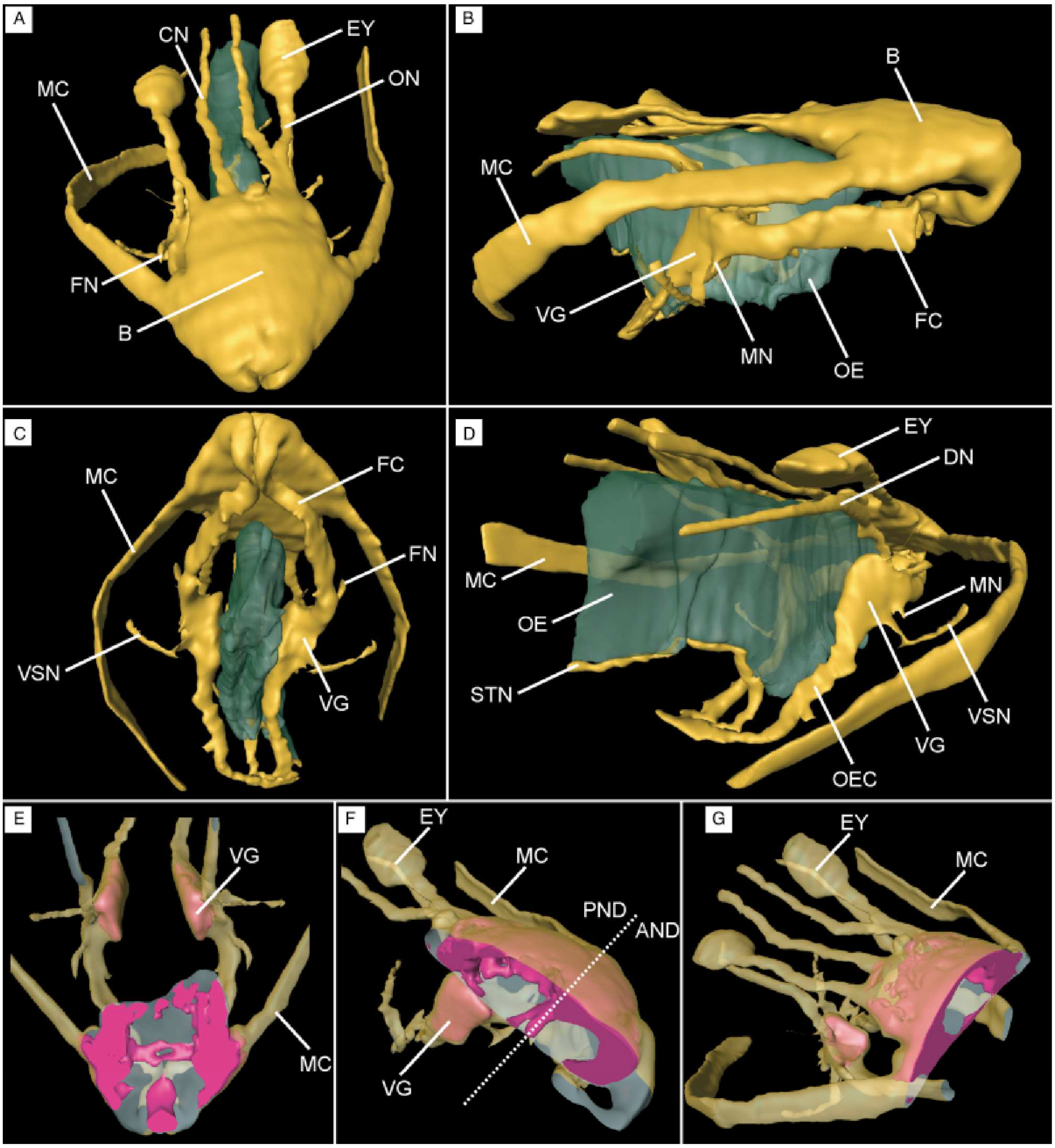

Fig. 2. A–D. 3D reconstruction of the cephalic nervous system in *Ferrosagitta hispida,* in relation to the gut based on a series of ~400 transverse semi-thin sections through the head; structures of the nervous system are colored yellow, the gut is stained green. The retrocerebral organ is not differentiated from the brain in the present model. **A.** Fronto-dorsal view. **B.** Lateral view. **C.** Fronto-ventral view. **D.** Posterio-lateral view. **E–G.** Same reconstruction with brain in cut-off perspective, showing the distribution of somata (purple color) in relation to its neuropil (not reconstructed) seen through a semitransparent basal matrix. **E.** Dorsal-horizontal view. **F.** Medio-sagittal view. **G.** transverse view. AND, anterior neuropil domain; B, brain; CN, coronal nerve; DN, dorsal nerve; EY, eye; FC, frontal connective; FN, frontal nerve; MC, main connective; MN, mandibulare nerve; OE, esophagus; OEC, esophageal commissure; ON, optic nerve; PND, posterior neuropil domain; STN, stomatogastric nerve; VG, vestibular ganglion; VSN, vestibular nerve.

structures, such as the head musculature, except for the coronal nerves that at least partly remain in a basiepidermal position (Fig. 4K). However, from a typological point of view, these parts of the nervous system have to be assigned to the basiepithelial type, as the ECM completely encases them. This is especially visible in the brain, which looks like a lens encapsulated by a thick ECM (Fig. 3D–F). The brain has a nearly pentagonal outline (Figs. 2A, 3C), the corner points of which are defined by (1) the paired frontal connectives that connect the brain with the vestibular ganglia (circumesophageal loop), (2) the paired main connectives that leave the brain laterally and extend obliquely in a posterior direction to target the ventral nerve center (circumintestinal loop), and (3) two nerve pairs at the posterior margin of the brain: the coronal nerves that link the corona ciliata to the brain, and the optic nerves that make contact with the eyes (Figs. 2A–C,G, 4G–K).

Cut-away reconstruction models reveal the presence of two distinct neuropil compartments (Figs. 2E,F, 4A–G) that can be also identified with immunohistochemical techniques. The anterior neuropil domain extends from the frontal horns (Fig. 4A,B) to the level of the bridge neuropil (Fig. 4C,D). The bridge neuropil has an elliptical shape, and the associated somata are mostly restricted to the dorsal and lateral side of this neuropil (Figs. 2G, 3D). Ventral clusters of somata are only present in the anterior half of the anterior neuropil domain (Fig. 4A,B). At the posterior end of the anterior neuropil domain, the bridge neuropil continues laterally into the main connectives (Fig. 4E). After their exit from the brain (Fig. 3E), the main connectives turn ventrolaterally in a half circle and enter the hood. They retain a subepidermal position, being always surrounded by a conspicuous layer of ECM (Figs. 2A,C,G, 3F–I). The posterior neuropil domain shows a central neuropil core with a mostly ovoid profile and is almost completely surrounded by a cortex of somata (Figs. 2E,F, 3E–G). The posterior neuropil domain is separated from the adjacent retrocerebral organ by a posterior layer of somata (Figs. 2E, 4G). The neuropil core tapers into a pair of dorsomedian coronal nerves, attached to the dorsal margin of the dorsal longitudinal muscles (musculus obliquus superficialis), as well as a pair of shorter, more dorsolaterally located optic nerves (Figs. 2A,G,I, 4G–K).

The vestibular ganglia are situated laterally and adjacent to the esophagus, crammed into the space between various vestibular and esophageal muscles. The vestibular ganglia are linked to the brain via the frontal connectives, which exit the brain anteriorly and then turn sharply ventrolaterally (Figs. 2C, 3A,B,D–G). The centrally located neuropil of the vestibular ganglia displays a circular or ovoid profile in transverse sections (Figs. 2C,D, 3H). The orientation of this neuropil in relation to the head, however, changes from a horizontal arrangement in the anterior portion to a vertical (dorsoventral) arrangement in the more voluminous posterior portion. In the anterior portion, the cortex of somata is restricted to the ganglion's dorsomedian border (Fig. 3H). In the larger posterior portion of the vestibular ganglion, the vertically oriented neuropil is either completely encased by a thin layer of somata, or again incompletely ensheathed by a cluster of somata arranged along its median border (not illustrated). Many nerves branch off the vestibular ganglion in various directions. The bilaterally paired frontal nerves come off the anterior tips of a vestibular ganglion, extend dorsolaterally, and ramify below the dorsolateral region of the cuticularized mouth integument (Fig. 2A,C). The paired mandibular nerves branch off the anterior ventrolateral edge of the vestibular ganglia (Fig. 2B,D). The mandibular nerves course between the external vestibular musculature (m. dilator vestibuli externus: Fig. 3H) and the lateral muscle-complex (m. complexus lateralis: Fig. 3I). More posteriorly, a second, larger nerve, with the same ventrolateral course, extends from each vestibular ganglion (Fig. 2C,D) and continues between the vestibular (m. dilator vestibuli externus: Fig. 3H) and the oral constrictor musculature (m. constrictor oris alter: Fig. 3G,H). On approaching the ventral integument, each vestibular nerve subdivides into two branches, the short inferior one that projects toward the mouth opening, and the longer exterior one that targets the space between the lateral region of the cuticularized mouth integument and the outer margin of the external vestibular muscle, where it further ramifies.

In the transition zone of the anterior and posterior portion of each vestibular ganglion, a thick dorsal nerve comes off, which ascends dorsally in close vicinity of the external vestibular muscle (m. dilator vestibuli externus: Fig. 3H) and the superior expansive muscle, partly moving the grasping spines (m. expansus superior: Fig. 3H). The dorsal nerves are the longest among all nerves branching off the vestibular ganglia and are clearly visible in 3D reconstructed models. Furthermore, we noticed several additional, much thinner, nerves that branch off the vestibular ganglia. Unfortunately, these nerves were too small and indistinctive to be unambiguously identified in histological sections, so we did not include them in the 3D reconstruction.

At their posterior end, the vestibular ganglia give rise to the strongly curved esophageal commissures that flank the mouth opening very close to the ventral integument (Fig. 2C,D). Both rami of the esophageal commissure meet ventrally of the bicornous muscle (m. bicornis: Fig. 3I). The stomatogastric nerve emerges from this junction. It first has an anterior course (Figs. 2D, 3I). The stomatogastric nerve changes direction upwards where the bicornous

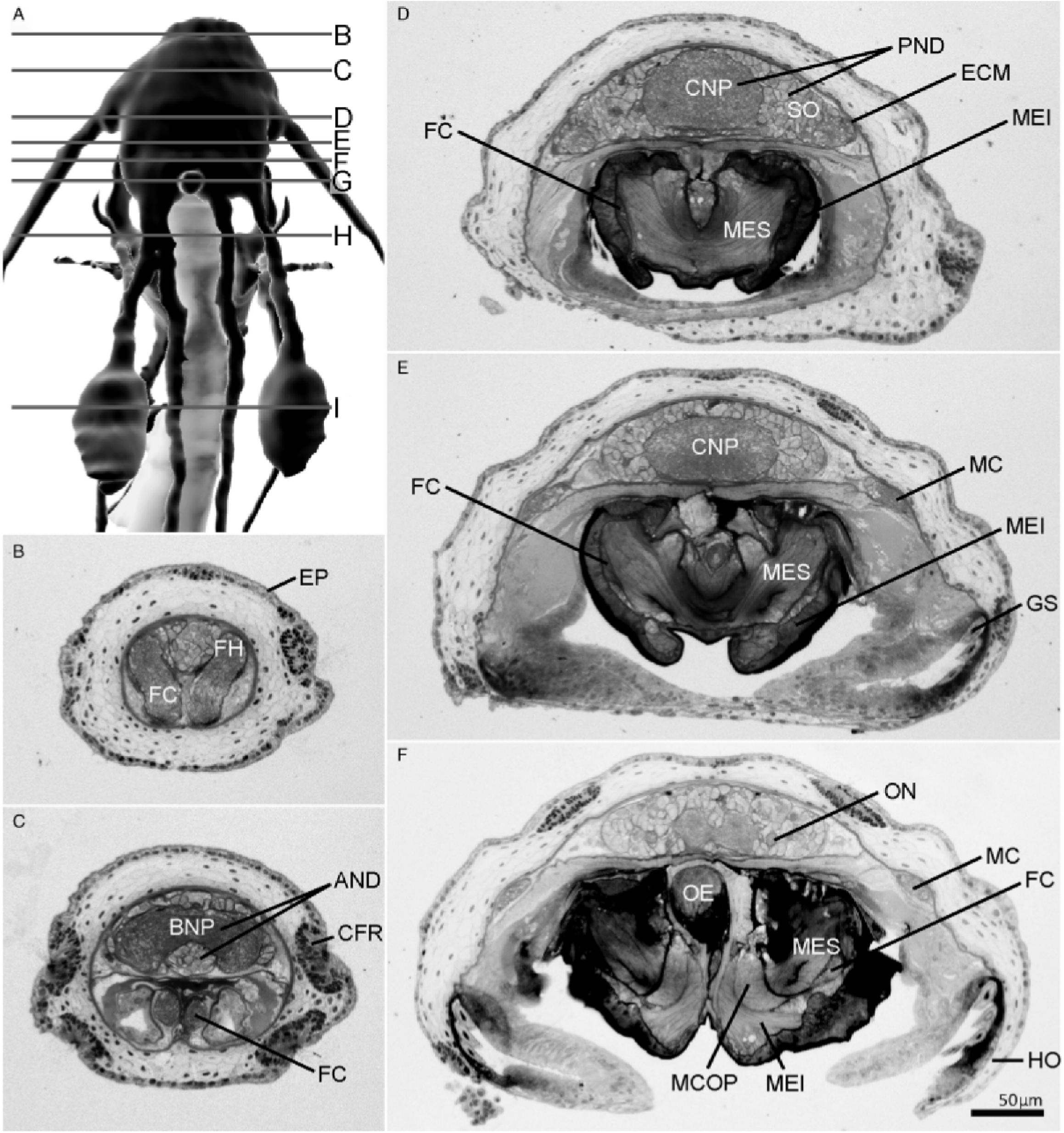

Fig. 3. Histological anatomy of the head in *Ferrosagitta hispida,* in resting position with complete hood coverage; images show examples from the section series, on which Fig. 2 is based. **A.** Approximate position of each section in relation to the cephalic nervous system. **B.** Dorsal region of frontal connectives merging with the anterior part of the brain and the vestibular ganglia. **C.** Anterior part of the brain. **D.** Anteromedian region of the brain. **E.** Median region of the brain with main connectives branching off, distal tip of grasping spines. **F.** Medioposterior region of the brain, anterior part of esophagus.

muscle splits into two horns and proceeds through the median space between these horns and joins the underside of the esophagus (Figs. 2D, 3I). The stomatogastric nerve then takes a posterior course and proceeds below esophagus (Fig. 2D).

Immunolocalization of tyr-tubulin

The anti-tyr-tubulin antibody proved to be a good general marker for labeling the various components of the nervous system (Fig. 5) to allow for a comparison with the 3D reconstruction (Fig. 2). Apparently, axons and dendrites are particularly rich in tyr-tubulin, a component of a relatively dynamic subclass of interphase microtubules. A combination of this marker with the nuclear dye bisbenzimide provided a detailed overview of the brain cytology (Fig. 5; see also Fig. 6B). Within the brain, substructures varying in labeling density can be distinguished (Fig. 6A). In *Spadella cephaloptera,* the retrocerebral organs, which are located slightly posteriorly to the brain, strongly express tyr-tubulin (Fig. 6A), but this organ was less obvious in the other species that we examined. The paired main connectives and the paired frontal connectives are also immunoreactive for tyr-tubulin, as is the pair of nerves that links the eyes to the brain (optic nerves), and the pair of nerves that connects the brain and the corona ciliata (coronal nerves: Figs. 5, 6). There seem to be differences between the genera concerning the arrangement of the main connectives. In Sagittidae, these exit the brain in a postero-lateral direction, whereas in Spadellidae they course slightly anteriorly before turning backwards toward the ventral nerve center. Because we observed this constellation in numerous species, we do not think that this is a fixation artifact but a true interspecific difference. All specimens represented here had their hood in an unretracted position.

Immunolocalization of synapsins

Synapsins are a class of presynaptic membrane proteins associated with the synaptic vesicles (Klagges et al. 1996). Hence, the SYNORF-1 antibody labels synaptic neuropil, whereas immunolocalization of tyr-tubulin more generally reveals the neuronal processes (neuritis: compare Fig. 6A,C). Immunohistochemistry against synapsins again confirmed that the chaetognath brain can be subdivided into an anterior and a poste-

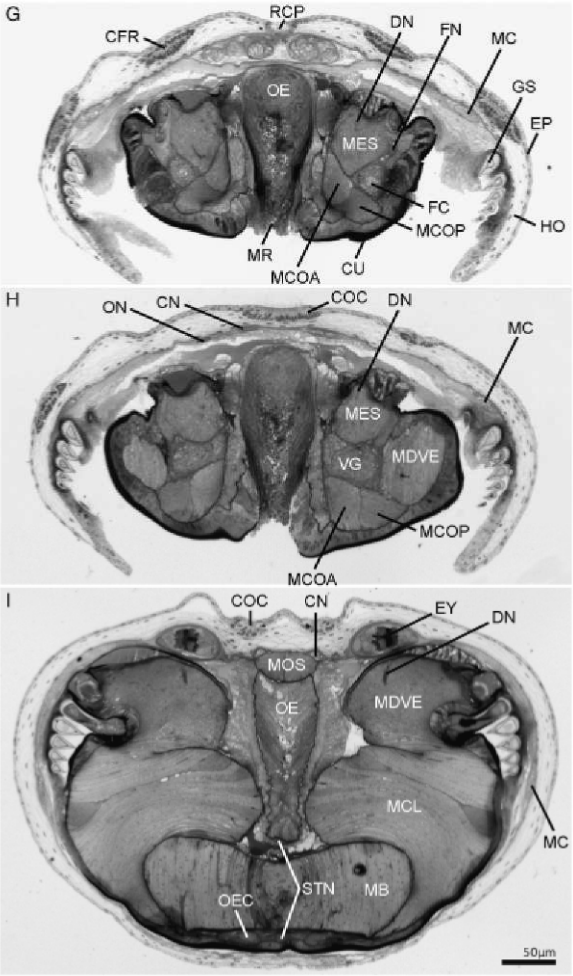

Fig. 3. Continued. G. Posterior end of the retrocerebral organ with pairs of coronal and optic nerves, mouth region. **H.** Anterior part of the corona ciliata, vestibular ganglia (anterior compartment in horizontal orientation), posterior mouth region. **I.** Eye region, anteriomedian part of the corona ciliata, slightly anterior to the subesophageal junction of esophageal commissure, basal zone of grasping spines. AND, anterior neuropil domain; BNP, bridge neuropil; CFR, ciliary fence receptors; CN, coronal nerve; CNP, core neuropil; COC, corona ciliata; CU, cuticle; DN, dorsal nerve; ECM, extracellular matrix; EP, epidermis; EY, eye; FC, frontal connective; FH, frontal horn; FN, frontal nerve; GS, grasping spine; HO, hood; MB, musculus bicornis; MC, main connective; MCL, musculus complexus lateralis; MCOA, musculus constrictor oris alter; MCOP, musculus constrictor oris primus; MDVE, musculus dilator vestibuli externus; MEI, musculus expansus inferior; MES, musculus expansus superior; MOS, musculus obliquus superficialis; MR, mouth region; OE, esophagus; OEC, esophageal commissure; ON, optic nerve; PND, posterior neuropil domain; RCP, pore opening of the retrocerebral organ; SO, somatic region; STN, stomatogastric nerve; VG, vestibular ganglion.

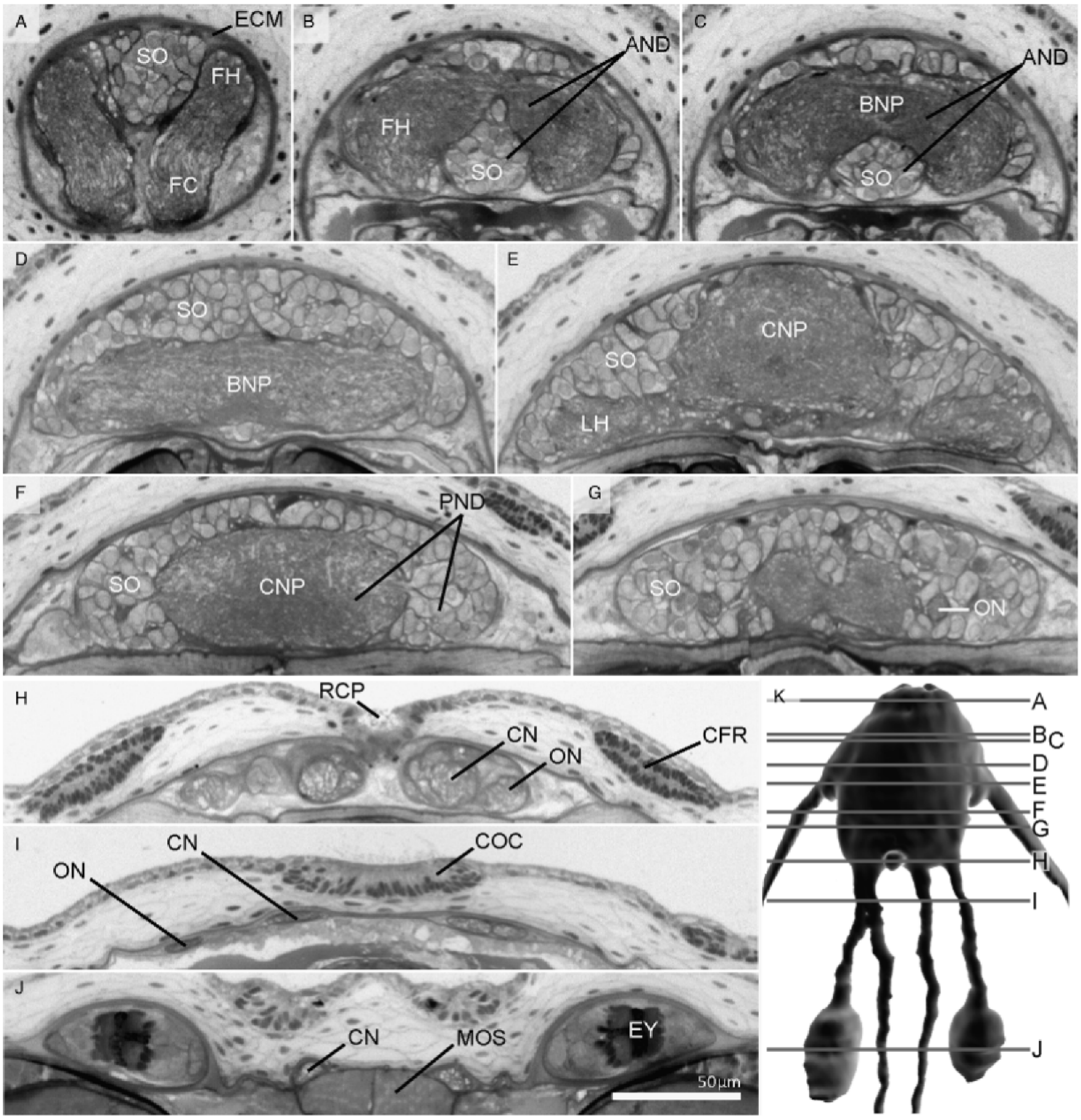

Fig. 4. Magnified views showing the histological anatomy of the brain and associated structures in *Ferrosagitta hispida* (A–G, I–K). **A.** Dorsal region of frontal connectives (frontal horn zone). **B.** Anterior neuropil domain posterior to A. **C.** Anterior part of the bridge neuropil. **D.** Posterior part of the bridge neuropil. **E.** Posterior neuropil domain. **F.** Posterior neuropil domain with core neuropil. **G.** Optic nerves detached from core neuropil. **H.** Posterior tip of the retrocerebral organ. **I.** Anterior part of the corona ciliata. **J.** Posterior part of the head, eyes, and coronal nerves remain close to mediosagittal plane. **K.** Position of each section in relation to the cephalic nervous system. AND, anterior neuropil domain; BNP, bridge neuropil; CFR, ciliary fence receptors; CN, coronal nerve; CNP, core neuropil; COC, corona ciliata; ECM, extracellular matrix; EY, eye; FC, frontal connective; FH, frontal horn; LH, lateral horn; MOS, musculus obliquus superficialis; ON, optic nerve; PND, posterior neuropil domain and associated cell cortex; RCP, pore opening of the retrocerebral organ; SO, somatic region.

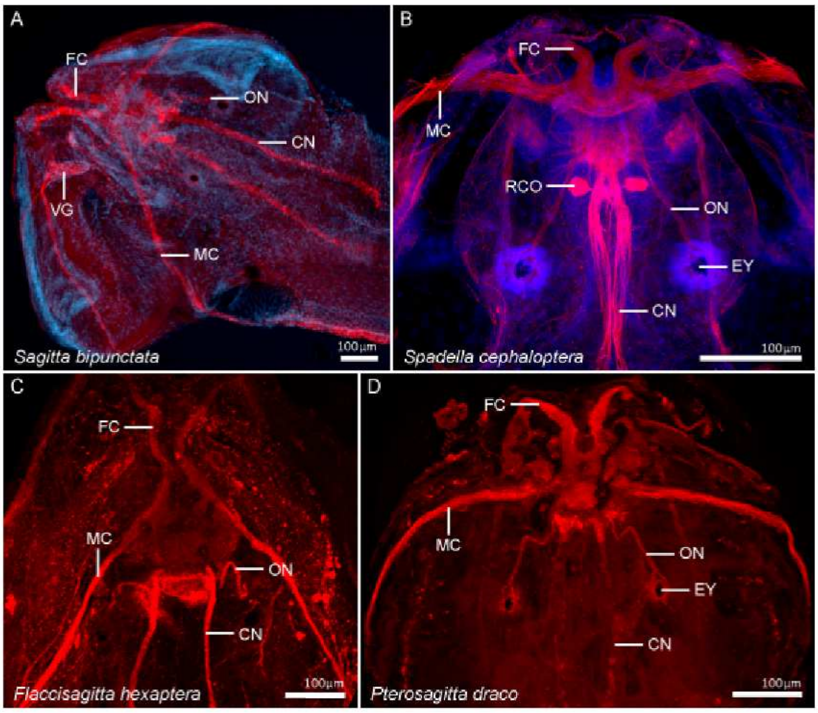

Fig. 5. Components of the cephalic nervous system of various chaetognath species, immunolocalization of tyrosinated tubulin (red) and histochemical labeling of nuclei (blue). (A) Conventional fluorescence microscopy combined with the Apotome structured illumination technique for optical sectioning; (B–D) confocal laser-scan microscopy. **A.** Head of *Sagitta bipunctata,* dorsolateral view. **B.** Brain of *Spadella cephaloptera,* dorsal view. **C.** Brain of *Flaccisagitta hexaptera,* dorsal view. **D.** Brain of *Pterosagitta draco,* dorsal view. CN, coronal nerve; EY, eye; FC, frontal connective; MC, main connective; ON, optic nerve; RCO, retrocerebral organ; VG, vestibular ganglia.

rior neuropil domain. This separation is also apparent in the specimens labeled for tyr-tubulin (Fig. 6C). The posterior neuropil domain is represented by what we named the core neuropil (Fig. 6C–G). In Sagittidae, the core neuropil is almost spherical, whereas in Spadellidae, it appears more or less rectangular. The immunohistochemical experiments support our previous result from the 3D reconstruction that the anterior neuropil domain is composed of the medially located bridge neuropil, from which the paired frontal horns and the paired lateral horns emerge (Fig. 6C,D). A DNA-specific marker confirmed that both neuropil domains are associated with neuronal somata (Fig. 6C,E), as shown by histological sections.

RFir neurons

Immunohistochemistry against RFamide-like neuropeptides labels a specific subset of neurons including their somata and arborizations (Figs. 6B, 7). In the beginning, we will describe the general labeling pattern present in all species that we have examined and then proceed with details of the groups. The description includes only strongly labeled structures that were consistently labeled in several specimens.

In the ventral nerve cord, a distinct set of individually identifiable RFir neurons is present (Harzsch et al. 2009). In this previous report, RFir neurites were seen to be present in the main connectives as they exit or enter the ventral nerve center, but it remained unclear if these are axons or dendrites, and what is the origin of these fibers. Likewise, these neurites were now traced in the main connectives as they feed into the brain. Furthermore, the frontal connectives contain RFir neurites. The pattern of RFir structures also revealed the two neuropil domains of the brain as the other methods did. RFir neurites can be seen crossing between the two neuropil domains. In the center of the core neuropil, RFir neurites form a dense neuropil plexus. A bilaterally arranged cluster is present, which comprises between one and three strongly labeled posterior lateral cells (PL: red arrowheads in Fig. 7; see also Fig. 8). These neurons project neurites into the core neuropil, and are the source of the RFir network in the core neuropil.

The posterior neurite bundle (PNB) extends transversely posterior to the bridge neuropil and merges with the core neuropil. Laterally, the PNB joins the main connectives that connect to the VNC. We could not unravel whether the axons of the large PL cells extend into the PNB to target the ventral

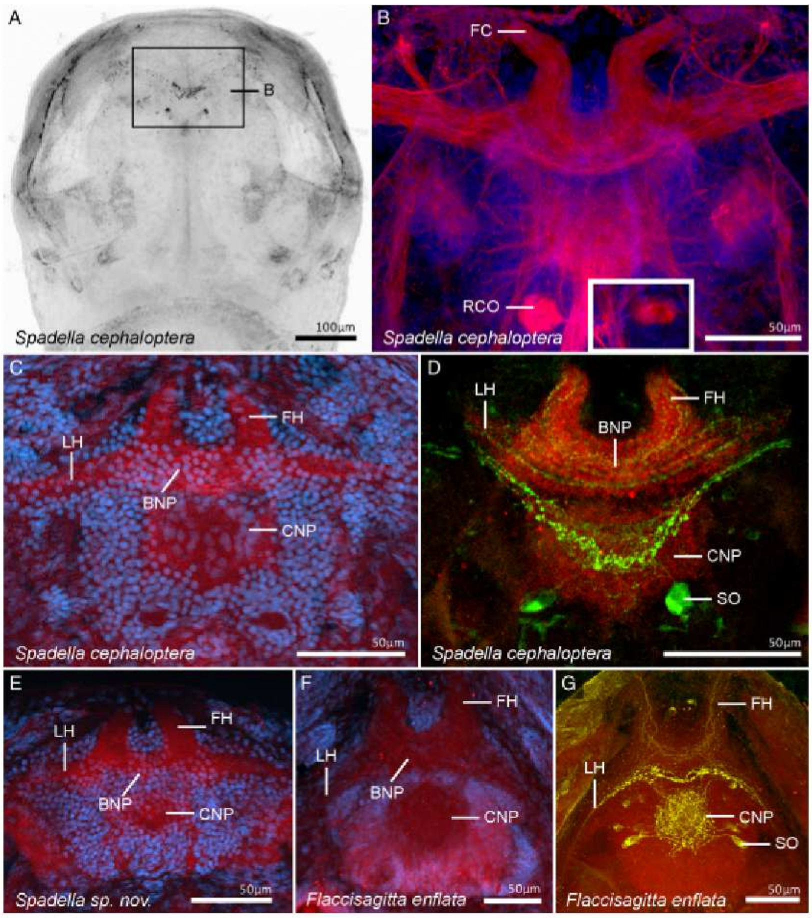

Fig. 6. **A.** Low magnification of the head of *Spadella cephaloptera,* immunolocalization of RFamide-like neuropeptides (black–white inverted image); the box indicates the labeled part of the brain. **B.** Immunolocalization of tyrosinated tubulin (red) and histochemical labeling of nuclei (blue) in the brain of *Spadella cephaloptera;* higher magnification of Fig 2. B. Inset: the core of the right retrocerebral organ is shown at a different exposure. **C.** Immunolocalization of synapsin (red) and histochemical labeling of nuclei (blue) in the brain of *S. cephaloptera.* **D.** Immunolocalization of synapsin (red) and RFamide-like neuropeptides (green) in the brain of *S. cephaloptera.* **E.** Immunolocalization of synapsin (red) and histochemical labeling of nuclei (blue) in the brain of *Spadella* sp. **F.** Immunolocalization of synapsin (red) and histochemical labeling of nuclei (blue) in the brain of *Flaccisagitta enflata.* **G.** Immunolocalization of synapsin (red) and RFamide-like neuropeptides (green) in the brain of *F. enflata.* A, B, D, G: confocal laser-scan microscopy; C, E, F: conventional fluorescence microscopy combined with the Apotome structured illumination technique for optical sectioning. B, brain; BNP, bridge neuropil; CNP, core neuropil; FC, frontal connective; FH, frontal horn; LH, lateral horn; RCO, retrocerebral organ; SO, somata.

nerve center, or if the PNB carries afferent axons from the ventral nerve center or both. Anteriorly to the PL cells, another bilaterally arranged RFir cell projects its neurite in the direction of the PNB, the median lateral cell (ML: blue arrowheads in Fig. 6; see also Fig. 7), but this neurite could not be traced further in most specimens. In the anterior neuropil domain, RFir fibers are present in the bridge neuropil, as well as the frontal and lateral horns, but the source of these fibers we could not trace. Transverse fibers in the base of the bridge neuropil extend in parallel to the PNB forming the median neurite bundle (MNB). The anterior neurite bundles (ANB) are closely associated with the frontal horns and within the bridge run in parallel to the MNB (Fig. 7). RFir neurites from the ANB establish a connection to the vestibular ganglia via the frontal connectives.

RFir in *Spadella*. In both *Spadella* species we examined, the pattern of RFir structures showed many similarities. Most notably, only a small portion of the core neuropil is filled with RFir fibers (Figs. 6D, 7A,B, 8). The PNB is the dominant RFir structure in the posterior domain of the brain. Its neurites ramify in the center of the core neuropil to give rise to the RFir network. The PNB has a V-like shape and extends laterally in anterior direction as a major contribution to the main connectives. Weakly labeled fibers establish a connection between the PNB and the MFB, thus linking the two brain domains. In the frontal horns, the neurites of the MFB seem to have lateral blind endings, and the somata that are the origin of these fibers could not be traced. The ANB is prominent and contains many fibers. In *S. cephaloptera,* three PL cells per side send projections to the neuropil. The somata are located on the

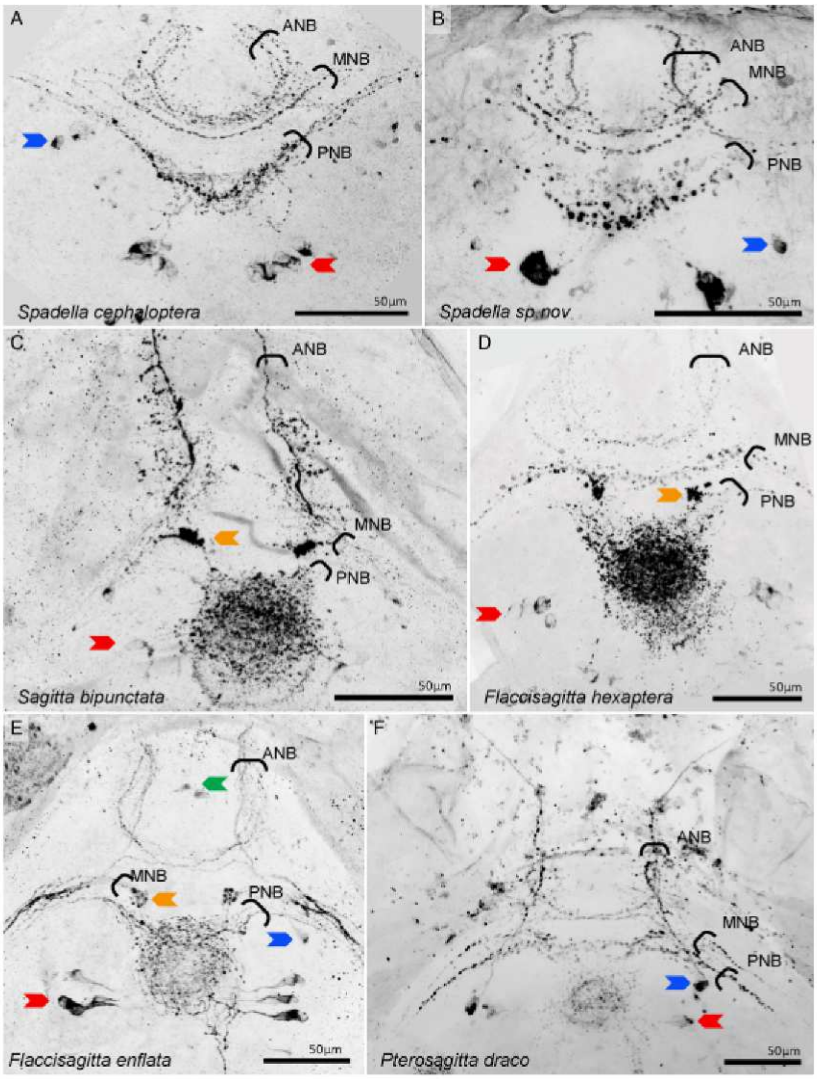
A
ANB
MNB
PNB
Spadella cephaloptera
50µm
B
ANB
MNB
PNB
Spadella sp.nov
50µm
C
ANB
MNB
PNB
Sagitta bipunctata
50µm
D
ANB
MNB
PNB
Flaccisagitta hexaptera
50µm
E
ANB
MNB
PNB
Flaccisagitta enflata
50µm
F
ANB
MNB
PNB
Pterosagitta draco
50µm

Fig. 7. RFamide-like immunoreactivity in the heads of various chaetognath species (species names are indicated); confocal laser-scan microscopy, black–white inverted images; red arrowheads, posterior lateral cells; blue arrowheads, median lateral cells; green arrowhead, anterior cells; orange arrowheads, satellite neuropils; for further information see text. ANB, anterior neurite bundle; MNB, median neurite bundle; PNB, posterior neurite bundle.

posterior side of the neuropil, slightly lateral. The ML cells send their axons in a median direction to join the PNB but the further course of these projections cannot be distinguished (Figs. 6D, 7A,B, 8). In *Spadella* sp., only one PL and one ML soma per side could be recognized, and the RFir structures in the fontal horns are labeled much weaker than in the core neuropil. In general, there seems to be less labeled structures compared with *S. cephaloptera,* which may be due to the small size of these organisms.

RFir in Sagittidae. In Sagittidae, the RFamidergic part of the core neuropil is circular, well defined, and located posteriorly to the PNB. It seems to be subdivided into two different regions, a smaller, densely labeled, dorsal part and a larger, but less strongly labeled, more ventral portion (Figs. 7C,D, 8). Furthermore, there are bilaterally paired small regions of neuropil, the satellite neuropils, in between the bridge neuropil and the PNB that exhibit an extremely strong signal of RFamide-like immunoreactivity (Fig. 7C–E). These satellites are linked to the core neuropil and have fiber connections to the ipsilateral main connectives, parallel to the other fibers that make up the MNB. The satellite neuropils are not present in Spadellidae. In addition to the connections to the satellite neuropils, the fibers in the main connectives can be subdivided according to their specific course. Some of these fibers seem to travel in the MNB to the other side, to establish a link between the contralateral main connectives, and they also give rise to immunolabeled ramifications in the core neuropil. However, some RFir fibers in the main connectives bypass the posterior brain domain to proceed toward the anterior domain (frontal horns) and into the frontal connectives. Some of these fibers remain on the ipsilateral side, whereas others cross to the contralateral side at the level of the bridge neuropil (Figs. 7E, 8).

Contrary to the Spadellidae, in which the neurites of the MNB seem to terminate blindly in the lateral horns, the MNB fibers of Sagittidae join the main connectives. In *Sagitta bipunctata,* except for MNB, most fibrous structures displayed strong immunreactivity, but were difficult to relate to the somata, because these were only weakly labeled. The ANB displayed small lateral branches that were not found in the other sagittid species so far. In *Flaccisagitta hexaptera,* the ML somata could not be traced. Up to three, paired, PL somata are present in most of the specimens, but frequently some of these were not labeled. The MNB is only weakly labeled in this species. In *Flaccisagitta enflata,* we noticed an additional pair of RFamid-expressing somata associated with the frontal horns, the anterior cells (green arrowheads). These cells could not be found in the other sagittid species. As in the other species, one pair of ML cells and usually three very prominent pairs of PL somata were found. Unlike the situation in other species, in *F. enflata,* especially in the ventral part of the core neuropil, single neurites could be distinguished and follow over some distance (Fig. 7E).

RFir in *Pterosagitta draco.* Unfortunately, we were able to successfully process only one specimen of *P. draco*. Nonetheless, we can say that the RFir pattern resembles the sagittid rather than the spadellid condition. Like in representatives of the genus *Sagitta,* the RFir network within the core neuropil is round and distinct from the more anterior PNB, to which it has connections (Fig. 7F). It receives projections from the PL cells that are located lateral to the neuropil. The number of PL cells could not be determined, because they exhibited only weak labeling. However, the paired ML somata are very prominent and their projections could be traced to join the ANB.

Discussion

General remarks on brain organization

The present study is the first that applied the technique of 3D reconstruction of histological section series to the nervous system in Chaetognatha. Moreover, we add a new species to the list of chaetognaths studied

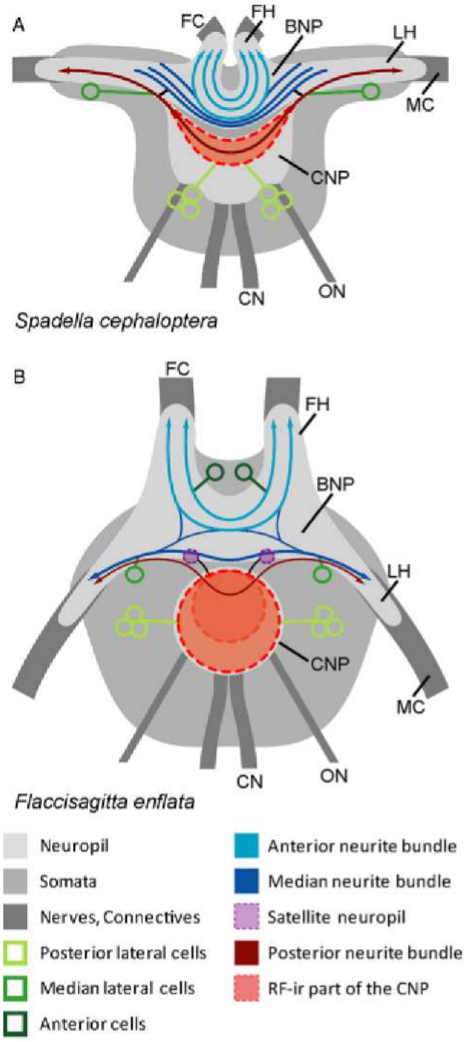

Fig. 8. Schematic drawings featuring the brains of *Spadella cephaloptera* and *Flaccisagitta enflata.* Only those structures are drawn that were strongly and consistently labeled in several specimens of the species represented here. The RFamide-like immunoreactive system is represented in color in relation to the neuropil, somata regions, and main nerves of the brain, which are shown in shades of gray. Those parts of the RFamidergic system within the posterior neuropil domain are colored in shades of red, whereas those within the anterior neuropil domain are represented in blue. The different types of neurons are coded by different shades of green. Note that the arrows at the end of fiber tracts are not meant to indicate a direction of information flow, but rather just indicate that these fibers proceed. Those parts of the anterior neuropil domain reaching into the frontal and main connectives and showing a high abundance of synapses are termed frontal and lateral horns. BNP, bridge neuropil; CN, coronal nerve; CNP, core neuropil; FC, frontal connective; FH, frontal horn; LH, lateral horn; MC, main connective; ON, optic nerve.

with regard to their neuroarchitecture (Table 1). Our data confirm previous reports (Krohn 1844; Hertwig 1880; von Ritter-Záhony 1909; Burfield 1927; Ahnelt 1980, 1984; Goto & Yoshida 1987; Salvini-Plawen 1988; Shinn 1997) that the cephalic nervous system is a complex of often deeply sunken basiepithelial ganglia that are interconnected by various connectives and commissures forming distinct circumesophageal and circumintestinal loops. In some aspects, however, the cephalic nervous system in *Ferosagitta hispida* differs considerably from those reported from other chaetognaths. Differences are, for instance, recognized in the pattern of nerves branching off the brain. The frontal and main connectives, as well as coronal and optic nerves, were found in all species examined so far (Table 1). Nonetheless, previous authors have illustrated, but not expressively named, additional fronto- and laterocerebral nerves (Hertwig 1880; Grassi 1883; Delage & Hérouard 1897). Later on, reinvestigations by von Ritter-Záhony (1909, 1911), Kuhl (1938), Burfield (1927), John (1933), and Goto & Yoshida (1987), partly on the same species, did not confirm the existence of these nerves. Therefore, the lack of fronto- and laterocerebral nerves in *F. hispida* seems to be less relevant for discussion, as their assumed absence is more likely due to misinterpretation rather than indicating interspecific divergences in the cephalic nervous system of the Chaetognatha.

However, there are clear indications that other aspects of nervous system architecture do diverge between chaetognath taxa. For instance, esophageal ganglia and esophageal nerves may be present or absent. In *F. hispida,* neither distinct esophageal ganglia nor esophageal nerves can be detected. The absence of these structures seems to be unusual, as nearly all previous authors have traced them in various chaetognath taxa (Table 1). Instead, we found a likewise unusual compartmentalization of the vestibular ganglia. It remains a matter of speculation whether the anterior portions of the vestibular ganglia in *F. hispida* resulted from a fusion of a formerly separated esophageal ganglion and less complex vestibular ganglia, or a loss of the esophageal ganglia and nerves. A similar problem concerns the absence of labial nerves and ganglia in *F. hispida* (Table 1). Interspecific variations are observed in the pattern of frontal, dorsal, mandibular, and vestibular nerves branching off the vestibular ganglia. The insertion pattern for these nerve pairs as described here for *F. hispida* differ from those of other sagittids (e.g., Hertwig 1880: figs. 2, 3; Kuhl 1938: figs. 15, 16; Goto & Yoshida 1987: fig. 1) as well as those of the spadellid species (John 1933: fig. 3B). This is in accordance with John (1933), who already mentioned considerable differences in shape of the vestibular ganglia, location of afferent/efferent nerves, and the inner cephalic course of these nerves between Sagittidae and Spadellidae.

All in all, we have to state that the nervous system in Chaetognatha, in general, and the cephalic nervous system, in particular, is not as constant as suggested by modern schematic reproductions (e.g., Goto & Yoshida 1987). Instead, it shows a certain degree of interspecific variation and divergence.

Division of the brain into two domains?

The present study is the first approach to compare the immunolocalization of several nervous system markers between several species in the genera *Spadella* and *Sagitta*. Immunolocalization data of tyr-tubulin as a general marker support several aspects of previous studies on brain architecture that used classical histological methods (e.g., Goto & Yoshida 1987; Shinn 1997 [review]; present report), such as the arrangement of the nerves and connectives, and the general brain composition of a neuropil surrounded by somata. However, our approach provides new insights into the internal organization of the entire cerebral complex (brain+retrocerebral organ *sensu* Salvini-Plawen 1988). Within the brain, we observed a clear subdivision into an anterior and a posterior neuropil domain. The immunohistochemical visualization of two distinct domains in the chaetognath brain is consistent with the results of the histological examinations.

In general, there are only a few studies that used electrophysiological methods to study possible functions of the various parts of the chaetognath nervous system, and these studies mainly focused on the neuromuscular system in the trunk (e.g., Bone & Pulsford 1984; Duvert & Savineau 1986; Savineau & Duvert 1986; Bone et al. 1987; Duvert et al. 1997; Tsutsui et al. 2000). Nonetheless, it is known that arrow worms display directional reactions to light, which are most likely mediated by the eyes (Goto & Yoshida 1981, 1984). Furthermore, arrow worms are able to detect vibrations in the water, which most likely helps them to detect prey (Feigenbaum & Reeve 1977). The posterior neuropil domain of the brain is connected to sensory systems of the arrow worm, namely the eyes and the corona ciliata, an organ with an unclear function but for which a role in chemoreception has been implicated (review: Shinn 1997).

Although electrophysiological information on the direction of excitation propagation in the cephalic nerves is missing, it seems likely that the optic nerves and coronal nerves, in addition to putative efferent components, also contain afferent fibers that provide sensory input to the posterior neuropil domain. Nonetheless, information about the exact termination site of this sensory input in terms of synaptic fields is missing. The vestibular papillae, presumably chemosensory or mechanosensory organs, are located on the ventral side of the chaetognath head, but the target of their afferents is not known (Bone & Pulsford 1984). Nonetheless, the retrocerebral organ is also closely associated with the posterior neuropil domain (Goto & Yoshida 1987; present study). Scharrer (1965) and Goto & Yoshida (1987) postulated this organ to be a baroreceptor, and suggested it to be composed of a network of microvilli. However, Shinn (1997) instead proposed some of these microvilli to be highly modified cilia. The fact that immunolocalization of tyr-tubulin showed a strong signal in the retrocerebral organ of *Spadella cephaloptera* supports the view that cilia may be present in this organ. Because tyr-tubulin is a component of a relatively dynamic subclass of interphase microtubules, an active growth and turnover of microtubules may take place in this organ.

The posterior neuropil domain of the brain is also linked to the ventral nerve center via the main connectives. The ventral nerve center most likely is involved in motor control (e.g., Bone & Pulsford 1984; Bone et al. 1987) and possibly also processes input from the fence receptor organs, mechanosensory structures that are distributed over the animal's body (Welsch & Storch 1983; Bone & Pulsford 1984). This mechanosensory input may also be communicated to the posterior neuropil domain via the main connectives. Fence receptor organs are also present on the head, but it is not known into which brain region their input is fed. Nonetheless, it would appear that one of the major tasks of the posterior neuropil brain domain may be to process and integrate different qualities of sensory input. Therefore, the posterior neuropil domain may be involved in the modulation of motor behaviors in response to changing sensory input.

The anterior neuropil brain domain is also linked to the ventral nerve center, but its main connections are with the esophageal, vestibular, and subesophageal ganglia via the frontal connectives and the esophageal commissure, which interconnects the vestibular ganglia. Likewise, most Protostomia possess specific neuronal structures that innervate the mouth opening, esophagus, and gut, collectively called the stomatogastric nervous system, a term that is being applied in a rather broad sense to describe a certain function rather than implying a homology of the nervous structures. These structures, in general, provide motor control of the associated muscles and relay afferent information from chemosensory and mechanosensory receptor cells associated with the feeding and digestion apparatus into the brain. As in chaetognaths, the stomatogastric innervation in most cases is part of the cephalic nervous system and is associated with the brain (e.g., Platyhelminthes: Reuter & Halton 2001; Nemertini: Bullock & Horridge 1965; Gastrotricha: Hochberg 2007a; Rothe & Schmidt-Rhaesa 2008, 2009; Nematoda: Bullock & Horridge 1965; Mollusca: Shigeno et al. 2007; Todt et al. 2008; Annelida: Orrhage & Müller 2005; Arthropoda: Bitsch & Bitsch 2009). However, the arrangement of the components of the stomatogastric nervous system show considerable variation between taxa projecting either anteriorly, ventrally, or posteriorly with regard to the brain. The arrangement of these structures naturally seems to be mainly dictated by the position of the mouth opening and esophagus.

Physiological data on the sensory and motor innervation of the feeding apparatus in Chaetognatha are not available and few studies have analyzed the physiological significance of the brain. Experiments on headless chaetognaths (Duvert et al. 2000) show that mature specimens can live, swim, attack prey, and display facets of mating behavior. These observations suggest that the ventral nerve center of Chaetognatha plays a major role in controlling feeding and reproduction behavior. However, the arrangement of the esophageal, vestibular ganglia, and their link via the frontal connectives and of the esophageal commissure, suggests that these structures also function as a stomatogastric nervous system. Considering the association of the stomatogastric nervous system with the anterior neuropil domain, we suggest that this part of the brain may assist in controlling the activity of the grasping spines by innervating the cephalic musculature, and may be involved in the innervation of the frontal and posterior teeth, the vestibular organs, and the musculature responsible for widening and closing the mouth. Finally, the anterior neuropil domain may also modulate the activity of the digestive system via the stomatogastric nerve that accompanies the esophagus subjacent to its bottom. The anterior and posterior parts of the brain together may function as a major coordination and integration center that interacts with the ventral nerve center in controlling the large scale behavior of these animals.

System of RFir neurons

RFamide-like immunoreactivity previously was studied in the brains of *Parasagitta setosa* (Bone et al. 1987) and *Paraspadella gotoi* (Goto et al.

1992). The results of these previous studies, specifically the arrangement of neuropils and fiber tracts, correspond well with our observations. Remarkably, in both *P. setosa* (Bone et al. 1987; their cell type one and two) and in *P. gotoi* (Goto et al. 1992), RFir neurons are present in number, position, and axonal projection pattern that which closely matches the posterior lateral cells reported here. The presence of individually identifiable neurons has now been firmly established for the ventral nerve center in Chaetognatha (Harzsch & Müller 2007; Harzsch et al. 2009). This means that neurons within the central nervous system can be treated as individuals that can be recognized from animal to animal of one species, or even in individuals belonging to different species that are more-or-less closely related. Our present data, in combination with those of previous studies, provide evidence for a group of identifiable neurons in the brain of Chaetognatha.

The RFir cell somata three and four, described for *P. setosa* by Bone et al. (1987: figs. 13, 14), most likely were mistaken for what we named the satellite neuropils, small regions of neuropil that display a very strong immunoreactivity. These may be neuromodulatory/neurosecretory sites, where the neuropetide is diffusely released into the surrounding neuronal tissue by varicosities that do not have point-to-point postsynaptic partners. Similar release sites of RFamide-like peptides are present in the anterior part of the ventral nerve center (Harzsch et al. 2009).

Comparison of Spadellidae and Sagittidae

The schematic drawings in Fig. 8 compare *S. cephaloptera* and *Flaccisagitta enflata* as individual representatives of the Spadellidae and Sagittidae. Only those structures are featured that were strongly and consistently labeled in several specimens of the species. In terms of general architecture, as seen in the tyr-tubulin labeling, there is a difference between Spadellidae and Sagittidae in the angle at which the main connective enters the brain. Another variation between these taxa is the shape of the core neuropil and especially the expansion of the RFir fiber network in the core neuropil. In *F. enflata,* this network is the most dominant structure, whereas in *S. cephaloptera* it appears to be little more than some side branches of the PNB that transverses the brain. The satellite neuropils found in all representatives of *Sagitta* are absent in *Spadella*. Differences between the two genera also concern the arrangement of the MNBs, but this warrants a more detailed look with other markers. Commonalties exist between the two taxa concerning the arrangement of the posterior and median lateral cells. Along the same lines, the pattern of RFir neurons in the ventral nerve centers displays many communal features down to the level of single individually identifiable neurons, but also distinct differences which may allow use of this set of characters to analyze the phylogenetic relationships within Chaetognatha (Harzsch et al. 2009).

Similar to the ventral nerve center (compare Harzsch et al. 2009), the pattern of RFir neurons in the brain of *Pterosagitta draco* corresponds more to that of Sagittidae than to Spadellidae. This result is consistent with the traditional phylogeny (e.g., Tokioka 1965a; Salvini-Plawen 1986), mainly based on the presence or absence of transverse muscles (phragms). However, on the basis of the 18S rRNA analysis (Papillon et al. 2006), the Spadellidae appear as a paraphyletic assemblage, from which *P. draco,* a species without phragms, derives. Interestingly, the status of *P. draco* also puzzled morphologists. In accordance with the molecular hypothesis, Tokioka (1965b) and Dallot & Ibanez (1972) also proposed a possible positioning of *P. draco* closer to Spadellidae than to Sagittidae. Because *P. draco* displays a set of morphological characters shared with Sagittidae and Spadellidae, new data from the Eukrohnidae, and the presumably basally branching Heterokrohniidae, are necessary for reconstructing the ancestral architecture of the arrow worm nervous system.

The first brain of Bilateria?

Considering that Chaetognatha may have branched off close to the split between deuterostomes and protostomes (Fig. 9) the structure of their nervous system may reveal insights into the evolution of the earliest bilaterian brains. Understanding the structure of the nervous system in the last common ancestor of Bilateria (LCBA) is a topic that is hotly debated (e.g., Holland 2003; Denes et al. 2007; Hirth & Reichert 2007; Lichtneckert & Reichert 2007; Lowe 2007; Schmidt-Rhaesa 2007; Arendt et al. 2008; Benito-Gutiérrez & Arendt 2009; Nomaksteinsky et al. 2009; Reichert 2009; Harzsch & Wanninger 2010). One of the important questions in this dispute is whether the nervous system of the LCBA was decentralized and structured as an epithelial plexus without concentrations, or had already centralized elements such as longitudinal chords or even a brain. Reichert and colleagues have repeatedly stressed striking similarities in topological expression patterns of conserved anterior–posterior and dorsoventral patterning genes during insect and mammalian nervous system development. This has led these authors to conclude that orthologous genes had been in-

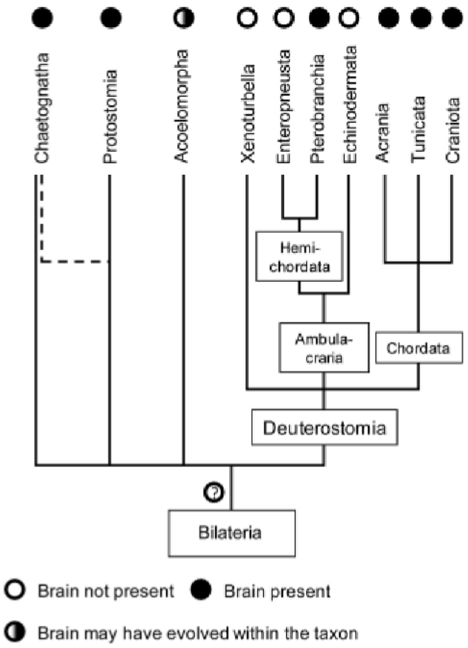

Fig. 9. Basal rooting of the Bilateria with the Chaetognatha considered an independent clade in relation to Protostomia, Acoelomorpha, and Deuterostomia, or as being the sister-group to Protostomia. The presence or absence of a brain in the various taxa is indicated.

volved in neural specification already in the LCBA (Lichtneckert & Reichert 2005, 2007; Reichert 2009).

Accordingly, two alternative hypotheses have been proposed to explain the matching gene expression patterns in insect and chordate brains: "The first of these postulates that the ancestral bilaterian nervous system was already centralized and had its development governed by conserved genetic mechanisms that are still apparent in extant insects and mammals (monophyletic origin of the brain). The second hypothesis is that the ancestral bilaterian nervous system was controlled by conserved genetic mechanisms that still operate in arthropods and vertebrates, but that centralization of the nervous system occurred independently in protostome and deuterostome lineages (polyphyletic origin of the brain)" (Lichtneckert & Reichert 2007:65). Accordingly, the question of whether or not CNS centralization occurred independently in protostomes or deuterostomes appears unresolved by molecular developmental analyses (Harzsch & Wanninger 2010).

In the following, we want to explore if neuroanatomy can contribute new aspects to this debate and will compare the brain of chaetognaths with that of other representatives of the Bilateria (larval characters will not be considered here, though). We suggest rather broad definition of the brain, as an anterior condensation of nervous tissue that receives and processes input from sensory organs. The taxon Xenoturbellida is a key player in any discussion on the characteristics of the LCBA. These animals were previously suggested to be allied to turbellarian flatworms or acoel flatworms (Raikova et al. 2000b; review: Telford 2008) but phylogenomic data recently provided compelling evidence that Xenoturbellida are deuterostomes (Bourlat et al. 2006, 2009; Dunn et al. 2008). Yet, the relationship of Xenoturbellida to the other deuterostome taxa remains unresolved (Stach et al. 2005; Telford 2008; Cannon et al. 2009) (Fig. 9). Despite the controversy on their phylogenetic position, there is no doubt that the nervous system of Xenoturbellida is an intraepidermal plexus that does not have any condensations such as cords or ganglia (Raikova et al. 2000a).

Considering the other deuterostome taxa, in the Echinodermata, a non-centralized nervous system organized as a plexus is present but, in addition, the radial cords and the circumoral nerve ring represent centralized elements. A brain is absent, however (e.g., García-Arrarás et al. 2001; Mashanov et al. 2006, 2007, 2009; Díaz-Balzac et al. 2007; review: Holland 2003). The Hemichordata as the sister group of Echinodermata comprise the Pterobranchia and Enteropneusta (Cameron 2005; Zeng & Swalla 2005; Cannon et al. 2009). Pterobranchia, in addition to an intraepidermal plexus, exhibit a ganglionic concentration of nervous tissue (Rehkämper et al. 1987) that may be considered as a brain. The Enteropneusta currently occupy a central role in the discussion on nervous system evolution in Deuterostomia (Lowe et al. 2003, 2006; Lowe 2007; Benito-Gutiérrez & Arendt 2009; Nomaksteinsky et al. 2009). Their adult bodyplan displays several forms of nervous systems, namely an intraepidermal plexus, and both a dorsal and a ventral nerve cord (Knight-Jones 1952; Dilly et al. 1970; Stach et al. 2005). A recent study on enteropneust neuroanatomy has emphasized the importance of the centralized components as opposed to the plexus (Nomaksteinsky et al. 2009), but it remains problematic if one of these concentrations functions as a brain. However, it is beyond any doubt that all taxa within Chordata, in addition to having retained parts of the ancestral bilaterian intraepidermal plexus, did evolve a brain (e.g., Tunicata/Ascidiacea: Meinertzhagen & Okamura 2001; Meinertzhagen et al. 2004; Tunicata/Apendicularia: Bollner et al. 1991; Cañestro et al. 2005; Søviknes et al. 2005; Tunicata/Thaliacea: Lacalli & Holland 1998; Stach 2005; Acrania: Wicht

& Lacalli 2005; reviews: Holland 2003; Mackie & Burighel 2005; Lacalli 2008).

Acoel flatworms (Acoela), in addition to Xenoturbellida, represent another taxon that is discussed as being among the earliest extant offshoots of Bilateria (review Deutsch 2008). Acoela traditionally have been classified within the Platyhelminthes, but molecular studies have subsequently suggested that they are among the earliest diverging Bilateria (Philippe et al. 2007; Sempere et al. 2007). In a most recent contribution to this question, the conflicting sets of morphological/developmental data and phylogenomic results were discussed (Egger et al. 2009). These authors conclude that both an inclusion of Acoela within Platyhelminthes and their separation from flatworms as basal bilaterians are well-supported alternatives. The nervous systems of representatives of the Acoela and the related Nemertodermatida have been thoroughly analyzed by Reuter colleagues (Raikova et al. 1998, 2000b, 2004; Reuter et al. 1998, 2001a–c) who demonstrated a great variability in the neuronal organization in this taxon.

In general, the acoel nervous system displays an architecture that is distinct from that in Platyhelminthes, suggesting a deep gap between members of these two taxa (Raikova et al. 2004). These authors suggest the acoel ancestor possessed a "diffuse, nerve net-like nervous system," and that a more complex neural organization may have occurred once or several times within the Acoela (Raikova et al. 2004). Because the vast majority of recent Acoelomorpha are free-living predators that actively hunt for prey, a secondary loss of an originally concentrated CNS seems unlikely. It would appear that the Acoela are an ideal taxon to study the emergence of a concentrated nervous system, and the evolution of the brain. In some acoel taxa, a symmetrical "brain-like" structure is represented by thickened commissural fibers, and hence was named "a commissural brain" (Raikova et al. 1998), but other neuroanatomists doubt if this structure can be called a brain (Harzsch & Wanninger 2010). This controversy mirrors a general difficulty to provide a definition of "what is a brain" that is satisfactory from a morphological and functional point of view.

Morphology and neurochemistry of the nervous system in Platyhelminthes have been thoroughly explored (reviews: Fairweather & Halton 1991; Halton & Gustafsson 1996; Reuter et al. 1998; Reuter & Halton 2001; Gustafsson et al. 2002; Umesono & Agata 2009). There is a long-standing record of studies on the general organization of the flatworm nervous system (e.g., Agata et al. 1998; Tazaki et al. 1999; Reuter et al. 2001a–c; Okamoto et al. 2005; Morris et al. 2007; Cebià 2008), and the nature and distribution of neuroactive substances is still being intensely explored (e.g., Nishimura et al. 2007, 2008a,b; McVeigh et al. 2009). Members of the Platyhelminthes have a distinct brain that is associated with sensory organs, and is formed by an outer cortex of neural somata surrounding a neuropil. This neuropil, according to a recent account on *Macrostomum lignano,* is subdivided into compartments or neuropil domains (Morris et al. 2007).

Moving further into the Protostomia, the presence of the brain is a unifying feature (Schmidt-Rhaesa 2007). Nielsen (2001, 2005) suggested that a perioral/circumesophageal brain, in addition to the intraepidermal nerve plexus, characterizes their ground pattern. Such a circumoral brain, in which the components of the cephalic nervous system are arranged around the esophagus, can be recognized in most protostomian groups and is by Nielsen considered to be one of the key apomorphies of the Protostomia. Basal molluscs do posses a well differentiated brain and ganglia (e.g., Polyplacophora: Moroz et al. 1994; Aplacophora: Shigeno et al. 2007; Solenogstares: Todt et al. 2008) as do most annelida (e.g., Polychaeta: Orrhage & Müller 2005; Müller 2006; Heuer & Loesel 2008; Oligochaeta: Spörhase-Eichmann et al. 1987a,b; Telkes et al. 1996). A new surge of neuroanatomical papers provides a more detailed insight into the brains of minute organisms such as Gastrotricha (Hochberg 2007a; Rothe & Schmidt-Rhaesa 2008, 2009) and members of the Gnathifera (Rotifera: Hochberg 2006, 2007b, 2009; Leasi et al. 2009; Acanthocephala: Miller et al. 1973; Dunagan & Miller 1975; Gee 1989; Gnathostomulida: Müller & Sterrer 2004). The brain architecture of Tentaculata and Cycloneurolia has been thoroughly reviewed by Schmidt-Rhaesa (2007), and that of Arthropoda by Burrows (1996).

In conclusion, it appears that in the deep metazoan nodes, concentration of the ancestral plexus to form a brain occurred independently at least twice, namely once after the protostome–deuterostome split on the branch leading to the protostomes, and once along the chordate line. The possible evolution of a brain within Acoelomorpha has been discussed above. If Chaetognatha represent a separate evolutionary lineage in addition to Protostomia and Deuterostomia, brains may have evolved at least 3 × convergently in Bilateria (Fig. 9). However, considering the great variation of the cephalic nervous systems within Protostomia, we cannot find any characteristics that would argue in favor of placing chaetognath brains outside of the Protostomia. Rather, we see the circumoral arrangement of their cephalic nervous system—the circumoral brain *sensu* Nielsen (2001)—as an argument that suggests protostome affinities (Marlétaz et al. 2006, 2008), in which case the protostomian ancestor most likely was already equipped with a brain.

Acknowledgments. The authors gratefully acknowledge E. Buchner (Würzburg) for generously providing samples of the SYNORF-1 antibody. We also wish to thank Mag. Gerwin Gretschel, director of the Meereschule in Pula (Croatia), for providing a boat and diving equipment for the collection of specimens of *Spadella* sp. nov. in Valsaline. Our special thanks go to Akihiro Shiroza and John Lamkin (University of Miami-RSMAS), as well as Gisèle Champalbert and Marc Pagano (Institute for Research and Development UR 167) for helping us to collect specimens. We are indebted to G. Shinn for providing specimens and constructive comments on the draft of this paper. This study was supported by grant HA 2540/7-2 in the DFG focus program "Metazoan Deep Phylogeny" and by the Max Planck Society.

References

Agata K, Soejima Y, Kato K, Kobayashi C, Umesono Y, & Watanabe K. 1998. Structure of the planarian central nervous system (CNS) revealed by neuronal cell markers. Zool. Sci. 15: 433–440.

Ahnelt P 1980. Das Coelom der Chaetognathen. Dissertation, University of Vienna. 380 pp.

——— 1984. Chaetognatha. In: Biology of the Integument. Vol. I. Invertebrates. Bereiter-Hahn J, Matolsky AG, & Richards KS, eds., pp. 746–755. Springer, Berlin, Germany.

Arendt D, Denes AS, Jekely G, & Tessmar-Raible K 2008. The evolution of nervous system centralization. Philos. Trans. R. Soc. Lond. B 363: 1523–1528.

Ax P 2001. Das System der Metazoa III. Spektrum Akademischer Verlag, Göttingen, Germany.

Benito-Gutiérrez E & Arendt D 2009. CNS evolution: new insight from the mud. Curr. Biol. 19: R640–R642.

Bitsch J & Bitsch C 2009. The tritocerebrum and the clypeolabrum in mandibulate arthropods: segmental interpretations. Acta Zoologica doi: 10.1111/j.1463-6395.2009.00402.x.

Bollner T, Storm-Mathisen J, & Ottersen OP 1991. GABA-like immunoreactivity in the nervous system of *Oikopleura dioica* (Appendicularia). Biol. Bull. 180: 119–124.

Bone Q & Goto T 1991. The nervous system. In: The Biology of Chaetognaths. Bone Q, Kapp H, & Pierrot-Bults AC, eds., pp. 18–31. Oxford University Press, Oxford, UK.

Bone Q & Pulsford A 1984. The sense organs and ventral ganglion of *Sagitta* (Chaetognatha). Acta Zool. 65: 209–220.

Bone Q, Grimmelikhuijzen CLP, Pulsford A, & Ryan KP 1987. Possible transmitter functions of acetylcholine an RFamide-like substance in *Sagitta* (Chaetognatha). Proc. R. Soc. Lond. B 230: 1–14.

Bourlat SJ, Juliusdottir T, Lowe CJ, Freeman R, Aronowicz J, Kirschner M, Lander ES, Thorndyke M, Nakano H, Kohn AB, Heyland A, Moroz LL, Copley RR, & Telford MJ 2006. Nature 444: 85–88.

Bourlat SJ, Rota-Stabelli O, Lanfear R, & Telford MJ 2009. The mitochondrial genome structure of *Xenoturbella bocki* (phylum Xenoturbellida) is ancestral within the deuterostomes. BMC Evol. Biol. 9: 107.

Bullock TH 1965. Chapter 27. Chaetognatha, Pogonophora, Hemichordata, and Chordata Tunicata. In: Structure and Function in the Nervous System of Invertebrates, Vol. II. Bullock TH & Horridge GA, eds., pp. 1559–1592. W.H. Freeman and Company, San Francisco, CA, USA.

Bullock TH, & Horridge GA, (eds.) 1965. Structure and Function in the Nervous Systems of Invertebrates, Vol. I. W.H. Freeman and Company, San Francisco, CA, USA.

Burfield ST 1927. Sagitta. L.M.B.C. Memoirs. XXVIII, Liverpool. Proc. Trans. Liverpool Biol. Soc. 42: 1–104.

Burrows M 1996. The Neurobiology of an Insect Brain. Oxford University Press, Oxford, UK.

Cameron CB 2005. A phylogeny of the hemichordates based on morphological characters. Can. J. Zool. 83: 196–215.

Cañestro C, Bassham S, & Postlethwait J 2005. Development of the central nervous system in the larvacean *Oikopleura dioica* and the evolution of the chordate brain. Dev. Biol. 285: 298–315.

Cannon JT, Rychel AL, Eccleston H, Halanych KM, & Swalla BJ 2009. Molecular phylogeny of hemichordata, with updated status of deep-sea enteropneusts. Mol. Phylogenet. Evol. 52: 17–24.

Cebià F 2008. Organization of the nervous system in the model planarian *Schmidtea mediterranea*: an immunocytochemical study. Neurosci. Res. 61: 375–384.

Dallot S & Ibanez F 1972. Etude préliminaire de la morphologie et de l'évolution chez les chaetognathes. Inv. Pesq. 36: 31–41.

Delage Y & Hérouard E 1897. Traité de Zoologie Concrète. Tome V. Les Vermidiens. Schleicher Frères, Paris, France. 364 pp.

Denes AS, Jekely G, Steinmetz PR, Raible F, Snyman H, Prud'homme B, Ferrier DE, Balavoine G, & Arendt D 2007. Molecular architecture of annelid nerve cord supports common origin of nervous system centralization in Bilateria. Cell 129: 277–288.

Deutsch JS 2008. Do acoels climb up the "Scale of Beings"? Evol. Dev. 10: 135–140.

Díaz-Balzac CA, Santacana-Laffitte G, San Miguel-Ruíz E, Tossas K, Valentín-Tirado G, Rives-Sánchez M, Mesleh A, Torres II, & García-Arrarás JE 2007. Identification of nerve plexi in connective tissues of the sea cucumber *Holothuria glaberrima* by using a novel nerve-specific antibody. Biol. Bull. 213: 28–42.

Dilly PN, Welsch U, & Storch V 1970. The structure of the nerve fibre layer and neurocord in the enteropneusts. Z. Zellforsch. 103: 129–148.

Dockray GJ 2004. The expanding family of RF-amide peptides and their effects on feeding behaviour. Exp. Physiol. 89: 229–235.

Dunagan TT & Miller DM 1975. Anatomy of the cerebral Ganglion of the male Acanthocephalan, *Miliformis dubius*. J. Comp. Neurol. 164: 483–494.

Dunn CW, Hejnol A, Matus DQ, Pang K, Browne WE, Smith SA, Seaver E, Rouse GW, Obst M, Edgecombe GD, Soerensen MV, Haddock SHD, Schmidt-Rhaesa A, Okusu A, Moebjerg Kristensen R, Wheeler WC, Martindale MQ, & Giribet G 2008. Broad phylogenomic sampling improves resolution of the animal tree of life. Nature 452: 745–749.

Duvert M & Barets AL 1983. Ultrastructural studies of neuromuscular junctions in visceral and skeletal muscles of the chaetognath *Sagitta setosa*. Cell Tissue Res. 233: 657–669.

Duvert M, Perez Y, & Casanova J 2000. Wound healing and survival of beheaded chaetognaths. J. Mar. Biol. Assoc. UK 80: 891–898.

Duvert M & Savineau J 1986. Ultrastructural and physiological studies of the contraction of the trunk musculature of *Sagitta setosa* (Chaetognath). Tissue Cell 18: 937–952.

Duvert M, Savineau JP, Campistron G, & Onteniente B 1997. Distribution and role of aspartate in the nervous system of the chaetognath *Sagitta*. J. Comp. Neurol. 380: 485–494.

Egger B, Steinke D, Tarui H, De Mulder K, Arendt D, Borgonie G, Funayama N, Gschwentner R, Hartenstein V, Hobmayer B, Hooge M, Hrouda M, Ishida S, Kobayashi C, Kuales G, Nishimura O, Pfister D, Rieger R, Salvenmoser W, Smith J III, Technau U, Tyler S, Agata K, Salzburger W, & Ladurner P 2009. To be or not to be a flatworm: the acoel controversy. PLoS One 4–5.

Fairweather I & Halton DW 1991. Neuropeptides in platyhelminths. Peptides 102: 77–92.

Feigenbaum D & Reeve MR 1977. Prey detection in the Chaetognatha: response to a vibrating probe and experimental determination of attack distance in large aquaria. Limnol. Oceanogr. 22: 1052–1058.

García-Arrarás JE, Rojas-Soto M, Jiménez LB, & Díaz-Miranda L 2001. The enteric nervous system of echinoderms: unexpected complexity revealed by neurochemical analysis. J. Exp. Biol. 204: 865–873.

Gee RJ 1989. The nervous system in the praesoma of *Echinorhynchus salmonis* (Acanthocephala: Echinorhynchidae). J. Morphol. 201: 273–284.

Goto T & Yoshida M 1981. Oriented light reactions of the arrow worm *Sagitta crassa* Tokioka. Biol. Bull. 160: 419–430.

——— 1984. Photoreception in Chaetognata. In: Photoreception and Vision in Invertebrates. Ali MA, ed., pp. 721–742. Plenum Publishing Corporation, New York, NY, USA.

——— 1987. Nervous system in Chaetognatha. In: Nervous Systems in Invertebrates. Ali MA, ed., pp. 461–481. Plenum Publishing Corporation, New York, NY, USA.

——— 1988. Histochemical demonstration of a rhodopsin-like substance in the eye of the arrow-worm, *Spadella schizoptera* (Chaetognatha). Exp. Biol. 48: 1–4.

Goto T, Takasu N, & Yoshida M 1984. A unique photoreceptive structure in the arrowworms *Sagitta crassa* and *Spadella schizoptera* (Chaetognatha). Cell Tissue Res. 235: 471–478.

Goto T, Terazaki M, & Yoshida M 1989. Comparative morphology of the eyes of *Sagitta* (Chaetognatha) in relation to depth of habitat. Exp. Biol. 48: 95–105.

Goto T, Katayama-Kumoi Y, Tohyama M, & Yoshida M 1992. Distribution and development of the serotonin- and RFamide-like immunoreactive neurons in the arrowworm, *Paraspadella gotoi* (Chaetognatha). Cell Tissue Res. 267: 215–222.

Grassi B 1881. Anatomia comparata. Intorno ai Chetognathi. Nota preliminare. Rend. Reale Ist. Lomb. Sci. Lett. 14: 199–214.

——— 1883. I Chetognathi. Anatomia a sistematica con aggiunte embriologiche. Fauna Flora Golfes Neapel 5: 1–126.

Greenberg MJ & Price DA 1992. Relationships among the FMRFamide-like peptides. Prog. Brain Res. 92: 25–37.

Grimmelikhuijzen CJP 1985. Antisera to the sequence Arg–Phe-amide visualize neuronal centralization in hydroid polyps. Cell Tissue Res. 241: 171–182.

Grimmelikhuijzen CJP & Spencer AN 1984. FMRFamide immunoreactivity in the nervous system of the medusa *Polyorchis penicillatus*. J. Comp. Neurol. 230: 361–371.

Gustafsson MKS, Halton DW, Kreshchenko ND, Movsessian SO, Raikova OI, Reuter M, & Terenina NB 2002. Peptides 23: 2053–2061.

Halton DW & Gustafsson MKS 1996. Functional morphology of the platyhelminth nervous system. Parasitology 113: 47–72.

Hanström B 1928. Vergleichende Anatomie des Nervensystems der wirbellosen Tiere unter Berücksichtigung seiner Funktion. Springer Verlag, Berlin, Germany. 189 pp.

Harzsch S & Hansson BS 2008. Brain architecture in the terrestrial hermit crab *Coenobita clypeatus* (Anomura, Coenobitidae), a crustacean with a good aerial sense of smell. BMC Neurosci. 9: 58.

Harzsch S & Müller CHG 2007. A new look at the ventral nerve centre of *Sagitta*: implications for the phylogenetic position of Chaetognatha (arrow worms) and the evolution of the bilaterian nervous system. Front. Zool. 4: 14.

Harzsch S & Wanninger A 2010. Evolution of invertebrate nervous systems: the Chaetognatha as a case study. Acta Zool. 91: 35–41.

Harzsch S, Anger K, & Dawirs RR 1997. Immunocytochemical detection of acetylated tubulin and *Drosophila* synapsin in the embryonic crustacean nervous system. Int. J. Dev. Biol. 41: 477–484.

Harzsch S, Müller CHG, Rieger V, Perez Y, Sintoni S, Sardet C, & Hansson BS 2009. Fine structure of the ventral nerve centre and interspecific identification of individual neurons in the enigmatic Chaetognatha. Zoomorphology 128: 53–73.

Hertwig O 1880. Die Chaetognathen. Mon. Jena Z. Med. Naturw. 14: 196–311.

Heuer CM & Loesel R 2008. Immunofluorescence analysis of the internal brain anatomy of *Nereis diversicolor* (Polychaeta, Annelida). Cell Tissue Res. 331: 713–724.

Hirth F & Reichert H 2007. Basic nervous system types: one or many? In: Evolution of Nervous Systems, Vol. 1. Kaas JH, ed., pp. 55–72. Academic Press, Oxford, UK.

Hochberg R 2006. On the serotonergic nervous system of two planktonic rotifers, *Conochilus coenobasis* and *C. dossuarius* (Monogononta, Flosculariacea, Conochilidae). Zool. Anz. 245: 53–62.

——— 2007a. Comparative immunohistochemistry of the cerebral ganglion in Gastrotricha: an analysis of FMRFamide-like immunoreactivity in *Neodasys cirritus* (Chatonotida), *Xenodasys riedli* and *Turbanella* cf. *hyalina* (Macrodasyida). Zoomorphology 126: 245–264.

——— 2007b. Topology of the nervous system of *Notommata copeus* (Rotifera: Monogononta) revealed with anti-FMRFamide, -SCPb, and -serotonin (5-HT) immunohistochemistry. Invertebr. Biol. 126: 247–256.

——— 2009. Three-dimensional reconstruction and neural map of the serotonergic brain of *Asplanchna brightwellii* (Rotifera, Monogononta). J. Morphol. 270: 430–441.

Holland ND 2003. Early central nervous system evolution: an era of skin brains? Nat. Rev. Neurosci. 4: 617–627.

John CC 1933. Habits, structure and development of *Spadella cephaloptera*. Q. J. Microsc. Sci. 75: 625–696.

Kapp H 1991. Morphology and anatomy. In: The Biology of Chaetognaths. Bone Q, Kapp H, & Pierrot-Bults AC, eds., pp. 5–17. Oxford University Press, Oxford, UK.

——— 2007. Chaetognatha, Pfeilwürmer. In: Spezielle Zoologie Teil 1. Westheide W & Rieger R, eds., pp. 898–904. Gustav Fischer Verlag, Stuttgart, Germany.

Klagges BRE, Heimbeck G, Godenschwege TA, Hofbauer A, Pflugfelder GO, Reifegerste R, Reisch D, Schaupp M, Buchner S, & Buchner E 1996. Invertebrate synapsins: a single gene codes for several isoforms in *Drosophila*. J. Neurosci. 16: 3154–3165.

Knight-Jones EW 1952. On the nervous system of *Saccoglossus cambrensis* (Enteropneusta). Philos. Trans. R. Soc. Lond. B 236: 315–354.

Kowalevsky A 1871. Entwicklungsgeschichte der *Sagitta*. Mém. Acad. Imp. Sci. St. Petersbourg (VII série) 16: 7–12.

Kreis TE 1987. Microtubules containing detyrosinated tubulin are less dynamic. EMBO J. 6: 2597–2606.

Kriegsfeld LJ 2006. Driving reproduction: RFamide peptides behind the wheel. Horm. Behav. 50: 655–666.

Krohn A 1844. Anatomisch physiologische Beobachtungen über die Sagitta bipunctata. Nestler & Melle, Hamburg, Germany. 16 pp.

Kuhl W 1938. Chaetognatha. In: Klassen und Ordnungen des Tierreiches, Bd IV, Abt. IV, Buch 2, Teil 1. Bronn HG, ed., pp. 1–226. Akademische Verlagsgesellschaft M. B. H. Leipzig, Leipzig, Germany.

Lacalli TC 2008. Basic features of the ancestral chordate brain: a protochordate perspective. Brain Res. Bull. 75: 3319–3323.

Lacalli TC & Holland LZ 1998. The developing dorsal ganglion of the salp *Thalia democratia,* and the nature of the ancestral chordate brain. Philos. Trans. R. Soc. Lond. 353: 1943–1967.

Langerhans P 1878. Das Nervensystem der Chaetognathen. Monatsber. Kön. Acad. Wiss. Berlin: 189–193.

Leasi F, Pennati R, & Ricci C 2009. First description of the serotonergic nervous system in a bdelloid rotifer: *Macrotrachela quadricornifera* Milne 1886 (Philodinidae). Zool. Anz. 248: 47–55.

Lichtneckert R & Reichert H 2005. Insights into the urbilaterian brain: conserved genetic patterning mechanisms in insect and vertebrate brain development. Heredity 94: 465–477.

——— 2007. Origin and evolution of the first nervous system. In: Evolution of Nervous Systems—A Comprehensive Reference. Vol. 1. Theories, Development, Invertebrates. Striedler GF & Rubenstein JLR, eds., pp. 289–316. Oxford Academic Press, Oxford, UK.

Lowe CJ 2007. Origins of the chordate central nervous system: insights from hemichordates. In: Evolution of Nervous Systems—A Comprehensive Reference. Vol. 2. Non-Mammalian Vertebrates. Kaas JH & Bullock TH, eds., pp. 25–38. Oxford Academic Press, Oxford, UK.

Lowe CJ, Wu M, Salic A, Evans L, Lander E, Stange-Thomann F, Grubner CE, Gerhart J, & Kirschner M 2003. Anteroposterior patterning in hemichordates and the origins of the chordate nervous system. Cell 113: 853–865.

Lowe CJ, Teraski M, Wu M, Freeman RM, Runft L, Kwan K, Haigo S, Aronowicz J, Lander E, Gruber C, Kirschner M, & Gerhart J 2006. Dorsoventral patterning in hemichordates: insights into early chordate evolution. PLoS Biol. 291: 1603–1619.

Mackie GO & Burighel P 2005. The nervous system in adult tunicates: current research directions. Can. J. Zool. 83: 151–183.

Marlétaz F & LeParco Y 2008. Careful with understudied phyla: the case of chaetognaths. BMC Evol. Biol. 8: 251.

Marlétaz F, Martin E, Perez Y, Papillon D, Caubit X, Lowe CL, Freeman B, Fasano L, Dossat C, Wincker P, Weissenbach J, & Le Parco Y 2006. Chaetognath phylogenomics: a protostome with deuterostome-like development. Curr. Biol. 16: R577–R578.

Marlétaz F, Gilles A, Caubit X, Perez Y, Dossat C, Samain S, Gyapay G, Wincker P, & Le Parco Y 2008. Chaetognath transcriptome reveals ancestral and unique features among bilaterians. Genome Biol. 9: R94.

Mashanov VS, Zueva OR, Heinzeller T, & Dolmatov IY 2006. Ultrastructure of the circumoral nerve ring and the radial nerve cords in Holothurioida (Echinodermata). Zoomorphology 125: 27–38.

Mashanov VS, Zueva OR, Heinzeller T, Aschauer B, & Dolmatov IY 2007. Developmental origin of the adult nervous system in a holothurian: an attempt to unravel the enigma of neurogenesis in echinoderms. Evol. Dev. 9: 244–256.

Mashanov VS, Zueva OR, Heinzeller T, Aschauer B, Naumann WW, Grondona JM, Cifuentes M, & Garcia-Arraras JE 2009. The central nervous system of sea cucumbers (Echinodermata: Holothuroidea) shows positive immunostaining for a chordate glial secretion. Front. Zool. 6: 11.

Matus DQ, Copley RR, Dunn CW, Hejnol A, Eccleston H, Halanych KM, Martindale MQ, & Telford MJ 2006. Broad taxon and gene sampling indicate that chaetognaths are protostomes. Curr. Biol. 16: R575–R576.

McVeigh P, Mair GR, Atkinson L, Ladurner P, Zamanian M, Novozhilova E, Marks NJ, Day TA, & Maule AG 2009. Discovery of multiple neuropeptide families in the phylum Platyhelminthes. Int. J. Parasitol. 39: 1243–1252.

Meinertzhagen IA & Okamura Y 2001. The larval ascidian nervous system: the chordate brain from its small beginnings. Trends Neurosci. 24: 401–410.

Meinertzhagen IA, Lemaire P, & Okamura Y 2004. The neurobiology of the ascidian tadpole larva: recent developments in an ancient chordate. Annu. Rev. Neurosci. 27: 453–485.

Miller DM, Dunagan TT, & Richardson J 1973. Anatomy of the cerebral Ganglion of the female Acanthocephalan, *Macracanthorhynchus hirudinaceus*. J. Comp. Neurol. 152: 403–494.

Moroz L, Nezlin L, Elofsson R, & Sakharov D 1994. Serotonin- and FMRFamide-immunoreactive nerve elements in the chiton *Lepidopleurus asellus* (Mollusca, Polyplacophora). Cell. Tissue Res. 275: 277–282.

Morris J, Cardona A, De Miguel-Bonet MDM, & Hartenstein V 2007. Neurobiology of the basal platyhelminth *Macrostomum lignano*: map and digital 3D model of the juvenile brain neuropile. Dev. Genes Evol. 217: 569–584.

Müller MCM 2006. Polychaete nervous systems: ground pattern and variations—cLS microscopy and the importance of novel characteristics in phylogenetic analysis. Int. Comp. Biol. 46: 125–133.

Müller MCM & Sterrer W 2004. Musculature and nervous system of *Gnathostomula peregrina* (Gnathostomulida) shown by phalloidin labeling, immunohistochemistry, and cLSM, and their phylogenetic significance. Zoomorphology 123: 169–177.

Nielsen C 2001. Animal Evolution. Oxford University Press, Oxford, UK.

——— 2005. Larval and adult brains. Evol. Dev. 7: 483–489.

Nishimura K, Kitamura Y, Inoue T, Umesono Y, Yoshimoto K, Takeuchi K, Taniguchi T, & Agata K 2007. Identification and distribution of tryptophan hydroxylase (TPH)-positive neurons in the planarian *Dugesia japonica*. Neurosci. Res. 59: 101–106.

Nishimura K, Kitamura Y, Inoue T, Umesono Y, Yoshimoto K, Taniguchi T, & Agata K 2008a. Characterization of tyramine β-hydroxylase in planarian *Dugesia japonica*: cloning and expression. Neurochem. Int. 53: 184–192.

Nishimura K, Kitamura Y, Umesono Y, Takeuchi K, Takata K, Taniguchi T, & Agata K 2008b. Identification of glutamic acid decarboxylase gene and distribution of GABAergic nervous system in the planarian *Dugesia japonica*. Neuroscience 153: 1103–1114.

Nomaksteinsky M, Röttinger E, Dufour HD, Chettouh Z, Lowe CJ, Martindale MQ, & Brunet JF 2009. Centralization of the deuterostome nervous system predates chordates. Curr. Biol. 19: 1264–1269.

Okamoto K, Takeuchi K, & Agata K 2005. Neural projections in planarian brain revealed by fluorescent dye tracing. Zool. Sci. 22: 535–546.

Orrhage L & Müller MCM 2005. Morphology of the nervous system of Polychaeta (Annelida). Hydrobiologia 535/536: 79–111.

Papillon D, Perez Y, Caubit X, & Le Parco Y 2006. Systematics of Chaetognatha under the light of molecular data, using duplicated ribosomal 18S DNA sequences. Mol. Phylogenet. Evol. 38: 621–634.

Philippe H, Brinkmann H, Martinez P, Riutort M, & Baguñà J 2007. Acoel flatworms are not platyhelminthes: evidence from phylogenomics. PLoS One 2: e717.

Price DA & Greenberg MJ 1989. The hunting of the FaRPs: the distribution of FMRFamide-related peptides. Biol. Bull. 177: 198–205.

Raikova OI, Reuter M, Kotikova EA, & Gustafsson MKS 1998. A commussiral brain! The pattern of 5-HT immunoreactivity in Acoela (Plathеminthes). Zoomorphology 118: 69–77.

Raikova OI, Reuter M, Jondelius U, & Gustafsson MKS 2000a. An immunocytochemical and ultrastructural study of the nervous and muscular systems of *Xenoturbella westbladi* (Bilateria inc. sed.). Zoomorphology 120: 107–118.

——— 2000b. The brain of the Nemertodermatida (Platyhelminthes) as revealed by anti-5HT and anti-FMRFamide immunostainings. Tissue Cell 32: 358–365.

Raikova OI, Reuter M, Gustafsson MKS, Maule AG, Halton DW, & Jondelius U 2004. Evolution of the nervous system in *Paraphanostoma* (Acoela). Zool. Scr. 33: 71–88.

Rehkämper G & Welsch U 1985. On the fine structure of the cerebral ganglion of *Sagitta* (Chaetognatha). Zoomorphology 105: 83–89.

Rehkämper G, Welsch U, & Dilly PN 1987. Fine Structure of the Ganglion of *Cephalodiscus gracilis* (Pterobranchia, Hemichordata). J. Comp. Neurol. 259: 308–315.

Reichert H 2009. Evolutionary conservation of mechanisms for neural regionalization, proliferation and interconnection in brain development. Biol. Lett. 5: 105–107.

Reuter M & Halton MD 2001. Comparative neurobiology of Platyhelminthes. In: The Interrelationships of Platyhelminthes. Littlewood TJ & Ray RA, eds., pp. 239–249. Academic Press, London, UK.

Reuter M, Mäntylä K, & Gustafsson MKS 1998. Organisation of the orthogon—main and minor nerve cords. Hydrobiologia 383: 175–182.

Reuter M, Raikova OI, & Gustafsson MKS 2001a. An endocrine brain? The pattern of FMRF-amide immunoreactivity in Acoela (Plathelminthes). Tissue Cell 30: 57–63.

——— 2001b. Patterns in the nervous and muscle systems in lower flatworms. Belg. J. Zool. 131: 47–53.

Reuter M, Raikova OI, Jondelius U, Gustafsson MKS, Halton DW, Maule AG, & Shaw C 2001c. Organization of the nervous system in the Acoela: an immunocytochemical study. Tissue Cell 33: 119–128.

Ritter-Zàhony R von 1909. Zur Anatomie des Chätognathenkopfes. Denkschr. Kaiserl. Akad. Wiss. Wien 84: 33–41.

Ritter-Záhony R von 1911. Das Tierreich. Vermes. Chaetognathi. Königl. Preuß. Akad. Wiss., Berlin, Germany. 34 pp.

Rothe BH & Schmidt-Rhaesa A 2008. Variation in the nervous system in three species of the genus *Turbanella* (Gastrotricha, Macrodasyida). Meiofauna Mar. 16: 175–184.

——— 2009. Architecture of the nervous system in two *Dactylopodola* species (Gastrotricha, Macrodasyida). Zoomorphology 128: 227–246.

Salvini-Plawen Lv 1986. Systematic notes on *Spadella* and on the Chaetognatha in general. Z. Zool. Syst. Evol. 24: 122–128.

——— 1988. The epineural (vs. gastroneural) cerebral complex of the Chaetognatha. Z. Zool. Syst. Evol. 26: 425–429.

Savineau J & Duvert M 1986. Physiological and cytochemical studies of Ca in the primary muscle of the trunk of *Sagitta setosa* (Chaetognath). Tissue Cell 18: 953–966.

Scharrer E 1965. The fine structure of the retrocerebral organ of *Sagitta* (Chaetognatha). Life Sci. 4: 923–926.

Schmidt-Rhaesa A 2007. The Evolution of Organ Systems. Oxford University Press, Oxford, UK.

Sempere LF, Martinez P, Cole C, Baguñà J, & Peterson KJ 2007. Phylogenetic distribution of microRNAs supports the basal position of acoel flatworms and the polyphyly of Platyhelminthes. Evol. Dev. 9: 409–415.

Shigeno S, Sasaki T, & Haszprunar G 2007. Central nervous system of *Chaetoderma japonicum* (Caudofoveata, Aplacophora): implications for diversified ganglionic plans in early molluscan evolution. Biol. Bull. 213: 122–134.

Shinn GL 1997. Chaetognatha. In: Microscopic Anatomy of Invertebrates, Vol. 15: Hemichordata, Chaetognatha, and the Invertebrate Chordates. Harrison FW & Ruppert EE, eds., pp. 103–220. Wiley-Liss Inc., New York, NY, USA.

Søviknes AM, Chourrout D, & Glover JC 2005. Development of putative GABAergic neurons in the appendicularian urochordate *Oikopleura dioica*. J. Comp. Neurol. 490: 12–28.

Spörhase-Eichmann U, Gras H, & Schürmann FW 1987a. Patterns of serotonin-immunoreactive neurons in the central nervous system of the earthworm *Lumbricus terrestris* L. I. Ganglia of the ventral nerve cord. Cell Tissue Res. 249: 601–614.

——— 1987b. Patterns of serotonin-immunoreactive neurons in the central nervous system of the earthworm *Lumbricus terrestris* L. II. Rostral and caudal ganglia. Cell Tissue Res. 249: 625–632.

Stach T 2005. Comparison of the serotonergic nervous system among Tunicata: implications for its evolution within Chordata. Org. Divers. Evol. 5: 15–24.

Stach T, Dupont S, Israelson O, Fauville G, Nakano H, Kånneby T, & Thorndyke M 2005. Nerve cells of *Xenoturbella bocki* (phylum uncertain) and *Harrimania kupfferi* (Enteropneusta) are positively immunoreactive to antibodies raised against echinoderm neuropeptides. J. Mar. Biol. Assoc. UK 85: 1519–1524.

Tazaki A, Gaudieri S, Ikeo K, Gojobori T, Watanabe K, & Agata K 1999. Neural network in planarian revealed by an antibody against planarian synaptotagmin homologue. Biochem. Biophys. Res. Commun. 260: 426–432.

Telford MJ 2008. Xenoturbellida: the fourth deuterostome phylum and the diet of worms. Genesis 46: 580–586.

Telkes I, Csoknya M, Buzás P, Gábriel R, Hámori J, & Elekes K 1996. GABA-immunoreactive neurons in the central and peripheral nervous system of the earthworm, *Lumbricus terrestris* (Oligochaeta, Annelida). Cell. Tissue Res. 285: 463–475.

Todt C, Büchinger T, & Wanninger A 2008. The nervous system of the basal mollusk *Wirenia argentea* (Solenogastres): a study employing immunocytochemical and 3D reconstruction techniques. Mar. Biol. Res. 4: 290–303.

Tokioka T 1965a. The taxonomical outline of chaetognaths. Publ. Seto Mar. Biol. Lab. 12: 335–357.

——— 1965b. Supplementary notes on the systematics of Chaetognatha. Publ. Seto Mar. Biol. Lab. 13: 231–242.

Tsutsui I, Inoue I, Bone Q, & Carre C 2000. Activation of locomotor and grasping spine muscle fibres in chaetognaths: a curious paradox. J. Muscle Res. Cell. Motil. 21: 91–97.

Umesono Y & Agata K 2009. Evolution and regeneration of the planarian central nervous system. Dev. Growth Differ. 51: 185–195.

Walker RJ 1992. Neuroactive peptides with an RFamide or Famide carboxyl terminal. Comp. Biochem. Physiol. 102C: 213–222.

Welsch U & Storch V 1983. Fine structural and enzyme histochemical observations on the epidermis and sensory cells *Sagitta elegans* (Chaetognatha). Zool. Anz. 1: 34–43.

Wicht H & Lacalli TC 2005. The nervous system of *Amphioxus*: structure, development, and evolutionary significance. Can. J. Zool. 83: 122–150.

Zajac J-M & Mollereau C 2006. Introduction: RFamide peptides. Peptides 27: 941–942.

Zeng L & Swalla BJ 2005. Molecular phylogeny of the protochordates: chordate evolution. Can. J. Zool. 83: 24–33.

8.3 Development of the nervous system in hatchlings of *Spadella cephaloptera* (Chaetognatha), and implications for nervous system evolution in Bilateria.

Rieger V, Perez Y, Müller CHG, Lacalli T, Hansson BS, Harzsch S (2011)

Development, Growth & Differentiation 53: 740-759

Development, Growth & Differentiation
The Japanese Society of Developmental Biologists

Develop. Growth Differ. (2011) **53**, 740–759
doi: 10.1111/j.1440-169X.2011.01283.x

Original Article

Development of the nervous system in hatchlings of *Spadella cephaloptera* (Chaetognatha), and implications for nervous system evolution in Bilateria

Verena Rieger,[1,2]* Yvan Perez,[3] Carsten H. G. Müller,[1] Thurston Lacalli,[4]
Bill S. Hansson[2] and Steffen Harzsch[1,2]

[1]*Zoologisches Institut und Museum, Cytologie und Evolutionsbiologie, Ernst Moritz Arndt Universität Greifswald, Soldmannstraße 23, 17487 Greifswald;* [2]*Department for Evolutionary Neuroethology, Max-Planck-Institute for Chemical Ecology, Hans-Knöll-Str. 8, 07745 Jena, Germany;* [3]*Institut Méditerranéen d'Ecologie et de Paléoécologie UMR CNRS 6116, Université de Provence, 3 Pl Victor Hugo Case 36, 13331 Marseille Cedex 3, France; and* [4]*Department of Biology, University of Victoria, Victoria, British Columbia V8W-3N5, Canada*

Chaetognaths (arrow worms) play an important role as predators in planktonic food webs. Their phylogenetic position is unresolved, and among the numerous hypotheses, affinities to both protostomes and deuterostomes have been suggested. Many aspects of their life history, including ontogenesis, are poorly understood and, though some aspects of their embryonic and postembryonic development have been described, knowledge of early neural development is still limited. This study sets out to provide new insights into neurogenesis of newly hatched *Spadella cephaloptera* and their development during the following days, with attention to the two main nervous centers, the brain and the ventral nerve center. These were examined with immunohistological methods and confocal laser-scan microscopic analysis, using antibodies against tubulin, FMRFamide, and synapsin to trace the emergence of neuropils and the establishment of specific peptidergic subsystems. At hatching, the neuronal architecture of the ventral nerve center is already well established, whereas the brain and the associated vestibular ganglia are still rudimentary. The development of the brain proceeds rapidly over the next 6 days to a state that resembles the adult pattern. These data are discussed in relation to the larval life style and behaviors such as feeding. In addition, we compare the larval chaetognath nervous system and that of other bilaterian taxa in order to extract information with phylogenetic value. We conclude that larval neurogenesis in chaetognaths does not suggest an especially close relationship to either deuterostomes or protostomes, but instead displays many apomorphic features.

Key words: development, evolution, immunohistochemistry, nervous system, neurotransmitter.

Introduction

The phylum Chaetognatha (Fig. 1D) comprises a group of small marine predators that are major components of the zooplankton throughout the world's oceans (Kapp 2007). Yet our knowledge of this taxon is limited in many respects, and its phylogenetic position is still a matter of considerable debate (reviewed in Harzsch & Müller 2007; Harzsch & Wanninger 2010). In the last 200 years, various phylogenetic affiliations have been proposed (summarized by Ghirardelli 1968), but the majority are not supported by modern phylogenomic analysis (Fig. 1F; reviewed in Telford 2004; Harzsch & Müller 2007; Harzsch & Wanninger 2010). Most such studies, using Bayesian inference and maximum likelihood methods to analyze broad datasets, support either a sister-group relationship with Lophotrochozoa (Papillon *et al.* 2004; Matus *et al.* 2006; Dunn *et al.* 2008; Philippe *et al.* 2011) or a position as a sistergroup to all Protostomia (Marlétaz *et al.* 2006, 2008; Philippe *et al.* 2007). However, other possible phylogenetic positions include a placement of the Chaetognatha within the Ecdysozoa (Paps *et al.* 2009), as a sistergroup to the Arthropoda (Zrzavý *et al.* 1998) or Nematoda (Halanych 1996; Peterson & Eernisse 2001), or as a sistergroup to all Ecdysozoa (Mallat & Winchell 2002). Close relations to Gnathostomulida

---

*Author to whom all correspondence should be addressed.
Email: verena.rieger@uni-greifswald.de

Received 10 February 2011; revised 23 March 2011; accepted 30 March 2011.

© 2011 The Authors
Development, Growth & Differentiation © 2011 Japanese Society of Developmental Biologists

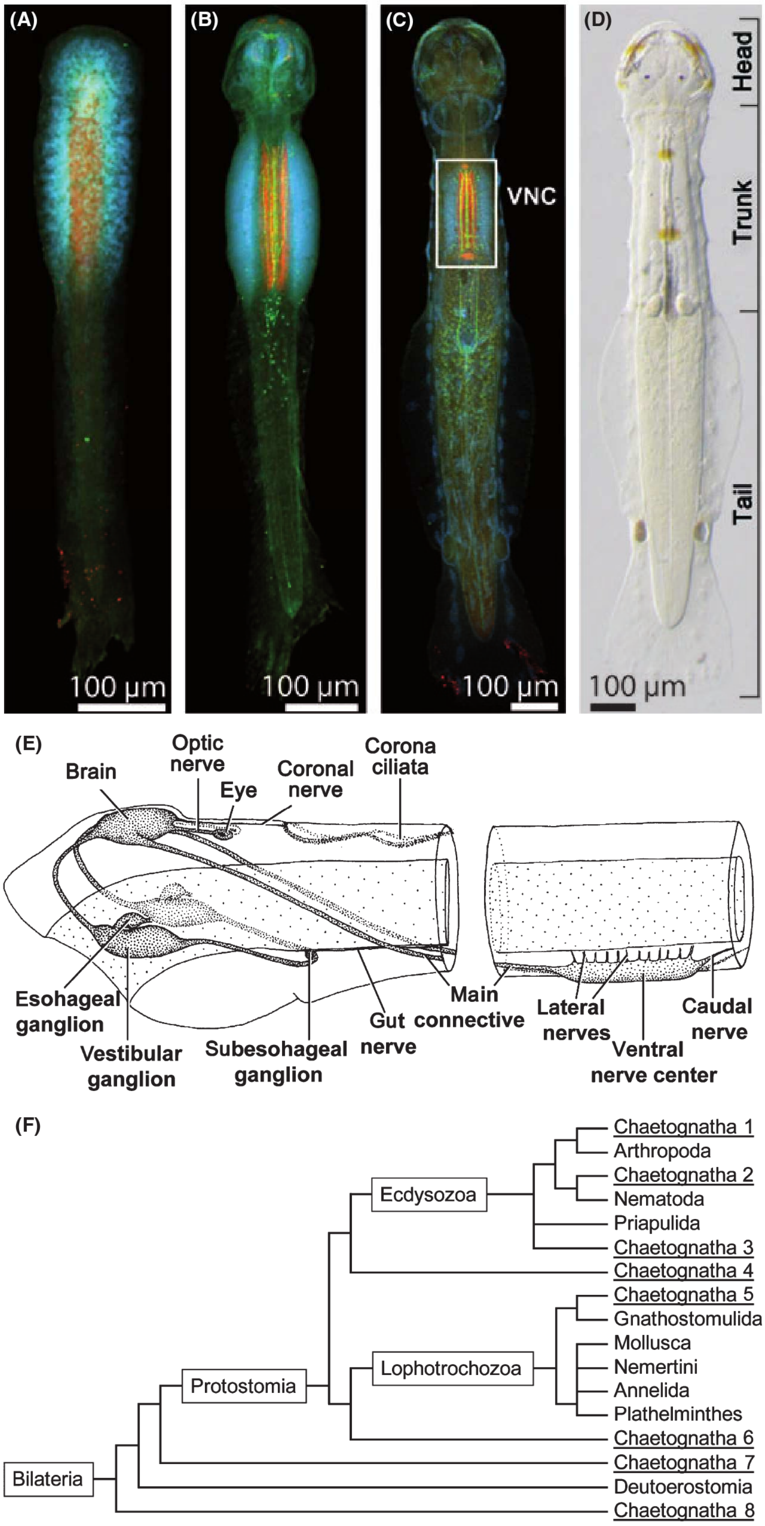
(A)
(B)
(C)
(D)
VNC
Head
Trunk
Tail
100 μm
100 μm
100 μm
100 μm
(E)
Brain
Optic nerve
Eye
Coronal nerve
Corona ciliata
Esohageal ganglion
Vestibular ganglion
Subesohageal ganglion
Gut nerve
Main connective
Lateral nerves
Ventral nerve center
Caudal nerve
(F)
Bilateria
Protostomia
Ecdysozoa
Lophotrochozoa
Chaetognatha 1
Arthropoda
Chaetognatha 2
Nematoda
Priapulida
Chaetognatha 3
Chaetognatha 4
Chaetognatha 5
Gnathostomulida
Mollusca
Nemertini
Annelida
Plathelminthes
Chaetognatha 6
Chaetognatha 7
Deutoerostomia
Chaetognatha 8

Fig. 1. Adult *Spadella cephaloptera*, developmental stages and an overview of the chaetognath nervous system. (A–C) Fluorescent micrographs of *Spadella cephaloptera,* immunohistochemistry against RFamide-like peptides (green), nuclei (blue), and synaptic proteins (red). (A) Hatchling age 24 h. (B) Hatchling age 120 h. (C) Adult (modified from Harzsch *et al.* 2009). (D) Light micrograph of a live adult specimen of *Spadella cephaloptera* (modified from Rieger *et al.* 2010). (E) General nervous system architecture of a chaetognath (modified from Kapp 2007). (F) Possible phylogenetic positions of the Chaetognatha based on molecular studies (modified from Harzsch & Müller 2007). 1: Zrzavý *et al.* (1998); 2: Halanych (1996), Peterson & Eernisse (2001); 3: Paps *et al.* (2009); 4: Mallat & Winchell (2002); 5: Littlewood *et al.* (1998); 6: Matus *et al.* (2006), Papillon *et al.* (2004), Dunn *et al.* (2008), and Philippe *et al.* (2011); 7: Giribet *et al.* (2000), Helfenbein *et al.* (2004), and Marlétaz *et al.* (2006); 8: Telford & Holland (1993) and Papillon *et al.* (2003). VNC, ventral nerve center.

(Littlewood *et al.* 1998) have been suggested, and some analyses favor the Chaetognatha as the sister-group to all other Bilaterians (Telford & Holland 1993; Papillon *et al.* 2003). In addition, a detailed survey of the chaetognath transcriptome and genome (Marlétaz *et al.* 2008) as well as new morphological data (Harzsch & Müller 2007; Harzsch *et al.* 2009; Harzsch & Wanninger 2010; Rieger *et al.* 2010) reveals both ancestral features shared with other Bilateria and derived characteristics, which suggests chaetognaths to be a key taxon for our understanding of the early events of bilaterian evolution. These new interpretations contradict many of the traditional models on chaetognath phylogenetic relationships, e.g. that chaetognaths are closely related to deuterostomes based on their embryonic development (Kuhl 1938; Hyman 1959). If, as suggested by some recent phylogenomic studies, chaetognaths may have branched off close to the split between protostomes and deuterostomes, an analysis of their ontogeny could potentially provide important insights into the development of the last common ancestor of modern bilaterians.

Chaetognaths are hermaphroditic and develop directly (Fig. 1A–D), so that the larvae at hatching (Fig. 1A) display a body organization that is in most respects similar to the adult (Fig. 1C,D). The embryonic development of chaetognaths is known from the fundamental studies by Hertwig (1880), Doncaster (1902), and John (1933) on *Spadella* and *Sagitta*. More recently, the embryology and various aspects of growth and reproduction in chaetognaths has been explored in laboratory cultures (Kuhl & Kuhl 1965; Reeve 1970; Kuhlmann 1977; Goto & Yoshida 1997; Shimotori & Goto 1999, 2001; Carré *et al.* 2002, review Pearre 1991; Kapp 2000) including the mating sequence (Goto & Yoshida 1985), the fertilization process (Goto 1999; Carré *et al.* 2002) and aspects of regeneration (Duvert *et al.* 2000). Furthermore, the embryonic expression patterns of actin genes (Yasuda *et al.* 1997), the *brachyury* gene (Takada *et al.* 2002) and a median *Hox* gene (Papillon *et al.* 2005) have been analyzed by whole mount *in situ* hybridization. The studies on embryology have used time-lapse imaging (Kuhl & Kuhl 1965) and injections of fluorescent tracer molecules (Shimotori & Goto 1999, 2001) to examine developmental fates of the blastomeres and the establishment of axial properties of the embryos. Carré *et al.* (2002) observed the fate of a Vasa-positive germ granule in eggs and traced it these through the development from embryo to adult. Thus, as in *Drosophila melanogaster*, Vasa-proteins here seem to be involved in germ cell specification.

Embryonic cleavage in chaetognaths is total and equal, and sufficiently close to the radial cleavage pattern of deuterostomes to suggest a deuterostome affinity. However, a recent analysis of the developmental fate of the first four blastomeres led Shimotori & Goto (2001) to suggest that chaetognaths are more similar to protostomes in their developmental program. In addition, their embryology is unusual and difficult to relate to other Bilateria so that Kapp (2000) coined a new term, *heterocoely*, to describe the mode of coelom formation during gastrulation. Chaetognath neurogenesis was first examined histologically by Doncaster (1902), who described the initial stages of neural development in some detail. According to this author, when the head coelom has formed, the ventral ectoderm of the trunk and the ectoderm above the mouth develop thickenings that become the rudiments of the ventral nerve center and the brain, respectively. Cell proliferation occurs along two ventro-lateral bands of somata in the trunk, which, just after hatching, are clearly marked off from the surrounding epidermis. These form the primordia of the ventral nerve center (VNC). At this point, the general organization of the VNC is well established. Some aspects of postembryonic development of the nervous system have been described by Doncaster (1902), and John (1933) for *Spadella cephaloptera*. Goto *et al.* (1992) have characterized the postembryonic development of some peptidergic and aminergic neurons in *Paraspadella gotoi* with immunofluorescence methods. However, beyond these basic studies, a good deal remains unknown about neural development in chaetognaths, especially regarding the development of specific neuronal subsystems in embryos and hatchlings.

Despite our limited knowledge of neurogenesis, the general organization of the adult nervous system of chaetognaths has been described by several authors, notably by Bone & Pulsford (1984), Goto & Yoshida (1984, 1987) and Shinn (1997; recently summarized in Harzsch & Müller 2007 and Rieger *et al.* 2010). Chaetognaths have a diffuse intraepidermal nerve plexus (Harzsch & Müller 2007) and two major condensed neuronal centers. The head contains a dorsally positioned brain subdivided into an anterior and a posterior part (Rieger *et al.* 2010) and is linked to several smaller cephalic ganglia (Fig. 1E). Paired frontal connectives link the frontal-most part of the brain with the more ventral and lateral to the esophagus positioned paired vestibular ganglia. The latter are connected to the esophageal ganglia and to the unpaired subesophageal ganglion that complete the circular arrangement around the esophagus. The trunk contains the VNC, the largest neuronal center of the animal, which is linked to the brain by the main connectives. Immunohistochemical studies on the nervous system include

© 2011 The Authors
Development, Growth & Differentiation © 2011 Japanese Society of Developmental Biologists

those by Goto *et al.* (1992), Harzsch & Müller (2007), Harzsch *et al.* (2009) and Rieger *et al.* (2010).

The present study explores features of postembryonic neurogenesis in *Spadella cephaloptera* (Fig. 1D) with immunofluorescence methods combined with the detailed analysis that is possible using laser scanning microscopy. We chose antisera against synaptic proteins, tubulin and RFamide-related neuropeptides because they were already used in adult specimens of various species (Fig. 1C; Goto *et al.* 1992; Harzsch & Müller 2007; Harzsch *et al.* 2009; Rieger *et al.* 2010). The results are discussed in a comparative context as, in our view, chaetognaths may provide a useful third and independent test for existing models of CNS evolution in bilaterians, which derive mainly from a consideration of how protostomes and deuterostomes differ from yet more basal metazoan taxa.

Materials and methods

Experimental animals

Adult specimens of *Spadella cephaloptera* (Busch, 1851) (Phragmophora, Spadellidae) were collected in Sormiou (Marseille, France) in June 2006 and August 2007. A plankton net was grazed over the sea grass beds by snorkeling. Animals were kept in aquaria containing natural seawater (21 ± 1°C) at the Université de Provence, Marseille. The eggs of these animals were collected on a daily basis and reared in separate tanks to obtain different developmental stages. The development of *Spadella cephaloptera* hatchlings proceeds rapidly and a few hours of developmental time can make a difference. Because we monitored the hatchling cultures once a day in the morning, a hatchling designated as 24 h old may be anywhere between 24 h old and just newly hatched. In this logic, an animal designated to be 48 h old may be between 24 and 48 h old. We tried to average out this variation by examining several randomly chosen individuals per stage, i.e. for each day of sampling.

Histology and transmission electron microscopy

Hatchlings of *Spadella cephaloptera* were fixed *in toto* according to Arnaud *et al.* (1978) for 2 h at 48°C in a mixture of 3% glutaraldehyde, 1% paraformaldehyde and 30% sea water in a 0.2 M sodium cacodylate buffer, pH 7.3 (final osmolarity adjusted to approximately 1240 mOsm with glucose), rinsed repeatedly in the same buffer for 2 h and post-fixed for 1 h in 1% OsO. They were dehydrated through a graded series of ethyl alcohol treatments before being embedded in Epon. Thin sections were cut with a Reichert Jung ultramicrotome using Diatome diamond knives and stained with uranyl acetate and lead citrate (Reynolds 1963), before being observed under a Zeiss EM 912 transmission electron microscope. Semithin sections (approximately 1 μm thick) through the trunk were prepared and stained using 1% toluidine blue in a solution of 1% Na-tetraborate (borax). Images were taken using a Nikon Eclipse 90i with the Nikon NIS-Elements Ar 3.10 software.

Fluorescent histochemistry and immunohistochemistry

Specimens were fixed for 4 h at room temperature (or alternatively overnight at 4°C) in 4% paraformaldehyde (PFA) in phosphate buffer (PB; 0.1 M, pH 7.4). Histochemistry and immunohistochemistry were carried out on free-floating whole mounts of hatchlings with primary and fluorochrome-conjugated secondary antibodies using standard protocols (Harzsch & Müller 2007). After fixation, the tissues were washed in several changes of phosphate-buffered saline (PBS) for at least 4 h. All specimens were preincubated in PBS-TX (1% normal goat serum, 0.3% Triton X-100, 0.05% Na-azide) for 1 h and then incubated overnight in either one or a combination of two of the following primary antibodies diluted in PBS-TX (room temperature):

1 Anti-acetylated α-tubulin from mouse (1:2000; Sigma).
2 Anti-FMRFamide polyclonal from rabbit (1:2000; ImmunoStar).
3 Anti-synapsin SYNORF 1 monoclonal from mouse (1:10; antibody kindly provided by Prof Dr E. Buchner, Universität Würzburg).

Specimens were then washed for at least 2 h in several changes of PBS and subsequently incubated in secondary antibodies against rabbit proteins conjugated to the fluorochrome Alexa Fluor 488 (1:500; Molecular Probes) and antibodies against mouse proteins conjugated to Cy3 (1:500; Jackson Immuno Research) for 4 h. The specimens were stained with a nuclear dye, either bisbenzimide (0.04%, 4 h at room temperature; Hoechst H 33258) or YOYO-1 (0.025%, 4 h at room temperature; Molecular Probes) during the secondary antibody incubations. Finally, the tissues were washed for at least 2 h in several changes of PBS and then mounted in MOWIOL (Calbiochem). The immunohistochemical observations reported in this paper are based on the analysis of at least six specimens for each stage.

Microscopic analysis

Digital images were obtained using a Zeiss Axioimager Z1 fluorescence microscope equipped with a structured

© 2011 The Authors

illumination device (ApoTome) and a digital camera AxioCamMRm (Zeiss) controlled by the AxioVision V 4.6.3-SP1 software package (Zeiss). In addition, samples were scanned with a Zeiss LSM 510 Meta Confocal Laser-Scanning Microscope. Those images are based on Z-stacks of several optical sections and were obtained using the LSM 510 V.4.0. SP2 software (Zeiss). Images were black-white inverted and processed in Adobe Photoshop CS4 V11.0 by using the global contrast and brightness adjustment features.

Measurement of animal length

Specimens of all ages and all experiments were photographed and measured from the tip of the head to the posterior end of the body, excluding the tailfin since this fin was often damaged. The length of specimens was measured using the AxioVision V 4.6.3-SP1 software package (Zeiss). Graphs were compiled using Sigma Plot 11.0 (Systat Software).

Specificity of the antisera

The tetrapeptide FMRFamide (Phe-Met-Arg-Phe-NH2) and FMRFamide-related peptides (FaRPs) form a large neuropeptide family with more than 50 members, all of which share the RFamide motif (reviews: Price & Greenberg 1989; Greenberg & Price 1992; Walker 1992; Dockray 2004; Kriegsfeld 2006; Zajac & Mollereau 2006) and which are widely distributed among invertebrates and vertebrates. The antiserum we used was generated in rabbit against synthetic FMRFamide (Phe-Met-Arg-Phe-NH2) conjugated to bovine thyroglobulin (DiaSorin, Cat. No. 20091, Lot No. 923602). According to the manufacturer, staining with this antiserum is completely eliminated by pre-treatment of the diluted antibody with 100 μg/mL of FMRFamide. We repeated this experiment and preincubated the antiserum with 10–4 M FMRFamide (16 h, 4°C). In this control, neuronal structures were not labeled. In an additional control experiment for possible non-specific binding of the secondary antiserum, we omitted the primary antiserum, replaced it with blocking solution, and followed the labeling protocol as above. In this control, staining was absent. We compared the labeling pattern obtained in our specimens with that in a previous study, in which a polyclonal antiserum to the sequence Arg-Phe-amide was used in *Parasagitta setosa* (Bone *et al.* 1987). This latter antiserum was obtained by immunizing rabbits with synthetic FMRFamide, which was coupled via glutaraldehyde to bovine thyroglobulin (Grimmelikhuijzen & Spencer 1984). Incubation of this antiserum with sepharose-bound FMRFamide, FLRFamide, or RFamide abolished all staining and this antiserum has been shown to be most sensitive to the C-terminal sequence -RFamide (Arg-Phe-NH2; Grimmelikhuijzen 1985). It has been used to label RFamide-like immunoreactive structures, e.g. in a medusa (Grimmelikhuijzen & Spencer 1984) and in several *Hydra* species (Grimmelikhuijzen 1985). Bone *et al.* (1987), using the antiserum generated by Grimmelikhuijzen & Spencer (1984) in *P. setosa*, concluded that the chaetognath peptide might be related to any peptide terminating with the sequence RFamide. Because the labeling pattern obtained by Bone *et al.* (1987) closely corresponds to that found in the present report we conclude that the ImmunoStar antiserum that we used most likely also labels any peptide terminating with the sequence RFamide. Therefore, we will refer to the labeled structures in our specimens as ''RFamide-like immunoreactive (RFir) neurons'' throughout the paper.

The monoclonal mouse anti-*Drosophila* synapsin ''SYNORF1'' was raised against a *Drosophila* GST-synapsin fusion protein and recognizes at least four synapsin isoforms (approximately 70, 74, 80, and 143 kDa) in western blots of *Drosophila* head homogenates (Klagges *et al.* 1996). Western blot analysis of brain homogenates of the anomuran crab *Coenobita clypeatus* showed that the epitope that SYNORF 1 recognizes is strongly conserved between the fruit fly and the crustacean (Harzsch & Hansson 2008). The antibody also labels neuromuscular synapses both in *Drosophila* and in *Crustacea* (Harzsch *et al.* 1997) as well as central synapses in Platyhelminthes (Cebrià 2008) suggesting that the epitope that this antiserum binds to is conserved over wide evolutionary distances. Our previous analysis on the ventral nerve center strongly suggested that this antibody also labels synaptic neuropil in the Chaetognatha (Harzsch & Müller 2007). In the present study, we found that this antibody labels an area of the ventral nerve centre which corresponds to the central neuropil we could identify in semithin sections (compare Figs 3E and 4E) suggesting that this antibody in fact labels the entire synaptic neuropil of the ventral nerve centre.

The monoclonal anti-acetylated tubulin (mouse IgG2b; Sigma Product Number T 7451, Clone 6-11B-1) was raised against acetylated tubulin from the sea urchin *Strongylocentrotus purpuratus*. According to the manufacturer, this antibody reacts with acetylated α-tubulin from many different species including protista, plants, invertebrates, and vertebrates, indicating that the antigen this antibody recognizes is evolutionarily conserved across a broad range of species. Tubulin is the major building block of microtubules and represents a heterodimer of alpha-tubulin and beta-tubulin.

Neuroanatomical nomenclature

The neuroanatomical nomenclature is according to Richter *et al.* (2010).

Results

Basic hatchling behavior and morphology

Hatchlings of *Spadella cephaloptera* are about 0.8 mm in length, and they grow about 20% in length during the following 5 days (Fig. 2). At hatching, they are already equipped with a distinct caudal fin. In contrast, the lateral fins are less well developed (Fig. 2A). The hatchlings lack a functional mouth opening with grasping spines and teeth as well as a functional anus (Fig. 2G), so they must rely entirely on yolk supplies for nutrition. In addition, typical adult cephalic structures such as grasping spines and the sensory organs associated with the head, including the eyes and the corona ciliata (a sensory organ for which a role in chemoreception has been suggested, see Shinn 1997), are either not yet present or are poorly developed at hatching.

Less than 1 h after hatching, each hatchling is able to react to external stimuli by escape movements, a reaction that most likely is mediated by hydrodynamic sensors, the fence receptor organs (see below). While the predatory adults swim by coordinated, alternating contractions of dorsal and ventral packages of longitudinal musculature (Bone & Duvert 1991; Shinn 1997) hatchlings swim in helicoidal spins. Furthermore, adults can attach themselves to the substrate with adhesive papillae localized in the mid ventral region of the body, whereas hatchlings adhere by the anterior ventral part of their head.

The head sensory organs and, in parallel, the brain develop rapidly during the first week of the hatchling's life. The mouth opens 24 h after hatching and eyes bear a pigmented cell 24 h later. In the following days, the hooks develop fully and the juvenile is now equipped for hunting prey.

Immunolocalization of tubulin reveals that directly after hatching, the head exhibits only a thin ring of

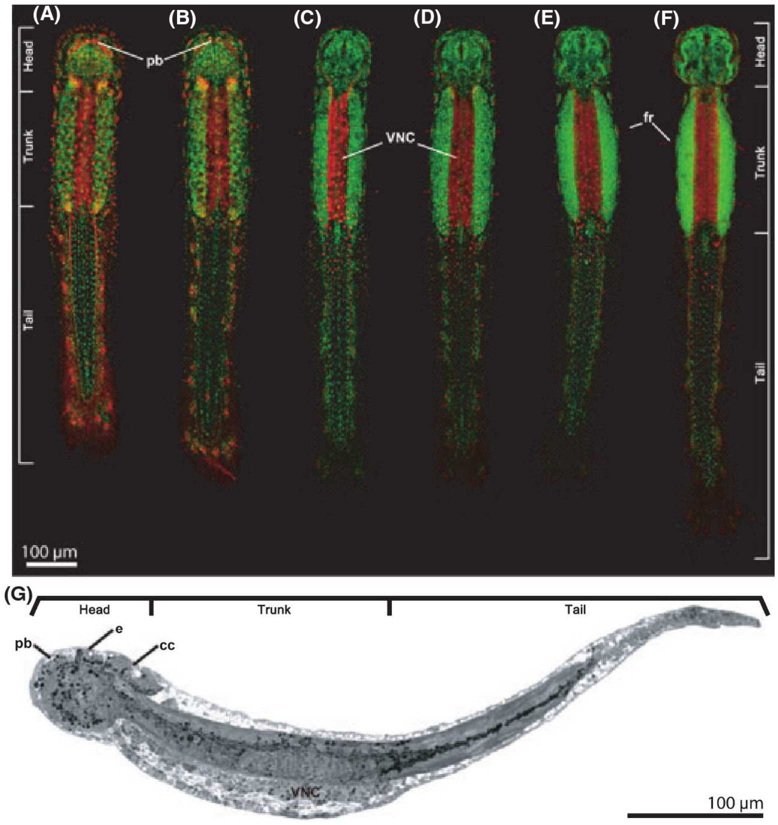

Fig. 2. *Spadella cephaloptera* hatchlings at 1–6 days after hatching. All hatchlings were stained against tubulin (red) and nuclei (green). (A) 24 h; (B) 48 h; (C) 72 h; (D) 96 h; (E) 120 h; (F) 144 h (compare material and methods section for the staging of the hatchlings). (G) Sagittal section showing the hatchling's body organization at low magnification. There is neither a mouth opening nor an anus visible. cc, corona ciliata; e, eye anlagen; fr, fence receptors; pb, primordial brain; VNC, ventral nerve center.

labeled fibers (Fig. 2A) belonging to the primordial brain. In contrast, the VNC is a most prominent structure that occupies the anterior half of the trunk almost completely (Fig. 2). It displays a well-developed neuropil, which is flanked by lateral bands of nuclei (Fig. 3). At hatching, the neuropil does show immunoreactivity for synapsins (synaptic proteins) suggesting the presence of functional synaptic contacts (Fig. 4E). The intensity of the synapsin-immunoreactivity in the VNC increases over the first 48–96 h (Fig. 5E–G). A comparison of the neuropil area in semithin cross sections of the VNC (Fig. 3E) with the area of the VNC, which is labeled by the synapsin antiserum (Fig. 4H) shows a close match, suggesting that this antiserum in fact labels the entire synaptic neuropil of the hatchling's VNC. Figure 3 shows a series of optical sections of an approximately 1 day-old hatchling from dorsal (A) to ventral (D). Anti-tubulin immunohistochemistry clearly shows that by this stage hatchlings are equipped with fence receptor organs (fr; hydrodynamic sensory organs), and adhesive papillae (ap) on the ventral surface. Furthermore, the corona ciliata (cc), a sensory organ of as yet unknown function, starts to develop.

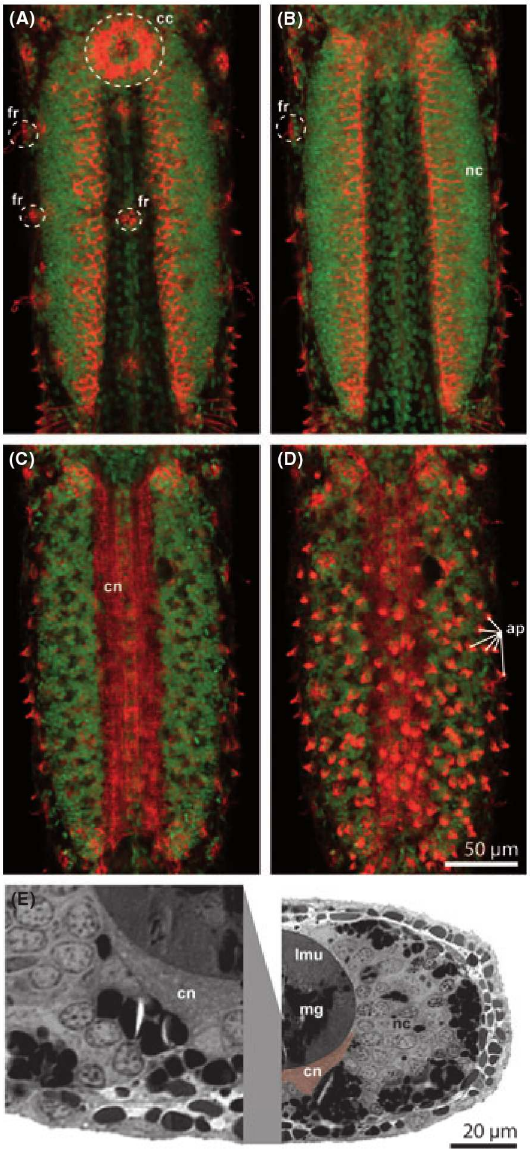

Fig. 3. Trunk and ventral nerve center of a 24 h old hatchling. Series of optical sections (confocal laser-scan microscopy) from dorsal (A) to ventral (D); Immunolocalization of tubulin (red) and histochemical staining of nuclei (green). (E) Semithin cross section through the ventral nerve centre of a hatchling shortly after hatching (age about 4 h), stained with toluidin blue. To the left, the ventral portion of the left half is shown in higher magnification. ap, adhesive papilla; cc, corona ciliata; cn, central neuropil; fr, fence receptors; lmu, longitudinal trunk musculature; mg, (unfunctional) mesodermal precursor cells of the midgut epithelium; nc, nuclei.

Development of individually identified peptidergic neurons in the ventral nerve center

In a previous paper we charted the system of individually identifiable neurons that show immunoreactivity for RFamide-related neuropeptides (RFamide-ir) in adult *Spadella cephaloptera* (Fig. 4D,H; Harzsch *et al.* 2009). One unpaired and two paired fiber bundles extend along the longitudinal axis of the adult VNC and paired RFamide-ir somata are arranged laterally to the fiber bundles. Anteriorly, we found a cluster of three labeled cell somata that we called lateral cells L1–L3, and another cell positioned more posteriorly closer to the midline (L4). Six serially arranged somata follow posteriorly in a regular spacing, the dorsal cells D1–6, a slightly larger cell (X) and another D-cell (Fig. 4D,H; compare Harzsch *et al.* 2009).

Compared to the pattern of RFamide-ir in the VNC of adult *S. cephaloptera*, this system is already well developed in juveniles. At 24 h of age, we observed two members of the L-group of somata. The most anterior one (Figs 4A and 5A) may correspond to Lc because this soma is most prominent in later stages (Fig. 4C,G). The Ld neuron is also immunolabeled, as are the neurons D1–4 (Figs 4A and 5A). Neurons D5 and D6 also seem to be present but because additional somata at the position of D4 and D5 were only inconsistently labeled in some preparations, we could not identify these cells with certainty. In addition, we could observe a pair of median cells at about the level of D2 that are not present in older hatchlings (Fig. 4A, circles). Medially directed projections, crossing the

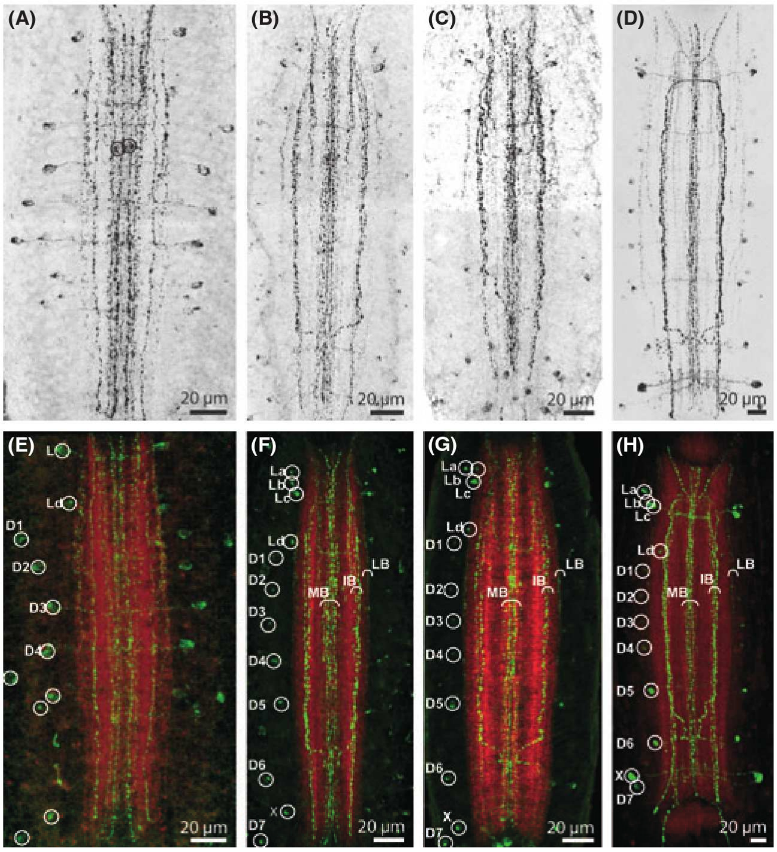

Fig. 4. RFamide-like immunoreactivity in the ventral nerve center (VNC). RFamide-ir was detected by confocal laser-scan microscopy in preparations of an adult (D, H) and hatchlings at 24 h (A), 48 h (E), 72 h (B, F), and 120 h (C, G). The upper row shows specimens stained against RFamide-like peptides, the images are black-white inverted. The lower row shows immunolocalization of RFamide-like peptides (green) and synapsin (red). La–d, lateral cells a–d; LB, lateral bundle; D1–7, dorsal cells 1–7; IB, intermediate bundle; MF, median bundle; X, X-cell.

main longitudinal fiber bundles, were visible for the Lc, Ld and D4 neurons. Projections towards the lateral fiber bundles, which could not be traced to any considerable length, were present for the cells D1–D3 and D5. About eight parallel longitudinal fibers are present, but they are not yet as clearly grouped into fiber bundles as they are in adults. The fibers extend anteriorly beyond the level of the Lc-neuron. Posteriorly, they extend further than D6 except for the most lateral fiber bundle, which only reaches as far as the level of D3 and forms the primordium of the lateral bundle (LB) in older hatchlings and adults. The second bundle from the midline on both sides is longer than the other bundles and will develop into the intermediate bundle (IB). The median fibers are later bundled into the median bundle (MB).

By 48 h, only minor progress in the development of the pattern of RFamide-ir structures is visible (Fig. 4E). From an age of 72 h onwards, all four L-cells are present, although in the beginning, the La-soma is rather faintly labeled (Fig. 4B,F). The D7 and X neurons now have also emerged, whereas the additional cells close to the position of D4 and D5 are barely observable any more. The cells Ld, D5–7, and X have developed medially directed projections. The longitudinal fibers are more prominent and grouped into bundles. The fibers of the LB now extend posteriorly to the level of D7. The longest fibers of the IB join each other and extend posteriorly along the midline, leaving the VNC. The connection between the fibers of the median and intermediate fiber bundle at a level between D5 and D6 is also present for the first time. At this age, the connection is labeled only inconsistently, but it is clearly visible in older hatchlings. Starting from 96 h onwards, cell bodies often display only a faint immunolabeling, especially the D1–5 somata. Of the L-cells, Lc is stained most brightly, and contralateral projections of all four L-cell pairs can be seen. These projections are also barely visible in hatchlings from 120 h onwards, whereas the longitudinal fibers become increasingly prominent (Fig. 4C,G).

Development of the brain

The brain is located dorsally within the head and is connected to the more ventral vestibular ganglia and

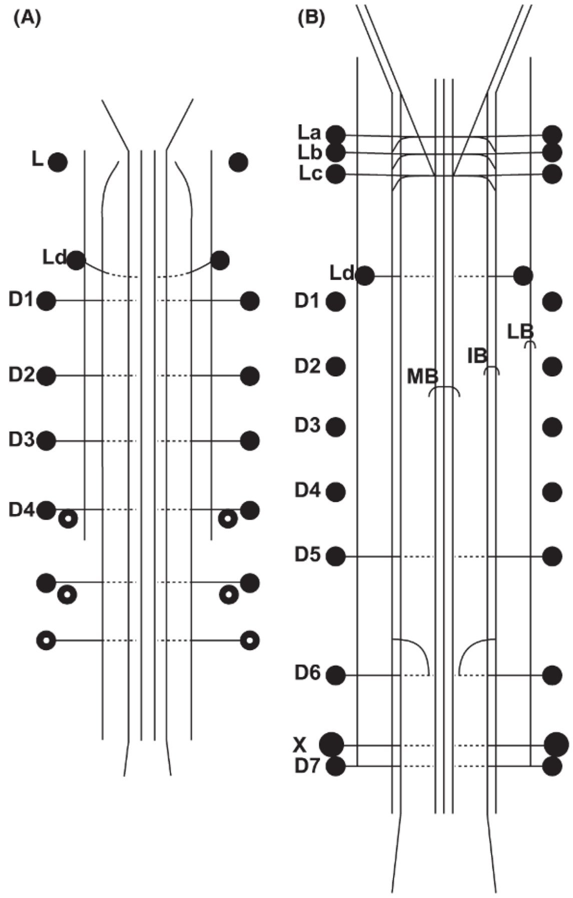

Fig. 5. Schematic representations comparing the RFamidergic system of the VNC of hatchlings during early development. The schematics represent stages of (A) 24 h and (B) 120 h. La–d, lateral cells a–d; LB, lateral bundle; D1–7, dorsal cells 1–7; IB, intermediate bundle; MF, median bundle; X, X-cell.

the subesophageal ganglion *via* the frontal connectives (Fig. 1E). We have recently analyzed the adult architecture of the cephalic nervous system of several chaetognath species using 3D reconstruction techniques from semithin serial sections and immunohistochemistry (Rieger *et al.* 2010). The brain consists of two domains, an anterior domain with connections to the VNC *via* the bilateral main connectives and to the vestibular ganglia *via* the paired frontal connectives, and a posterior domain that receives afferents from the eyes and corona ciliata. Here, we include two pictures of the adult brain for comparison with the brain in hatchlings (Fig. 6G,H). Other than in hatchlings the vestibular ganglia are not visible in adult preparations.

RFamide-ir in the dorsal part of the adult cephalic nervous system shows the brain's division into an anterior and a posterior component corresponding to the median and posterior neurite bundles, respectively (Fig. 6G,H). A paired group of three somata, in the posterior domain of the brain, the posterior lateral cells, sends neurites anteriorly into this posterior neurite bundle (PNB). The fibers of the PNB extend on both sides into the main connectives and establish a connection to the VNC. On both sides of the midline, another more lateral and anterior positioned cell, the median lateral cell, sends its axon to join the PNB. In the rostral part of the brain, additional fibers are present that form the brain's anterior domain (Fig. 6G,H). Some of these fibers constitute the median neurite bundle (MNB), which extends in parallel to the PNB but does not leave the brain. Anteriorly, additional RFamide-ir fibers are arranged in a hornlike shape, the anterior neurite bundle (ANB; compare Rieger *et al.* 2010 for more details).

In young hatchlings, the cephalic nervous system is simply composed of a loop of fibers connected to the VNC that exhibits tubulin-immunoreactivity (Figs 2A,B and 6b). At hatching, the brain does not display any immunoreactivity for synaptic proteins (synapsins). The first signs of synapsin-immunoreactivity (syn-ir) appear around 48 h (Fig. 6B). At first the anterior domain of the brain expresses synapsins more widely and intensively than the posterior domain. Rudiments of the frontal and lateral horns are clearly visible at 72 h (Fig. 6D) and become more distinct during the next 2 days (Fig. 6F). At this point RFamide-immunoreactivity (RFamide-ir) is already quite strong (see below), and those fibers are embedded within the neuropils indicated by synapsin-ir. First synapsin-ir in the posterior domain is found as a band along the RFamide-ir PNB (Fig. 6D). Later synapsins are expressed more widely and an almost rectangular shape is present (Fig. 6F). This posterior part is the developing core neuropil. However, the anterior and posterior parts of the neuropil are not yet clearly separated from each other (Fig. 6F). In addition to the brain, the formation of the more ventrally positioned vestibular ganglia can be observed (Fig. 6D,F). The vestibular ganglia are first visible by 72 h (Fig. 6D). The emergence of synapsin-ir coincides with the development of RFamide-ir in the brain (see below). The two vestibular ganglia are characterized by slightly curved and longitudinal extending masses of neuropil that end in medially directed tips at their posterior ends. The intensity of synapsin-ir in this ganglia increases over the first 76–96 h.

In contrast to the situation in the ventral nerve cord, the pattern of RFamide-ir in the hatchling brain does not resemble the adult pattern at all. For the first 24 h, only one thin fiber bundle is present, which forms a loop in the head (Fig. 6A). The anterior part of this loop will develop into the brain neuropil and is strongly

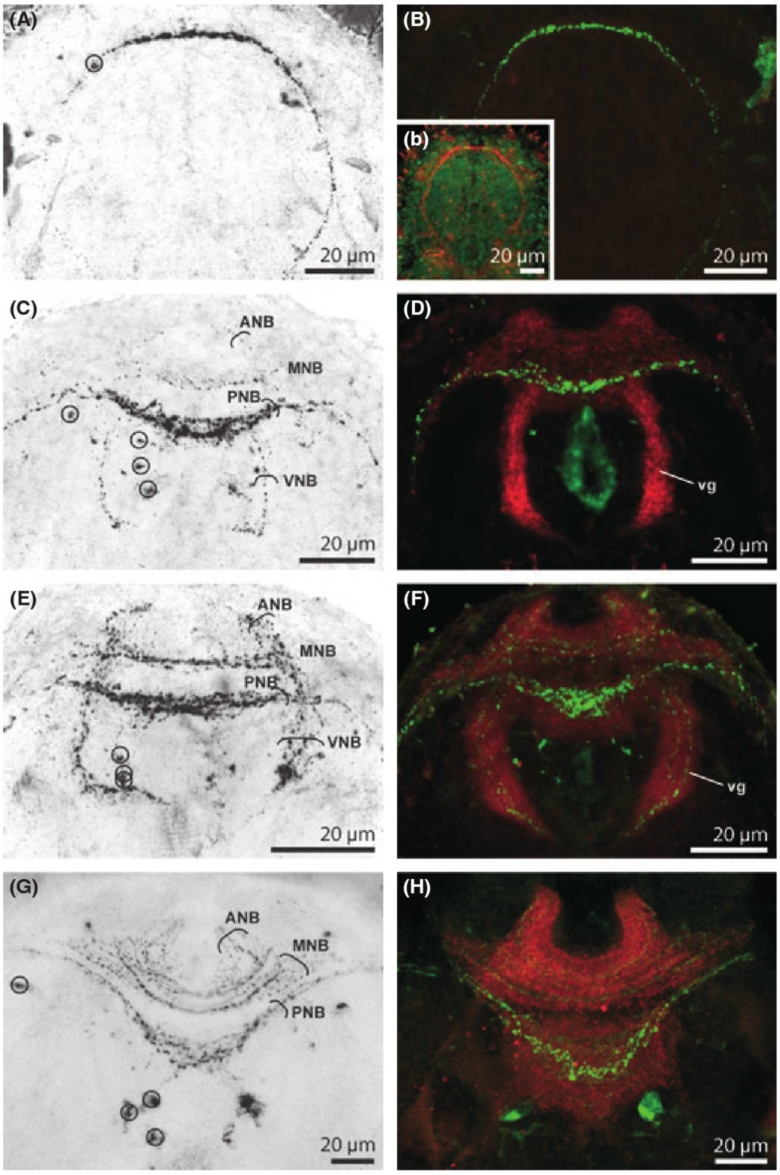

Fig. 6. RFamide-like immunoreactivity (confocal laser-scan microscopy) in the head of adult specimens (G, H) and hatchlings at 24 h (A), 48 h (B), 72 h (C, D), and 120 h (E, F). The left column shows specimens stained against RFamide-like peptides, the images are black-white inverted. The right column shows immunolocalization of RFamide-like peptides (green) and synapsin (red). (b) Inset in (B) 24 h old hatchlings stained against tubulin (red) and nuclei (green). ANB, anterior neurite bundle; MNB, median neurite bundle; PNB, posterior neurite bundle; vg, vestibular ganglion, VNB, ventral neurite bundle.

labeled, while the remaining, lateral fibers of the loop are part of the main connectives that link brain and VNC (Figs 6A and 7A). One pair of cell somata, lateral to the most anterior part of the fiber loop, is inconsistently labeled in the youngest hatchlings and can be seen to project medially in some preparations (Fig. 6A). We could not determine if these cells are the sole source of fibers in the loop or if ascending fibers from the VNC also participate in forming the loop. In addition, one-to-three pairs of inconsistently immunolabeled structures are positioned laterally along the loop of fibers. Even though these structures were labeled in some preparations, we do not consider them to be neuronal somata since they are less prominent than other neuronal structures, are bigger than other observed somata, and probably lie outside the boundaries of the brain (Fig. 6A). From 48 h onwards, additional pairs of RFamide-ir somata were inconsistently detected. Starting with a single additional pair (Fig. 6D), two or three pairs of this type emerge during the following days (circles in Figs 6C,E and 7B,C). These are located more posteriorly and less laterally than the first pair of somata. We therefore assume them to correspond to the adult posterior lateral cells (compare Rieger *et al.* 2010). By 48 h, yet another pair of RFamide-ir cells was observed in some preparations.

This pair is located even more posteriorly and laterally to the loop, with neurites extending medially to the fiber loop. However, it is likely not positioned within the brain and was not observed in older specimens.

Extensive changes are visible between 48 and 72 h regarding the system of RFamide-ir neurites, in that many additional immunolabeled fibers emerge in the developing brain. The frontal part of the primary fiber loop is now strongly labeled, consists of many more immunolabeled profiles, and is slightly curved backwards to prefigure the future posterior neurite bundle (PNB). A few fibers separate laterally from this bundle to extend anteriorly and then course in parallel to the more posterior fiber bundle, thereby forming the developing median neurite bundle (MNB). Some of these fibers also form a hornlike structure in the most anterior part of the brain, the first sign of the anterior neurite bundle (ANB), although at this age the labeling is still inconsistent. These anterior fibers are the first sign of the anterior domain of the brain (Figs 6C,D and 7B). At the same time the vestibular ganglia start to exhibit RFamide-ir. We found inconsistently labeled lateral fibers extending to the posterior part of the brain, slightly curving towards the midline. The same labeling patterns persist in the brain and vestibular ganglia with small changes until 96 h. The somata are labeled less intensely, though, and the processes of single neurons could not be distinguished. However, during the following 2 days, the pattern of fibers becomes more prominent until all structures of the adult brain of *S. cephaloptera* can be distinguished (Figs 6E,F and 7C). Especially the RFamide-ir part of the developing core neuropil, surrounding the PNB, increases in labeling intensity. It is also possible to track fibers from the frontal horns to the vestibular ganglia *via* the frontal connectives. From 120 h onwards, three pairs of posterior lateral somata, that in some preparations can be seen projecting anteriorly to the core neuropil, are constantly visible.

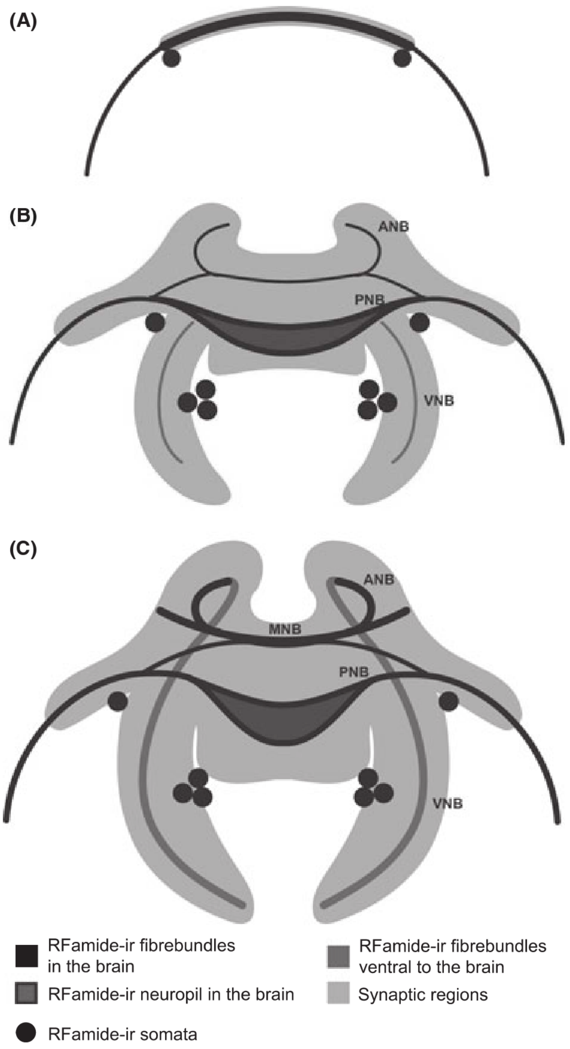
(A)
(B)
ANB
PNB
VNB
(C)
ANB
MNB
PNB
VNB
RFamide-ir fibrebundles in the brain
RFamide-ir fibrebundles ventral to the brain
RFamide-ir neuropil in the brain
Synaptic regions
RFamide-ir somata

Fig. 7. Schematic representations comparing the RFamidergic system of the head in hatchlings during early development. The schematics represent stages of (A) 24 h, (B) 72 h and (C) 120 h. ANB, anterior neurite bundle; MNB, median neurite bundle; PNB, posterior neurite bundle; vg, vestibular ganglion; VNB, ventral neurite bundle.

Discussion

Development of the nervous system and behavior of the hatchlings

The brain in adult arrow worms is subdivided into an anterior and a posterior domain as described by Rieger *et al.* (2010). The posterior domain receives input from the sensory organs and hence, according to Rieger *et al.* (2010) is probably involved in the modulation of motor behavior in response to changing sensory input. The anterior domain is associated with the stomatogastric nervous system and therefore is likely to assist in controlling the activity of the grasping spines, teeth, and the musculature responsible for opening and closing the mouth. Considering that the hatchlings neither feed nor are equipped with the adult set of sensory organs, it is not surprising that the brain is poorly developed at hatching, consisting only of a fiber loop linked to the well developed VNC. During the first 48 h of postembryonic development, zones of synaptic neuropil emerge in the brain, new RFamide-like immunoreactive neurons appear, and a system of RFamide-like immunoreactive fibers is elaborated, all of which implies that a functional brain is present by the time the hatchlings switch from feeding on yolk supplies to active predation.

In contrast to the brain, the VNC is well developed at hatching and is a dominant organ in young hatchlings. The system of RFamidergic neurons in many respects already resembles that in adults, though some postembryonic elaboration occurs. The arrangement of neurons in the species that we studied closely resembles those present in hatchlings of *Paraspadella gotoi* (compare Goto *et al.* 1992) although these authors did not identify the neurons on an individual basis. In adults, the VNC controls swimming by initiating contractions of the body wall musculature and coordinating mechanosensory input from the numerous ciliary fence receptors in the epidermis. For motor control, the VNC closely interacts with the peripheral, exclusively epidermal plexus that innervates the muscles (reviewed in Harzsch & Müller 2007; Harzsch & Wanninger 2010). Similar to the situation in the adult, we suggest here that the VNC modulates body movements in hatchlings, enabling them to escape predators and control their attachment to seaweed, the preferred substrate for attachment in this species. From our studies it appears that the hatchlings are already equipped with some functional fence receptor organs, sensory organs that perceive hydrodynamic stimuli, and an array of papillae on the ventral surface of the body that probably mediate substrate attachment (Müller & Perez, unpubl. data, 2009).

Swimming methods do differ between hatchlings and adults, however, in that the former swim in helicoïdal movements, whereas the adults swim or hunt with rapid, jerking, dorso-vental movements. In this context, it is useful to point out that although the RFamidergic system of the VNC is already implemented in the hatchling, indicating the presence of at least some functional neuronal circuits, experiments using the proliferation marker bromodeoxyuridin (BrdU) indicate that neurogenesis persists during the first 4–5 days after hatching (Rieger, Perez, Müller & Harzsch, unpub. data, 2009). This mitotic activity shows that the VNC is far from being completely differentiated at hatching. Instead, concurrent with changes in locomotion, new neurons are added and existing neuronal systems continue to differentiate. Likewise, our unpublished results suggest that new fence receptor organs are added on the body surface, that provide new sensory input to the VNC that needs to be integrated. In conclusion, the newly hatched, non-feeding animals mostly rely on a set of embryonic fence receptors that perceive hydrodynamic stimuli for navigating in their habitat, predator avoidance, and attachment to their preferred substrate. Because these fence receptors feed into the VNC and because the VNC is essential for swimming behavior, this major neuronal center for sensory-motor integration must be functional to a degree at hatching.

Developmental features and chaetognath affinities: gastrulation patterns

Chaetognath embryology has been explored in laboratory cultures (Kuhl & Kuhl 1965; Reeve 1970; Kuhlmann 1977; Goto & Yoshida 1997; Shimotori & Goto 1999, 2001; Carré *et al.* 2002, review Pearre 1991 and Kapp 2000) including studies using time-lapse imaging (Kuhl & Kuhl 1965) and injections of fluorescent tracer molecules (Shimotori & Goto 1999, 2001) to examine developmental fates of the blastomeres and the establishment of axial properties of the embryos. Chaetognath blastomeres undergo total and equal divisions to generate the blastula. Cleavage has traditionally been perceived as ''radial'' and thus suggestive of a deuterostome affinity. However, recent embryological studies in which the developmental fate of the first four blastomeres was investigated have led Shimotori & Goto (2001) to suggest that chaetognaths may be more similar to protostomes in their developmental program than previously supposed. These authors point out, for example, that the modified spiral cleavage in crustaceans, which have a tetrahedral 4-cell stage, resembles the cleavage pattern of chaetognaths, and they discuss the evolutionary implications. However, considering the diversity of cleavage patterns in Crustacea, the uncertainty over whether crustacean cleavage is derived from spiral cleavage, and the controversy over ancestral cleavage patterns in arthropods more generally (Alwes & Scholtz 2004; Gerberding & Patel 2004) it is doubtful that such patterns, in themselves, can be taken as a very meaningful basis for understanding the phylogenetic relationship between chaetognaths and crustaceans.

Gastrulation describes the process of germ layer formation and is intimately linked to the formation of a digestive system that includes mouth opening, gut and anus. Gastrulation patterns play essential roles in discussions on bilaterian evolution (e.g. Arendt & Nübler-Jung 1997; Nielsen 2001, 2005a,b, 2010; Hejnol & Martindale 2009; Martindale & Hejnol 2009; Lacalli 2010). The blastopore is the site of tissue internalization, and two major phylogenetic concepts are based on the fate of the blastopore. In protostomes, the blastopore becomes the mouth, and the anus (if present) is formed secondarily at a different site (reviewed in Hejnol & Martindale 2009; Martindale & Hejnol 2009). In deuterostomes, the blastopore becomes the anus while the mouth is formed secondarily at a different site in the animal hemisphere of the embryos.

However, Hejnol & Martindale (2009) have pointed out that, on closer examination, a considerable variation in gastrulation patterns is evident between subtaxa, especially in protostomes, which leads them to stress the extreme variability in blastopore fate. In ctenophores and cnidarians the mouth and the blastopore have a common origin, and these animals gastrulate at the animal pole. Nevertheless, bilaterians gastrulate at the vegetal pole (Hejnol & Martindale 2009; Martindale & Hejnol 2009). The authors propose that in Bilateria a separation of the signaling centers that determine the sites of mouth formation *versus* site of germ layer specification has taken place, and that this ancient separation explains the variation of the spatial relation of blastopore and mouth in Bilateria. Furthermore, they critically review the concept of *amphistomy*, which refers to the lateral closure of a slit-like, elongate blastopore. The latter, by staying open at both ends, can account in principle for the formation of both the bilaterian mouth and the anus (e.g. Arendt & Nübler-Jung 1997; Nielsen 2001). Amphistomy appears, however, to occur in this idealized way in only a few protostomian taxa.

Kapp (2000) considers the embryology of the Chaetognatha to be unusual, possibly unique, and difficult to relate to embryological patterns in other bilaterians. She coined a new term, *heterocoely*, to describe the mode of coelom formation during gastrulation. After the invagination of the entoderm, germ cells become localized opposite to the blastopore inside of the cavity enclosed by entoderm. Traditionally, this cavity is termed the archenteron, but Kapp argues against this term as it implies a function as gut anlagen, which is not the case in chaetognaths (see below). The primary body cavity lying between the ecto- and entoderm, the blastocoel, is very narrow. The mesoderm does not form by cells migrating into the blastocoel (schizocoely) nor does it form from diverticulae surrounded by blastocoel that eventually separate from the entoderm (i.e. by enterocoely). Instead, the entoderm folds inwards in two places into the cavity enclosed by entoderm (the archenteron) and the blastocoel subsequently vanishes (this is the ''heterocoely'' referred to by Kapp). Entodermal folds separate part of the cavity enclosed by entoderm opposite to the blastopore into three hollows. The upper tip of the middle space is the area in which the mouth will form and a second opening develops. For a short period the embryo possesses a stomodaeum and a blastopore. The middle hollow shrinks as its walls move towards each other. These cell-layers will eventually form the intestine. The other two hollows will be part of the coelom. The mouth then closes, followed shortly afterwards by the blastopore, so that young hatchlings for a time have neither a mouth opening nor an anus. Both openings are re-established some days after hatching.

In summary, chaetognath gastrulation displays a mosaic of both protostome and deuterostome features, which undoubtedly accounts for the abundance of hypotheses on their phylogenetic relationships (summarized in Harzsch & Müller 2007). The mode of gastrulation has been one of the key reasons for allying them to deuterostomes (summarized in Takada *et al.* 2002), but this link should not necessarily be taken at face value. In a recent review, Lacalli (2010) raises the point that deuterostomy could have emerged more than once in the taxa conventionally assigned to the Deuterostomia. The condition is linked to a delay in mouth formation in the developing dipleurula larvae of one subgroup, the Ambulacraria (echinoderms plus hemichordates), and this could be associated with their distinctive mode of feeding, which relies on a ciliated food-collecting domain that surrounds the mouth. In contrast, there is little evidence as yet that the other subgroup (chordates) ever had feeding larvae of this type (Lacalli 2005) but the delay in mouth formation (and hence deuterostomy) in chordates may instead be more a consequence of the reorganization of the head region required by dorsoventral inversion, a feature of chordates but not the Ambulacraria. In chordates, in fact, the embryonic anus closes as well, so both the mouth and the definitive anus are formed quite late, and neither occupies the precise site of the blastopore. Since the hatching stages of chordates rely on a substantial store of yolk, there is a greater freedom to rearrange the openings to the gut without compromising function. It is possible, in this way, to view deuterostomy as a secondary change that may have occurred several times and for different adaptive reasons.

If, in fact, the mouth has been the subject of evolutionary experiments of this type in taxa conventionally assigned to the deuterostomes, it is a short step to suggesting that chaetognaths may simply represent a third such experiment in which a mode of gastrulation has evolved that is clearly distinct from protostomes, but without necessarily meaning that chaetognaths are taxonomically close to deuterostomes. This conclusion, that chaetognaths display a third and independently evolved variant of deuterostomy, allows their mode of gastrulation to be more easily accommodated with interpretations of phylogenomic data that place chaetognaths either closer to or fully within the protostomes (compare Fig. 1F). At the same time, it supports the conclusions of Takada *et al.* (2002) on *brachyury* expression in a closely related chaetognath species, *Paraspadella gotoi*, that the expression pattern of this gene in the embryonic chaetognath blastopore and

© 2011 The Authors

mouth resembles that of hemichordates and echinoderms, whereas the pattern in the region of the new mouth opening of the hatchling appears to be novel.

CNS development in chaetognaths and insights into the basal bilaterian condition

The structure of the nervous system in the last common bilaterian ancestor (LCBA) is currently a topic of considerable controversy (e.g. Holland 2003; Hirth & Reichert 2006; Denes *et al.* 2007; Lichtneckert & Reichert 2007; Lowe 2007; Schmidt-Rhaesa 2007; Arendt *et al.* 2008; Benito-Gutiérrez & Arendt 2009; Nomaksteinsky *et al.* 2009; Reichert 2009; Harzsch & Wanninger 2010; Kaul & Stach 2010; Miyamoto *et al.* 2010; Rieger *et al.* 2010). One of the important questions is whether the LCBA had a decentralized nervous system, structured as an epithelial plexus without ganglia or other concentrations of neuronal cell somata, or had already centralized elements such as longitudinal cords or even a brain. The available data leads some authors (Rieger *et al.* 2010; Semmler *et al.* 2010) to assume that centralized structures may not have been part of the ground pattern, though the necessary ''genetic toolkit'' for producing such structures was already present. This would explain how a centralized nervous system could evolve independently in protostome and deuterostome taxa. The circumesophageal nature common to all protostome nervous systems implies that the protostomian ancestor had a centralized brain. In contrast, within deuterostomes centralized structures may have formed independently at least twice (Rieger *et al.* 2010; Semmler *et al.* 2010). Ultimately, however, this issue remains unresolved, even by molecular developmental analyses (Harzsch & Wanninger 2010). We have previously discussed the impact of the adult chaetognath brain on such debates at some length, and will therefore repeat only our conclusion here, that the arrangement of the chaetognath cephalic nervous system is suggestive of protostome affinities (Harzsch & Müller 2007; Rieger *et al.* 2010).

The developmental data reported here provide some further insight into this issue. Clearly, the brain of chaetognath hatchlings is delayed in development when compared to the ventral nerve center. At hatching, the brain is represented simply by a fiber loop that extends anteriorly from the ventral nerve center and surrounds the area, where a few days later the new mouth opening and its connection to the gut will form (Fig. 8A). This ''primary brain'', which topologically can be viewed as a circumoral nerve ring, will develop into the posterior brain domain of the adult. Acting as a kind of ''sensory brain'', it receives input from the sensory organs and may be involved in the modulation of motor behaviors in response to changing sensory input (Rieger *et al.* 2010). Slightly later, a second brain component develops in hatchlings that topologically can also be viewed as being arranged in a circumoral pattern (Fig. 8B,C), and this develops into the anterior brain domain. This anterior domain gives rise to the stomatogastric nervous system, which, in the adult, is involved in controlling the activity of the grasping spines, the innervation of the teeth, and the musculature responsible for opening and closing the mouth (Rieger *et al.* 2010). The circumesophageal arrangement of the adult cephalic nervous system including, in addition to the brain, vestibular and subesophageal ganglion (compare Fig. 1) has already been recognized by Nielsen (2001). However, the situation in the hatchlings clearly shows that we do not only face *one* but *two* brain components that have a basically circumoral arrangement (Fig. 8A–C).

In other bilaterian invertebrates, the ventral cords, with suitable cross-connections, are typically also circumoral in arrangement (or circum-blastoporal, Nielsen's equivalent, in some cases). Together with the oral and/or stomatogastric innervation, one then has much the same condition as in chaetognaths, a CNS comprised of two essentially separate circumoral subsystems. Figure 8(D–I) shows this, taking a selection of examples taken from early development (e.g. from larvae) on the supposition that these better reveal more of the basic developmental plan than the adult anatomy. Considering the secondary modifications seen in many larvae, this is not necessarily the case, but it is useful as a starting point for a phylogenetic analysis.

Thus, among ecdysozoans and spiralian protostomes, there is a well-defined stomodeal derivative (e.g. a foregut or similar) supplied with stomatogastric nerves and ganglia (Fig. 8D,E) quite separate from the ventral cords supplying the body wall and muscles of the trunk. The innervation pattern is more diffuse and more complex in the case of flatworms (Fig. 8F), but exhibits an otherwise similar pattern. The situation in lophophorate taxa is less straightforward: the mouth here typically leads to a tapered esophagus, but a ciliated preoral vestibule, funnel or hood is usually present, which serves to concentrate food particles during filter feeding. These preoral structures are usually supplied with suboral nerve tracts, in the form of innervated ciliated ridges in the case of the cyphonautes larva (Santagata 2008), or innervated tentacles in the case of phoronids (Hay-Schmidt 1990a,b). The postoral esophagus, in contrast, appears to have a very limited nerve supply if any, at least at early developmental stages. The various neural elements associated with the mouth are basically circumoral in

© 2011 The Authors

Fig. 8. Schematic drawings of the nervous system in Chaetognaths (A–C) and various other species. (A, B) Highlight the differences between a hatchling (A) and an adult (B) specimen, whereas (C, C′) show the adult nervous system from two different angles. For comparison we also included a highly schematic survey of the main stomatogastric and longitudinal nerve tracts in a selection of invertebrates, most shown in two different views, of which the larger is frontal (E, F) or dorsal (C, D, G, H) and the smaller is lateral (C′–H′). Nerves and ganglia are drawn in yellow; with ganglia shown as bulbous swellings. Frontal views of the oral junction between ectoderm and entoderm are indicated by a heavy circle, with a surrounding green domain to indicate the zone occupied by the stomodeum or, in the case of (I), its probable deuterostome equivalent. Hence, the anatomical ''mouth'' in these diagrams lies along the dotted circle, while the anus, where shown, is smaller and outlined with a thinner solid line. The longitudinal tracts, where paired, are assumed to represent a potentially circumblastoporal component (*sensu* Nielsen) even where they do not form a complete loop; the stomatogastric nerves more typically do form a loop, with or without ganglia, around the mouth, though the relation of the latter to the blastopore clearly differs between groups. Taxa with a clearly identifiable stomodeal invagination include arthropods (D, D′; a crustacean [egg] nauplius stage, modified from Fabritius-Vilpoux *et al.* 2008) and protostomes with a muscular pharynx, e.g. annelids (E, E′; a serpulid polychaete trochophore larva, where the transition between larva and juvenile can be followed, from Lacalli 1988; see also McDougall *et al.* 2006). For polyclad flatworms, the arrangement of nerves in Muller's larva is shown (F, F′; from Rawlinson 2010; see also Lacalli 1982); there are basic similarities with the arrangement of nerves in the trochophore despite other differences, e.g. the absence of an anus (see Lacalli 1984). Lophophorates are not included in the figure, as the diffuse innervation of both the oral region and the body wall makes comparison with other taxa more difficult, but there are similarities (see text). In basal deuterostomes, represented here by a very schematic pluteus larva (I), the oral region is well innervated, at least in the larval stages where the muscular esophagus is used for swallowing. There is typically either a suboral ring of neurons at the junction of the vestibule and esophagus (asteroids, Chee & Byrne 1999) that later produces a quite extensive plexus (Nakajima *et al.* 2004) or a pair of adoral ganglia that flank the mouth (Nakajima *et al.* 2004). These are linked in most instances by small nerve tracts to nerve tracts from the apical organ supplying the ciliary bands. The tornaria has a similar complement of tracts running along the underside of the esophagus (Lacalli *et al.* 1999; Miyamoto *et al.* 2010). Such larvae lack an obvious counterpart to the trunk innervation of protostome taxa, which instead will develop only at the juvenile stage (hemichordates) or not at all because of secondary modifications to the body plan (echinoderms). For comparison we also included schematics on the hypothetic development of an ancestral protostome (G, G′, H, H′; see Nielsen 2010). and, anterior neuropil domain of the brain; cc, corona ciliata; pb, primordial brain; pnd, posterior neuropil domain of the brain; sog, sub-oesophageal ganglion; vg, vestibular ganglion; VNC, ventral nerve center.

---

arrangement, as is evident in phoronid larvae in both the major and minor nerve rings and the epistome margin nerves (Hay-Schmidt 1990a,b; Santagata 2002). Likewise, the larvae of Brachiopoda have the dorsal and ventral lophophore nerves that circle the mouth opening (Hay-Schmidt 1992), but trunk innervation, as in the other lophophorate groups, is more difficult to relate directly to the arrangement observed in spiralians and ecdysozoans.

Basal deuterostomes, in their larvae at least (Fig. 8I), have a well-innervated esophagus used for muscular swallowing. In asteroid larvae, this begins as a suboral ring of neurons at the junction of the vestibule and esophagus (Chee & Byrne 1999) that later produces a quite extensive plexus (Nakajima *et al.* 2004) or a pair of adoral ganglia that flank the mouth opening (Nakajima *et al.* 2004). These are linked in most instances by small nerve tracts to the ciliary band nerves, but there is no clear counterpart to the trunk innervation of protostomes owing to the unusual body plan of echinoderms. Hemichordates would be more informative from a comparative standpoint if more were known of relevant aspects of their neural development and early neuroanatomy. Their larva, the tornaria, has irregular tracts running along the underside of the esophagus (Lacalli & Gilmour 2001; Miyamoto *et al.* 2010), derived apparently from scattered cells rather than ganglia. Transition to the adult in this case generates a preoral vestibule, but how its innervation develops in relation to that of the trunk is not known. Chordates are not included in the figure because of the problem of relating their nerve cord in a meaningful way to the ventral cords of other invertebrate taxa (Burke 2011), but among invertebrate chordates: tunicates have a coronal organ consisting of a ring of sensory cells around the mouth that synapse to nerves whose cell bodies lie in the central ganglion (e.g. Manni *et al.* 2006); amphioxus has a circumoral ring nerve containing fibers from both peripherally and centrally located neurons (Lacalli *et al.* 1999; Kaji *et al.* 2009). Whether these two are homologous or otherwise related is not clear, but both are circumoral complexes positioned at the opening of the pharynx.

The widespread occurrence among invertebrates of a CNS consisting of two essentially separate circumoral components, one for oral innervation and one for the rest of the body, prompts us to look more closely at how this situation might have arisen. Current hypotheses for bilaterian origins and body plan evolution are of basically two types, depending on whether the ancestral forms are supposed to be radial in organization or to have already had an established anteroposterior axis. The latter typically take the acoelomorph worms as likely models, though recent

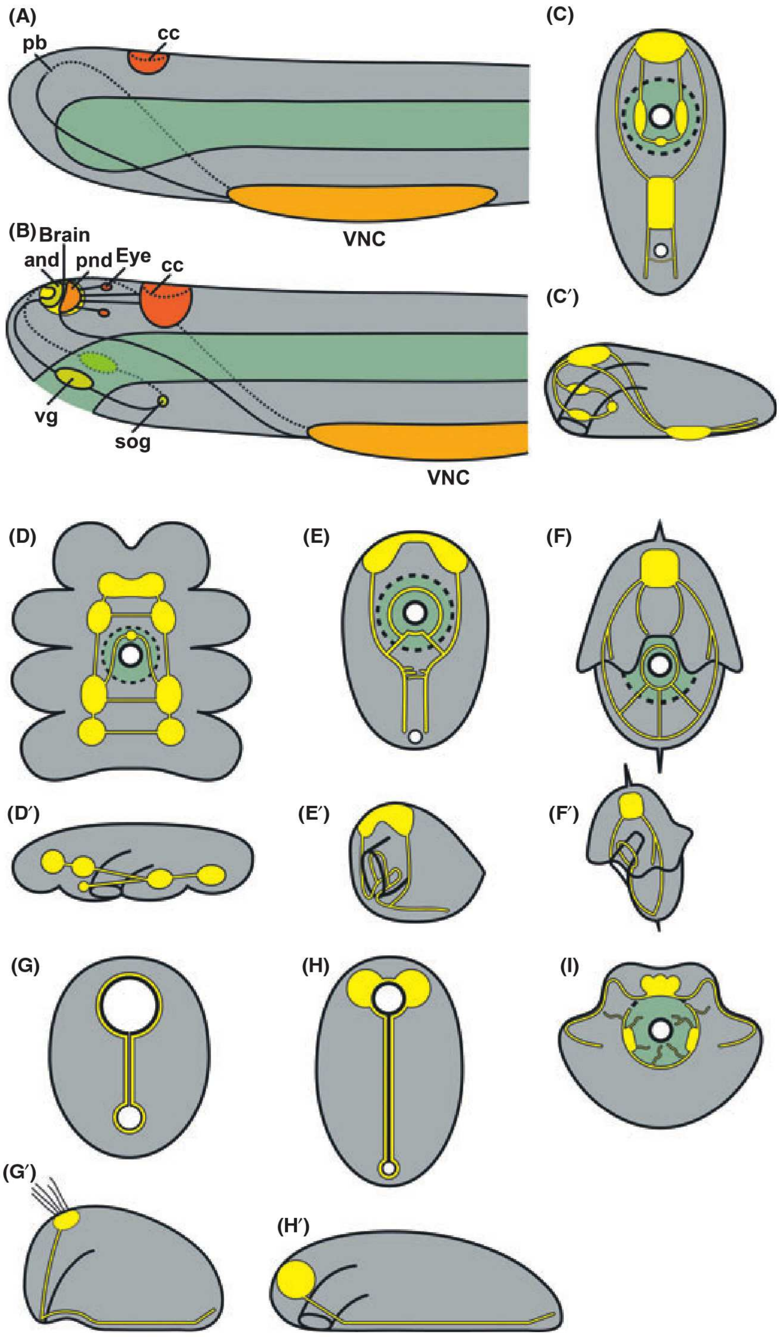

results (Philippe *et al.* 2011) have raised questions as to how basal the acoelomorphs really are. Nevertheless, the LCBA may have been like acoels in having longitudinal nerves projecting to the trunk in order to control body shape and locomotory effectors, whether muscles or cilia. But if the LCBA mouth was transitory, as in acoels, one can suppose there was much less involvement of nerves in the process of food ingestion. In consequence, the axial nerves devoted to locomotory control, whether arranged in a circumoral fashion or not, may have evolved before an oral innervation of any complexity was established. In such scenarios, a well-defined stomatogastric innervation might well be a quite late innovation.

In contrast, for hypotheses that invoke a radial ancestor that feeds, the expectation is for there to be a common plan across the Bilateria in the way the innervation of the oral region and feeding apparatus (e.g. tentacles, if present) is organized. Circumoral loops are likely, possibly patterned along lines seen in modern radiate animals such as cnidarians (Mackie & Meech 1995, 2008; Martindale *et al.* 2004). One then needs to consider how such systems changed during the progressive evolution of the trunk and associated changes in locomotory capabilities. Among the better-known treatments of this issue is Nielsen's trochaea hypothesis (Nielsen 2005a,b, 2010): here the blastopore, which would originally have formed just the mouth, is stretched axially along the ventral surface of the body as the trunk evolves. If one then assumes a zone of neurogenic tissue along the blastopore margin, longitudinal nerve tracts can be derived from this (Fig. 8G). Supplemented with an anterior pair of cerebral ganglia, this generates a typical protostome arrangement of brain and paired ventral tracts (Fig. 8H). Whether a similar explanation applies to deuterostomes is less evident. Nevertheless, for protostomes at least, the circumoral component of the CNS is intimately associated with the expanding domain of the trunk, while the tubular digestive tract with separate mouth and anus arises as a natural consequence of the process. Nothing specific is said, however, about the stomodeal innervation, which presumably arises secondarily.

An alternative, assuming again a radial ancestor, is to view the trunk as an addition to the ancestral radial body instead of a consequence of modifying its shape by stretching. The *radial head hypothesis* developed by Shankland and colleagues (Bruce & Shankland 1998; Shankland & Seaver 2000) is an example. Here, the radial ancestor is represented in the LCBA in the head, and the mouth and its innervation derives from the circumoral nerves supplying the oral region of that ancestor. How the trunk evolved, presumably associated with the eventual evolution of an actively motile mode of life, is a separate issue. So regardless of details, the trunk is conceived of essentially as a later addition, attached to one side of the ancestral body. One could argue that the Hox gene cluster, being so similar among modern bilaterian taxa, argues for an extended trunk-like body region with a role in locomotion being at least as old as the LCBA. There are alternatives, however. It is possible, for example, that the original function of such genes was unrelated to trunk evolution and locomotion, but had instead to do with gonad specification, as suggested by Arenas-Mena (2010). Scenarios in which a change in locomotory mode is not the key event in bilaterian evolution therefore also need to be considered. In terms of conserved innervation patterns, the key feature carried through from the radial ancestor might thus be the supply to the oral region, in the form of circumoral nerves like those seen in radial animals (e.g. cnidarians) today.

The above analysis highlights the question of whether stomatogastric innervation in bilaterians might be older than, contemporary with, or more recent in origin than their trunk innervation. This point is worth emphasizing, because knowing which of the main targets of the two circumoral systems of tracts evolved first, the specialized mouth or the muscular trunk, tells us something about the nature of the LCBA. If the latter sprang from radial animals with nerves encircling an orifice that is both mouth and blastopore, did the trunk and creeping habit then evolve first, before a stomodeal feeding apparatus? Or did the latter come first, to be later adapted variously by taxa as diverse locomotory specializations evolved, some for a creeping, motile habit, others for a sedentary and less active habit? In this respect, understanding the homologies of the stomodeal innervation and its relation to the ventral nerve cord serves as a proxy for the more difficult problem of discovering how blastopores first became mouths and anuses, and how the trunks and nerve cords that arose with this transition originated. The present results, on chaetognaths, do not as yet help in choosing between alternatives. However, by defining more clearly the issues involved, there is a better prospect for more focused research on the subject that might do so.

Acknowledgments

The authors gratefully acknowledge E. Buchner (Würzburg) for generously providing samples of the SYNORF-1 antibody. We also wish to thank Claus Nielsen for comments on an earlier version of the manuscript. This study was supported by grant HA 2540/7-2 in the DFG focus program ''Metazoan Deep Phylogeny'' and by the Max Planck Society.

References

Alwes, F. & Scholtz, G. 2004. Cleavage and gastrulation of the euphausiacean *Meganyctiphanes norvegica* (Crustacea, Malacostraca). *Zoomorphology* **123**, 125–137.

Arenas-Mena, C. 2010. Indirect development, transdifferentiation and the macroregulatory evolution of metazoans. *Philos. Trans. R. Soc. Lond. B Biol. Sci.* **365**, 653–669.

Arendt, D., Denes, A. S., Jékely, G. & Tessmar-Raible, K. 2008. The evolution of nervous system centralization. *Philos. Trans. R. Soc. Lond. B Biol. Sci.* **363**, 1523–1528.

Arendt, D. & Nübler-Jung, K. 1997. Dorsal or ventral: similarities in fate maps and gastrulation patterns in annelids, arthropods and chrodates. *Mech. Dev.* **61**, 7–21.

Arnaud, J., Brunet, M. & Mazza, J. 1978. Studies on the midgut of *Centropages typicus* (Copepod, Calanoida). I. Structural and ultrastructural data. *Cell Tissue Res.* **187**, 333–353.

Benito-Gutiérrez, È. & Arendt, D. 2009. CNS evolution: new insight from the mud. *Curr. Biol.* **19**, R640–R642.

Bone, Q. & Duvert, M. 1991. Locomotion and buoyancy. In *The Biology of Chaetognaths* (Eds Q. Bone, H. Kapp & A. C. Pierrot-Bults), pp. 32–44, Oxford University Press, New York.

Bone, Q., Grimmelikhuijzen, C. J. P., Pulsford, A. & Ryan, K. P. 1987. Possible transmitter functions of acetylcholine and an RFamide-like substance in *Sagitta* (Chaetognatha). *Proc. R. Soc. Lond. B* **230**, 1–14.

Bone, Q. & Pulsford, A. 1984. The Sense Organs and Ventral Ganglion of *Sagitta* (Chaetognatha). *Acta Zool.* **65**, 209–220.

Bruce, A. E. E. & Shankland, M. 1998. Expression of the head gene *Lox22-Otx* in the leach *Helobdella* and the origin of the bilaterian body plan. *Dev. Biol.* **201**, 101–112.

Burke, R. D. 2011. Deuterostome neuroanatomy and the body plan paradox. *Evol. Dev.* **13**, 110–115.

Carré, D., Djediat, C. & Sardet, C. 2002. Formation of a large Vasa-positive germ granule and its inheritance by germ cells in the enigmatic Chaetognaths. *Development* **129**, 661–670.

Cebrià, F. 2008. Organization of the nervous system in the model planarian *Schmidtea mediterranea*: an immunocytochemical study. *Neurosci. Res.* **61**, 375–384.

Chee, F. & Byrne, M. 1999. Development of the larval serotonergic nervous system in the sea star *Patiriella regularis* as revealed by confocal imaging. *Biol. Bull.* **197**, 123–131.

Denes, A. S., Jékely, G., Steinmetz, P. R. H., Raible, F., Snyman, H., Prud'homme, B., Ferrier, D. E. K., Balavoine, G. & Arendt, D. 2007. Molecular architecture of annelid nerve cord supports common origin of nervous system centralization in bilateria. *Cell* **129**, 277–288.

Dockray, G. J. 2004. The expanding family of RF-amide peptides and their effects on feeding behaviour. *Exp. Physiol.* **89**, 229–235.

Doncaster, L. 1902. On the Development of *Sagitta*; with Notes on the Anatomy of the Adult. *Q. J. Microsc. Sci. s2* **46**, 351–395.

Dunn, C. W., Hejnol, A., Matus, D. Q., Pang, K., Browne, W. E., Smith, S. A., Seaver, E., Rouse, G. W., Obst, M., Edgecombe, G. D., Sørensen, M. V., Haddock, S. H. D., Schmidt-Rhaesa, A., Okusu, A., Kristensen, R. M., Wheeler, W. C., Martindale, M. Q. & Giribet, G. 2008. Broad phylogenomic sampling improves resolution of the animal tree of life. *Nature* **452**, 745–749.

Duvert, M., Perez, Y. & Casanova, J. 2000. Wound healing and survival of beheaded chaetognaths. *J. Mar. Biol. Ass. UK* **80**, 891–898.

Fabritius-Vilpoux, K., Bisch-Knaden, S. & Harzsch, S. 2008. Engrailed-like immunoreactivity in the embryonic ventral nerve cord of the Marbled Crayfish (Marmorkrebs). *Invert. Neurosci.* **8**, 177–197.

Gerberding, M. & Patel, N. H. 2004. Gastrulation in crustaceans: germ layers and cell lineages. In *Gastrulation: From Cells to Embryos* (Ed. C. Stern), pp. 78–89, CSHL Press, Cold Spring Harbor.

Ghirardelli, E. 1968. Some Aspects of the Biology of the Chaetognaths. *Adv. Mar. Biol.* **6**, 271–375.

Giribet, G., Distel, D. L., Polz, M., Sterrer, W. & Wheeler, W. C. 2000. Triploblastic relationships with emphasis on the Acoelomates and position of Ganthostomulida, Cycliophora, Plathelminthes and Chaetognatha: a combined approach to 18S rDNA sequences and morphology. *Syst. Biol.* **49**, 539–562.

Goto, T., Katayama-Kumoi, Y., Tohyama, M. & Yoshida, M. 1992. Distribution and development of the serotonin-and RFamide-like immunoreactive neurons in the arrowworm, *Paraspadella gotoi* (Chaetognatha). *Cell Tissue Res.* **267**, 215–222.

Goto, T. & Yoshida, M. 1984. Photoreception in Chaetognatha. In *Photoreception and Vision in Invertebrates* (Ed. M. A. Ali), pp. 727–742, Plenum Publishing Corporation, New York.

Goto, T. & Yoshida, M. 1985. The mating sequence of the benthic arrowworm *Spadella schizoptera*. *Biol. Bull.* **169**, 328–333.

Goto, T. & Yoshida, M. 1987. Nervous System in Chaetognatha. In *Nervous Systems in Invertebrates* (Ed. M. A. Ali), pp. 461–481, Plenum Publishing Corporation, New York.

Goto, T. & Yoshida, M. 1997. Growth and reproduction of the benthic arrowworm *Paraspadella gotoi* (Chaetognatha) in laboratory culture. *Invert. Reprod. Dev.* **32**, 201–207.

Goto, T. 1999. Fertilization process in the arrow worm *Spadella cephaloptera* (Chaetognatha). *Zool. Sci.* **16**, 109–114.

Greenberg, M. J. & Price, D. A. 1992. Relationships among the FMRFamide-like peptides. *Prog. Brain Res.* **92**, 25–37.

Grimmelikhuijzen, C. J. P. & Spencer, A. N. 1984. FMRFamide immunoreactivity in the nervous system of the medusa *Polyorchis penicillatus*. *J. Comp. Neurol.* **230**, 361–371.

Grimmelikhuijzen, C. J. P. 1985. Antisera to the sequence Arg-Phe-amide visualize neuronal centralization in hydroid polyps. *Cell Tissue Res.* **241**, 171–182.

Halanych, K. M. 1996. Testing hypotheses of chaetognath origins: long branches revealed by 18S ribosomal DNA. *Syst. Biol.* **45**, 223–246.

Harzsch, S., Anger, K. & Dawirs, R. R. 1997. Immunocytochemical detection of acetylated tubulin and *Drosophila* synapsin in the embryonic crustacean nervous system. *Int. J. Dev. Biol.* **41**, 477–484.

Harzsch, S. & Hansson, B. S. 2008. Brain architecture in the terrestrial hermit crab *Coenobita clypeatus* (Anomura, Coenobitidae), a crustacean with a good aerial sense of smell. *BMC Neurosci.* **9**, 58.

Harzsch, S., Müller, C. H. G., Rieger, V., Perez, Y., Sintoni, S., Sardet, C. & Hansson, B. 2009. Fine structure of the ventral nerve centre and interspecific identification of individual neurons in the enigmatic Chaetognatha. *Zoomorphology* **128**, 53–73.

Harzsch, S. & Müller, C. H. G. 2007. A new look at the ventral nerve centre of *Sagitta*: implications for the phylogenetic position of Chaetognatha (arrow worms) and the evolution of the bilaterian nervous system. *Front. Zool.* **4**, 14.

Harzsch, S. & Wanninger, A. 2010. Evolution of invertebrate nervous systems: the Chaetognatha as a case study. *Acta Zool.* **91**, 35–43.

Hay-Schmidt, A. 1990a. Distribution of catecholamine-containing, serotonin-like and neuropeptide FMRFamide-like immunoreactive neurons and processes in the nervous system of the actinotroch larva of *Phoronis muelleri* (Phoronida). *Cell Tissue Res.* **259**, 105–118.

Hay-Schmidt, A. 1990b. Catecholamine-containing, serotonin-like, and FMRFamide-like immunoreactive neurons and processes in the nervous system of the early actinotroch larva of *Phoronis vancouverensis* (Phoronida): distribution and development. *Can. J. Zool.* **68**, 1525–1536.

Hay-Schmidt, A. 1992. Ultrastructure and immunocytochemistry of the nervous system of the larvae of *Lingula anatina* and *Glottidia* sp. (Brachiopoda). *Zoomorphology* **112**, 189–205.

Hejnol, A. & Martindale, M. Q. 2009. The mouth, the anus and the blastopore – open questions about questionable openings. In *Animal Evolution: Genes, Genomes, Fossils and*

© 2011 The Authors

Trees (Eds M. J. Telford & D. T. J. Littlewood), pp. 33–40, Oxford University Press, Oxford.

Helfenbein, K. G., Fourcade, H. M., Vanjani, R. G. & Boore, J. L. 2004. The mitochondrial genome of Paraspadella gotoi is highly reduced and reveals that chaetognaths are a sister group to prostostomes. *PNAS* **101**, 10639–10643.

Hertwig, O. 1880. Die Chaetognathen Ihre Anatomie, Systematik und Entwicklungsgeschichte. In *Studien zur Blättertheorie*, Vol. 2 (Eds O. Hertwig & R. Hertwig) Gustav Fischer Verlag, Jena.

Hirth, F. & Reichert, H. 2006. Basic nervous system types: one or many? In *Evolution of Nervous Systems*, Vol. 1 (Ed. J. H. Kaas), pp. 55–72. Academic Press, Oxford.

Holland, N. D. 2003. Early central nervous system evolution: an era of skin brains? *Nat. Rev. Neurosci.* **4**, 617–627.

Hyman, L. 1959. The enterocoelous coelomates-phylum Chaetognatha. In *The Invertebrates: Smaller Coelomate Groups*, Vol. 5, pp. 1–71. McGraw-Hill, New York.

John, C. C. 1933. Habits, Structure, and Development of *Spadella cephaloptera*. *Q. J. Microsc. Sci.* **75**, 625–696.

Kaji, T., Shimizu, K., Artinger, K. B. & Yasui, K. 2009. Dynamic Modification of Oral Innervation During Metamorphosis in *Branchiostoma belcheri*, the Oriental Lancelet. *Biol. Bull.* **217**, 151–160.

Kapp, H. 2000. The Unique Embryology of Chaetognatha. *Zool. Anz.* **239**, 263–266.

Kapp, H. 2007. Chaetognatha, Pfeilwürmer. In *Spezielle Zoologie*, Vol. 1 (Eds W. Westheide & R. Rieger), pp. 898–904, Gustav Fischer Verlag, Stuttgart.

Kaul, S. & Stach, T. 2010. Ontogeny of the collar cord: neurulation in the hemichordate *Saccoglossus kowalevskii*. *J. Morphol.* **271**, 1240–1259.

Klagges, B. R. E., Heimbeck, G., Godenschwege, T. A., Hofbauer, A., Pflugfelder, G. O., Reifegerste, R., Reisch, D., Schaupp, M., Buchner, S. & Buchner, E. 1996. Invertebrate synapsins: a single gene codes for several isoforms in *Drosophila*. *J. Neurosci.* **16**, 3154–3165.

Kriegsfeld, L. J. 2006. Driving reproduction: RFamide peptides behind the wheel. *Horm. Behav.* **50**, 655–666.

Kuhl, W. & Kuhl, G. 1965. Die Dynamik der Frühentwicklung von *Sagitta setosa*. *Helgol. Mar. Res.* **12**, 260–301.

Kuhl, W. 1938. Chaetognatha. In *Klassen und Ordnungen des Tierreichs*, Vol. 4, Section 4, Part 2 (Ed. H. G. Bronn), pp. 1–226, Akademische Verlagsgesellschaft M. B. H. Leipzig, Leipzig.

Kuhlmann, D. 1977. Laboratory studies on the feeding behavior of the chaetognaths *Sagitta setosa* J. Müller and *S. elegans* Verrill with special reference to fish eggs and larvae as food organisms. *Kieler Meeresforsch* **25**, 163–171.

Lacalli, T. C., Gilmour, T. H. J. & Kelly, S. J. 1999. The oral nerve plexus in amphioxus larvae: function, cell types and phylogenetic significance. *Proc. R. Soc. Lond. B Biol. Sci.* **266**, 1461–1470.

Lacalli, T. C. & Gilmour, T. H. J. 2001. Locomotory and feeding effectors of the tornaria larva of *Balanoglossus biminiensis*. *Acta Zool.* **82**, 117–126.

Lacalli, T. C. 1982. The nervous system and ciliary band of Müller's larva. *Proc. R. Soc. Lond. B Biol. Sci.* **217**, 37–58.

Lacalli, T. C. 1984. Structure and organization of the nervous system in the trochophore larva of *Spirobranchus*. *Philos. Trans. R. Soc. Lond. B Biol. Sci.* **306**, 79.

Lacalli, T. C. 1988. Foregut innervation in juvenile *Spirobranchus spinosus* (Polychaeta). *Can. J. Zool.* **66**, 1488–1491.

Lacalli, T. C. 2005. Protochordate body plan and the evolutionary role of larvae: old controversies resolved? *Can. J. Zool.* **83**, 216–224.

Lacalli, T. C. 2010. The emergence of the chordate body plan: some puzzles and problems. *Acta Zool.* **91**, 4–10.

Lichtneckert, R. & Reichert, H. 2007. Origin and evolution of the first nervous system. In *Evolution of Nervous Systems. A Comprehensive Reference*, Vol. 1 (Ed. J. H. Kaas), pp. 289–315, Academic Press, Amsterdam.

Littlewood, T. J., Telford, M. J., Clough, K. A. & Rohde, K. 1998. Gnathostomulida – an enigmatic metazoan phylum from both morphological and molecular perspectives. *Mol. Phylogenet. Evol.* **9**, 72–79.

Lowe, C. J. 2007. Origins of the chordate central nervous system: insights from hemichordates. In *Evolution of Nervous Systems – A Comprehensive Reference*, Vol. 2, Non-mammalian Vertebrates (Eds J. H. Kaas & T. H. Bullock), pp. 25–38, Oxford Academic Press, Oxford.

Mackie, G. O. & Meech, R. W. 1995. Central circuitry in the jellyfish *Aglantha digitale* I. The relay system. *J. Exp. Biol.* **198**, 2261–2270.

Mackie, G. O. & Meech, R. W. 2008. Nerves in the endodermal canals of hydromedusae and their role in swimming inhibition. *Invert. Neurosci.* **8**, 199–209.

Mallat, J. & Winchell, C. J. 2002. Testing the new animal phylogeny: first use of combined large-subunit and small sub-unit rRNA gene sequences to classify the protostomes. *Mol. Biol. Evol.* **19**, 289–301.

Manni, L., Mackie, G. O., Caicci, F., Zaniolo, G. & Burighel, P. 2006. Coronal organ of ascidians and the evolutionary significance of secondary sensory cells in chordates. *J. Comp. Neurol.* **495**, 363–373.

Marlétaz, F., Gilles, A., Caubit, X., Perez, Y., Dossat, C., Samain, S., Gyapay, G., Wincker, P. & Le Parco, Y. 2008. Chaetognath transcriptome reveals ancestral and unique features among bilaterians. *Genome Biol.* **9**, R94.

Marlétaz, F., Martin, E., Perez, Y., Papillon, D., Caubit, X., Lowe, C. J., Freeman, B., Fasano, L., Dossat, C., Wincker, P., Weissenbach, J. & Le Parco, Y. 2006. Chaetognath phylogenomics: a protostome with deuterostome-like development. *Curr. Biol.* **16**, R577–R578.

Martindale, M. Q., Pang, K. & Finnerty, J. R. 2004. Investigating the origins of triploblasty: 'mesodermal' gene expression in a diploblastic animal, the sea anemone *Nematostella vectensis* (phylum, Cnidaria; class, Anthozoa). *Development* **131**, 2463–2474.

Martindale, M. Q. & Hejnol, A. 2009. A developmental perspective: changes in the position of the blastopore during bilaterian evolution. *Dev. Cell* **17**, 162–174.

Matus, D. Q., Copley, R. R., Dunn, C. W., Hejnol, A., Eccleston, H., Halanych, K. M., Martindale, M. Q. & Telford, M. J. 2006. Broad taxon and gene sampling indicate that chaetognaths are protostomes. *Curr. Biol.* **16**, R575–R576.

McDougall, C., Chen, W. C., Shimeld, S. M. & Ferrier, D. E. K. 2006. The development of the larval nervous system, musculature and ciliary bands of *Pomatoceros lamarckii* (Annelida): heterochrony in polychaetes. *Front. Zool.* **3**, 16.

Miyamoto, N., Nakajima, Y., Wada, H. & Saito, Y. 2010. Development of the nervous system in the acorn worm *Balanoglossus simodensis*: insights into nervous system evolution. *Evol. Dev.* **12**, 416–424.

Nakajima, Y., Kaneko, H., Murray, G. & Burke, R. D. 2004. Divergent patterns of neural development in larval echinoids and asteroids. *Evol. Dev.* **6**, 95–104.

© 2011 The Authors
Development, Growth & Differentiation © 2011 Japanese Society of Developmental Biologists

Nielsen, C. 2001. *Animal Evolution. Interrelationships of the Living Phyla*, 2nd edn. Oxford University Press, Oxford.

Nielsen, C. 2005a. Larval and adult brains. *Evol. Dev.* **7**, 483–489.

Nielsen, C. 2005b. Trochophora larvae: cell-lineages, ciliary bands and body regions. 2. Other groups and general discussion. *J. Exp. Zool.* **304B**, 401–447.

Nielsen, C. 2010. Some aspects of spiralian development. *Acta Zool.* **91**, 20–28.

Nomaksteinsky, M., Röttinger, E., Dufour, H. D., Chettouh, Z., Lowe, C. J., Martindale, M. Q. & Brunet, J. F. 2009. Centralization of the deuterostome nervous system predates chordates. *Curr. Biol.* **19**, 1264–1269.

Papillon, D., Perez, Y., Fasano, L., Le Parco, Y. & Caubit, X. 2003. *Hox* gene survey in the chaetognath Spadella cephaloptera: evolutionary implications. *Dev. Genes Evol.* **213**, 142–148.

Papillon, D., Perez, Y., Caubit, X. & Le Parco, Y. 2004. Identification of chaetognaths as protostomes is supported by the analysis of their mitochondrial genome. *Mol. Biol. Evol.* **21**, 2122–2129.

Papillon, D., Perez, Y., Fasano, L., Parco, Y. L. & Caubit, X. 2005. Restricted expression of a median *Hox* gene in the central nervous system of chaetognaths. *Dev. Genes Evol.* **215**, 369–373.

Paps, J., Baguñà, J. & Riutort, M. 2009. Lophotrochozoa internal phylogeny: new insights from an up-to-date analysis of nuclear ribosomal genes. *Proc. R. Soc. Lond. B Biol. Sci.* **276**, 1245–1254.

Pearre, S. 1991. Growth and reproduction. In *The Biology of Chaetognaths* (Eds Q. Bone, H. Kapp & A. C. Pierrot-Bults), pp. 61–75, Oxford University Press, New York.

Peterson, K. J. & Eernisse, D. J. 2001. Animal phylogeny and the ancestry of bilaterians: inferences from morphology and 18S rDNA gene sequences. *Evol. Dev.* **3**, 170–205.

Philippe, H., Brinkmann, H., Martinez, P., Riutort, M., Baguñà, J. & Volff, J. 2007. Acoel Flatworms Are Not Platyhelminthes: evidence from Phylogenomics. *PLoS ONE* **2**, e717.

Philippe, H., Brinkmann, H., Copley, R. R., Moroz, L. L., Nakano, H., Poustka, A. J., Wallberg, A., Peterson, K. J. & Telford, M. J. 2011. Acoelomorph flatworms are deuterostomes related to *Xenoturbella*. *Nature* **470**, 255–258.

Price, D. A. & Greenberg, M. J. 1989. The hunting of the FaRPs: the distribution of FMRFamide-related peptides. *Biol. Bull.* **177**, 198–205.

Rawlinson, K. A. 2010. Embryonic and post-embryonic development of the polyclad flatworm *Maritigrella crozieri*; implications for the evolution of spiralian life history traits. *Front. Zool.* **7**, 12.

Reeve, M. R. 1970. Complete Cycle of Development of a Pelagic Chaetognath in Culture. *Nature* **227**, 381.

Reichert, H. 2009. Evolutionary conservation of mechanisms for neural regionalization, proliferation and interconnection in brain development. *Biol. Lett.* **5**, 112–116.

Reynolds, E. S. 1963. The use of lead citrate at high pH as an electron-opaque stain in electron microscopy. *J. Cell Biol.* **17**, 208–212.

Richter, S., Loesel, R., Purschke, G., Schmidt-Rhaesa, A., Scholtz, G., Stach, T., Vogt, L., Wanninger, A., Brenneis, G., Döring, C., Faller, S., Fritsch, M., Grobe, P., Heuer, C. M., Kaul, S., Møller, O. S., Müller, C. H. G., Rieger, V., Rothe, B. H., Stegner, M. E. J. & Harzsch, S. 2010. Invertebrate neurophylogeny: suggested terms and definitions for a neuroanatomical glossary. *Front. Zool.* **7**, 29.

Rieger, V., Perez, Y., Müller, C. H. G., Lipke, E., Sombke, A., Hansson, B. S. & Harzsch, S. 2010. Immunohistochemical analysis and 3D reconstruction of the cephalic nervous system in Chaetognatha: insights into the evolution of an early bilaterian brain? *Invertebr. Biol.* **129**, 77–104.

Santagata, S. 2002. Structure and metamorphic remodeling of the larval nervous system and musculature of *Phoronis pallida* (Phoronida). *Evol. Dev.* **4**, 28–42.

Santagata, S. 2008. Evolutionary and structural diversification of the larval nervous system among marine bryozoans. *Biol. Bull.* **215**, 3–23.

Schmidt-Rhaesa, A. 2007. *The Evolution of Organ Systems*. Oxford University Press, Oxford.

Semmler, H., Chiodin, M., Bailly, X., Martinez, P. & Wanninger, A. 2010. Steps towards a centralized nervous system in basal bilaterians: insights from neurogenesis of the acoel *Symsagittifera roscoffensis*. *Develop. Growth Differ.* **52**, 701–713.

Shankland, M. & Seaver, E. C. 2000. Evolution of the bilaterian body plan: what have we learned from annelids? *PNAS* **97**, 4434–4437.

Shimotori, T. & Goto, T. 1999. Establishment of axial properties in the arrow worm embryo, *Paraspadella gotoi* (Chaetognatha): developmental fate of the first two blastomeres. *Zool. Sci.* **16**, 459–469.

Shimotori, T. & Goto, T. 2001. Developmental fates of the first four blastomeres of the chaetognath *Paraspadella gotoi*: relationship to protostomes. *Develop. Growth Differ.* **43**, 371–382.

Shinn, G. L. 1997. Chapter 3: Chaetognatha. In *Microscopic Anatomy of Invertebrates. Hemichordata, Chaetognatha, and the Invertebrate Chordates*, Vol. 15 (Eds F. W. Harrison & E. E. Ruppert), Wiley-Liss, New York, 103–220.

Takada, N., Goto, T. & Satoh, N. 2002. Expression Pattern of the *Brachyury* Gene in the Arrow Worm *Paraspadella gotoi* (Chaetognatha). *Genesis* **32**, 240–245.

Telford, M. J. 2004. Affinity for arrow worms. *Nature* **431**, 254–256.

Telford, M. J. & Holland, P. W. H. 1993. The phylogenetic affinities of the chaetognaths: a molecular analysis. *Mol. Biol. Evol.* **10**, 660–676.

Walker, R. J. 1992. Neuroactive peptides with an RFamide or Famide carboxyl terminal. *Comp. Biochem. Physiol.* **102C**, 213–222.

Yasuda, E., Goto, T., Makabe, K. W. & Satoh, N. 1997. Expression of Actin Genes in the Arrow Worm *Paraspadella gotoi* (Chaetognatha). *Zool. Sci.* **14**, 953–960.

Zajac, J. M. & Mollereau, C. 2006. Introduction: RFamide peptides. *Peptides* **27**, 941–942.

Zrzavý, J., Mihulka, S., Kepka, P. & Bezděk, A. 1998. Phylogeny of the Metazoa based on morphological and 18S ribosomal DNA evidence. *Cladistics* **14**, 249–285.

© 2011 The Authors
Development, Growth & Differentiation © 2011 Japanese Society of Developmental Biologists

8.4 Neurogenesis in an early protostome relative: stem cells in the ventral nerve centre of chaetognath hatchlings are arranged in a highly organized geometrical pattern.

Perez Y, **Rieger** V, Martin E, Müller CHG, Harzsch S (submitted)

Journal of Experimental Zoology B: Molecular and Developmental Evolution 9999B: 1-15

RESEARCH ARTICLE

JOURNAL OF EXPERIMENTAL ZOOLOGY
PART B
MOLECULAR AND DEVELOPMENTAL EVOLUTION

Neurogenesis in an Early Protostome Relative: Progenitor Cells in the Ventral Nerve Center of Chaetognath Hatchlings Are Arranged in a Highly Organized Geometrical Pattern

YVAN PEREZ[1], VERENA RIEGER[2], ELISE MARTIN[3], CARSTEN H.G. MÜLLER[2], AND STEFFEN HARZSCH[2]*

[1]Institut Méditerranéen de Biodiversité et d'Ecologie "Evolution Genome Environment", IMBE—UMR CNRS 7263/IRD 237 Aix-Marseille Université/Centre St Charles, Marseille cedex 3, France
[2]Ernst-Moritz-Arndt-Universität Greifswald, Zoologisches Institut und Museum, Cytologie und Evolutionsbiologie, Greifswald, Germany
[3]INSERM U845—Centre de Recherche "Croissance et Signalisation", Hôpital Necker, Paris, France

ABSTRACT

Emerging evidence suggests that Chaetognatha represent an evolutionary lineage that is the sister group to all other Protostomia thus promoting these animals as a pivotal model for our understanding of bilaterian evolutionary history. We have analyzed the proliferation of neuronal progenitor cells in the developing ventral nerve center (VNC) of *Spadella cephaloptera* hatchlings. To that end, for the first time in Chaetognatha, we performed in vivo incorporation experiments with the S-phase specific mitosis marker bromodeoxyuridine (BrdU). Our experiments provide evidence for a high level of mitotic activity in the VNC for *ca.* 3 days after hatching. Neurogenesis is carried by presumptive neuronal progenitor cells that cycle rapidly and most likely divide asymmetrically. These progenitors are arranged in a distinct grid-like geometrical pattern including about 35 transverse rows. Considering Chaetognaths to be an early offshoot of the protostome lineage we conclude that the presence of neuronal progenitor cells with asymmetric division seems to be a feature that is rooted deeply in the Metazoa. In the light of previous evidence indicating the presence of serially iterated peptidergic neurons with individual identities in the chaetognath VNC, we discuss if these neuronal progenitor cells give rise to distinct lineages. Furthermore, we evaluate the serially iterated arrangement of the progenitor cells in the light of evolution of segmentation. *J. Exp. Zool. (Mol. Dev. Evol.) 9999B:1–15, 2013.* © 2013 Wiley Periodicals, Inc.

J. Exp. Zool. (Mol. Dev. Evol.) 9999B:1–15, 2013

How to cite this article: Perez Y, Rieger V, Martin E, Müller CHG, Harzsch S. 2013. Neurogenesis in an early protostome relative: progenitor cells in the ventral nerve center of Chaetognath hatchlings are arranged in a highly organized geometrical pattern. J. Exp. Zool. (Mol. Dev. Evol.) 9999:1–15.

Grant sponsor: Metazoan Deep Phylogeny (DFG Focus Program); grant number: HA 2540/7-3.

Additional supporting information may be found in the online version of this article.

*Correspondence to: Steffen Harzsch, Ernst-Moritz-Arndt-Universität Greifswald, Zoologisches Institut und Museum, Cytologie und Evolutionsbiologie, Johann Sebastian Bach Str. 11/12, 17497 Greifswald, Germany. E-mail: steffen.harzsch@uni-greifswald.de

Received 27 September 2012; Revised 29 December 2012; Accepted 23 January 2013

DOI: 10.1002/jez.b.22493

Published online XX Month Year in Wiley Online Library (wileyonlinelibrary.com).

© 2013 WILEY PERIODICALS, INC.

Despite the ever increasing number of molecular phylogenetic studies and an emerging consensus for protostome affinities, today the position of the Chaetognatha is still among the most enigmatic issues of metazoan phylogeny. The latest phylogenomic and morphological studies suggest that Chaetognatha have branched off close to the split between protostomes and deuterostomes (Marlétaz et al., 2006, 2008; Matus et al., 2006; reviews Nielsen, 2012; Perez et al., in press). The chaetognath genome is likely the product of a unique evolutionary history and shows a long isolation of this group. Furthermore, morphological characters provide evidence for the long evolutionary distance that separates the Chaetognatha from its closest (unknown) metazoan relative and suggest that this taxon in many aspects seems to have explored its own evolutionary pathways in generating tissue and organ diversity. Both, the genome and morphological characters include many autapomorphies of this group in addition to a character mix of protostome and deuterostome features, promoting this taxon as a pivotal model for our understanding of bilaterian evolutionary history (Perez et al., in press).

Hence, analyzing their ontogeny may be revealing concerning developmental aspects of the last common bilaterian ancestor. Chaetognaths are hermaphroditic and develop directly so that the hatchlings display a body organization that is in many aspects similar to the adult (Fig. 1A). However, because the mouth and also the blastopore close again after gastrulation, the hatchlings have neither a mouth opening nor an anus. The embryonic development of Chaetognatha is known from the fundamental studies by Hertwig (1880), Doncaster ('02), and John ('33) on animals of the genera *Spadella* and *Sagitta*. More recently, the embryology and many aspects of growth and reproduction of Chaetognatha have been explored in laboratory cultures (Kuhl and Kuhl, '65; Reeve, '70; Kuhlmann, '77; Goto and Yoshida, '97; Shimotori and Goto, '99, 2001; Carré et al., 2002; reviews Pearre, '91; Kapp, 2000; Perez et al., submitted) including the mating sequence (Goto and Yoshida, '85), the fertilization process (Goto, '99; Carré et al., 2002) and aspects of regeneration (Duvert et al., 2000). Furthermore, the embryonic expression patterns of actin genes (Yasuda et al., '97), the *brachyury* gene (Takada et al., 2002), and the median *Hox* gene *Scemed4* (Papillon et al., 2005) have been analyzed by whole mount in situ hybridization.

The general organization of the nervous system in adult Chaetognaths has been described by several authors and was summarized by Bone and Pulsford ('84), Goto and Yoshida ('84, '87), and Shinn ('97). In the last few years new interest has arisen in analyzing the Chaetognath nervous system against an evolutionary background (reviews Harzsch and Wanninger, 2009; Perez et al., in press). Immunofluorescence studies combined with confocal laser-scan microscopy have revealed new details on the architecture of individually identifiable neurons in the ventral nerve center (VNC) (Harzsch and Müller, 2007; Harzsch et al., 2009), the brain (Rieger et al., 2010), and the morphology of sensory organs (Müller et al., submitted) and have discussed implications for nervous system evolution in Bilateria ("neurophylogeny"; Harzsch, 2006; Richter et al., 2010). As for development of the nervous system, Doncaster ('02) has provided the first histological data on chaetognath neurogenesis. However, apart from this study, neurogenesis in Chaetognatha is poorly understood and in the last years was only studied by Rieger et al. (2011) using contemporary neurodevelopmental methods. These authors analyzed postembryonic neurogenesis in *Spadella cephaloptera* with histochemical and immunohistochemical methods and used antisera against tubulin, RFamide-related neuropeptides and synaptic proteins to analyze the maturation of the VNC and brain in hatchlings. In *S. cephaloptera*, at hatching, the basic neuronal architecture of the VNC is already established, whereas the brain and the associated vestibular ganglia are still rudimentary (Rieger et al., 2011). The development of the brain proceeds rapidly over the next six days to reach a state resembling the adult pattern. During the first 2 days of postembryonic development, new zones of synaptic neuropil emerge in the brain, new neurons with RFamide-like immunoreactivity appear, and the system of RFamide-like immunoreactive fibers is elaborated. In contrast to the brain, the ontogeny of the VNC appears to be more advanced at hatching. This center is a dominant organ in young hatchlings. The system of neurons that express RFamide-related neuropeptides in the VNC in many respects already resembles that in adults. The number of somata with RFamide-like immunoreactivity increases very little from hatching onwards but the system of their neurites becomes more complex as development proceeds (Rieger et al., 2011). In the present contribution, we asked the question if in addition to the apparent maturation of existing RFamide-like immunoreactive neurons in the VNC other neuronal systems may still be developing. Specifically, we wanted to know if mitotic neuronal progenitor cells are present in the postembryonic central nervous system of Chaetognath hatchlings. To that end, for the first time in Chaetognatha, we used the S-phase specific cell cycle marker bromodeoxyuridine (BrdU) to document spatial and temporal patterns of neuronal proliferation in the developing VNC.

MATERIALS AND METHODS

Experimental Animals

Adult specimens of *Spadella cephaloptera* (Busch, 1851) (Phragmophora, Spadellidae) were collected in Sormiou (Marseille, France) in June 2006 and August 2007. A plankton net was grazed over the sea grass beds by snorkeling. Animals were kept in aquaria containing natural seawater (21 ± 1°C) at the Aix-Marseille University (France). The eggs of these animals were collected on a daily basis and reared in separate tanks to obtain different developmental stages. Because we monitored the hatchling cultures once a day in the morning, a hatchling designated as 24 hr old may be anywhere between 24 hr old and

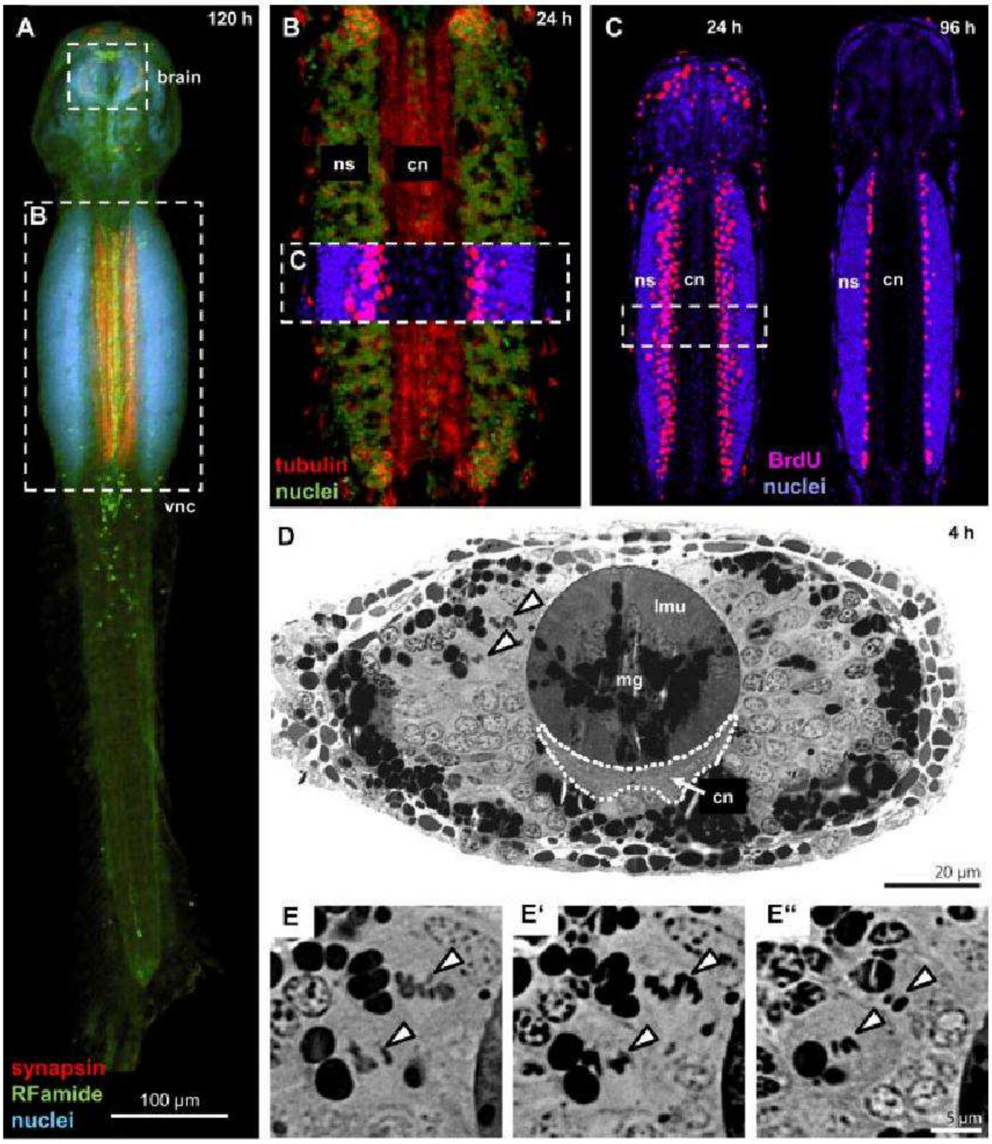

Figure 1. The ventral nerve center of *Spadella cephaloptera*. **A**: Hatchling at 120 hr triple labeled for nuclei (blue), synaptic proteins (red), and the neuropeptide RFamide (green; reprinted with permission from Rieger et al., 2011). Boxes identify the brain and the ventral nerve center. **B**: Higher magnification of the ventral nerve center (as indicated in A) of a 24 hr old hatchling double labeled for tubulin (red) to show the central neuropil that is flanked by neuronal somata labeled by a nuclear marker (green; reprinted with permission from Rieger et al., 2011). The inset shows a higher magnification of the boxed area in C. **C**: Hatchlings at 24 hr (left) and 96 hr (right) after 4 hr BrdU labeling. The cells in S-phase (red) are located at the interface of the central neuropil and the peripheral layers of neuronal somata (blue). Note the decreasing mitotic activity in the older hatchling. **D**: Semithin cross-section (toluidin blue) through the ventral nerve center of a hatchling. The hatchling was fixed shortly after hatching (age about 4 hr). Arrowheads identify two nuclei of dividing cells (see higher magnifications in E). The dotted line surrounds the central neuropil of the ventral nerve center. **E–E″**: Higher magnifications of three consecutive sections (1 µm) showing mitotic cells in M-phase (arrowheads). Abbreviations: cn, central neuropil; lmu, longitudinal muscles; mg, mid gut; nc, neuronal somata; vnc, ventral nerve center.

just newly hatched. In this logic, an animal designated to be 48 hr old may be between 24 and 48 hr old. We averaged out this variation by examining several randomly chosen individuals per stage ($n > 5$), that is per day of sampling.

Histology and Light Microscopy

Hatchlings of *S. cephaloptera* were fixed in toto for 12 hr in a cold solution of Karnovsky's prefixative (1965), consisting of 2% glutaraldehyde, 2% paraformaldehyde, 1.52% NaOH, and 5.0 g d-glucose, dissolved in 2.25% Na-hydrogen phosphate buffer (pH 7,4). After washing in the same buffer (12 hr), the specimens were then postfixed for 6 hr in 2% OsO_4 solution (same buffer) at room temperature and, following dehydration in a graded series of acetone, embedded in epoxide resin (Araldite, FLUKA). Serial semithin cross-sections (approximately 1 µm thick) through the trunk were prepared and stained using 1% toluidine blue in a solution of 1% Na-tetraborate (borax). Images were taken using a Nikon Eclipse 90i with the Nikon NIS-Elements Ar 3.10 software.

BrdU Labeling

For labeling with the S-phase specific proliferation marker BrdU (for details see e.g., Harzsch and Dawirs, '94, '96; Harzsch et al., 2006), live animals were incubated in seawater with BrdU (0.2 µg/mL; GE Healthcare, Heidelberg, Germany, Amersham cell proliferation kit RPN20). The incubation time ("pulse") for the first set of experiments was 4 hr and hatchlings were fixed immediately afterwards. For the second set, the pulse-chase experiments, the pulse was 10 min. A part of the hatchlings were fixed immediately afterwards, the others were reared in seawater without BrdU for additional 1, 2, 4, 8, or 24 hr before fixation. Specimens were fixed for 4 hr at room temperature (or alternatively overnight at 4°C) in 4% paraformaldehyde (PFA) in phosphate buffer (PB; 0,1 M, pH 7.4). Histochemistry and immunohistochemistry were carried out on free-floating whole mounts of hatchlings specimens with primary and fluorochrome-conjugated secondary antibodies using standard protocols (Harzsch and Dawirs, '94; Rieger et al., 2011). After fixation, the tissues were washed in several changes of phosphate-buffered saline (PBS) for at least 4 hr. Specimens were incubated in 2 N HCl for 20 min and washed for 2 hr in several changes of PBS, then preincubated in PBS-TX (1% normal goat serum, 0.3% Triton X-100, 0,05% Na-azide) for 1 hr. Incubation in the anti-BrdU monoclonal antibody from mouse (1:50 in PBS-TX; GE Healthcare, Amersham cell proliferation kit RPN20) was carried out for 4 hr at room temperature. Specimens were then washed for at least 2 hr in several changes of PBS and subsequently incubated with an anti-mouse secondary antibody conjugated to Cy3 (1:500; Jackson Immuno Research, Suffolk, UK) for 4 hr. Some specimens were counterstained with a nuclear dye, bisbenzimide (0.04%, 4 hr at room temperature; Hoechst H 33258) during the secondary antibody incubations. Finally, the tissues were washed for at least 2 hr in several changes of PBS and then mounted in MOWIOL (Calbiochem, Darmstadt, Germany). Batches of hatlings were analyzed in this way at 24 hr intervals and the immunohistochemical observations reported in this paper are based on the analysis of at least six specimens for each time point.

Microscopic Analysis and Cell Counts

Digital images were obtained using a Zeiss Axioimager Z1 fluorescence microscope equipped with a structured illumination device (ApoTome) and a digital camera AxioCamMRm (Zeiss) controlled by the AxioVision V 4.6.3-SP1 software package (Zeiss). In addition, samples were scanned with a Zeiss LSM 510 Meta confocal laser-scanning microscope. Those images are based on Z-stacks of several optical sections obtained with the LSM 510 V.4.0. SP2 software (Zeiss). Images were black-white inverted and processed in Adobe Photoshop CS4 V11.0 by using the global contrast and brightness adjustment features.

The number of labeled BrdU cells was counted in a defined rectangular sector of the VNC (viewed from a ventral perspective) that had the same size in all examined developmental stages. For the counts, we analyzed Z-stacks of optical sections taken at 1 µm intervals and covering the entire Z-extension of the VNC. All optical sections were printed on A4 sheets and cells counted manually thus avoiding double counts of nuclei that appeared in several sections.

RESULTS

Mitotic Cells in the Ventral Nerve Center Are Arranged in a Highly Organized Pattern

The VNC is an easily visible, dominating organ in the hatchlings that extends through the entire trunk (Fig. 1A; compare Rieger et al., 2011). Its medioventral (here termed "central") neuropil (CN), which contains both dendritic and axonal processes, is already well developed. The neuronal somata (NS) of the VNC are organized into two bilaterally arranged lateral clusters (Fig. 1B,D; Rieger et al., 2011). Our experiments with the S-phase specific proliferation marker BrdU revealed an intense mitotic activity in many tissues of the hatchlings (data not shown). In the VNC, BrdU incorporating (BrdU+) nuclei were arranged on both sides of the VNC at the interface between the central neuropil and the lateral soma clusters both in 24- and 96 hr-old hatchlings (Fig. 1C). In histological cross-sections of the VNC (Fig. 1D) cells in M-phase could be seen in corresponding positions (Fig. 1E–E″). In a series of optical sections through a 48 hr old hatchling after a 4 hr pulse of BrdU, about 10 BrdU+ nuclei were seen distributed along the midline on the ventral side of the VNC (Fig. 2A). About 30–35 transverse rows of nuclei of mitotic cells were present on both sides of the VNC (Figs. 1C, 2B–E, and 3A). From the double labeling experiments (Fig. 1C) we know that these cells are located at the interface between the central neuropil and the lateral soma clusters of the VNC. The Supplementary Videos 1 and 2 revealed the geometrical arrangement of the labeled cells in the anterior-

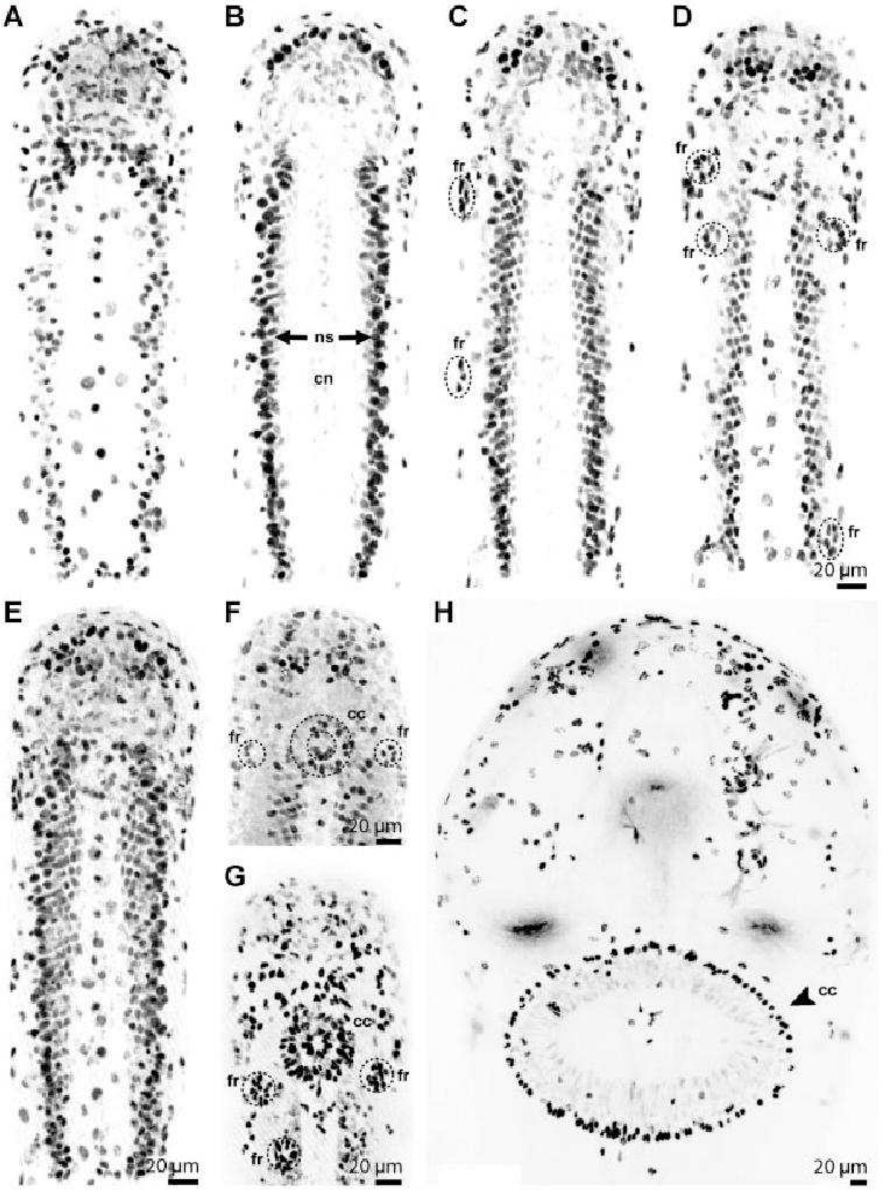

Figure 2. Localization of proliferating cells in hatchlings (whole mounts) as analyzed by BrdU-labeling and confocal laser-scan microscopy (all images were black-white inverted). A 4 hr BrdU pulse was given except for (G) with an incubation time of only 10 min. **A–E**: Hatchlings at 48 hr, series of single optical sections from ventral (A) to dorsal (D). Mitotic cells in the ventral nerve center flank the central neuropil on both sides and are arranged in a grid-like pattern. Circles identify mitotic cells within developing epidermal fence receptor organs. E: Same specimen as A–E, maximum projection of the entire image stack showing the whole specimen. **F**: Head of a 48 hr old hatchling showing the developing corona ciliata and fence receptor organs (maximum projection of the entire image stack). **G**: Head of a hatchling incubated in BrdU (4 hr) at 48 hr, after 24 hr chase (maximum projection of the entire image stack). **H**: Head of an adult showing mitotic activity persists mostly in epidermal cells as well as the corona ciliata (maximum projection). Abbreviations: cc, corona ciliata; cn, central neuropil; nc, neuronal somata; fr, fence receptors.

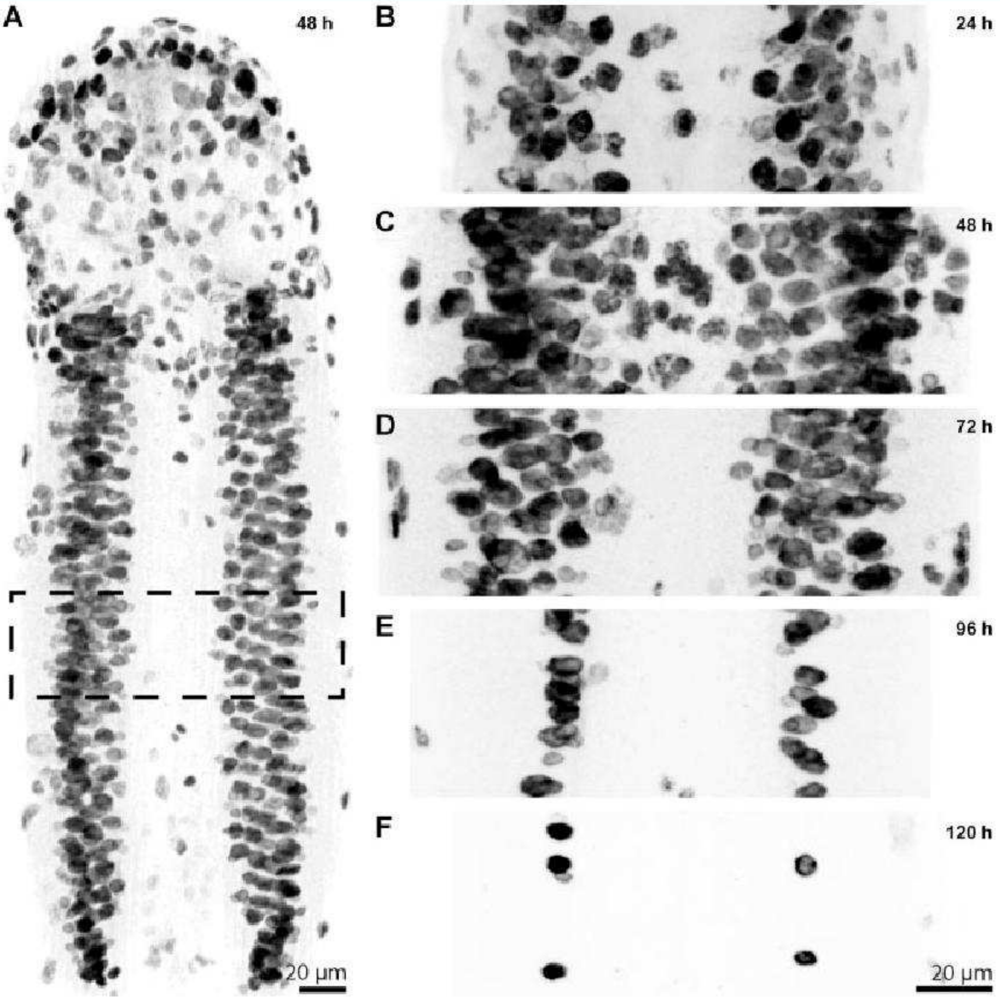

Figure 3. Cell proliferation in hatchlings of different ages as analyzed by BrdU-labeling and confocal laser-scan microscopy (4 hr BrdU). **A**: Hatchling at 48 hr. **B–F**: Higher magnifications of the VNC in the middle of the trunk (see boxed area in A) in hatchlings of various ages: 24 hr (B), 48 hr (C), 72 hr (D), 96 hr (E), and 120 hr (F). All images are maximum projections of image stacks covering the entire trunk and were black-white inverted.

posteriorly repeated rows and that individual cells in the rows seem to curve around the medially located anlagen of the longitudinal musculature and the intestine or gut (Fig. 1D). In these preparations and histological transverse sections (Fig. 1D) we found a maximum of six BrdU+ cells per row. Because the rows of mitotic cells are arranged in an angle with respect to the antero-posterior body axis and the inner boundary formed by the mesoderm (Fig. 2D), the progenitor cells are not arranged in a chess-board like pattern but every three rows there is a lateral shift. At the anterior and posterior ends of the VNC there were fewer than six cells per row and these rows could not be distinguished as clearly as in the middle of the VNC.

In the head region, many BrdU+ nuclei were present but it was difficult to decide whether these cells were associated with neuronal structures of the cephalic nervous system based on the position of the labeled nuclei alone (Figs. 1C and 2A–E). Within the epidermis of the head, but also in the developing trunk, clusters of BrdU+ nuclei arranged like a rosette were present, that contributed to the development of fence receptor organs (FR in Fig. 2C,D,F,G), mechanosensory epidermal sense organs

(Shinn, '97) the cytoarchitecture and ontogenetic elaboration of which we currently analyze (Müller, Perez, Rieger, Harzsch; unpublished data). Furthermore, embedded within the dorsal epidermis of the hatchlings at the transition point between head and trunk was another area with great proliferative activity, the developing corona ciliata (CC in Fig. 2F,G), a putative sensory organ. In pulse-chase experiments (24 hr of chase), the labeled nuclei were arranged in two rings, a smaller one surrounded by the second larger one located across the body-midline (Fig. 2G). The cells within the corona ciliata retained mitotic activity even in adult specimens (Fig. 2H).

Time Course of Neurogenesis in the Hatchling's Ventral Nerve Center

We compared the number of proliferating cells in the VNC after a single 4 hr pulse in hatchlings of different ages (Figs. 1C, 3, and 4). In an attempt to obtain quantitative data on the number of BrdU+ nuclei, we analyzed Z-stacks of optical sections taken at 1 µm intervals covering the entire Z-extension of the VNC. The number of labeled nuclei in a defined rectangular sector of the VNC was counted as indicated in Figure 3A. We analyzed only one hatchling per stage so that our quantitative data can only serve as a support for the histological observations. In our preparations, it appeared that the number of mitotic nuclei was highest on the second day (Fig. 3C) and then decreases rapidly from 72 hr onwards (Figs. 3E,F and 4). These findings were supported by our counts of labeled nuclei (Fig. 5). By 96 and 120 hr, few cells were still in S-phase as determined by a 4 hr BrdU pulse, and the remaining labeled nuclei in these late hatchlings were arranged in one longitudinal column on each side of the central neuropil region (Figs. 1C, 3E,F, and 4). By 120 hr, only about 10 labeled nuclei per side remained throughout the entire VNC (Figs. 4 and 5). In hatchlings that were 7 and 10 days old (Fig. 4), we did not encounter any nuclei anymore that incorporated BrdU in a 4 hr pulse suggesting that the mitotic activity of neuronal progenitor cells had either ceased or slowed down dramatically. We recorded a considerable variation in the size of the BrdU+ nuclei in the different stages that we analyzed ranging from between 20 and 40 µm^2 but larger nuclei up to about 90 µm^2 were also present (Fig. 5).

Pulse-Chase Experiments: Tentative Evidence for Asymmetrically Dividing Neuronal Progenitor Cells

Pulse-chase experiments were carried out to follow the arrangement of the newborn cells in the VNC. For these experiments, we used a shorter BrdU pulse (10 min) so that fewer cells were labeled than in the previous experiment (Fig. 6). In both experimental groups (pulsed at 48 and 120 hr), we observed that with increasing chase period the number of labeled nuclei increased while the nuclear size decreased (Fig. 6). Counts of labeled cells in a single specimen before and after a chase of 24 hr suggested that the number of labeled cells in a defined rectangular sector of the VNC almost quadrupled over this time (Fig. 7 left; only one specimen counted). At the same time, the average size of the nuclei strongly decreased (Fig. 7 right) most likely due to the ongoing proliferation. Before the chase, most nuclei had a diameter around 20–40 µm^2 ($n = 53$; mean: 31,6 µm^2; median: 25 µm^2), but after a 24 hr chase most nuclei measured about 10 µm^2 ($n = 165$; mean: 11,8 µm^2; median: 10 µm^2; Fig. 7).

Because these experiments had raised the possibility that multiple divisions take place during the 24 hr chase period, we wanted to explore the mode of cell division in more detail. In a 48 hr hatchling, right after the pulse, the majority of BrdU+ nuclei was large (Fig. 8A), whereas during the chase, more and more smaller nuclei emerged closely associated with the larger nuclei. Close inspection of confocal image stacks of the VNC revealed that already after 1 hr of chase, small labeled nuclei were present in addition to the large labeled nuclei (Fig. 8B). After 2 hr of chase, about one small nucleus was located nearby each large cell. This pattern can be interpreted such that the large nuclei belong to neuronal progenitor cells that divide asymmetrically and generate smaller progeny (Fig. 8C). After 4 hr of chase, two to three small labeled nuclei were consistently located close to each large (Fig. 8D). After 8 hr, the majority of nuclei was small and the large cells were only weakly labeled because most likely the BrdU label that was taken up during the initial pulse gets diluted during subsequent divisions (Fig. 8E). After a chase of 24 hr, large cells could hardly be detected anymore (Fig. 8F).

DISCUSSION

Neurogenesis in the Ventral Nerve Center (VNC) in Relation to Hatchling Behavior

The basic architecture of the VNC is well established at hatching and this structure is one of the most dominant organs in the young hatchlings (Rieger et al., 2011). In adults, the VNC controls swimming by initiating contractions of the body-wall musculature and coordinating mechanosensory input from the numerous ciliary fence receptors in the epidermis. For motor control, the VNC closely interacts with the peripheral, exclusively epidermal plexus that innervates the muscles (reviewed in Harzsch and Müller, 2007; Harzsch and Wanninger, 2009). We assume that the VNC is essential for swimming behavior in the hatchlings, too, so that this major neuronal center for sensory-motor integration must be functional to a certain extent at hatching. In our previous study on the development of neurons, that are immunoreactive for the neuropeptide RFamide, we found that the system of these neurons already resembles that in adults as far as numbers of identifiable neurons are concerned. Nevertheless, significant postembryonic changes occur in that the fiber system of these neurons becomes more complex as development proceeds (Rieger et al., 2011). However, although the RFamidergic system of the VNC is already implemented in the hatchlings indicating the presence of at least some functional neuronal circuits, our BrdU

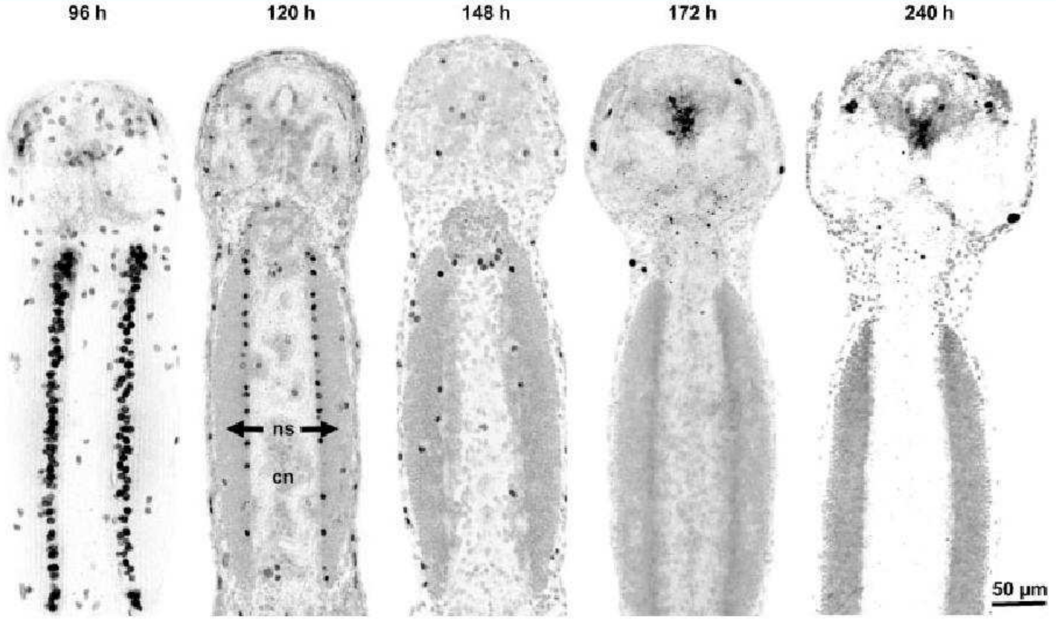

Figure 4. Cell proliferation in late hatchlings of different ages as analyzed by BrdU-labeling and confocal laser-scan microscopy (4 hr BrdU) to show that the mitotic activity of neuronal progenitor cells gradually slows down in the ventral nerve center and stops at around one week after hatching. All images are maximum projections of image stacks covering the entire trunk and were black-white inverted. Abbreviations: cn, central neuropil; nc, neuronal somata.

experiments nevertheless provide evidence for a high rate of neurogenesis during the first four to five days after hatching. This mitotic activity shows that the VNC is far from being completely differentiated at hatching but that, concurrent with changes in larval locomotion, new neurons are added and existing neuronal systems differentiate further.

The hatchlings of *S. cephaloptera* do neither have a functional mouth opening with grasping spines and teeth nor do they have a functional anus so that they have to fully rely on yolk supplies for nutrition. Likewise, sensory organs associated with the head such as the eyes and the corona ciliata, a sensory organ for which a role in chemoreception has been suggested (Shinn, '97; Müller et al., submitted), are not yet present or are poorly developed at hatching. Because the newly hatched, non-feeding animals must perceive hydrodynamic stimuli for navigating in their habitat, predator avoidance and attachment to their preferred substrate we have to assume that they can rely on a set of embryonic fence receptors. These organs in adult arrow worms have been shown to perceive such hydrodynamic stimuli (Shinn, '97). However, our results suggest that new fence receptor organs are added on the body surface to provide new sensory input to the VNC that needs to be integrated. Our experiments with the proliferation marker BrdU also showed intense mitotic activity in the area, where the corona ciliata will develop which suggests that this sensory organ is assembled during the first few days after hatching. Interestingly, our experiments also showed distinct mitotic activity in the adult corona ciliata as was already observed by Shinn ('97) suggesting that either this organ grows during adult life or that a turn-over of sensory neurons takes place.

Postembryonic Neurogenesis in the VNC: Mode of Division of Neuronal Progenitor Cells

Our data provided evidence for a high rate of neurogenesis in the VNC especially on days 2–4 posthatching. Pulse-chase experiments revealed cells with large BrdU-labeled nuclei that after a certain chase interval were accompanied by smaller nuclei which all fall into one size category. The number of these small nuclei increased with longer chase periods. One explanation for this pattern is that the large nuclei belong to neuronal progenitor cells that divide asymmetrically and generate smaller progeny, but alternative interpretations of these data are possible as outlined below. After 4 hr of chase, two to three small-labeled nuclei were consistently located close to each large nucleus. Without having done any statistics these data nevertheless suggest that, if neurogenesis is in fact driven by progenitor cells that divide asymmetrically, these progenitors cells in a 2-day old hatchling

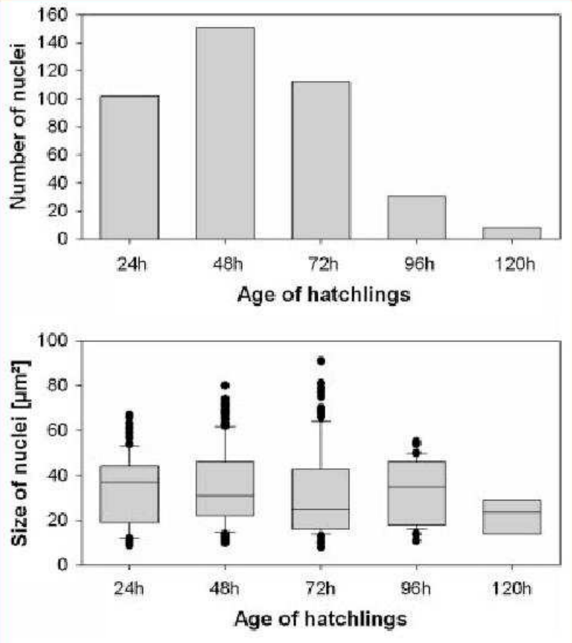

Figure 5. Upper panel: Number of BrdU-incorporating nuclei (4 hr pulse) in identical sample areas of the ventral nerve center (compare boxed area in Figure 3; only one hatchling was counted per time point). Lower panel: Box-and-whisker diagram showing the size of BrdU-incorporating nuclei (4 hr pulse) in identical sample areas of the ventral nerve center (compare boxed area in Figure 3; only one hatchling was counted per time point).

divide two to three times in 4 hr suggesting a cell cycle length of between 1.5 and 2 hr. The pulse-chase experiments did not provide evidence that the small daughter cells undergo additional divisions which raises the possibility that they are postmitotic and differentiate into neurons. Such a mode of progenitor cell division is also present in other Bilateria (see discussion below), for example, in Arthropoda/Tetraconata in which large progenitor cells, the neuroblasts, divide asymmetrically to generate progeny, the ganglion mother cells. One difference is that these daughter cells in Tetraconata (Crustacea and Hexapoda) go through one or multiple additional division cycles, before the products of these divisions differentiate into neurons (reviews e.g., Harzsch, 2003; Harzsch et al., 2005).

However, pulse-chase experiments only provide indirect evidence about the cell division characteristics. Can our data be interpreted in a different way other than indicating asymmetric divisions? The presence of a mixed population of small and large BrdU-labeled nuclei next to each other could mirror cell-cycle dynamics, more specifically that the nuclear size changes during the cell cycle. If the nuclear size differences that we found were due to changes as the nuclei enter a certain cell cycle phase, looking at the entire pool of labeled nuclei, one should expect a mix of sizes immediately after the 4 hr pulse (that is at zero hour chase) unless all labeled cells go through the cell cycle in full synchrony. Our preparations showed two distinct size classes from 2 hr of chase onwards. If size differences were due to nuclear dynamics we should expect to encounter a continuum of cell sizes at this time point of the chase unless, again, there are two populations of mitotic cells that have fully synchronized their cell cycle. However, if this were the case we should already see these two populations immediately after the BrdU pulse. What is more, the number of small nuclei associated with the large ones appeared to increase with longer chase periods, a point that further supports our claim of asymmetric divisions. The fact that the BrdU-label gets diluted out from the large cells during the chase is consistent with the claim that they divide asymmetrically and hence pass on 50% of the BrdU to the daughters with every division. Double labeling experiments with additional mitosis markers (e.g., Sintoni et al., 2012) will be useful to unravel more details concerning the cell cycle dynamics of the Chaetognath neuronal progenitors.

Postembryonic Neurogenesis in the VNC: Serial Arrangement of Neuronal Progenitor Cells

Our BrdU-experiments provided the exciting result that the progenitor cells associated with the VNC are arranged in a conspicuous, serially iterated geometrical pattern that in principal was consistent from specimen to specimen (Fig. 7A–F). The formation of geometrical patterns in living tissues has puzzled scientists for centuries. Hexagonal (triangular) patterns are remarkably similar even in unrelated organisms and unrelated organ systems and display spiral lines which represent successive numbers in the famous series discovered by Leonardo Fibonacci, in which each number is the sum of the previous two (1, 1, 2, 3, 5, 8, 13, 21, 34, ...; Klar, 2002). Much of our knowledge about these patterns comes from phyllotaxis studies in plants (flowers, bracts, stickers; Klar, 2002; Shipman and Newell, 2004) but phyllotactic-like patterns are also known in animals as for instance the hexagonal array of ommatidia in the compound eyes of insects (Cagan, 2009), the two-dimensional patterns of specific vertebrate retinal neurons (Stenkamp and Cameron, 2002), the firing field of grid cells in the entorhinal cortex (Fyhn et al., 2008; Kropff and Treves, 2008) and the pre- and parasubiculum of vertebrates (Boccara et al., 2010). However, the physical and chemical processes which give rise to these strikingly similar patterns are not sufficiently understood.

At hatching, progenitor cells in the VNC show a two-dimensional arrangement of spheres, whose centers form a triangular point system so that each sphere representing one progenitor cell is in contact with four others (Fig. 7A,B,G). In describing patterns of spheres on a cylinder surface, it is possible to characterize the parastichies (spiral lines) which might be

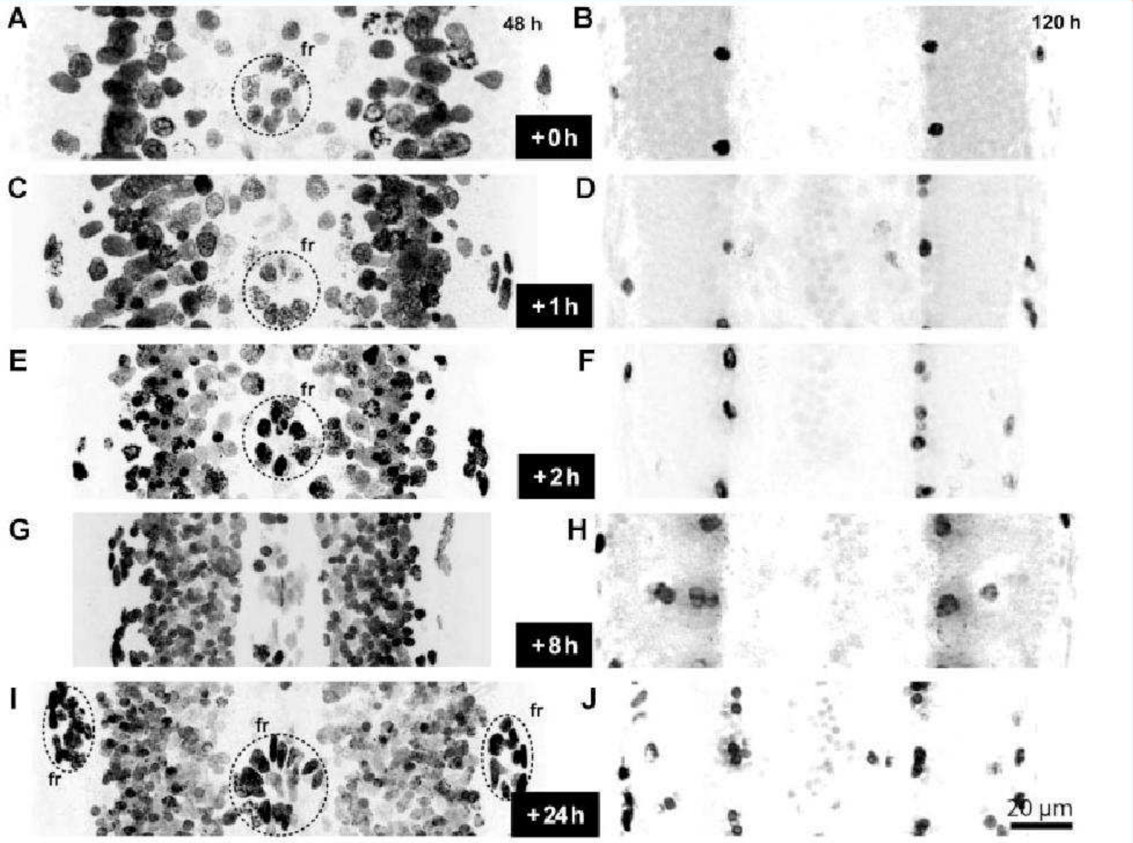

Figure 6. Pulse-chase experiments to track the arrangement of BrdU-incorporation nuclei in the ventral nerve center. A 10 min BrdU-pulse was given to two groups of animals at 48 hr (left column) or 120 hr (right column). Specimens from these groups were killed and processed after a period of chase as follow: no chase (**A,B**), 1 hr (**C,D**), 2 hr (**E,F**), 8 hr (**G,H**), 24 hr (**I,J**). The same sample area in the middle of the trunk is shown (compare Fig. 3A). All images are maximum projections of image stacks covering the entire trunk and were black-white inverted. Abbreviations: fr, fence receptors.

defined as the polygonal sequence of straight lines connecting the centers of a given rank of spheres (Erickson, '73; Veen and Lindenmayer, '77; Douady and Couder, '96). In *S. cephaloptera*, the progenitor cells' arrangement (Fig. 7G) is similar to a conjugate pattern named (2,3)-parastichy pattern (Veen and Lindenmayer, '77). This packing is not optimal so that we can expect a trade off between a maximum number of progenitor cells and the available space for progeny in the developing nerve center. Furthermore, biochemical constraints related to cell-cell interactions and mitotic spindle orientation may play a role in defining the progenitor cell arrangement.

The iteration of the (2,3)-pattern (in a frontal plane of view) gives rise to a periodic 2-dimensional grid composed of about 35 progenitor cells rows (Fig. 7H). Considering the inclination angle of each row with respect to the AP axis and the boundary formed by the mesoderm, a lateral shift of the progenitor cells occurs every three rows. This pattern may be interpreted as revealing serially organized domains of the VNC (Fig. 7H). We have previously provided evidence for individually identifiable, serially arranged neurons in the VNCs of four chaetognath species, based on immunohistochemitry against RFamide-related neuropeptides (Harzsch and Müller, 2007; Harzsch et al., 2009; see also Goto et al., '92). Double labeling experiments may reveal the spatial relationship of these serially arranged neurons and the rows of progenitor cells.

Harzsch and Müller (2007) have pointed out that a serial arrangement of individual neurons cannot only be found in protostomians with typical segmentation such as annelids and arthropods, but also in unsegmented organisms such as Nematoda and Plathelminthes, and in organisms the segmental organization

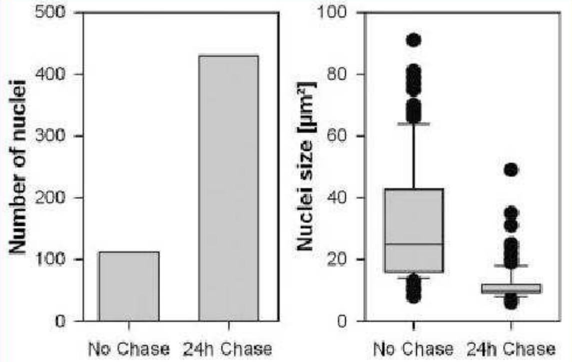

Figure 7. Pulse-chase experiments, number (left panel) and size (right panel) of BrdU-incorporating nuclei in the ventral nerve center. A 10 min BrdU-pulse was given at 48 hr and sample areas of similar size and location (see Fig. 3A) were counted in hatchlings immediately processed after the pulse and after 24 hr chase. The number and size of nuclei was counted in single specimens only. The size of the nuclei is displayed in a box-and-whisker diagram (right panel). Before the chase, most nuclei had a diameter around 20–40 µm^2 ($n = 53$; mean: 31,6 µm^2; median: 25 µm^2), but after a 24 hr chase most nuclei measured about 10 µm^2 ($n = 165$; mean: 11,8 µm^2; median: 10 µm^2).

of which is unclear such as basal Mollusca. According to Budd (2001), segmentation must have been acquired in a series of functional intermediates so that the sudden imposition of eusegmentation on a non-segmental progenitor seems highly unlikely. In this view, the organization of individual organ systems such as the central nervous system (but not the entire organism) into serially repeated structures may be the starting point in an evolutionary trajectory from which segmentation as we see it in annelids and arthropods emerged (Budd, 2001). The present report and the findings of Harzsch et al. (2009) suggest that developmental program to generate neurons with individual identities and serially iterated neuronal structures is part of the chaetognath ground pattern (Harzsch et al., 2009). Considering the basal position of Chaetognatha within the Bilateria (review Perez et al., submitted), we suggest that a serially repeated organization in the central nervous system may be one essential step towards true metamerism.

Neurogenesis in a Comparative Context

The most recent phylogenomic studies promote chaetognaths as a pivotal model for our understanding of bilaterian evolutionary history. Rieger et al. (2010) and Perez et al. (submitted) have discussed brain evolution in Bilateria based on the working hypothesis that Chaetognatha represent an evolutionary lineage that is the sister group to all other Protostomia. Considering that Chaetognatha may have branched off close to the split between protostomes and deuterostomes, their ontogeny may be revealing concerning modes of neurogenesis in the earliest bilaterian nervous systems. In the following, we want to briefly explore this idea by comparing neurogenetic mechanisms across two selected metazoan taxa, Cnidaria and Platyhelminthes, in which neurogenesis has been intensively studied. In a broader context, such comparison is hampered by the fact that data on neuronal stem cells are scarce, if available at all, in other basal bilaterian taxa that are phylogenetically meaningful for comparison with Chaetognatha such as basal Lophotrochozoa and basal Ecdysozoa (Hartenstein, 2013).

Cnidaria, and specifically *Hydra* have served as model organisms to understand neurogenesis in a basal metazoan taxa and, specifically, to understand molecular aspects of neurogenic regulators. These studies suggest that Cnidaria share with Bilateria a large number of genetic tools that regulate neurogenic functions. Studies on neurogenesis in Cnidaria have focused the *Hydra* polyp (reviews e.g., Bode, '96; Bosch, 2009; Galliot et al., 2009; Galliot and Quiquand, 2011) which in general is characterized by a constant turnover of cells (Otto and Campbell, '77; Bosch et al., 2010). Today, we know that in *Hydra* three distinct progenitor cell populations provide all cell types, namely the ectodermal epithelial cells, the endodermal for gastrodermal cells, and the interstitial cells (reviews Bode, '96; Bosch, 2009; Galliot et al., 2009). One of these three types of progenitor cells in Cnidaria, the interstitial cells, are multipotent progenitor cells restricted to the ectoderm and continuously provide neurons, mechanoreceptor cells (nematocytes), gland cells and, during the sexual cycle, gametes (Galliot et al., 2009). Bosch (2009) and Hemmrich et al. (2012), based on findings in *Hydra* suggested asymmetric cell divisions in general to be common to all multicellular animals.

Platyhelminthes possess extraordinary regenerative abilities, which require undetermined stem cells at all times during their life-cycle. Totipotent stem cells (neoblasts) are supposed to be the only dividing cells in these animals and are thought to be responsible for the renewal of all cell types during growth, development, and regeneration (reviews Baguna, '98; Agata, 2008; Rink, 2013). The neoblast system has been suggested to be unique in the Animal Kingdom because renewal of the 20–30 differentiated cell types rests upon a singly type of stem cell (Ladurner et al., 2000; Newmark and Alvarado, 2000). Neoblasts are a heterogenous group of cells (Baguna, '98) including self-renewing stem cells as well as several generations of progenitor cells with progressively restricted proliferation potential (Bode et al., 2006; Rink, 2013). There is not any morphological evidence that neoblasts divide asymmetrically. BrdU-pulse chase experiments show that after division some of the cells differentiate into various tissues like epidermis and germ cells, but also neuronal tissue (Ladurner et al., 2000; Bode et al., 2006). In the course of differentiation, the postmitotic cells undertake distinct migrations to their tissue of destination (Bode et al., 2006). These authors

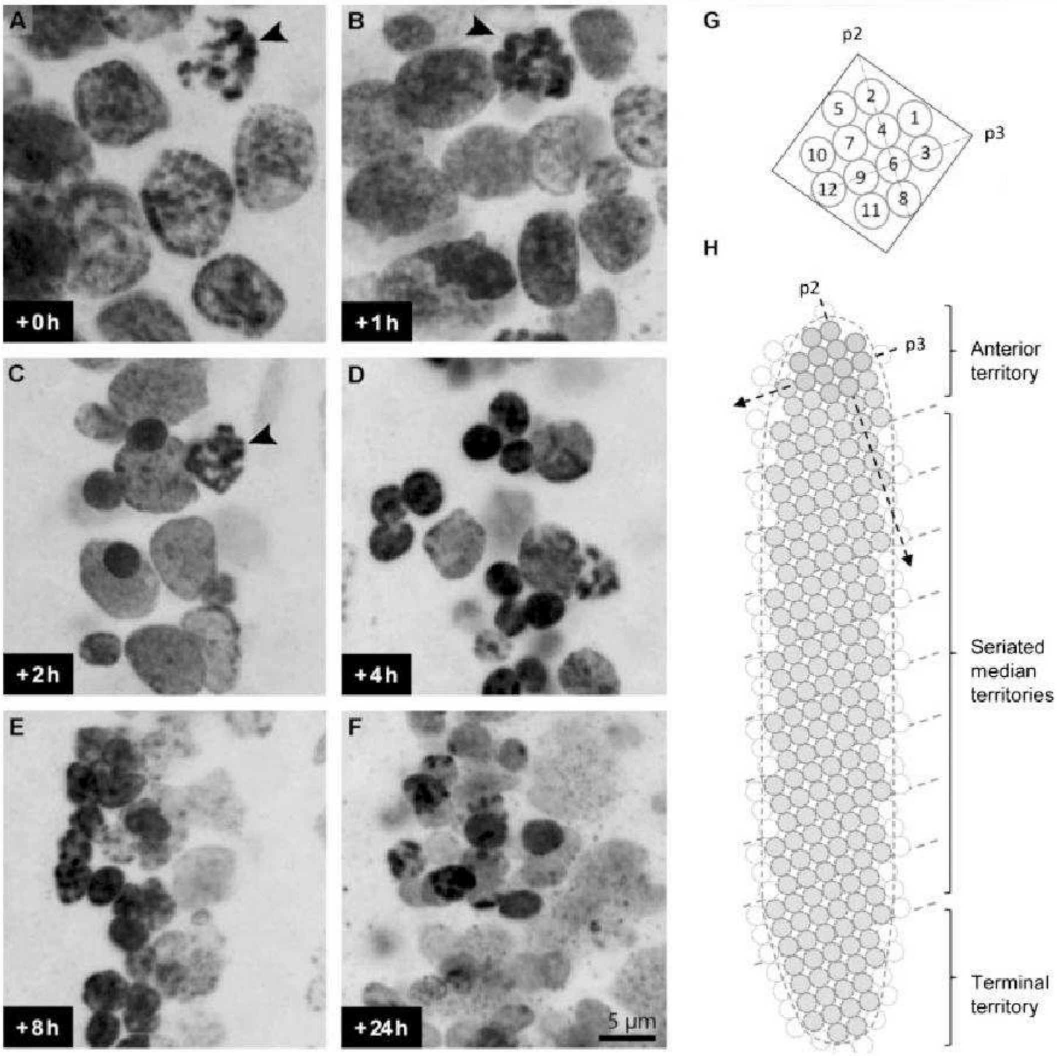

Figure 8. Pulse-chase experiments to track the mode of cell division in the ventral nerve center of hatchlings. A 10 min BrdU-pulse was given a group of hatchlings at 48 hr. Specimens from these groups were killed and processed after a period of chase as follow: no chase (**A**), 1 hr (**B**), 2 hr (**C**), 4 hr (**D**), 8 hr (**E**), 24 hr (**F**). The images are single optical sections (confocal laser-scan microscopy) that were black-white inverted. The excerpts chosen are located left of the neuropil, anterior is towards the top. The arrowheads indicate nuclei in Pro-Metaphase. **G**: Packed circles pattern on an unrolled cylinder surface. On the unrolled surface the 2–3 parastichies through point 0 are shown (after Veen and Lindenmayer, '77). **H**: Schematic diagram representing the organization of neuronal stem cells in a frontal plane of the ventral nerve center (left cluster) after iteration of the 2–3 pattern. Note the serially organized domains.

mention that the majority of neoblasts in S-phase are located close to the main lateral nerve cords, specifically to neurites with RFamide-like immunoreactivity, and suggest that the nervous system may exert a guiding function on neoblasts via cell-cell connections or via neurosecretion. Although here is a long-standing record of studies on the general organization of the flatworm nervous system (e.g., Raikova et al., '98, 2000; Reuter et al., '98, 2001a,b; Okamoto et al., 2005; Morris et al., 2007; Cebrià, 2008; review Umesono and Agata, 2009) and, the nature and distribution of neuroactive substances is still being intensely explored (e.g., Nishimura et al., 2007a,b, 2008a,b; McVeigh et al., 2009) the contribution of neoblasts to neurogenesis needs to be explored in more depth.

In the absence of a molecular fingerprint of the chaetognath neuronal progenitor cells, it is difficult to set these into a meaningful relation to well characterized stem cell systems of basal Metazoa such as Cnidaria and Platyhelminthes (compare discussion in Hartenstein, 2013). On a cytological level, we have tentative evidence that the chaetognath progenitor cells divide asymmetrically, cycle rapidly, and are arranged in a distinct geometrical pattern (see above). Future studies may reveal if this asymmetric type of division is a prerequisite for generating neurons with individual identities (lineage) and what the molecular and cellular basis for the strict geometrical arrangement in iterated rows may be. A comparison on this cytological level does not yet yield any meaningful insights when compared to Cnidaria or Plathyelminthes.

ACKNOWLEDGMENTS

This study was supported by grant HA 2540/7-3 in the DFG focus program "Metazoan Deep Phylogeny." We greatly appreciate the technical and logistic support provided by Bill S. Hansson (Max-Planck-Institute for Chemical Ecology, Jena) during the initial phase of this project.

LITERATURE CITED

Agata K. 2008. Stem cells in planarian. In: Bosh TG, editor. Stem cells: from hydra to man. Heidelberg, Germany: Springer. p 59–74.

Baguna J. 1998. Planarians. In: Ferretti P, Geraudie J, editors. Cellular and molecular basis of regeneration: from invertebrates to human. South Dacota, U.S.A.: John Wiley & Sons Ltd. p 135–165.

Boccara CN, Sargolini F, Thoresen VH, et al. 2010. Grid cells in pre- and parasubiculum. Nat Neurosci 13:987–994.

Bode HR. 1996. The interstitial cell lineage of hydra: a stem cell system that arose early in evolution. J Cell Sci 109:1155–1164.

Bode A, Salvenmoser W, Nimeth K, et al. 2006. Immunogold-labeled S-phase neoblasts, total neoblast number, their distribution, and evidence for arrested neoblasts in *Macrostomum lignano* (Platyhelminthes, Rhabditophora). Cell Tissue Res 325:577–587.

Bosch TCG, editor. 2009. Stem cells from hydra to man. Berlin, Heidelberg: Springer.

Bosch TC, Anton-Erxleben F, Hemmrich G, Khalturin K. 2010. The *Hydra* polyp: nothing but an active stem cell community. Dev Growth Differ 52:15–25.

Bone Q, Pulsford A. 1984. The sense organs and ventral ganglion of *Sagitta* (Chaetognatha). Acta Zool 65:209–220.

Budd GE. 2001. Why are arthropods segmented? Evol Dev 3:332–342.

Cagan R. 2009. Principles of *Drosophila* eye differentiation. Curr Top Dev Biol 89:115–135.

Carré D, Djediat C, Sardet C. 2002. Formation of a large Vasa-positive germ granule and its inheritance by germ cells in the enigmatic Chaetognaths. Development 129:661–670.

Cebrià F. 2008. Organization of the nervous system in the model planarian *Schmidtea mediterranea*: an immunocytochemical study. Neurosci Res 61:375–384.

Doncaster L. 1902. On the development of *Sagitta*; with notes on the anatomy of the adult. Q J Microsc Sci s2–46:351–395.

Douady S, Couder Y. 1996. Phyllotaxis as a dynamical self organizing process Part I: the Spiral modes resulting from time periodic iterations. J Theor Biol 178:225–274.

Duvert M, Perez Y, Casanova J. 2000. Wound healing and survival of beheaded chaetognaths. J Mar Biol Assoc UK 80:891–898.

Erickson RO. 1973. Tubular packing of spheres in biological fine structure. Science 181:705–716.

Fyhn M, Hafting T, Witter MP, Moser EI, Moser MB. 2008. Grid cells in mice. Hippocampus 18:1230–1238.

Galliot B, Quiquand M. 2011. A two-step process in the emergence of neurogenesis. Eur J Neurosci 34:847–862.

Galliot B, Quiquand M, Ghila L, et al. 2009. Origins of neurogenesis, a cnidarian view. Dev Biol 332:2–24.

Goto T, Yoshida M. 1984. Photoreception in Chaetognatha. In: Ali MA, editor. Photoreception and vision in invertebrates. New York: Plenum Publishing Corporation. p 727–742.

Goto T, Yoshida M. 1987. Nervous system in Chaetognatha. In: Ali MA, editor. Nervous systems in invertebrates. New York: Plenum Publishing Corporation. p 461–481.

Goto T. 1999. Fertilization process in the arrow worm *Spadella cephaloptera* (Chaetognatha). Zool Sci 16:109–114.

Goto T, Katayama-Kumoi Y, Tohyama M, Yoshida M. 1992. Distribution and development of the serotonin-and RFamide-like immunoreactive neurons in the arrowworm, *Paraspadella gotoi* (Chaetognatha). Cell Tissue Res 267:215–222.

Goto T, Yoshida M. 1997. Growth and reproduction of the benthic arrowworm *Paraspadella gotoi* (Chaetognatha) in laboratory culture. Invert Reprod Dev 32:201–207.

Goto T, Yoshida M. 1985. The mating sequence of the benthic arrowworm *Spadella schizoptera*. Biol Bull 169:328–333.

Hartenstein V. 2013. Stem cells in the context of evolution and development. Dev Genes Evol 223:1–3.

Harzsch S. 2003. Ontogeny of the ventral nerve cord in malacostracan crustaceans: a common plan for neuronal development in Crustacea, Hexapoda and other Arthropoda? Arthropod Struct Dev 32:17–37.

Harzsch S. 2006. Neurophylogeny: architecture of the nervous system and a fresh view on arthropod phyologeny. Comp Integr Biol 46:162–194.

Harzsch S, Dawirs RR. 1994. Neurogenesis in larval stages of the spider crab *Hyas araneus* (Decapoda, Brachyura): proliferation of neuroblasts in the ventral nerve cord. Roux's Arch Dev Biol 204:93–100.

Harzsch S, Dawirs RR. 1996. Neurogenesis in the developing crab brain: postembryonic generation of neurons persists beyond metamorphosis. J Neurobiol 29:384–398.

Harzsch S, Müller CHG. 2007. A new look at the ventral nerve centre of *Sagitta*: implications for the phylogenetic position of Chaetognatha (arrow worms) and the evolution of the bilaterian nervous system. Frontiers Zool 4:14.

Harzsch S, Müller CHG, Wolf H. 2005. From variable to constant cell numbers: cellular characteristics of the arthropod nervous system argue against a sister-group relationship of Chelicerata and "Myriapoda" bur favour the Mandibulata concept. Dev Genes Evol 215:53–68.

Harzsch S, Müller CH, Rieger V, et al. 2009. Fine structure of the ventral nerve centre and interspecific identification of individual neurons in the enigmatic Chaetognatha. Zoomorphology 128:53–73.

Harzsch S, Wanninger A. 2009. Evolution of invertebrate nervous systems: the Chaetognatha as a case study. Acta Zool 91:35–43.

Harzsch S, Vilpoux K, Blackburn DC, et al. 2006. Development of the eyes and central visual pathway of the horseshoe crab *Limulus polyphemus* Linnaeus, 1758 (Chelicerata, Xiphosura). Developmental Dynamics 235:2641–2655.

Hemmrich G, Khalturin K, Boehm A-M, et al. 2012. Molecular signatures of the three stem cell lineages in *Hydra* and the emergence of stem cell function at the base of multicellularity. Mol Biol Evol 29:3267–3280.

Hertwig O. 1880. Die chaetognathen ihre anatomie, systematik und entwicklungsgeschichte. Hertwig O, Hertwig R, series editors, Studien zur Blättertheorie. Jena: Gustav Fischer Verlag.

John CC. 1933. Habits, structure, and development of *Spadella cephaloptera*. Q J Microsc Sci 75:625–696.

Kapp H. 2000. The unique embryology of Chaetognatha. Zool Anz 239:263–266.

Klar AJ. 2002. Fibonacci's flowers. Nature 417:595.

Kropff E, Treves A. 2008. The emergence of grid cells: intelligent design or just adaptation? Hippocampus 18:1256–1269.

Kuhl W, Kuhl G. 1965. Die Dynamik der Frühentwicklung von *Sagitta setosa*. Helgoland Marine Res 12:260–301.

Kuhlmann D. 1977. Laboratory studies on the feeding behavior of the chaetognaths Sagitta setosa J. Müller and *S. elegans* Verrill with special reference to fish eggs and larvae as food organisms. Kieler Meeresforsch 25:163–171.

Ladurner P, Rieger R, Baguñà J. 2000. Spatial distribution and differentiation potential of stem cells in hatchlings and adults in the marine Platyhelminth *Macrostomum* sp.: a bromodeoxyuridine analysis. Dev Biol 226:231–241.

Matus DQ, Copley RR, Dunn CW, et al. 2006. Broad taxon and gene sampling indicate that chaetognaths are protostomes. Curr Biol 16: R575–R576.

Marlétaz F, Martin E, Perez Y, et al. 2006. Chaetognath phylogenomics: a protostome with deuterostome-like development; Supplemental data. Curr Biol 16:R577–R578.

Marlétaz F, Gilles A, Caubit X, et al. 2008. Chaetognath transcriptome reveals ancestral and unique features among bilaterians. Genome Biol 9:R94.

McVeigh P, Mair GR, Atkinson L, et al. 2009. Discovery of multiple neuropeptide families in the phylum Platyhelminthes. Int J Parasitol 39:1243–1252.

Morris J, Cardona A, Miguel-Bonet MDM, Hartenstein V. 2007. Neurobiology of the basal platyhelminth *Macrostomum lignano*: map and digital 3D model of the juvenile brain neuropile. Dev Genes Evol 217:569–584.

Müller CHG, Rieger V, Perez Y, Harzsch S. submitted. Multicellular ciliary sense organs of arrow worms (Chaetognatha): a comparative immunhistochemical and ultrastructural study.

Newmark PA, Alvarado AS. 2000. Bromodeoxyuridine specifically labels the regenerative stem cells of planarians. Dev Biol 220:142–153.

Nielsen C. 2012. Animal evolution: interrelationships of the living phyla. Oxford: Oxford University Press.

Nishimura K, Kitamura Y, Inoue T, et al. 2007a. Reconstruction of dopaminergic neural network and locomotion function in planarian regenerates. Dev Neurobiol 67:1059–1078.

Nishimura K, Kitamura Y, Inoue T, et al. 2007b. Identification and distribution of tryptophan hydroxylase (TPH)-positive neurons in the planarian *Dugesia japonica*. Neurosci Res 59:101–106.

Nishimura K, Kitamura Y, Inoue T, et al. 2008a. Characterization of tyramine beta-hydroxylase in planarian *Dugesia japonica*: cloning and expression. Neurochem Int 53:184–192.

Nishimura K, Kitamura Y, Umesono Y, et al. 2008b. Identification of glutamic acid decarboxylase gene and distribution of GABAergic nervous system in the planarian *Dugesia japonica*. Neuroscience 153:1103.

Okamoto K, Takeuchi K, Agata K. 2005. Neural projections in planarian brain revealed by fluorescent dye tracing. Zool Sci 22:535–5546.

Otto JJ, Campbell RD. 1977. Budding in *Hydra attenuata*: bud stages and fate map. J Exp Zool 200:417–428.

Papillon D, Perez Y, Fasano L, Parco YL, Caubit X. 2005. Restricted expression of a median Hox gene in the central nervous system of chaetognaths. Dev Genes Evol 215:369–373.

Pearre S. 1991. Growth and reproduction. In: Bone Q, Kapp H, Pierrot-Bults AC, editors. The biology of Chaetognaths. New York: Oxford University Press. p 61–75.

Perez Y, Müller CHG, Harzsch S. (in press). The Chaetognatha: an anarchistic taxon between Protostomia and Deuterostomia. In: Wägele W, editor. Metazoan deep phylogeny.

Raikova OI, Reuter M, Jondelius U, Gustafsson MKS. 2000. The brain of the Nemertodermatida (Platyhelminthes) as revealed by anti-5HT and anti-FMRFamide immunostainings. Tissue Cell 32:358–365.

Raikova OI, Reuter M, Kotikova EA, Gustafsson MK. 1998. A commissural brain! The pattern of 5-HT immunoreactivity in Acoela (Plathelminthes). Zoomorphology 118:69–77.

Reuter M, Raikova OI, Jondelius U, et al. 2001. Organisation of the nervous system in the Acoela: an immunocytochemical study. Tissue Cell 33:119–128.

Reuter M, Raikova OI, Gustafsson MKS. 1998. An endocrine brain? The pattern of FMRF-amide immunoreactivity in Acoela (Platyhelminthes). Tissue Cell 30:57–63.

Reuter M, Raikova OI, Gustafsson MKS. 2001. Patterns in the nervous and muscle systems in lower flatworms. Belg J Zool 131:47–53.

Reeve MR. 1970. Complete cycle of development of a pelagic Chaetognath in culture. Nature 227:381.

Richter S, Loesel R, Purschke G, et al. 2010. Invertebrate neurophylogeny—suggested terms and definitions for a neuroanatomical glossary. Front Zool 7:29.

Rieger V, Perez Y, Müller CHG, et al. 2010. Immunohistochemical analysis and 3D reconstruction of the cephalic nervous system in Chaetognatha: insights into the evolution of an early bilaterian brain? Invert Biol 129:77–104.

Rieger V, Perez Y, Müller CHG, et al. 2011. Development of the nervous system in hatchlings of *Spadella cephaloptera* (Chaetognatha), and implications for nervous system evolution in Bilateria. Dev Growth Differ 53:740–759.

Rink J. 2013. Stem cell systems and regeneration in Planaria. Dev Genes Evol 223:67–84.

Shipman PD, Newell AC. 2004. Phyllotactic patterns on plants. Phys Rev Lett 92:168102.

Stenkamp DL, Cameron DA. 2002. Cellular pattern formation in the retina: retinal regeneration as a model system. Mol Vision 8:280–293.

Shinn GL. 1997. Chapter 3: chaetognatha. In: Harrison FW, Ruppert EE, editors. Hemichordata, chaetognatha, and the invertebrate chordates. New York: Wiley-Liss. p 103–220 [Harrison FW (Series Editor) Microscopic Anatomy of Invertebrates, Vol. 15].

Shimotori T, Goto T. 1999. Establishment of axial properties in the arrow worm embryo, *Paraspadella gotoi* (Chaetognatha): developmental fate of the first two blastomeres. Zool Sci 16:459–469.

Shimotori T, Goto T. 2001. Developmental fates of the first four blastomeres of the chaetognath *Paraspadella gotoi*: relationship to protostomes. Dev Growth Differ 43:371–382.

Sintoni S, Benton JL, Beltz BS, Hansson BS, Harzsch S. 2012. Neurogenesis in the central olfactory pathway of adult decapod crustaceans: development of the neurogenic niche in the brains of Procambarid Crayfish. Neural Dev 7:1.

Takada N, Goto T, Satoh N. 2002. Expression pattern of the *brachyury* gene in the arrow worm *Paraspadella gotoi* (Chaetognatha). Genesis 32:240–245.

Umesono Y, Agata K. 2009. Evolution and regeneration of the planarian central nervous system. Dev Growth Differ 51:185–195.

Veen AH, Lindenmayer A. 1977. Diffusion mechanism for phyllotaxis. Theoretical physico-chemical and computer study. Plant Physiol 60:127–139.

Yasuda E, Goto T, Makabe KW, Satoh N. 1997. Expression of actin genes in the arrow worm *Paraspadella gotoi* (Chaetognatha). Zool Sci 14:953–960.

8.5 Multicellular ciliary sense organs of arrow worms (Chaetognatha): a comparative immunohistochemical and ultrastructural study.

Müller CHG, **Rieger** V, Perez Y, Harzsch S (submitted)

Zoomorphology

Zoomorphology

Multicellular ciliary sense organs of arrow worms (Chaetognatha): a comparative immunohistochemical and ultrastructural study

--Manuscript Draft--

Manuscript Number:	
Full Title:	Multicellular ciliary sense organs of arrow worms (Chaetognatha): a comparative immunohistochemical and ultrastructural study
Article Type:	Original Paper
Keywords:	ciliary fence organs, ciliary tuft organs, corona ciliata, individual neurite/neuron identification, mechanoreceptor, chemoreceptor, aspartate, tubulin
Corresponding Author:	Carsten H.G. Müller University of Greifswald Greifswald, Mecklenburg-Vorpommern GERMANY
Corresponding Author Secondary Information:	
Corresponding Author's Institution:	University of Greifswald
Corresponding Author's Secondary Institution:	
First Author:	Carsten H.G. Müller
First Author Secondary Information:	
Order of Authors:	Carsten H.G. Müller
	Verena Rieger, Dipl. Biol.
	Yvan Perez, Researcher
	Steffen Harzsch, Professor, head of the department
Order of Authors Secondary Information:	
Abstract:	This study sets out to explore details of structure and innervation of multicellular ciliary sense organs in Chaetognatha, highly abundant marine predators which effectively prey on zooplankton in various depths and habitats. We examined the epibenthic species Spadella cephaloptera and Spadella valsalinae as well as the pelagic species Parasagitta setosa by immunohistofluorescence with confocal laser-scan microscopy to detect tubulin and cell nuclei in whole mount preparations. Furthermore, we used scanning and transmission electron microscopy to analyse ultrastructural details of multicellular ciliary sense organs (including a further pelagic species, Sagitta bipunctata) and a mitosis marker to detect proliferating cells. Chaetognaths, and in particular the examined species, are equipped with several epidermal sensory organs including the three types of ciliary sense organs that are the focus of the present study: the transversally oriented ciliary fence organs (1), the longitudinally (parallel to the anterior-posterior axis) oriented ciliary tuft organs (2) and a ciliary loop, the corona ciliata (3). The outer shape of those sense organs, especially the corona ciliata, may vary widely among Chaetognatha. Shape, number and distribution of the ciliary fence organs and the corona ciliata are species-specific and can be easily highlighted by immunohistochemical techniques making these a useful tool for taxonomic studies. Two different types of multilayered and partly pooled receptor cells constitute the ciliary fence and ciliary tuft organs. Each receptor cell extends a single, non-locomotory cilium from the narrow apex so that multiple rows of highly ordered cilia are formed. The ciliary fence and ciliary tuft organs are distributed in large numbers along the entire body. They are known to have a mechanosensory function, detecting hydrodynamic stimuli to initiate attack or escape movements. Their axons project in bundles towards the ventral nerve centre. The corona ciliata consists of numerous ciliary cells forming a loop on the animal's dorsal neck region and shows an extensive and intricate pattern of innervation. Many of the cells in the corona ciliata of adult specimens of S. cephaloptera show mitotic activity suggesting a turnover of cells. In S. cephaloptera

Powered by Editorial Manager® and Preprint Manager® from Aries Systems Corporation

	and S. valsalinae, the corona ciliate shares a nearly identical cellular architecture. The outer cellular population of the corona ciliata comprises epithelial cells with a single motile cilium, whereas the larger inner cell population contains two types of epithelial cells: absorptive cells extending two or several cilia and sensory cells with a single cilium. TEM studies show that the two latter ciliary cell types surround an annular extracellular cavity which is, although almost completely enclosed, accessible by water from outside. The axons of the sensory cells become bundled to the centre of the corona ciliata, where they pass into the dorsomedian coronal nerves that house approximately 400 neurites and project into the posterior area of the brain. Synapses are found throughout the coronal nerves, close to the ECM and the subjacent longitudinal dorsomedian musculature of the trunk. The function of the corona ciliata is not yet known, but the new insights into the microscopic architecture strengthens speculations of a sensory function, and suggest that it is most likely a chemosensory organ.

Powered by Editorial Manager® and Preprint Manager® from Aries Systems Corporation

Manuscript
Click here to download Manuscript: Receptors_Vers_01.09.12g.doc
Click here to view linked References

Multicellular ciliary sense organs of arrow worms (Chaetognatha): a comparative immunohistochemical and ultrastructural study

Carsten H.G. Müller[1],Verena Rieger[1], Yvan Perez[2] & Steffen Harzsch[1]

[1] Ernst-Moritz-Arndt-Universität Greifswald, Zoologisches Institut und Museum, Cytologie und Evolutionsbiologie, Soldmannstrasse 23, 17497 Greifswald, Germany
[2] Université de Provence, Institut Méditerranéen d'Ecologie et de Paléoécologie, UMR CNRS 6116 3 Pl Victor Hugo Case 36, 13338 Marseille cedex 3, France

Abstract:

This study sets out to explore details of structure and innervation of multicellular ciliary sense organs in Chaetognatha, highly abundant marine predators which effectively prey on zooplankton in various depths and habitats. We examined the epibenthic species *Spadella cephaloptera* and *Spadella valsalinae* as well as the pelagic species *Parasagitta setosa* by immunohistofluorescence with confocal laser-scan microscopy to detect tubulin and cell nuclei in whole mount preparations. Furthermore, we used scanning and transmission electron microscopy to analyse ultrastructural details of multicellular ciliary sense organs (including a further pelagic species, *Sagitta bipunctata*) and a mitosis marker to detect proliferating cells. Chaetognaths, and in particular the examined species, are equipped with several epidermal sensory organs including the three types of ciliary sense organs that are the focus of the present study: the transversally oriented ciliary fence organs (1), the longitudinally (parallel to the anterior-posterior axis) oriented ciliary tuft organs (2) and a ciliary loop, the corona ciliata (3). The outer shape of those sense organs, especially the corona ciliata, may vary widely among Chaetognatha. Shape, number and distribution of the ciliary fence organs and the corona ciliata are species-specific and can be easily highlighted by immunohistochemical techniques making these a useful tool for taxonomic studies. Two different types of multilayered and partly pooled receptor cells constitute the ciliary fence and ciliary tuft organs. Each receptor cell extends a single, non-locomotory cilium from the narrow apex so that multiple rows of highly ordered cilia are formed. The ciliary fence and ciliary tuft organs are distributed in large numbers along the entire body. They are known to have a mechanosensory function, detecting hydrodynamic stimuli to initiate attack or escape movements. Their axons project in bundles towards the ventral nerve centre. The corona ciliata consists of numerous ciliary cells forming a loop on the animal's dorsal neck region and shows an extensive and intricate pattern of innervation. Many of the cells in the corona ciliata of adult specimens of *S. cephaloptera* show mitotic activity suggesting a turnover of cells. In *S. cephaloptera* and *S. valsalinae,* the corona ciliate shares a nearly identical cellular architecture. The outer cellular population of the corona ciliata comprises epithelial cells with a single motile cilium, whereas the larger inner cell population contains two types of epithelial cells: absorptive cells extending two or several cilia and sensory cells with a single cilium. TEM studies show that the two latter ciliary cell types surround an annular extracellular cavity which is, although almost completely enclosed, accessible by water from outside. The axons of the sensory cells become bundled to the centre of the corona ciliata, where they pass into the dorsomedian coronal nerves that house approximately 400 neurites and project into the posterior area of the brain. Synapses are found throughout the coronal nerves, close to the ECM and the subjacent longitudinal dorsomedian musculature of the trunk. The function of the corona ciliata is not yet known, but the new insights into the microscopic architecture strengthens speculations of a sensory function, and suggest that it is most likely a chemosensory organ.

Key Words: ciliary fence organs, ciliary tuft organs, corona ciliata, individual neurite/neuron identification, mechanoreceptor, chemoreceptor, aspartate, tubulin

Introduction:

Chaetognaths are small, translucent and widely distributed marine predators that feed mainly on zooplankton. They are found at various depths and inhabit both pelagic and benthic environments. Their body can be divided into three distinct parts: the head, trunk and tail (Fig 1A). Several sense organs are present, most of which are located in the epidermis of the head, where they are used for orientation and prey detection. These include a pair of eyes (Goto and Yoshida 1981, 1983), and the retrocerebral organ (Shinn 1997) both innervating the posterior end of the brain and positioned on the dorsal side of the head. The function of the retrocerebral organ is yet unclear. However, based on the occurrence of ciliary bodies and rootlets along the apical membranes of some microvilli-bearing epithelial cells constituting the organ, Shinn (1997) suspected that it might be a baroreceptor. Other, structurally less complex ciliary organs, are the peristomatic, presumably chemosensory “enclosed ciliary slit receptors” (Bone and Pulsford 1978) on the head as well as “large cilia” extended by single sensory cells which occur in various positions of the body and are assumed to function as vibration receptors (Horridge and Boulton 1967, Bone and Pulsford 1978).

The multicellular ciliary fence and ciliary tuft organs (*sensu* Malakhov et al. 2005), also termed as “bristles”, “hairs fans”, “sensory cells”, “ciliary sensory organs”, “ciliary fence organs”, ciliary fence receptors”, or just “fence receptors” (e.g. Bone and Pulsford 1978, Feigenbaum 1978, Nagasawa and Marumo 1982, Welsch and Storch 1983, Shinn 1997), are the two main targets of this study. They are embedded in the epidermis and are distributed in great numbers over the whole body surface (Fig. 1B-D), but differ with respect to their orientation relative to the body and several ultrastructural characters as detailed below. These organs consist of numerous ciliary receptor cells and are discussed as either representing a primary (Bone and Pulsford 1978) or a secondary type of receptor (Reisinger 1969, Welsch and Storch 1983). Bone and Pulsford (1978) and also Nagasawa and Marumo (1982) failed to show the primary synapses which remained undetected. Shinn (1997) suggested that reports according to which the fence receptors are secondary sensory cells were more reliable. The appearance of their organelles resembles that of neurons (Horridge and Boulton 1967). In *Spadella cephaloptera*, for example, about 50-300 rigid cilia emerge from these cells, positioned in a straight row. The cilia have the typical 9x2+2 microtubular configuration (Bone and Pulsford 1984) and are surrounded by a collar of microvilli at their base (Shinn 1997). A typical cilium of a receptor cell is 60-70 µm long and 0.2 µm thick (Horridge and Boulton, 1967). It is known that the ciliary fence and ciliary tuft organs of chaetognaths innervate the ventral nerve centre (e.g. Hertwig 1880, Bone and Pulsford 1984). Several authors have studied the outer and internal ultrastructure of ciliary fence and ciliary tuft organs utilizing electron microscopic (SEM and TEM) techniques (e.g., Horridge and Boulton 1967, Bone and Pulsford 1978, Welsch and Storch 1983, Ahnelt 1984, Bone and Pulsford 1984, Goto and Yoshida 1987, Shinn 1997, Malakhov et al. 2005). The typology separating ciliary fence organs from ciliary tuft organs, as used in this paper, refers in a slightly modified way to the latest TEM study of Malakhov et al. (2005), who differentiated "ciliary fence receptors" and "ciliary tuft receptors" in the species *Parasagitta elegans* und *Serratosagitta pseudoserratodentata* according to their orientation relative to the body and several ultrastructural characters. Ciliary fence receptors in a strict sense are clusters of sensory cells that are arranged perpendicular to the longitudinal body axis and include an elongated, unstriated and electron-dense apical structure subjacent to the basal body of the cilium (compare Fig. 1C-D). These receptors were suggested to perceive different oscillation/vibration frequencies propagating in the water. Ciliary tuft receptors, however, are exclusively arranged in parallel to the anterior-posterior axis and contain sensory cells with very long and cross-striated ciliary rootlets (compare Fig. 1C-D), which anchor in the basal body and extend deeply into the cell body (see Fig. 2 in Malakhov et al. 2005).

Experiments showed that the receptor cells in ciliary fence and ciliary tuft organs react to close-range mechanosensory input and are used for prey detection and coordination of swimming behavior (Horridge and Boulton 1967, Feigenbaum and Reeve 1977, Feigenbaum and Maris 1984, Bone and Goto 1991). In their experimental setup, Horridge and Boulton (1967) used a probe vibrating at different frequencies. They found that in *S. cephaloptera* the probe could elicit a directed feeding attack at close proximity (1-3mm) and for a narrow range of frequencies (9-20 Hz) and amplitudes (100-50 µm). Newbury (1972) suggested that this range of detected frequencies is similar to the vibration rates emitted by some copepod species. Feigenbaum and Reeve (1977) demonstrated that for other species the detection range varies and that exposition to other frequencies resulted in either an escape movement or no response at all. Another goal of the study by Feigenbaum and Reeve (1977) was to determine the density of prey organisms necessary for a pelagic chaetognath to find enough food to sustain maximal growth and reproduction rates, since a chaetognath only detects organisms that are less than 3 mm away. Therefore, Feigenbaum and Reeve (1977) concluded that these animals must use other sensory modalities to detect patches of prey organisms with a high enough organism density.

The distribution pattern of ciliary fence and ciliary tuft organs is species-specific, although minor intraspecific variances are common (Feigenbaum 1978). Patterns have been described by various authors for several species and with several methods (e.g. *Ferosagitta hispida*: Conant 1895; *S. cephaloptera*: Hertwig 1880, John 1933, Horridge and Boulton 1967). The most substantial study of this topic was published by Feigenbaum (1978, see Fig. 1C), who collected data on several species of various chaetognath subtaxa and described the distribution patterns of ciliary fence and ciliary tuft organs in great detail. He illustrated that the total number of these sensory organs varies with age and taxonomic affiliation. Amongst the studied chaetognath taxa, the lowest number of ciliary fence and ciliary tuft organs in an adult was present in *Spadella schizoptera* with about 125 receptors, whereas *Flaccisagitta enflata* had the highest number with about 600 receptors. During development, the number of ciliary fence and ciliary tuft organs increases, but while in Sagittidae the final number of receptors depends on the size of the animal, in Spadellidae the final number is established a few days after hatching and remains unaffected by growth. Feigenbaum (1978) also showed that fence receptors are either aligned with the longitudinal body axis or are arranged transversally to this axis, whereas a diagonal orientation is rare. Bone and Pulsford (1978) concluded that the sensitivity of chaetognaths to water movement depends on the orientation of the ciliary fence and ciliary tuft organs on the animal, since they are likely most sensitive to currents that run transversally to their row of cilia.

The corona ciliata, the third multicellular ciliary sensory organ analyzed in the present report, is located on the dorsal side of the body and extends along the dorso-posterior ("neck") region (Bone and Goto 1991, Shinn 1997). Even though the corona ciliata is a very prominent feature of chaetognaths, its functional role is not yet known with certainty. The various suggested functions include chemo- and mechanoreception, the secretion of a substance that governs sperm movement and a nephridium-like function (reviewed by Ghirardelli 1968). A role as a tactile receptor was discussed and dismissed by Horridge and Boulton (1967). The ultrastructure of the corona ciliata has been described in different chaetognath species by several authors (Horridge and Boulton 1967, Nagasawa and Marumo 1982, Malakhov and Frid 1984, Shinn 1997, Giulianini et al. 1999, Malakhov et al. 2005). The corona ciliata is arranged in a loop that is normally closed, but it may remain open at their posterior end in a few species (Casanova 1991). The macroscopic shape and orientation of this organ were suggested to be species-specific (Shinn 1997), although some intraspecific variations of its size, shape and position on the body may occur (Ghirardelli 1968). Transverse sections through either side of the corona ciliata show that the epithelium is condensed into a cell cluster comprising a dozen of ciliary cells with a putative sensory function as well as secretory cells. The secretory cells are arranged at the inner margin of the cluster, while the ciliary cells occupy the centre and outer margin of the cluster (Reisinger 1969, Shinn 1997). However, secretory cells are not present in ciliary loops of pelagic species (Ghirardelli 1968). Two types of cilia have been described. The first type of cilium is visible from outside and is protruded outwards from a collar-surrounded apical depression of each ciliary cell (Shinn 1997). These cilia have been reported to move rhythmically in live specimens (Horridge and Boulton 1967). The second type of cilium is formed by medially arranged ciliary cells. These cilia are not visible from outside, as they extend into a subsurface canal that is also lined and accessed by the secretory cells. Whether or not the corona really contains sensory cells, has long been a matter of dispute (Bone and Pulsford 1984, Malakhov and Frid 1984), but Shinn (1997) reported the presence of neurites basal to the outer margin of the coronal cell cluster. Because he did not observe any synapses, he concluded that these neurites may extend from the coronal cells into the coronal nerve.

The current study sets out to explore the structure and innervation patterns of the ciliary fence and ciliary tuft organs as well as of the corona ciliata in higher detail by using a combination of different methods, some of which have yet not been used to examine these particular sense organs of chaetognaths. We applied immunohistochemistry (labeling against acetylated tubulin or tyrosinated α-tubulin as well as aspartate and actin combined with a histochemical marker for nuclei), confocal laser scanning microscopy, light microscopy (histological staining), and scanning and transmission electron microscopy. The data presented in this comparative approach was obtained from the epibenthic species *Spadella cephaloptera* (Fig. 1) and *Spadella valsalinae* as well as from the pelagic species *Parasagitta setosa* and *Sagitta bipunctata*. We also present histological aspects of the ciliary sense organs of *S. cephaloptera* and *Ferosagitta hispida*. Furthermore, we examined the ultrastructural organization of multicellular ciliary sense organs in *S. cephaloptera* and *S. valsalinae*, with a special emphasis on the microtubular system and the various afferents projecting from receptor cells into the coronal nerves and the intraepidermal nerve plexus.

Material & Methods

Experimental animals

Several hundreds adult specimens of *Spadella cephaloptera* (Busch, 1851) (Phragmophora, Spadellidae) were collected in Sormiou (near Marseille, France) in June 2006 and August 2007. A plankton-net was grazed over the *Posidonia oceanica*-seagrass beds by snorkeling. Animals were kept in aquaria containing natural seawater in the lab of Y. Perez at the University of Provence, Marseille, before immunohistochemical processing. Additionally, specimens of the Northern Adriatic species *Spadella valsalinae* recently described by Winkelmann et al. (in press) were examined. This species was discovered and collected on a poorly assorted *Amphioxus*-sediment at 10 m depth during a diving expedition in the bay of Valsaline (Pula, Croatia) in April until July 2009. One specimen of the tropical West Atlantic *Ferosagitta hispida* (Conant, 1895), generously provided by G. Shinn, was obtained in surface water of the Indian River Lagoon (271140N, 801900W) near Fort Pierce, FL, USA, with a plankton net suitable for capturing macrofauna organisms (300-mm mesh size). Adult specimens of *Parasagitta setosa* (Müller, 1847) were obtained during a collection trip to the Biologische Anstalt Helgoland (German Bight) in August 2006. Specimens were obtained by horizontal (surface water samples) as well as by vertical (down to 20 meters depth) plankton hauls with the research vessel "MS Aade". Several adult specimens of *Sagitta bipunctata* were captured in shallow waters (0-5 m depth) of the Brazilian basin using a PLA plankton net (79th cruise of research vessel “FS METEOR” exploring deep-sea diversity and atlantic seamounts: DIVA-3 expedition). Some unidentified *Sagitta* specimens were also captured with a small plankton net during a plankton survey in the coastal waters of the Balearic Island Ibiza (March 2006), approximately 2 kilometers south of Eivissa harbour.

Histology

For histology, dissected body parts (head, trunk, tail) of several adult individuals of *Ferosagitta hispida* and *Spadella cephaloptera* (the former species treated by G. Shinn, Northeast Missouri State University) were prefixed in a cold solution modified after Karnovsky (1965) consisting of 2.5% paraformaldehyde and 2.5% glutaraldehyde dissolved in 0.2 M phosphate buffer. Postfixation of the material included bathing into 2% OsO_4 in 0.2 M posphate buffer. Dissected body parts of two individuals of *F. hispida* were then dehydrated in a graded series of ethanol, transferred through three changes of propylene oxide solutions, and embedded in Epon 812. Tissues were sectioned transversally in several series of approximately 400 sections (1.5 µm in thickness) with a rotating MICROM HM 355S histomicrotome. Dissected body parts (head, trunk) of *S. cephaloptera* were embedded into epoxide resin (Araldit, FLUKA), then sectioned serially and transversally at a thickness of 0.5 µm with a LEICA UCT ultramicrotome. Semithin and thick sections of both species were then stained in a 1% toluidine blue solution in a solution of 1% Na-tetraborate (borax) and afterwards digitalized with a Nikon Eclipse 90i microscope equipped with a Nikon D-2MBWc camera using the Nikon NIS-Elements Ar 3.10 software.

Scanning electron microscopy and transmission electron microscopy

For scanning electron microscopy (SEM), several adult individuals of *Parasagitta setosa*, *Sagitta bipunctata*, *Spadella cephaloptera* and *Spadella valsalinae* were fixed *in toto* either in 70% ethanol (*P. setosa*, *Spadella* spp.) or 4% paraformaldehyde (*S. bipunctata*). After washing in 0.1 M sodium phosphate buffer (at pH 7.4), the animals were critical-point-dried, mounted on standard conductive adhesive tabs, sputter-coated with gold, and finally examined at an accelerating voltage of 15-30 kV under different scanning electron microscopes: *P. setosa*: Zeiss DSM 960A (Electron Microscopic Centre, University of Rostock), *S. valsalinae*: Zeiss EVO LS10 (Electron Microscopic Unit, University of Greifswald), *S. bipunctata*: LEO 1525 (Microscopy Section, Biocentre Grindel and Zoological Museum, University of Hamburg).

For transmission electron microscopy (TEM), adult specimens of *S. cephaloptera* and *S. valsalinae*, all measuring 4–6 mm in length, were fixed either by immersing the entire specimen or by cutting the body into three pieces (head, trunk and tail). The tissues were immersed for 12 h in a cold solution of Karnovsky's (1965) prefixative, consisting of 2% glutaraldehyde, 2% paraformaldehyde, 1.52% NaOH, and 1.2 g D-glucose, dissolved in 2.25% Na-hydrogenphosphate buffer (pH 7.4). After washing in the same buffer (12 h), the specimens were postfixed for 4 h in 1% OsO_4 solution (same buffer) at room temperature and, following dehydration in a graded series of acetone, embedded in epoxide resin (Araldit, FLUKA). Serial ultrathin sections (thickness: 55-70 nm) were mounted on Formvar-coated slotgrids, stained with uranyl acetate and lead citrate for 4 min each, and then examined under Zeiss 902A (Electron Microscopic Centre, University of Rostock) and Jeol-1011 (Dept. General and Systematic Zoology, University of Greifswald) transmission electron microscopes operated at 80 kV. In some specimens, up to 30 digital TEM micrographs were compiled using the software ITEM to provide an overview of an entire ciliary sense organ.

Fluorescent histochemistry and immunohistochemistry

For the BrdU (Bromodeoxyuridine, S-phase specific mitosis marker) experiment, numerous adult specimens of *Spadella cephaloptera* were kept in seawater with added BrdU (0.2 µg/ml) for 4 h prior to the fixation (compare Harzsch and Dawirs 1994). Several specimens of *Parasagitta setosa*, *Spadella cephaloptera* and *Spadella valsalinae* were fixed for 4 h at room temperature (or alternatively overnight at 4°C) in 4% paraformaldehyde (PFA) in 0.1 M sodium phosphate buffer (pH 7.4). Histochemistry and immunohistochemistry were carried out on free-floating whole mounts of hatchlings with primary and fluorochrome-conjugated secondary antibodies using standard protocols (Harzsch and Müller 2007, Harzsch et al. 2010, Rieger et al. 2011). After fixation, the tissues were washed in several changes of phosphate buffered saline (PBS) for at least 4h. All specimens were pre-incubated in PBS-TX (1% normal goat serum, 0.3% Triton X-100, 0.05% Na-azide) for 1 h and then incubated overnight in either one or a combination of two of the following primary antibodies diluted in PBS-TX (room temperature):

- anti-acetylated α-tubulin from mouse (1:2000; Sigma)
- anti-tyrosinated tubulin from mouse (1:1000; Sigma)
- anti-conjugated aspartate from rabbit (1:2000; MoBiTec)
- anti-BrdU monoclonal from mouse (1:50; GE Healthcare, Amersham cell proliferation kit RPN20)

Specimens were then washed for at least 2 h in several changes of PBS and subsequently incubated in secondary antibodies against rabbit proteins conjugated to the fluorochrome Alexa Fluor 488 (1:500; Molecular Probes) and antibodies against mouse proteins conjugated to Cy3 (1:500; Jackson Immuno Research) for 4 h. The specimens were stained with a nuclear dye, either bisbenzimide (0.04%, 4 h at room temperature; Hoechst H 33258) or YOYO-1 (0.025%, 4 h at room temperature; Molecular Probes) during the secondary antibody incubations. Finally, the tissues were washed for at least 2 h in several changes of PBS and then mounted in MOWIOL (Calbiochem). The immunohistochemical observations reported in this paper are based on the analysis of at least six specimens for each stage.

Microscopic analysis

Digital images were obtained using a Zeiss Axioimager Z1 fluorescence microscope equipped with a structured illumination device (ApoTome) and a digital camera AxioCamMRm (Zeiss) controlled by the AxioVision V 4.6.3-SP1 software package (Zeiss). In addition, samples were scanned with a Zeiss LSM 510 Meta Confocal Laser-Scanning Microscope. Those images are based on Z-stacks of several optical sections and were obtained using the LSM 510 V.4.0. SP2 software (Zeiss). Images were black-white inverted and processed in Adobe Photoshop CS4 V11.0 by using the global contrast and brightness adjustment features.

Specificity of the antisera

As a control for unspecific binding of the secondary antisera, we treated some specimens of *Spadella cephaloptera* according to the protocol described above, but replaced the primary antibody with a pure PBS-TX. This treatment created an unspecific, homogenous background in all body areas relevant to this study.

The monoclonal anti-acetylated tubulin (mouse IgG2b; Sigma Product Number T 7451, Clone 6-11B-1) was raised against acetylated tubulin from the sea urchin *Strongylocentrotus purpuratus*. According to the manufacturer, this antibody reacts with acetylated α-tubulin from many different species including protists, plants, invertebrates, and vertebrates, indicating that the antigen this antibody recognizes is evolutionarily conserved across a broad range of species. Tubulin is the major building block of microtubules and represents a heterodimer of α-tubulin and β-tubulin.

The monoclonal anti-tyrosinated tubulin (mouse IgG3; Sigma Product Number T 9028, Clone TUB-1A2) was raised against a peptide containing the carboxy-terminal amino acids of α-tubulin. In recent studies, this antibody was used to label commissures and nerves, as for example in acoels (Heynol and Martindale 2009, Semmler et al. 2010). According to the manufacturer, this antibody reacts with tyrosinated tubulin from bovine brain, African monkey green kidney cells, dog kidney, marsupial kidney, mouse pituitary tumor (AtT-20), yeast, and *Xenopus*-frogs. This again indicates that the antigen which this antibody recognizes is evolutionarily conserved across a broad range of species. Microtubules grow and turn over rapidly, but some populations of interphase microtubules are more stable, such as acetylated α-tubulin (Kreis 1987). Tubulin tyrosinylation is involved in the assembly status of tubulin. Tyrosinated tubulin (tyr-tubulin) represents a relatively dynamic subclass of interphase microtubules (Kreis 1987).

The polyclonal anti-conjugated aspartate (rabbit IgG3; MoBiTec Product Number 1011GE) was raised against aspartate-glutaraldehyde-carriers. According to the manufacturer, this antibody reacts with aspartate coupled to glutaraldehyde. Very weak cross-reactivity occurs with conjugated glutamate and GABA, almost no cross-reactivity was found for conjugated taurine, glycine, β-alanine and unconjugated aspartate.

Neuroanatomical nomenclature

Our neuroanatomical nomenclature conforms with Richter et al. (2010).

Results

Ciliary fence and ciliary tuft organs

General arrangement

Immunohistochemistry clearly labels the ciliary sense organs on which this study is focused, but cannot resolve all subtypes (ciliary fence and ciliary tuft organs) which are described here by means of histological and ultrastructural characters. Ciliary sense organs appear at low magnification as aggregations of labeled cell nuclei distributed along the surface of the chaetognath body (Fig. 1D). Ciliary fence and ciliary tuft organs are numerous and distributed in a bilaterally symmetrical fashion in an arrangement that resembles the pattern described in Feigenbaum (1978 reproduced in Fig. 1C, compare with Fig. 1B,D). As an example, we will illustrate the pattern in *Spadella cephaloptera* which we analyzed in detail and for which we prefer to use the following terminology. In this species, several longitudinal 'lines' of receptors, the ciliary tuft organs, with their fences aligned parallel to the anterior-posterior axis as well as numerous ciliary fence organs, located perpendicular to the former type, are present along the head, trunk and tail (dorsal aspects are highlighted in color in Fig. 1C for comparison). Ten unpaired ciliary tuft organs are positioned along the midline of the dorsal surface in the dorsomedian line (red). The average distance between the ciliary tuft organs of the dorsomedian line is about 290 µm with a maximum of about 380 µm and a minimum of 210 µm in a 3,6mm long specimen (tip of the head to tip of the tail fin, distances may vary depending on the size of the animal). The most anteriorly located ciliary tuft organ is positioned in the centre of the corona ciliata. More laterally, a second line of ciliary fence organs with mediolaterally orientated fences form the dorsolateral line (green, see Fig. 1C). Further five ciliary fence and/or ciliary tuft organs are aligned laterally along the side of the trunk (turquoise, see Fig. 1C). The ventral lines of receptors (Feigenbaum 1978) were not considered in this study. Each one ciliary fence tuft and one ciliary tuft organ is present at the median and posterior rim of the lateral fins; another ciliary fence organ is situated anterior of each seminal vesicle (blue, see Fig. 1C). A varying number of receptors is present on the tail fin: three anterior ciliary fence organs are present on both sides of the tail fin (yellow, see Fig. 1C), the anteriormost of which is larger than the other two. A bilaterally symmetrical group of 3-4 ciliary fence and ciliary tuft organs is arranged along the posterior rim of the tail fin (orange, see Fig. 1C). The oblique arrangement of the ciliary fence of the latter group of sense organs makes it difficult to unambiguously assign them to one of the two subtypes, if based on immunhistochemistry.

Histology and immunhistochemistry

The typology of ciliary sense organs, as depicted from fluorescence microscopic and/or confocal laser-scanning microscopic observations, is illustrated in more detail by the examination of semithin (histological) sections and ultrastructure (see below). Histology clearly reveals the existence of tightly packed multiple bands of cilia. These cilia protrude either from a flattened unilayer of sensory epithelial cells with their apices coming together in a narrow, deep and elongated groove in the epidermis (ciliary tuft organs, Fig. 2A-B,D) or from a larger, stratified apparatus of epithelial cells with their apices tapering into an only slightly depressed area of the epidermis (ciliary fence organs, Fig. 2C,E). Furthermore, histological sections reveal that in ciliary tuft organs the peripheral ciliary epithelial cells lie almost parallel to the body surface, whereas the central ones are oriented at a 90° angle to the body surface (Fig. 2B).

In semithin sections (Fig. 2) and fluorescence images with the nuclear marker (Fig. 3), the ciliary fence and ciliary tuft organs can be distinguished from surrounding epidermis as distinct custers of densely packed nuclei. In *Spadella cephaloptera*, local aggregations of nuclei associated with ciliary fence or ciliary tuft organs exhibit a rhombus-like shape. The multiple bands of cilia emanate along the shorter diagonal of such a rhombus (Figs. 1D, 3A). The nuclei are concentrated in the proximal regions. Nuclei of ciliary epithelial cells mostly appear stacked horizontally, especially obvious in ciliary fence organs (Fig. 3B). In contrast, ciliary tuft organs display at most two horizontal layers of nuclei (e.g. Fig. 3D). An extensive filamentous mass of tubulin is clearly visible which pass through the ciliary epithelial cells, surround the nuclei and converge towards the apical region of the ciliary sense organ (Figs. 3B-D, 4B). Towards the midline of the receptor cells, the tubulin filament bundles converge, where the cilia breach the surface in a well ordered, densely packed array (Figs. 3B-D, 4B).

Experiments with an antibody against aspartate show immunreactivity in some of the cell somata of the ciliary fence and ciliary tuft receptor cells. Immunreactivity against aspartate is restricted to central populations of ciliary epithelial cells (located basally of the ciliary multiband, see Fig. 11C-D).

Ciliary fence and ciliary tuft organs: nervous connections

Immunohistochemistry against acetylated α-tubulin reveals that each ciliary fence organ is proximally associated with neurites that provide a link to the centralized parts of the nervous system. However, this method does not allow for a distinction if these are axons or dendrites. Ciliary fence and ciliary tuft organs located on the head and the anterior part of the trunk innervate the main connective (Fig. 3B), while those on the posterior part of the trunk, tail and fins are linked to the looped caudal nerve, neurite bundles which extend laterally along the tail region and are connected to the ventral nerve center (VNC) (Fig. 4A-C-D). A comparison of fence receptors on the tail fin of *S. cephaloptera* and *Parasagitta setosa* highlights a difference in their innervation. The neurites of *S. cephaloptera* are collected in a single neurite bundle (Fig. 4A-B), whereas in *P. setosa* several fiber bundles seem to be linked to a ciliary fence or ciliary tuft organ (Fig. 4C-D).

Fine structure

A SEM survey of the epidermis of those chaetognaths examined in this study reveals tangles of numerous fine and long cilia, often appearing coiled at their tips (Fig. 2A,C). The cilia are arranged in a multiple rows and are ordered in strongly parallel fashion, resembling a ‘fence’ (e.g. Figs. 1, 5C). The ‘fences’ are aligned either perpendicular (ciliary fence organs: Fig. 5A) or parallel (ciliary tuft organs: Fig. 1, 5B) to the anterior-posterior body axis. In some specimens, and in particular in Sagittidae, artifactual losses of tissue material, as they for instance occured in the distal layer of epidermal cells and sheath cells surrounding the ciliary sense organs during TEM preparation, provided insights into the cellular organization of the ciliary fence and ciliary tuft organs. Fig. 5B for example shows numerous spheres clustered at the periphery of a ciliary tuft organ (outer cellular portion). These spherical bodies correspond to the somata of ciliary sensory cells (for details see description below). At the centre, numerous tubes are visible, interspersed by some additional spheres (somata of the inner cellular portion, see also TEM description below). The closer these tubes come to the 'fence' region, the higher ordered they look. The spheres may appear also tapered to their lateral margin. These short tubes are however less obvious and often disappear in the cluster of spheres.

The cellular organization of ciliary fence and ciliary tuft organs as well as their multiple ciliary bands becomes even more obvious in TEM. The following description is based mainly on observations on the species *Spadella cephaloptera* and *Spadella valsalinae*, but we have also TEM-analyzed sagittid species (except *Sagitta bipunctata*) for a comparative approach, but did not find cellular constituents others than documented here for spadellids. Despite different orientation of multiple ciliary bands relative to the body and some other ultrastructural characters, ciliary fence and ciliary tuft organs in principle share the same cellular organization. The large cluster of sensory cells of both types of ciliary sense organs is always encapsulated by specialized sheath cells. The distal tip of the cell cluster is in part overlain by typical distal epidermal cells rich in electron-opaque vacuoles and numerous secretory granules (Figs. 5D; 7A,C). Additionally, the sensory cell cluster is covered upon its distal periphery by ramified and extremely flattened sheath cells, which exhibit a highly condensed, osmiophilic and filamentous cytoplasmic compartment overlying a less osmiophilic cytoplasmic portion with an indistinct nucleus (Figs. 5D,F; 7B-D). Sheath cells located at the distolateral margin of the sensory cell cluster are equipped with osmiophilic granules with a point-screen inner matrix and elongated microvilli extending from their apices (Figs. 5D; 6C; 7A-C). Only the apices of the sensory cells are free of any sheath cells or distal epidermal cell coverage (e.g., Figs. 5D, 7A,B-C). There are two different kinds of monociliated, primary sensory cells found in ciliary fence and ciliary tuft organs, distinguishable by (1) the location of somata in the cluster, (2) the osmiophyly and composition of the cytoplasm, (3) and the construction of the basal region of the cilia. An inner (central) portion of type 1 sensory cells can be separated from a larger outer (peripheral) portion of type 2 sensory cells (e.g., Figs. 5D, 7A). In both types, a more or less stretched apical cytoplasmic process, termed here the inner dendritic segment according to generally used terminology for ciliary sensory cells (e.g. Arthropoda: Müller et al. 2011), extends from the distally tapering soma (e.g., Figs. 5E; 7A-B,D). These inner dendritic segments become slender continuously (Figs. 5E; 6F; 7A-B,D) and are precisely aligned into several rows (Figs. 5D-E, 6A, 7A-B). At its tip, the inner dendritic segment carries a collar of slender microvilli that contain clearly discernible, tightly adjoined longitudinal filaments (Fig. 6B,E). A single cilium (=outer dendritic segment) protrudes from the centre of the microvillar collar (Figs. 5E, 6A, 7C). The apices of ciliary sensory cells as well as of the distal sheath cells come together either on the same (ciliary fence organs, Fig. 5D-E) or on different epidermal surface level(s) (ciliary tuft organs, Fig. 7A,C). In the latter case, the apices of all constituting cells form a deep, cup-like depression in the epidermis (Fig. 7A,C) corresponding to the groove visible on SEM images (Fig. 5B and SEM section above). The cilium bears a long hair shaft traversed by microtubules in a conventional 9x2+2 configuration, the axoneme. Each microtubule encloses a highly electron-dense inner matrix. The axoneme is connected to the inner dendritic segment by (1) a ciliary (basal) body, (2) a filamentous anchoring structure, (3) a conspicuous, more or less elongated electron-dense body and, eventually, (4) a cross-striated ciliary rootlet of various lengths (Figs. 5E; 6B,E; 7A-C). An accessory centriole is not found. The cross-striation of the ciliary rootlets is usually interspersed with less conspicuous longitudinal striation. This complex basal apparatus appears to be most suitable to strengthen our typology of sensory cells. In type 1 sensory cells, the axoneme of the sensory shaft may be incorporated into the inner dendritic segment (Fig. 6D). The electron-dense body is mostly longer and slender in type 1 sensory cells, particularly obvious in ciliary fence organs (Figs. 5E; 6B,E). A dense felt of radial filaments connects the often amorphous electron-dense body to hemidesmosome-like adhering junctions that diversify the apical cell membrane (Fig. 6B,E). Below that level, dendritic inner segments are tightly adjoined by septate junctions (e.g. Fig. 6E). According to our TEM examinations, a cross-striated ciliary rootlet is only present in the inner dendritic segments of type 1 sensory cells and reaches an extraordinary length in ciliary tuft organs (compare Figs. 5E and 7B). The cross-striated rootlets are not always strictly separated from the distally attached electron-dense body as seen on the upper right of Fig. 6E, but may also be merged in type 1 sensory cells, thus forming an intermediate zone with the cross-striated rootlet becoming a core cylinder (Fig. 5E). Lateral branches of the cross-striated ciliary rootlet are present on rare occasions. Instead, condensations of the radial apparatus of microfibrils may occur locally and in particular along the intermediate zone of the electron-dense body and the cross-striated ciliary rootlet (see arrows in Fig. 5E). In both types of sensory cells, the entire inner dendritic segment is endowed with dispersed or sometimes also aggregated microtubules. A considerable portion of these microtubules, along with other microfilaments, is attached to the proximal tip of the electron-dense body. Other cytoplasmic organelles typically found in type 1 and 2 sensory cells are mitochondria of the tubular type, cisternae of the rough endoplasmatic reticulum often in direct vicinity of the nucleus (characteristic for type 2 sensory cells), one or several supranuclear Golgi stack(s) (characteristic for type 2 sensory cells), coated vesicles (at the distal tip of the inner dendritic segment), multivesicular bodies, and late lysosomes (e.g. Figs. 5E,G-H; 6B,E-F; 7B-C). Generally, the cytoplasm of type 1 sensory cells appears less condensed than that of the type 2 ones in ciliary fence organs (Fig. 5E). In ciliary tuft organs, this holds also true, but there some type 1 sensory cells with a very strong osmiophyly can also be observed (Fig. 7A). A more condensed caryoplasm in combination with high portions of distinct heterochromatin make it also possible to differ nuclei of type 2 sensory cells from type 2 ones in ciliary fence organs; the nucleus of a type 1 sensory cell looks indistinctly granular (Fig. 5G-H). In ciliary tuft organs, it is possible to identify most type 1 sensory cells by weaker electron-density of the euchromatic portion

(Fig. 7A-B,D). Nuclei of type 2 sensory cells nest in the centre of a ciliary fence or ciliary tuft organ and are, moreover, often located above the nuclear level of the type 1 sensory cells, thus placing their somata closer to the central ciliary multiband. This gradual separation of nuclear levels becomes particularly evident in ciliary fence organs which include much more cells (Fig. 5D-E). There, central clusters of type 2 sensory cell somata organize the course of the inner dendritic segments of the type 1 sensory cells by forcing them into breakthroughs between the clusters through which they project to their respective somata (Fig. 5E). This pattern leads to a local bundling of the more abundant type 1 sensory cells.

Synapses could not be found in the closest vicinity of ciliary fence or ciliary tuft organs, potentially adjoining the bottom of type 1 and/or 2 sensory cells. In contrast, we discovered that most sensory cells extend axonal processes. Axons of neighboring sensory cells are grouped together and leave the organ as bundles of primary axons (Fig. 5F). The ordering principle according to which primary axon bundles are formed could not be revealed by our TEM examinations, but likely the first sorting of inner dendritic segments (e.g, Fig. 5E) may play a pivotal role.

Corona ciliata

Histology and immunhistochemistry

The corona ciliata of those species examined here varies in shape, but always exhibits a closed ring of numerous, tightly adjoined cilia. In *Spadella cephaloptera*, the cilia are arranged in multiple rows along an oval across the animal's dorso-posterior cephalic ("neck") region (Figs. 1,9A). In *Spadella valsalinae*, the corona ciliata looks similar but is less spherical and looks slightly like a rhombus (Fig. 10C,E). In contrast, in *Parasagitta setosa* and another unidentified *Sagitta* species from Ibiza, the corona ciliata is elongated and stretches from a point anterior to the eyes onto the trunk (Fig. 10A-B,D). In histological semithin sections, the cellular organization of the corona ciliata appears generally similar to those found in the ciliary fence and ciliary tuft organs in a way that densely clustered nuclei are arranged in a flat or slightly cup-like epithelium. When comparing transverse section through the ciliary loop, it is obvious that *Ferosagitta hispida* (Fig. 8A-F) and *Parasagitta setosa* have fewer cells in a given section plane than *Spadella cephaloptera* (Fig. 8G-K). However, the corona ciliata of those sagittid species examined in this study enclose a much wider area by projecting deeply into the trunk region (e.g. Fig. 10B). Based on the location of cells gathered within the cluster, their cytoplasmic composition as well as the shape, size and staining intensity of their nuclei, it is possible to distinguish an outer cellular portion of highly ordered, flattened epithelial cells producing the cilia from an inner cellular portion containing voluminous, granular cells in less ordered fashion (Figs. 8; 9C-D; 10A,C; 12B). Within the inner cellular portion, the nuclei are aligned on two stacked horizontal levels, whereas cells of the outer portion carry their nuclei close to basal pole (e.g. Figs. 8K, 12B). The typological separation of constituting cells is even more evident on the ultrastructural level (see below).

In whole mounts labeled against nuclear material and acetylated α-tubulin, the two-level arrangement of nuclei becomes even more obvious. Tightly packed nuclei surround a tubulin-rich central filamentous mass (Figs. 9; 10A,C-E). The cells constituting the corona ciliata are arranged in a circular cluster in dorsal aspects, similar to the arrangement in ciliary fence and ciliary tuft organs which results in the same distribution of nuclei, several layers in the periphery, mostly one layer underneath the cilia (Fig. 9). In dorsal aspects, two distinctive rings of nuclei are visible in the corona ciliata of *Spadella* spp. by means of fluorescence labelling (Figs. 9C-D; 10C,E; 11B). In accordance with our histological and fine structural analyses, an outer cellular portion with somata that house small nuclei and extend many cilia contrasts with an inner cellular portion the somata of which contain larger, elongated and less densely packed nuclei (e.g. *S. cephaloptera*: Fig. 9C-D). *P. setosa*, too, has two rings of densely packed nuclei, however we could not distinguish different sizes of nuclei (Fig. 10A). Such size differences were also absent in *Ferrosagitta hispida* (Fig. 8A-F) and other sagittids (Fig. 10D). Inbetween the rings, the cilia emerge in a highly ordered, multilayered array, similar to the one observed for fence receptors (e.g., Fig. 8D-F,K). The corona and the brain are linked *via* a pair of coronal nerves (Figs. 9B, 10E). The nerves are composed of neurites that are associated with the sensory cells and are only clearly discernible under the TEM (see Fig. 9E and EM description below). However, our immunohistochemical experiments did not allow us to determine if these neurites are axons emerging from the corona or dendrites that are postsynaptic to those ciliary cells forming the corona ciliata. From the cilia to the brain, these neurites form bundles that become increasingly thicker (Figs. 9B-C, E; 10E), designated here as branches of the coronal nerve (see also EM description below). These bundles converge into either the right or the left coronal nerve. There appears to be no contralateral connection between both nerves along their entire course to the brain (e.g., Fig. 9B). Experiments with the s-phase specific proliferation marker bromodeoxyuridine (BrdU) show that in adult specimens, the outer perimeter of the corona ciliata contains cells in s-phase of the cell cyle, indicating a high rate of mitotic activity (Fig. 11A). Like the ciliary fence and ciliary tuft organs, the corona ciliata also expresses aspartate. This labeling, however, is restricted to the inner cellular portion, namely the absorptive and/or sensory cells (Fig. 11B).

Fine structure

In contrast to the ciliary fence and ciliary tuft organs, the cilia of the corona ciliata are short and arranged in a loop, when viewed from a dorsal perspective. A surface view of *Parasagitta setosa* using SEM shows distinct differences in size and length between cilia produced by the ciliary fence and ciliary tuft receptor cells and related epithelial cells of the corona ciliata forming motile cilia (Fig. 5A, almost invisible in *Spadella valsalinae*: Fig. 12A). Our TEM studies reveal the existence of four different cell types constituting the corona ciliata in *Spadella* spp. (Fig. 12B). In a longitudinal perspective (transverse sections through the collarette region), two cellular portions become obvious. The outer cellular portion comprises several rows of elongated and thinned epithelial cells each forming a single motile cilium (1). The inner cellular portion contains two types of epithelial cells: absorptive cells extending two or several cilia (2) and sensory cells extending a single cilium (3). The entire corona ciliata is encompassed by elongated sheath cells (4) that are derivatives of the proximal epidermal cells.

The bottle-shaped absorptive cells and sensory cells are arranged in the form of a cup, the upper cells of which are oriented obliquely till horizontally (Fig. 12B). At their apex, these cells surround a rounded extracellular cavity which contains their microvilliform protrusions and ciliary processes (Fig. 12B-C). Besides the typical, highly ordered microtubular apparatus (axoneme) in all coronal cilia, dispersed microtubules can be found in the narrowed apical region of all contributing ciliary cell types (1-3), with highest density in the sensory cells (Fig. 12C-E). The nuclei of the sensory cells are always located distally to those of the absorptive cells (Fig. 12B). Proximally to the nuclear region, the somata of each sensory cell tapers into an axon that contains specialized microtubules and is wrapped by radial processes of a surrounding absorptive cell. The axons of neighboring sensory cells are grouped together (Fig. 12F) and leave the inner cell cluster and to course medially towards and come together in either of the two lateral branches of the coronal nerves (Fig. 12G). At the distal tip of the corona ciliata, the two lateral branches become more compact to form the definite coronal nerves that project to the posterior margin of the brain (Fig. 12H). Several synapses are present at the ventral margin of the coronal nerves adjoining the extracellular matrix (ECM) and innervating the dorsal longitudinal musculature (Fig. 12I). Our TEM data, however, are not significant enough to determine whether these synapses are terminations of either afferent (formed by sensory cells of the corona ciliata) or efferent fibres (formed by interneurons of the brain).

This TEM study revealed many characters which are new to science. A thorough description of the ultrastructural organization of the corona ciliata will be provided in an additional manuscript.

Discussion

Added value of multimethodological analyses in chaetognath research

In the present study, we examined the general and specific organization of multicellular ciliary sense organs in various pelagic and benthic Chaetognatha with a broad mix of microscopic methods. The correlative and comparative application of light microscopy, electron microscopy and fluorescence/confocal laser scanning microscopy with respect to multicellular ciliary sense organs is unparalleled in literature on chaetognath morphology. The benefits of a multimethodological approach in “modern” zoomorphology are clearly underlined by this study, especially concerning the often difficult correlation of immunohistochemistry, fluorescence microscopy and transmission electron microscopy (TEM). In our case, the complex cellular architecture of ciliary fence and ciliary tuft organs, as revealed by TEM (two types of ciliary sensory cells instead of a single one known so far), is also indicated by differential occurrence of aspartate in these organs. Furthermore, the presence and distribution of acetylated α-tubulin in the cells constituting the ciliary fence and ciliary tuft organs as well as the corona ciliata is convincingly shown by the immunoreactivity of the protein molecules and by the unique ultrastructure of tubulin filaments. In particular, intracellular distribution patterns of tubulin as revealed by immunohistochemistry provided an overview of the neurite branching patterns in the corona ciliata much more accurately, realisticly and effectively than it would have been possibly by 3D reconstructioning based on semi- or ultrathin section series. However, even the exclusive usage of immunohistochemistry against acetylated α-tubulin would certainly be a powerful, fast and reliable tool to locate, distinguish and map ciliary sense organs in Chaetognatha. This is nicely exemplified in ciliary fence and ciliary tuft organs.

Ultrastructure of ciliary fence and ciliary tuft organs

Previous authors discussed controversially whether the ciliary fence and ciliary tuft organs are true sense organs at all. Reisinger (1969) as well as Bone and Pulsford (1978) emphasized that the bent and tangled appearance of the cilia in SEM images is likely a fixation problem, since they are naturally straight and arranged in parallel in live animals. Shinn (1997) considered a sensory function of these organs to be likely and attributed the following potential functions to the ciliary fence and ciliary tuft organs: the (1) sensitivity to touch (Grassi in Bone and Pulsford 1978), the (2) sensitivity to non-vibrating sweeps (Feigenbaum and Reeve 1977), a (3) “fright response” to movements near the posterior end of the body (Feigenbaum and Maris 1984), (4) initiation and/or regulation of mating behaviour (Goto and Yoshida 1985), and (5) the sensitivity to detect water flow past the body during swimming and sinking (Sweatt and Forward 1985). Even though our new dataset can contribute little to understanding the function of these organs, our data provide additional evidence that they are truly sensory. We were able to visualize the massive connection between these organs and intraepidermal nerve plexus by applying an antiserum against acetylated α-tubulin (for aspartate immunoreactivity see discussion below). Moreover, we described the ultrastructure of two different types of sensory cells, whose somata taper proximally to form an axonal process. A third, perhaps less striking hint comes from the ultrastructure of the axoneme that contains microtubules with an electron-dense core. Microtubules with an electron-dense core, if present, have been frequently described from ciliated sensory cells in various invertebrates (e.g. Brachiopoda: Lüter 1996).

Proposition of an elaborated classification of sensory cells in ciliary fence and ciliary tuft organs: indications from immunohistochemistry and ultrastructure

The main benefit of this paper probably comes from the multimethodological approach which provided a high-detail resolution of the ciliary fence and ciliary tuft organs. Admittedly, immunohistochemical stainings of acytylated α-tubulin can only contribute in part to the question whether the typological separation between ciliary fence and ciliary tuft organs according to Malakhov et al. (2005), who based their analysis on the pelagic species *Parasagitta elegans* and *Serratosagitta pseudoserratodentata*, is supportable. Therefore, the ciliary fence and ciliary tuft receptor cells have to be examined and discussed on the ultrastructural level. It is in particular the extraordinarily good preservation of sensory tissues by Karnovsky's (1965) prefixative that now enables us to evaluate and confirm the classification of Malakhov and co-workers that was initially introduced for pelagic Sagittidae, also for representatives of the benthic Spadellidae (*Spadella* spp.). Besides obvious differences in the orientation of multiple ciliary rows relative to the body's longitudinal axis and the numbers and arrangement of constituting sensory and sheath cells, we discovered that on the ultrastructural level ciliary fence and ciliary tuft organs may be reliably distinguished by morphological features of the basal apparatus of their cilia. In sensory cells of ciliary tuft organs, the cross-striated rootlet, if present, is much longer, whereas the curious electron-dense body to which this rootlet is attached proximally appears chunky and jagged. The latter aspect is different from the schematic reconstruction of ciliary tuft organs provided by Malakhov et al. (2005) (compare Fig. 2B, p. 70). Our subdivision into type 1 and 2 sensory cells in ciliary fence and ciliary tuft organs in *Spadella* spp. is however new to science and chaetognath research. One indication for this distinction of cell types comes from the differential immunolocalization of aspartate the presence of which seems to be restricted to centrally located type 1 sensory cells in both ciliary fence and ciliary tuft organs. Aspartate-immunoreactive ciliary fence and ciliary tuft sensory cells have been already detected in *Sagitta friderici* by Duvert et al. (1997), who broadly reported an immunoreactivity in a "subpopulation" of cells. Since double-labelling with nuclear markers was not conducted by these authors, the exact location of this subpopulation within the cell cluster could not be determined. Often co-localized with the metabolically linked amino acid glutamate, aspartate is a putative excitatory neurotransmitter in the central nervous system of vertebrates (e.g., Nadler et al. 1976, Pettersson et al. 1996, Dingledine and McBain 1999). In the optic neuropils of various insects with achromatic photoreceptors, aspartate immunoreactivity was used to characterize various types of visual interneurons (Sinakevitch and Strausfeld 2004). Duvert et al. (1997) discovered strong immunoreactivity against aspartate in the central nervous system (brain, ventral nerve centre) and in the intraepidermal nerve plexus of *Sagitta friderici*, especially in the trunk and the tail regions. Based on electrophysiological recordings, these authors hypothesized that aspartate-immunoreactive neurons in chaetognaths, in contrast to those known from vertebrates, may act as an inhibitor of muscular contractions induced by acetylcholine. As further morphological key characters that help to distinguish type 1 from type 2 secretory cells in ciliary fence and ciliary tuft organs of Chaetognatha we propose ultrastructural features, such as (1) the different location of somata in the cluster, (2) the osmiophyly and composition of the cytoplasm, (3) the length of the axoneme, and most importantly (4) the construction of the basal region of the cilia, including in particular the presence and dimensions of the conspicuous electron-dense body and the cross-striated rootlet attached to it.

Phylogenetic significance of ciliary components

One may surely ask how legitimate it is to base a cell classification and phylogenetic considerations on ultrastructural characters, such for example basal parts of the ciliary apparatus. However, we agree with Tyler (1979) who resumed that "cilia, though small in size, are sufficiently complex to bear a number of resolvable characters – characters of tip shape, axonemal termination pattern, basal body and transition region structure, and of rootlet structure as well as a number of special characters specific to particular groups such as morphology of flagellar appendages" (p. 398). In the same paper, he also concluded that "ultrastructural characters are as valid as macroscopic ones for phylogeny and systematics" (p. 399). In an outstanding account, Todt and Tyler (2007) for instance distinguished five different types of ciliary receptors in various Acoela based on the ultrastructure of the basal apparatus of the cilia. In fact, the entire ciliary ultrastructure, and in particular a cross-striated ciliary rootlet, is considered a highly conserved character in ciliated cells of larval calcareous and homoscleromorph Porifera as well as of adult Placozoa and Bilateria (Rieger 2007, Nielsen 2012). The plesiomorphic condition in Eumetazoa most likely includes monociliated and primarily locomotory epithelial cells whose single cilium is associated with a corona of microvilli, a basal body, a bifurcated (horizontal + caudal component), cross-striated rootlet, and an accessory centriole (e.g., Ax 1995, Rieger 1976, 2007). Multiciliated cells with bifurcated or multiply ramified, often interconnected rootlets have been reported from various Acoelomorpha (e.g., Hendelberg and Hedlund 1974) and Gastrotricha (e.g., Rieger 1976) and are assumed to have derived from the monociliated state independently, but are valuable constitutive characters of their respective groups (read summaries by Rieger 2007, Schmidt-Rhaesa 2007). In contrast, the basal ciliary apparatus is thought to have been somewhat simplified in many demospongian Porifera or larval/adult Anthozoa (absent or single cross-striated ciliary rootlet, torsion or absence of the accessory centriole; see Fig. 123 in textbook contribution of Rieger 2007). Our TEM examinations reveal that the type 1 and 2 sensory cells in the ciliary fence and ciliary tuft organs of *S. cephaloptera* and *S. valsalinae* contain a single cilium which is surrounded by a corona of only few slender microvilli (see also Fig. IIb of Bone and Pulsford 1978) and anchored in the apical cytoplasm by a basal body, an electron-dense body and a radiating microfibrillar system. In addition, a sometimes extremely elongated, cross-striated ciliary rootlet is clearly indicated in type 1 sensory cells. This ciliary rootlet seems to correspond to the "main rootlet" described by many authors to extend deep into the cytoplasm of metazoan epithelial cells (e.g., Hendelberg and Hedlund 1974, Tyler 1979, Lundin 1997), equivalents of "lateral", "caudal" or "rostral rootlet" are hardly observed in spadellid Chaetognatha (Nagasawa and Marumo 1982, Welsch and Storch 1983, Shinn 1997, Malakhov et al. 2005, this study). A ciliary rootlet is thought to be an essential element of a ciliated cell, be it either locomotory or sensory. It is suggested to anchor the basal body within its cytoplasm/inner dendritic segment (e.g. Moran and Rawley 1975), to maintain the long-term stability of the cilium (Yang et al. 2005), to establish intracellular transport processes by direct interaction of the protein component rootletin and kinesin light chains (Yang and Li 2005), and/or participate in the sensory transduction or adaptation (Wolfrum 1991). Whereas the monociliary appearance of sensory cells and the collar-like arranged microvilli fit well into the assumed ground pattern of

Eumetazoa (only ciliary sense organs of *Zonosagitta nanae* appear to be biciliated: Nagasawa and Marumo 1982), the (almost complete) absence of a lateral cross-striated rootlet and an accessory centriole more resembles the secondarily simplified cilia of some Porifera and Anthozoa. Besides ciliary fence and ciliary tuft organs of sagittid and spadellid Chaetognatha (Bone and Pulsford 1978, Shinn 1997, Malakhov et al. 2005, this study), monociliated cells with a single (primarily unbranched), mostly slender, extremely elongated and cross-striated ciliary rootlet have been reported from anthoathecate Hydrozoa ("rootlet cells": Holtmann and Thurm 2001), some Acoela (Crezée and Tyler 1976, Popova and Mamkaev 1987, Todt and Tyler 2007), proseriate and neorhabdocoel turbellarians (Ehlers and Ehlers 1977, Rohde and Watson 1993 1995), the enigmatic *Xenoturbella westbladi* (see Raikowa et al. 2000), and arthropod scolopidia (see Wolfrum 1991 for summary). The often elongated and cylindrical electron-dense body below the basal body of the chaetognath cilia investigated in this study, however, seems to be unparalleled among metazoans, along with the system of radiating filaments making that make contact to a hemidesmosome-like structure strengthening the apical membrane around the ciliary basis. Of course, there are many examples for heavily derived basal complexes associated with sensory cilia described in various invertebrate groups, in which they perform a large variety of different functions. As striated rootlets with all kinds of structural variations seem to be associated with the base of sensory cilia as well as of motile cilia (see discussion in Wolfrum 1991), it is difficult for us to tell from functional ultrastructure how the different basal ciliary structures in type 1 and 2 sensory cells may influence or cause different mechanisms of stimuli transmission. However, one may speculate that these radiating filaments, especially if present in condensed formation, may functionally compensate the lack of lateral elements in the rootlet system and/or initiate stimulus transmission. Either way, likely unique ultrastructures like (1) the elongated electron-dense body underneath the basal body associated with (2) an apparatus of radiating filaments may be added to the long list of apomorphies of the Chaetognatha. The continuously growing list of chaetognath apomorphies appears less and less surprising considering that this animal group has most probably passed through a long time of independent evolution as an early offshoot of the Bilateria (reviewed by Harzsch and Wanninger 2010).

Ciliary fence and ciliary tuft organ patterns as systematic character

Ciliary fence and ciliary tuft receptors are distributed widely over the chaetognath body. So far, this distribution had been studied primarily with light microscopy using phase contrast and differential interference (Feigenbaum 1978) and our data confirm the distribution patterns described by these authors for *Spadella cephaloptera*. Their work was based on the observation of live, immobilized animals and the translucent nature of most chaetognaths means that an accurate survey of all fence receptors is difficult and requires much time and great care. However, due to the dense packing of somata of the ciliary fence and ciliary tuft receptor cells, simply staining their nuclei provides a good, quick and reliable overview of the number and distribution of fence receptors, as we demonstrated in our study. Combined with the immunohistochemistry against acetylated α-tubulin, the position of the sensory cilia is also revealed. This allows a reliable mapping and detailed description of fence receptor organs in Chaetognatha. Histochemistry works well on fixed specimens and even allows discerning fence receptors, whose cilia were damaged or lost during the processing, as long as the epidermis itself is not damaged. When considering *S. cephaloptera*, the pattern we found was very consistent with all previous accounts. The only variance in number of ciliary fence and ciliary fence organs occurred on the tail fin, as was already noted by Feigenbaum (1978). This author considered the distribution of fence receptors as a "poor systematic character" (p. 536) and argued that only 4 out of today's known 150 chaetognath species were named after morphological or distributional characters of their ciliary fence and ciliary tuft organs. However, with immunohistochemistry, we now have a fast, reliable and simple way to gain accurate information on the distribution of the ciliary fence and ciliary tuft organs, which might justify to re-evaluate their value for a systematic discussion. Indeed, it would be an interesting task to map the exact distribution of the ciliary fence and ciliary tuft organs/receptors along the chaetognath body, which could be provided using serial TEM.

Functional disparity of type 1 and 2 sensory cells

This technique could also be helpful in the debate about whether the type 1 and 2 sensory cells in these organs belong to either primary (with an axon) or secondary (without an axon) receptors. Reisinger (1969), Welsch and Storch (1983), and Shinn (1997) proposed that the fence receptors are secondary sensory cells whereas our TEM observations rather suggest that they are all primary sensory cells. Results from immunohistochemistry remain ambiguous: we were able to confirm a direct connection between both ciliary fence and ciliary tuft receptors and the centralized part of the nervous system. What is more, our previous immunolocalization experiments against synapsins (presynaptic proteins) in *Parasagitta setosa* (see Harzsch and Müller 2007) and *S. cephaloptera* (head region: see Rieger et al. 2010; trunk region: Thiele and Müller, unpubl. data) did not result in any notable signal around the ciliary fence and ciliary tuft organs. However, we are aware of the fact that we might have overlooked some synapses at the bottom of type 1 and/or type 2 sensory cells during our TEM studies. Also, the absence of a noticeable synapsin immunoreactivity does not necessarily imply the absence of synapses in the region in question, as their abundance may be too low to be detected with immunohistochemical techniques. What is more, aspartate immunoreativity only labeled the somata of the sensory cell and not any axonal extensions which might be expected if aspartate were the primary (and only) transmitter of these cells. Yet, aspartate may not act as a transmitter at all in these sensory cells but fulfill another physiological role restricted to the soma. Therefore, we have to remain cautious until the aforementioned serial TEM examination will have been carried out.

Studies on the architecture of the corona ciliata in various Chaetognatha

Even though Hertwig (1880) already recognized two different horizontal layers of nuclei in the corona ciliata (see his plate IV, Fig.1), it took another 50 years until Reisinger (1934) first noticed two types of differently shaped cells in this organ, arranged in an inner and outer ring (species: *S. cephaloptera*). Ghirardelli (1958) re-examined the corona ciliata of *S. cephaloptera* and confirmed Reisinger's results by distinguishing an outer corona containing sensory cells ("corona esterna", "cellule nervose e presentano caratteristiche morfologiche …… a quelle delle eminenze sensitive della epidermide") from an inner corona with secretory function ("corona interna ghiandolare") which he identified in histological sections by means of their large secretory granules (p. 89). One year later, Ghirardelli (1959) expanded his studies to several pelagic species, such as *Flaccisagitta enflata*, *Sagitta bipunctata* and *Pterosagitta draco*, and noted that the latter two species are devoid of secretory cells in the corona interna. However, Shinn (1997) opposed this view based on new TEM data. He described two different functional types of cells within the corona ciliata of *Adhesisagitta hispida*: (1) ciliated, putative sensory cells each producing one vibratile cilium which protrudes above the body surface and (2) glandular (in part ciliated) cells releasing their secretion into a subsurface cavity. Unfortunately, Shinn's (1997) description is based on a schematic drawing (Fig. 53) which nevertheless allows to assign the glandular cells to a medial and inner population of coronal epithelial cells, whereas the motile ciliated cells belong to the outer population of coronal epithelial cells. The position of the neurite bundle in his drawing suggests that the neurites therein are associated with the outer ciliated cells. However, Shinn (1997) was uncertain whether these neurites have an afferent or efferent nature. In contrast, Malakhov and Frid (1984) mentioned only one type of cells constituting the corona ciliata in *Sagitta glacialis*, the "flagellar cells" which form bladder-like outgrowths around the "intraepithelial canal" and form flagella that protrude outside the body surface. These authors therefore did not distinguish an outer from an inner population of coronal cells. However, we assume that their cell classification and localization was misled anyway, since they attributed the motile ciliated ("flagellar") cells to the inner population of cells in *S. cephaloptera*. Malakhov et al.'s contribution from 2005 has corrected this wrong localization by subdividing the corona ciliata of *Parasagitta elegans* into "an internal canal with inflated electron-lucent microvilli, and an external part carrying cilia" (p. 67). In their Fig. 6, Malakhov et al. (2005) showed that all coronal epithelial cells carry a cilium, but neither in the English abstract of this contribution in Russian nor in the included schematic drawing did we find an indication for specialized secretory cells. Concerning the corona ciliata of *S. cephaloptera*, TEM observations of Ahnelt (1980) and Giulianini et al. (1999) revealed the existence of secretory granules in a dual-type epithelium of monociliated cells ("innere und äußere Corona-Zellen", "flask shaped ciliated cells with collars" and "a vacuolar secretory area"). Giulianini et al. (1999) moreover confirmed previous observations by Shinn (1997) for *A. hispida* in that these authors found "a lateral electron-dense, putatively proliferative area" as well as "an apoptotic, degenerative area" in *S. cephaloptera*, as well. Our own TEM data now reveal that the architecture of the corona ciliata of *S. cephaloptera* and *S. valsalinae* is considerably more complex than had been reconstructed by previous authors. The finding of bi- or multiciliated, presumably absorptive cells and monociliated primary sensory cells within the inner population of coronal epithelial cells suggest a functional mechanism to be active in the corona ciliata that is much different from those assumed so far.

Functional morphology of the corona ciliata: new insights from Immunohistochemistry and TEM

The various suggested functions of the corona ciliata include chemo- and mechanoreception, the secretion of a substance that governs sperm movement and a nephridium-like function (reviewed by Ghirardelli 1968). A role as a tactile receptor was discussed and dismissed by Horridge and Boulton (1967). Immunohistochemistry and TEM data demonstrate that the corona ciliata has a direct neuronal connection to the posterior sensory part of the brain so that we can provide new insight into the extent and the pattern of this neuronal link. Anti-tyrosinated tubulin immunoreactivity suggests that individual sensory (ciliated) cells of the corona ciliata extend single axons that join into larger bundles which target the brain. Whether or not the corona ciliata really contains sensory cells has long been a matter of dispute (Bone and Pulsford 1984, Malakhov and Frid 1984). Our finding that the actual sensory cells represent "only" a smaller portion in the inner population of coronal epithelial cells conflicts with previous authors, as for instance Malakhov and Frid (1984) and Shinn (1997), who reported the presence of neurites basal to the medial part of the corona and thus allocated them to the outer population of vibratile, monociliated cells. Like Shinn (1997) we did not find evidence for any synapses within the periphery of either side of the corona ciliata. There are clearly visible basal cytoplasmic extensions of the putative sensory cells that contain many microtubules and tend to become bundled when they leave the inner population of coronal epithelial cells. Therefore, we have to interpret them as primary axons that project into one of the two coronal nerves and not vice versa. Of course, immunohistochemistry or transmission electron microscopy cannot differentiate beyond doubt whether the coronal nerves contain afferent or efferent fibres. Nevertheless, the clear separation of the innervation of the left and right halves of the corona ciliata may indicate a directional sensitivity. If the only role of the corona were secretory or excretory, as predicted by some previous authors, we might expect a less elaborate neuronal investment, since maintaining nervous and sensory tissues is very costly from a metabolic point of view (e.g., Laughlin et al. 1998, Niven and Laughlin 2008, Niven and Farris 2012). It is unlikely that such a differentiated control would be essential for a secretory or excretory function alone. In addition, our TEM data show that the paired dorsal longitudinal musculature of *S. cephaloptera* and *S. valsalinae* is innervated and controlled by most ventral axons that contact the extracellular matrix (ECM) by conspicuous synaptic swellings. Therefore, efferent neurites must exist in the coronal nerves, too. Yet, it still is problematic to decide whether these neurites extend from neurons in the sensory, posterior compartment of the brain or from coronal sensory cells. Immunohistochemical methods cannot clarify this particular point but electrophysiological experiments and single cell injections of tracers may be necessary. For sure, the detection of the neurotransmitter aspartate in the inner cellular population and in the centre of the corona ciliata of *S. cephaloptera* makes the presence of synapses in the direct vicinity of this organ more likely. As outlined in the previous chapter, aspartate-immunoreactive neurons are commonly found in the intra- and basiepidermal plexus of chaetognaths (Bone and Goto 1991, Duvert et al. 1992). Based on physiological experiments and immunohistochemical labeling against L-aspartate in the nervous system of *Sagitta friderici*, Duvert et al. (1997) concluded that this neurotransmitter most likely has a pivotal role in motor and sensory functions in chaetognaths acting as an inhibitory modulator of acetylcholine-induced muscle contractions.

Taken together, these morphological data suggest that the corona ciliata in addition to its presumed secretory function also acts as a highly sophisticated sensory organ and a potential modulator of muscular activity in the trunk. As mentioned before, one suggested function of the corona ciliata is that of an olfactory organ. Previous analyses of the corona ciliata by Shinn (1997) already indicated a high level of mitotic activity suggesting a massive turnover. This author observed single dividing cells in the periphery of the corona ciliata, and also degenerating ones between the ciliary sensory cells and the glandular cells. Even though mitosis figures could only been rarely observed in histological (LM) and ultrathin (TEM) sections, our approach using the s-phase-specific marker BrdU indeed confirms the presence of a substantial number of mitotic cells suggesting a constant production of new sensory cells. This is a trait known from olfactory systems in many metazoan taxa, from crustaceans to mammals (Harrison et al. 2001; Malnic and Armelin-Correa 2010). However, there is not yet any compelling evidence that chaetognaths react to chemical stimuli. Hunting behavior seems to be primarily dependent on mechanosensory cues (Horridge and Boulton 1967, Feigenbaum and Reeve 1977, Feigenbaum and Maris 1984, Bone and Goto 1991, Shinn 1997). We may speculate that finding a mating partner might depend on pheromones, but pheromones in chaetognaths have not been found yet. Also, the corona ciliata is not the only organ speculated to be involved in mating behavior, during which the animals touch their heads (Goto and Yoshida 1985). Thuesen et al. (1988) associated the same possible functions to the transvestibular pores of the head of chaetognaths.

The motility of the cilia of the outer cell population as reported by some authors (e.g., Reisinger 1934, Ghirardelli 1968, Malakhov and Frid 1984, Shinn 1997) is also of little help in determining the exact function of the corona ciliata. Motile cilia can serve a mechanosensory as well as a chemosensory purpose in other species and sometimes they are equipped for both functions (Bloodgood 2010). Neither function has yet been backed up by any definitive experimental evidence in Chaetognatha. The present knowledge of the corona ciliata is still not deep enough to determine its function, although as discussed above accumulating evidence suggests that the corona serves a sensory purpose. The persistent adult cell proliferation, in analogy to other metazoan chemosensory systems, may points to an olfactory function, whereas a mechanosensory function seems redundant in the light of the extensive system of ciliary fence and ciliary tuft receptors. Our TEM observations, however, let us doubt that the monociliated cells of the outer cellular portion are indeed involved in the sensory process, as will be outlined in the following. There are no indications that the three cell types constituting the corona ciliata of *S. cephaloptera* discharge their secretions mainly into the subsurface cavity or outside the body. We never observed the more or less extended cilia of the sensory cells to reach the surface of the body. One explanation is that the vibratile cells of the outer portion create a directed water current which flushes the subsurface cavity *via* the network of minute extracellular canals ranging from the extended apices of the motile ciliated cells to the subsurface cavity. At this point it is important to point out that this subsurface cavity is surrounded not only by the apices of the monociliated sensory cells but also the apices of the bi- or multiciliated absorptive cells. Our functional interpretation is so far based on the peculiar zonation in the cytoplasm of these absorptive cells. They display a strongly diversified apex with numerous microvilli, endosomes, cytoplasmic tubules, and Golgi stacks as well as several huge, heterogenous lysosomes located at the bottom of the cell. This cytoplasmic pattern is strikingly similar to that described from intestinal cells in *Parasagitta setosa* and *S. cephaloptera* (compare Perez et al. 1999, 2000) so that we speculate that the absorptive cells take up cavity liquids. This uptake may modify the chemical environment of the subsurface cavity and thereby influence and potentially improve the sensitivity of the sensory cilia extending through the cavity. This mechanism, as deduced from ultrastructure, seems to fit the requirements of a chemoreceptor organ. This scenario is currently tested by experiments with ferritin particles in which we incubate live specimens of *S. cephaloptera*. The putative uptake of ferritin particles from the cavity water will be visualized using TEM techniques and will hopefully provide the definite evidence for our functional predictions. However, we are aware of the necessity to flank morphological studies with behavioral observations or electrophysiological recordings that may link the corona ciliata to a certain stimulus. Without progress on these fields the topic will likely not be settled.

Acknowledgement:

We would like to thank the team of the „Gastforschung“ at the Biologische Anstalt Helgoland for assistance in collecting *Parasagitta setosa* and Prof. Dr. B. S. Hansson from the Max-Planck-Institute for Chemical Ecology in Jena for providing laboratory facilities during the initial stages of this study. We are indebted to Prof. George Shinn for providing resin-embedded specimens of *Ferosagitta hispida* for the semithin sections. Our electron microscopic studies were supported by Prof. Gabriele Uhl from University of Greifswald, PD Dr. Markus Franck and his technician team from the Electron Microscopic Centre of the University of Rostock, Renate Walter and Helga Kapp of the Biocentre Grindel and Zoological Museum of Hamburg University as well as by Gabriele Ladwig working at the Electron Microscopic Unit of the University Hospital Essen. Dipl. Biol. Charlotte Winkelmann helped sampling specimens of *Spadella valsalinae* in Southern Istria and kindly provided a SEM image of its corona ciliata. Dipl. Biol. Franziska Glück (Institute of Baltic Sea Research, Warnemünde) kindly provided a SEM image of *Sagitta bipunctata*, whose capture was made possible by the organizers and scientists of the DIVA-3 survey; special thanks go to PD Dr. Andreas Bick from University of Rostock who sorted out chaetognath material from plankton samples during that survey. This study was supported by grant HA 2540/7-1/2/3 in the DFG focus program SPP 1174 „Metazoan Deep Phylogeny“.

Literature:

Ahnelt PK (1980) Das Coelom der Chaetognathen. Dissertation, University of Vienna, 209 p. + 180 figs.

Ahnelt PK (1984) Chaetognatha (Chapter 40). In: Bereiter-Hahn J, Matoltsy AG, Richards KS (eds) Biology of the integument. 1. Invertebrates. Springer, Berlin Heidelberg, pp 746-755.

Arnaud J, Brunet M, Mazza J (1978) Studies on the midgut of *Centropages typicus* (Copepod, Calanoida). I. Structural and ultrastructural data. Cell Tissue Research 187:333-353.

Ax P (1995) Das System der Metazoa I. Ein Lehrbuch der phylogenetischen Systematik. Gustav Fischer Verlag, Stuttgart, Jena, 226 p.

Bloodgood RA (2010) Sensory reception is an attribute of both primary cilia and motile cilia. Journal of Cell Science 123:505-509.

Bone Q, Pulsford A (1978) The arrangement of ciliated sensory cells in *Spadella* (Chaetognatha). Journal of Marine Biological Association UK 58:565-570.

Bone Q, Pulsford A (1984) The sense organs and ventral ganglion of *Sagitta* (Chaetognatha). Acta Zoologica (Stockholm) 65:209-220.

Bone Q, Goto T (1991) The nervous system. In: Bone Q, Kapp H, Pierrot-Bults AC (ed) The biology of chaetognaths. Oxford University Press, New York, pp 18-31.

Casanova JP (1991) Chaetognaths from the Alvin dives on the seamount Volcano 7 (east tropical Pacific). Journal of Plankton Research 13:539-548.

Conant FS (1895) Description of two new chaetognaths (*Spadella schizoptera* and *Sagitta hispida*). The Annals and Magazine of Natural History (6th series) 16:288-292.

Crezée M, Tyler S (1976) *Hesiolicium* gen.n. (Turbellaria Acoela) and observations on its ultrastructure. Zoologica Scripta 5:207-216.

Dingledine R, McBain CJ (1999) Glutamate and aspartate. In: Siegel GJ (ed in chief) Basic neurochemistry. Molecular, cellular and medical aspects. Lippincott-Raven, Philadelphia, pp. 317-333.

Duvert M, Tramu G, Salat C (1992) Recherches immunohistochimiques sur la présence de neuro-modulateurs chez l'invertébré *Sagitta* (Chaetognathes). Société des Neurosciences Abstr. 27:185.

Duvert M, Savineau J-P, Campistron G, Onteniente B (1997) Distribution and role of aspartate in the nervous system of the chaetognath *Sagitta*. The Journal of Comparative Neurology 380:485-494.

Ehlers U, Ehlers B (1977) Monociliary receptors in interstitial Proseriata and Neorhabdocoela (Turbellaria Neoophora). Zoomorphology 86:197-222.

Feigenbaum DL, Maris RC (1984) Feeding in the Chaetognatha. Oceanography and Marine Biology Annual Reviews 22:343-392.

Feigenbaum D, Reeve MR (1977) Prey detection in the Chaetognatha: Response to a vibrating probe and experimental determination of attack distance in large aquaria. Limnology and Oceanography 22:1052–1058.

Feigenbaum DL (1978) Hair-fan patterns in the Chaetognatha. Canadian Journal of Zoology 56:536-546.

Ghirardelli E (1958) Osservazioni preliminari sulla corona ciliata in *Spadella cephaloptera* Busch (Chaetognatha). Dai "Rendiconti dell'Accademia Nazionale dei Lincei" (Serie VIII) 25:87-91.

Ghirardelli E (1959) Osservazioni sulla corona ciliata nei Chetognati. Bollettino di Zoologia 26:413-421.

Ghirardelli E (1968) Some aspects of the biology of the chaetognaths. Advances in Marine Biology 6:271-375.

Giulianini PG, Ghirardelli E, Ferrero EA (1999) Ultrastruttura comparativa della corona ciliate in *Spadella cephaloptera* e *Sagitta setosa* (Chaetognatha). Biologia Marina Mediterranea 6:666–669.

Goto T, Yoshida M (1981) Oriented light reactions of the arrow worm *Sagitta crassa* Tokioka. Biological Bulletin 160:419-430.

Goto T, Yoshida M (1983) The role of the eye and CNS components in phototaxis of the arrow worm, *Sagitta crassa* Tokioka. Biological Bulletin 164:82-92.

Goto T, Yoshida M (1985) The mating sequence of the benthic arrowworm *Spadella schizoptera*. Biological Bulletin 169:328-333.

Goto T, Yoshida M (1987). Nervous system in Chaetognatha. In: Ali MA (ed) Nervous systems in invertebrates. Plenum Publishing Corporation, New York, pp 461-481.

Grassi B (1883) I chetognathi. Anatomia e sistematica con aggiunte embriologiche (Die Chaetognathen). Fauna und Flora des Golfes von Neapel, 5: 1-126.

Harrison PJH, Cate HS, Swanson ES, Derby CD (2001) Postembryonic proliferation in the spiny lobster antennular epithelium: rate of genesis of olfactory receptor neurons is dependent on molt stage. Journal of Neurobiology 47:51-66.

Harzsch S, Dawirs RR (1994) Neurogenesis in larval stages of the spider crab *Hyas araneus* (Decapoda, Brachyura): proliferation of neuroblasts in the ventral nerve cord. Roux's Archives of Developmental Biology 204: 93-100.

Harzsch S, Müller CHG (2007) A new look at the ventral nerve centre of *Sagitta*: implications for the phylogenetic position of Chaetognatha (arrow worms) and the evolution of the bilaterian nervous system. Frontiers in Zoology 4:14.

Harzsch S, Wanninger A (2010). Evolution of invertebrate nervous systems: the Chaetognatha as a case study. Acta Zoologica (Stockholm) 91:35-43.

Harzsch S, Rieger V, Müller CHG, Perez Y, Sintoni S, Sardet C, Hansson B (2009) Fine structure of the ventral nerve centre and interspecific identification of individual neurons in the enigmatic Chaetognatha. Zoomorphology 128: 53-73.

Hendelberg J, Hedlund JO (1974) On the morphology of the epidermal ciliary rootlet system of the acoelous turbellarian *Childia groenlandica*. Zoon 2:13-24.

Hertwig O (1880) Die Chaetognathen Ihre Anatomie, Systematik und Entwicklungsgeschichte. In Hertwig O, Hertwig R (eds) Studien zur Blättertheorie, vol 2. Gustav Fischer Verlag, Jena.

Heynol A, Martindale M (2009) Coordinated spatial and temporal expression of *Hox* genes during embryogenesis in the acoel *Convolutriloba longifissura*. BMC Biology 7:65.

Holtmann M, Thurm U (2001) Variations of concentric hair cells in a cnidarian sensory epithelium (*Coryne tubulosa*). The Journal of Comparative Neurology 432:550-563.

Horridge GA, Boulton PS (1967) Prey detection by Chaetognatha via a vibration sense. Proceedings of the Royal Society (London) B 168: 413-419.

John CC (1933) Habits, Structure, and Development of *Spadella cephaloptera*. Quarterly Journal of Microscopic Science 75:625-696.

Karnovsky MJ (1965) A formaldehyde-glutaraldehyde fixative of high osmolality for use in electron microscopy. Journal of Cell Biology 27:137-138.

Kreis TE (1987) Microtubules containing detyrosinated tubulin are less dynamic. EMBO J 6: 2597-2606.

Laughlin SB, de Ruyter van Steveninck RR, Anderson JC (1998) The metabolic cost of neural information. Nature Neuroscience 1:36-41.

Lundin K (1997) Comparative ultrastructure of the epidermal ciliary rootlets and associated structures in species of the Nemertodermatida and Acoela (Plathelminthes). Zoomorphology 117:81-92.

Lüter C (1996) The median tentacle of the larva of *Lingula anatina* (Brachiopoda) from Queensland, Australia. Australian Journal of Zoology 44:355-366.

Malakhov VV, Frid MG (1984) Structure of the ciliary loop and retrocerebral organ in *Sagitta glacialis* (Chaetognatha). Dokl Akad Nauk SSSR (Marine Biology) 277:763-765.

Malakhov VV, Berezinskaya TL, Solovyev KA (2005) Fine structure of sensory organs in the chaetognaths. 1. Ciliary fence receptors, ciliary tuft receptors and ciliary loop. Invertebrate Zoology 2:67-77.

Malnic B, Armelin-Correa L (2010) Neurogenesis in the olfactory epithelium. In Ulrich H (ed) Perspectives of stem cells. Springer, Dordrecht, Heidelberg, London, New York, pp. 35-45.

Moran DT, Rawley JC (1975). The fine structure of the cockroach subgenual organ. Tissue and Cell 7:91-106.

Nadler JV, Vaca KW, White WF, Lynch GS, Cotman CW (1976) Aspartate and glutamate as possible transmitters of excitatory hippocampal afferents. Nature 260:538-540.

Nagasawa S, Marumo R (1982) Ultrastructure of ciliary sense organs of a pelagic chaetognath Sagitta nagae Alvarifio. La Mer 20:141-150.

Nielsen C (2012) Animal evolution. Interrelationships of the living phyla (3rd edition). Oxford University Press, New York, 402 p.

Niven JE, Farris SM (2012) Miniaturization of nervous systems and neurons. Current Biology 22:R323-R329.

Niven JE, Laughlin SB (2008) Energy limitation as a selective pressure on the evolution of sensory systems. The Journal of Experimental Biology 211:1792-1804.

Newbury TK (1972) Vibration perception by chaetognaths. Nature 236:459-460.

Perez Y, Casanova J-P, Mazza J (2000) Changes in the structure and ultrastructure of the intestine of *Spadella cephaloptera* (Chaetognatha) during feeding and starvation experiments. Journal of Experimental Marine Biology and Ecology 253:1-15.

Perez Y, Arnaud J, Brunet M, Casanova J-P, Mazza J (1999) Morphological study of the gut in *Sagitta setosa*, *S. serratodentata* and *S. pacifica* (Chaetognatha). Functional implications in digestive processes. Journal of the Marine Biological Association of the United Kingdom 79:1079-1109.

Pettersson E, Herrera-Marschitz M, Rodriguez-Puertas R, Xu Z-Q, You Z-B, Hughes J, Elde RP, Ungerstedt U, Hökfelt T (1996) Evidence for aspartate-immunoreactive neurons in the neostriatum of the rat: modulation by the mesencephalic dopamine pathway via D_1-subtype of receptor. Neuroscience 74:51-66.

Popova NV, Mamkaev YV (1987) On types of sensillae in the acoel turbellarians. USSR Academy of Sciences (Proceedings of the Zoological Institute, Leningrad) 167:85-89.

Raikowa OI, Reuter M, Jondelius U, Gustafsson MKS (2000) An immuncytochemical and ultrastructural study of the nervous and muscular systems of *Xenoturbella westbladi* (Bilateria inc. sed.). Zoomorphology 120:107-118.

Reisinger E (1934) Zur Exkretionsphysiologie von *Spadella*. Thalassia 1:3-16.

Reisinger E (1969) Ultrastrukturforschung und Evolution. Bericht der physikalisch-medizinischen Gesellschaft zu Würzburg NF 77:4-47.

Reynolds ES (1963) The use of lead citrate at high pH as an electron-opaque stain in electron microscopy. Journal of Cell Biology 17:208-212.

Richter S, Loesel R, Purschke G, Schmidt-Rhaesa A, Scholtz G, Stach T, Vogt L, Wanninger A, Brenneis G, Döring C, Faller S, Fritsch M, Grobe P, Heuer CM, Kaul S, Møller OS, Müller CHG, Rieger V, Rothe BH, Stegner MEJ, Harzsch S (2010) Invertebrate neurophylogeny: suggested terms and definitions for a neuroanatomical glossary. Frontiers in Zoology 7:29.

Rieger R (1976) Monociliated epidermal cells in Gastrotricha: significance of concepts of early metazoan evolution. Journal of Zoological Systematics and Evolutionary Research 14:198-226.

Rieger R (2007). Metazoa. In: Westheide W, Rieger R (eds), Spezielle Zoologie. Teil 1: Einzeller und Wirbellose Tiere (2nd edition). Spektrum Akademischer Verlag, Heidelberg, pp. 69-90.

Rieger V, Perez Y, Müller CHG, Lipke E, Sombke A, Hansson BS, Harzsch S (2010) Immunohistochemical analysis and 3D reconstruction of the cephalic nervous system in

Chaetognatha: insights into the evolution of an early bilaterian brain? Invertebrate Biology 129:77-104.

Rieger V, Perez Y, Müller CHG, Lacalli T, Hansson BS, Harzsch, S (2011) Development of the nervous system in hatchlings of *Spadella cephaloptera* (Chaetognatha), and implications for nervous system evolution in Bilateria. Development, Growth and Differentiation 53:740-759.

Rohde K, Watson NA (1993) Ultrastructure of sensory receptors of an undescribed species of Luridae (Plathelminthes: Rhabdocoela). Australian Journal of Zoology 41:53-65.

Rohde K, Watson NA (1995) Sensory receptors and epidermal structures of a meiofaunal turbellarian (Proseriata: Monocelididae). Australian Journal of Zoology 43:69-81.

Schmidt-Rhaesa A (2007) The evolution of organ systems. Oxford University Press, New York, 385 p.

Semmler H, Chiodin M, Bailly X, Martinez P, Wanninger A (2010) Steps towards a centralized nervous system in basal bilaterians: Insights from neurogenesis of the acoel *Symsagittifera roscoffensis*. Development, Growth and Differentiation 52:701-713.

Shinn GL (1997) Chapter 3: Chaetognatha. In: Harrison FW, Ruppert EE (eds) Microscopic Anatomy of Invertebrates. Hemichordata, Chaetognatha, and the Invertebrate Chordates, vol 15. Wiley-Liss, New York, pp 103-220.

Sinakevitch I, Strausfeld NJ (2004). Chemical neuroanatomy of the fly’s movement detection pathway. The Journal of Comparative Neurology 468:6-23.

Sweatt AJ, Forward RB (1985). Diel vertical migration and photoresponses of the chaetognath *Sagitta hispida* Cihabt. Biological Bulletin 168:18-31.

Thuesen EV, Nagasawa S, Bieri R, Nemoto T (1988) Transvestibular pores of chaetognaths with comments on the function and nomenclature of the vestibular anatomy. Bulletin of Plankton Society of Japan 35:133-141.

Todt C, Tyler S (2007) Ciliary receptors associated with the mouth and pharynx of Acoela (Acoelomorpha): a comparative ultrastructural study. Acta Zoologica (Stockholm) 88:41-58.

Tyler S (1979) Distinctive features of cilia in metazoans and their significance for systematics. Tissue & Cell 11:385-400.

Welsch U, Storch V (1983) Fine structural and enzyme histochemical observations on the epidermis and the sensory cells of *Sagitta elegans* (Chaetognatha). Zoologischer Anzeiger 210:34-43.

Winkelmann C, Gasmi S, Gretschel G, Müller CHG, Perez Y (in press) Description of *Spadella valsalinae* sp. nov., a neo-endemic benthic chaetognath from Northern Adriatic Sea (Croatia) with remarks on its morphology, phylogeny and biogeography. Organisms Diversity & Evolution (DOI 10.1007/s13127-012-0108-0).

Wolfrum U (1991) Centrin- and α-actinin-like immunoreactivity in the ciliary rootlets of insect sensilla. Cell and Tissue Research 266:231-238.

Yang J, Li T (2005) The ciliary rootlet interacts with kinesin light chains and may provide a scaffold for kinesin-1 vesicular cargos. Experimental Cell Research 309:379-389.

Yang J, Gao J, Adamian M, Wen X-H, Pawlyk B, Zhang L, Sanderson MJ, Zuo J, Makino CL, Li T (2005) The ciliary rootlet maintains long-term stability of sensory cilia. Molecular and Cellular Biology 25:4129-4137.

Figure legends:

Figure 1: Adult *Spadella cephaloptera* portrayed with different techniques, dorsal view. (A) Live specimen viewed through a stereo microscope (from Rieger et al. 2010); (B) Specimen photographed using SEM (from Bone and Pulsford 1978); (C) Schematic drawing showing the distribution of the three types of ciliary sense organs (modified from Feigenbaum 1978), various rows of cilia are indicated with color: dorsomedian line (red); dorsolateral line (green); lateral line (blue); receptors on the lateral fin (purple); anteriolateral receptors on the tail fin (yellow); posterior receptors on the tail fin (orange). (D) Specimen labeled with immunohistochemistry against acetylated tubulin (red) counterstained with a nuclear dye (YOYO-1, green). Abbreviations: cc, corona ciliata; cfo, ciliary fence organ; cto, ciliary tuft organ; ey, eye; h, head; ta, tail; tr, trunk. Scalebars: (A,B,D) 200 µm.

Figure 2: Toluidine-blue-stained transverse semithin sections of the head of *Ferosagitta hispida* showing the general anatomy of ciliary sense organs: (A-B,D) ciliary tuft organs; (C,E) ciliary fence organs. (A) Overview of the histological anatomy of the head; (B,D) Excerpts from the transverse section series through a ciliary tuft organ, proceeding from the median (B) and posterior (D) part of the receptor; (C,E) Excerpts from the section series of a lateromedially oriented ciliary fence organ cut longitudinally exhibiting the median (C) and lateral (E) part of the receptor. Abbreviations: c, stiff cilia produced by sensory cells; cc, corona ciliata; cn, coronal nerve; cto, ciliary tuft organ; cu, cuticle; dlm, paired dorsomedian longitudinal musculature; ey, eye; ecm, extracellular matrix; ep, epidermis; edp, epidermal depression; gs, grasping spine; ho, hood (praeputium); mc, main connective; m, musculature (of the head); mo, mouth opening; n, nuclei of sensory cells; oe, oesophagus; sc, sensory cells; shc, sheath cells. Scalebars: (E) 10 µm; (A) 50 µm.

Figure 3: Ciliary sense organs of *Spadella cephaloptera* labeled with antibodies against acetylated tubulin (red) and a nuclei dye (green). The exact types of ciliary sense organs could be revealed only occasionally by immunhistochemistry and only in case of an unambiguous orientation of the cell cluster relative to the body's longitudinal axis by immunhistochemistry. (A) Top view of two ciliary sense organs. (B-D) Lateral view of several ciliary sense organs. That one shown in B stands perpendicular to the main connectives and, therefore, has to be interpreted as a ciliary fence organ. (D) is a single image of the cLSM Z-stack that was used for creating the composite image given in (C). Abbreviations: c, stiff cilia produced by sensory cells; cmic, condensed microtubules; ep, epidermis; iepl, profiles of the intraepidermal nerve plexus; mc, main connective; n(epc), nucleus of an epidermal cell; n(sc), nucleus of a sensory cells; ncfo, afferent nerve of a ciliary sense organ. Scalebars: (A) 50 µm; (B) 20 µm; (C,D) 10 µm.

Figure 4: In part unspecifiable ciliary sense organs located on the tail fin of (A-B) *Spadella cephaloptera* and (C-D) *Parasagitta setosa* labeled with antibodies against tyrosinated tubulin (A,B) or acetylated tubulin (C,D). The upper ciliary sense organ (A) stands perpendicular to the tail's longitudinal axis and should therefore be a ciliary fence organ. Assignment to subtypes is however somewhat difficult or virtually impossible on the tail fin, where ciliary sense organs mostly have an oblique orientation. Note that immunhistochemistry against tubulin shows strong reactivity in the apical region of the ciliary sense organs; branches of the afferent nerves are sharply visible in all images (especially in D). Abbreviations: bncfo, branch of an afferent nerve of a ciliary sense organ; c, stiff cilia produced by sensory cells; can, caudal nerve; cfo, ciliary fence organ; cmic, condensed microtubules; cso, ciliary sense organ; iepl, profiles of the intraepidermal nerve plexus; n(epc), nucleus of an epidermal cell; ncfo, afferent nerve of a ciliary fence organ; ncfo, afferent nerve of a ciliary sense organ; tf, tail fin. Scalebars: (A,C) 100 µm; (B,D) 20 µm.

Figure 5: Ultrastructure of ciliary fence and ciliary tuft organs in various Chaetognatha as revealed by SEM (A-C) and TEM (D-H): *Parasagitta setosa* (A), *Sagitta bipunctata* (B), *Spadella valsalinae* (C-H) (A) Dorsal aspect of the transition zone between the head and trunk regions showing anterior third of the corona ciliata and several ciliary fence organs. (B) Close-up of a ciliary tuft organ of the trunk. The tightly packed somata and inner dendritic segments of the sensory cells are clearly visible due to a loss of the distal epidermis cells and the distal sheath cell layer. Note the primary sensory function of constituting cells based on the presence of axons (white arrow). (C) Close-up of a cliary fence organ of the trunk. (D) Longitudinal section of a ciliary fence organ providing an overview of its cellular organization. Note the four different types of constituting cells including an inner and outer population of sensory cells. (E-H) High-power magnifications of some sectors of D, detailed sections are highlighted by dashed boxes in D: (E) Medial, apical region of a ciliary fence organ showing the compartimentalization within the cluster of sensory cells (note arrows pointing on locally condensed radial microfibrils providing strong lateral mounting of the ciliary basis); (F) Basal pole of a ciliary fence organ with extended axons and subjacent primary axon bundle; (G) Somata of type 2 sensory cells; (H) Somata of type 1 sensory cells. Abbreviations: ac, alveolated cell; c, ciliae; cb, ciliary (basal) body; cc, corona ciliata; cfo, ciliary fence organ; cr, cross-striated ciliary rootlets; edb, electron-dense body; dep, distal epidermal cell; ecm, extracellular matrix; fin, fibrilar intercellular matrix; h, head; ids, inner dendritic segment of a sensory cells; ip, inner cellular portion of the ciliary fence organ (type I sensory cells); iz, intermediate zone; lys, lysosome; mcib, multiple and highly ordered bands of cilia; mi, mitochondrion (tubular type); mic, microtubules; miv, microvilli; n, nucleus (sensory cells type 1 and 2); op, outer cellular portion of the ciliary fence organ (type 2 sensory cells); p, pit; pab, primary axon bundle of sensory cells; pc, peripheral cells; pep, proximal epidermal cell; rER, rough endoplasmatic reticulum; rus, regional subset of type 1 or type 2 sensory cells; sc, sensory cell; sc1, type 1 sensory cell; sc2, type 2 sensory cell; sg, secretory granule; shc, sheath cell; so, somata of sensory cells; tr, trunk. Scalebars: (A) 50 µm; (B-D) 10 µm; (E) 2 µm; (F-H) 1µm.

Figure 6: Ultrastructure of ciliary fence organs on the head and in the collarette region of *Spadella valsalinae* (A, C-F) and *Spadella cephaloptera* (B) as revealed by TEM. (A) High-power magnification of some cilia extended by type 2 sensory cells: basal part of the axoneme and the ciliary body (longitudinal view). (B) Detailed longitudinal view of the apical (tip of the inner dendritic segment) region of several type 2 sensory cells. The ciliary bodies are underlain by elongated, unstriated electron-dense bodies connected to hemidesmosome-like adhering junctions by conspicuous radial filamentous matrix. (C-F) Details of apical region (inner dendritic segment zone) of type 1 sensory cells: (C) Oblique-transverse view with cuttings of the cross-striated ciliary rootlets; (D) Transverse sections of cilia extended by type 1 and 2 sensory cells; (E-F) Detailed longitudinal view of the short, electron-dence body from which long and slim cross-striated ciliary rootlets emanate. Region illustrated in F is slightly more proximal to E. Abbreviations: axn, axoneme; c, cilia; cb, ciliary (basal) body; cov, coated vesicle; cr, cross-striated ciliary rootlets; daj, hemidesmosome-like adhering junction; edb, electron-dense body; fia, fibrillous anchoring structure; gs, Golgi stack; ids, inner dendritic segment of type 1 or 2 sensory cells; lbr, (putative) lateral branch of the cross-striated ciliary rootlet, mi, mitochondrion (tubular type); mic, microtubules; miv, microvilli; mvb, multivesicular body; n, nucleus (type 2 sensory cell); rER, rough endoplasmatic reticulum; rfm, radial filamentous matrix; sc1, type 1 sensory cell; sc2, type 2 sensory cell; sej, septate junctions; shc, sheath cell; ssg, structured secretory granules. Scalebars: (C) 1µm, (A,D-F) 0.5 µm, (B) 0.2 µm.

Figure 7: Ultrastructure of ciliary tuft organs in the collarette region of *Spadella valsalinae* as revealed by TEM. (A) Longitudinal section of a ciliary tuft organ with characteristic medio-apical notch located at the lateral tip of the collarette giving an overview of the arrangement of type 1 and 2 sensory cells. Peripheral type 1 sensory cells may also exhibit a strongly electron-dense cytoplasm. (B) Detailed view of the ventral periphery of the ciliary tuft organ shown in A (dashed box). Type 1 sensory cells contain enormously elongated cross-striated ciliary rootlets and condensed system of microtubules. (C) Conkave medio-apical region of a ciliary tuft organ in higher detail. Note the double or triple apical sheath consisting of distal epidermal cells and one or two layers of sheath cells, the latter are rich in secretory granules and extend long, slender microvilli. The electron-dense body of type 2 sensory cells do not continue in cross-striated ciliary rootlets. Longitudinal section. (D) High-power magnification of the medial region of a lateroventral ciliary tuft organ exhibiting a cluster of type 2 sensory cells with a voluminous electron-dense body and some microtubules, but without obvious cross-striated ciliary rootlets. Longitudinal section. Abbreviations: c, cilia; cb, ciliary (basal) body; de, depression in the medio-apical region of a ciliary tuft organ; dep, distal epidermal cell; do, dorsal direction; ecr, elongated and cross-striated ciliary rootlet; edb, electron-dense body; ids, inner dendritic segment of type 1 or 2 sensory cells; mc, main connective; mi, mitochondrion (tubular type); mic, microtubules; miv, microvilli; n, nucleus (type 2 sensory cell); pep, proximal epidermis cells; rER, rough endoplasmatic reticulum; sc1, type 1 sensory cell; sc2, type 2 sensory cell; shc, sheath cell; ssg, structured secretory granules. Scalebars: (A) 5µm, (D) 2 µm, (B-C) 1µm.

Figure 8: Toluidine-blue-stained semithin sections of the head of *Ferosagitta hispida* (A-F) and *Spadella cephaloptera* (G-K) showing excerpts from the section series of the corona ciliata sorted from anterior end (A, G) to the centre (F, J-K). Abbreviations: abc, absorptive cells; ac, alveolated cell of the collarette region; c, locomotory cilia; cplc, epithelial cells producing locomotory cilia; dlm, paired dorsal longitudinal musculature; ecm, extracellular matrix; ep, epidermis; in, intestine; ind, intestinal diverticle; ltm, longitudinal trunk musculature; n, nucleus of an epithelial cell producing a locomotory cilium; sc, sensory cells; shc, sheath cell. Scalebars: (A-F) 10 µm; (K) 20 µm; (G-J) 50 µm.

Figure 9: Corona ciliata of *Spadella cephaloptera* labeled with antibodies against acetylated (A) or tyrosinated (C,D) tubulin (red) and a nuclei dye (green). (A) Overview of the dorsal head; (B) Innervation patterns of the corona ciliata labeled with anti-tyrosinated tubulin, image black-white inverted; (C) Innervation of the corona ciliata labeled with anti-tyrosinated tubulin in higher magnification, note the ciliary fence organ lateral to the corona ciliata; (D) Details of the nuclei of the outer cellular portion housing epithelial cells producing locomotory cilia and of the inner cellular portion comprising absorptive cells and sensory cells; (E) Details of the branched innervation patterns and formation of the coronal nerve projecting from the corona cilata, same image as in (C), black-white inverted. Abbreviations: cn, coronal nerve. Abbreviations: abc, absorptive cells; bcn, lateral branches of a coronal nerve; c, locomotory cilia; cc, corona ciliata; cfo, ciliary fence organ; cmic, condensed microtubules; cn, caudal nerve; cplc, epithelial cells producing locomotory cilia; cso, ciliary sense organ; h, head; iepl, profiles of the intraepidermal nerve plexus; in, intestine; ip, inner cellular portion of the corona ciliata; mcib, multiple and highly ordered ciliary bands; op, outer cellular portion of the corona ciliata; pab, primary axon bundle of coronal sensory cells; sc, sensory cell; tr, trunk. Scalebars: (A,B) 50 µm; (C,E) 20 µm; (D) 10 µm.

Figure 10: Corona ciliata of *Parasagitta setosa*. (A,B), *Sagitta* sp. (D) and *Spadella valsalinae* (C,E) labeled with antibodies against actin (A,B) and acetylated tubulin (D) or tyrosinated tubulin (C,E). Note the different shapes of the corona ciliata ranging from longitudinal-elliptical in Sagittidae (A,B,D) to transverse-oval in Spadellidae (C,D). Images A, B and E were black-white inverted. Abbreviations: abc, absorptive cells; bcn, lateral branches of a coronal nerve; cc, corona ciliata; cfo, ciliary fence organ; cmic, condensed microtubules; cn, coronal nerve; cplc, epithelial cells producing locomotory cilia; cto, ciliary tuft receptor; ey, eye; h, head; ip, inner cellular portion of the corona ciliata; mcib, multiple and highly ordered bands of locomotory cilia; op, outer cellular portion of the corona ciliata; pab, primary axon bundle of coronal sensory cells; sc, sensory cell; tr, trunk. Scalebars: (A,B) 200 µm; (D) 100 µm; (C,E) 50 µm.

Figure 11: The corona ciliata as well as ciliary fence and ciliary tuft organs of *Spadella cephaloptera*. (A) Distribution of BrdU in the corona ciliata and head of an adult specimen; (B) Aspartate (red) and nuclei (green) in the corona ciliata. (C,D) Aspartate (red) and nuclei (green) in ciliary sense organs documented on the tail fin (C) and on the trunk (D). Note that only a small central population of sensory cell somata in the ciliary sense organs (C,D) shows

a distinctive immunoreactivity against aspartate antibody (white arrows). Abbreviations: abc, absorptive cells; cc, corona ciliata; cfo, ciliary fence organ; cplc, epithelial cells producing locomotory cilia; cso ciliary sense organ; ip, inner cellular portion of the corona ciliata; op, outer cellular portion of the corona ciliata; sc, sensory cell. Scalebars: (A) 100 µm; (B,C) 50 µm; (D) 25 µm.

Figure 12: Ultrastructure of the corona ciliata of *Spadella cephaloptera* revealed by SEM (A) and TEM (B-I). (A) Overview of corona ciliata, dorsal view. (B-E) Longitudinal sections demonstrating the ultrastructural architecture of the corona ciliata: (B) Multiple image alignment of the right half of the corona ciliata giving an overview of the distribution of the four cell types involved in its forming; (C) High-power magnification of the apical region of absorptive cells and sensory cells displaying an enormous microtubular apparatus. The apices surround a subsurface cavity narrowed by partly ramified microvilliform projections and cilia (not shown!); (D) Close-up of the apical region of the outer cellular portion, which forms a highly ordered system of multilayered, narrowed, collar-like tips from which the locomotory cilia are protruded. The microtubular system of the ciliary epithelial cells becomes considerably condensed; (E) Details of the apical region of one ciliary epithelial cell at the level of the basal body and distal portion of the ciliary rootlet encompassed by microtubules. (F-I) Innervation of the corona ciliata following the a gradient of complexity starting from (F) primary axon bundles formed by several local sensory cells of the inner cellular portion, which (G) become collected in lateral branches (H) passing into and subsequently forming both coronal nerves. (I) The coronal nerve may contain both afferent and efferent fibres. At the ventral margin of each coronal nerve several synapses are found that may innervate the paired dorsomedian longitudinal musculature. Abbreviations: abc, absorptive cells; bci, basal region of the locomotory cilia (surrounded by cytoplasmic collars); bcn, lateral branches of a coronal nerve; c, locomotory cilia; ca, subsurface cavity (filled with cilia and microvilli); cb, ciliary (basal) body; cc, corona ciliata; cn, coronal nerve; co, collar-like infolding of the ciliary epithelial cells; cplc, epithelial cells producing locomotory cilia; cr, ciliary rootlet; ctu, cytoplasmic tubules; dep, distal epidermal cell; dlm, paired dorsomedian longitudinal musculature; ecm, extracellular matrix; end, (primary) endosome; h, head; ip, inner cellular portion of the corona ciliata; ltm, longitudinal trunk musculature; mcib, multiple and highly ordered bands of locomotory cilia; mi, mitochondrion (tubular type); mic, microtubules; miv, microvilliform apical projections of the absorptive cells and sensory cells; n, nucleus (absorptive cell); ne, neck-like lateral protuberance at the head-trunk transition zone (collarette region); neu, neurites; nt, neurotubules; op, outer cellular portion of the corona ciliata; pab, primary axon bundle of coronal sensory cells; pep, proximal epidermal cells; sc, sensory cell; shc, sheath cell; sy, synapse; syv, synaptic vesicles; tr, trunk. Scalebars: (A) 30 µm; (B) 10 µm; (G,H) 2 µm; (C,D,F,) 1 µm; (E,I) 0.5 µm.

Figure 1
Click here to download high resolution image

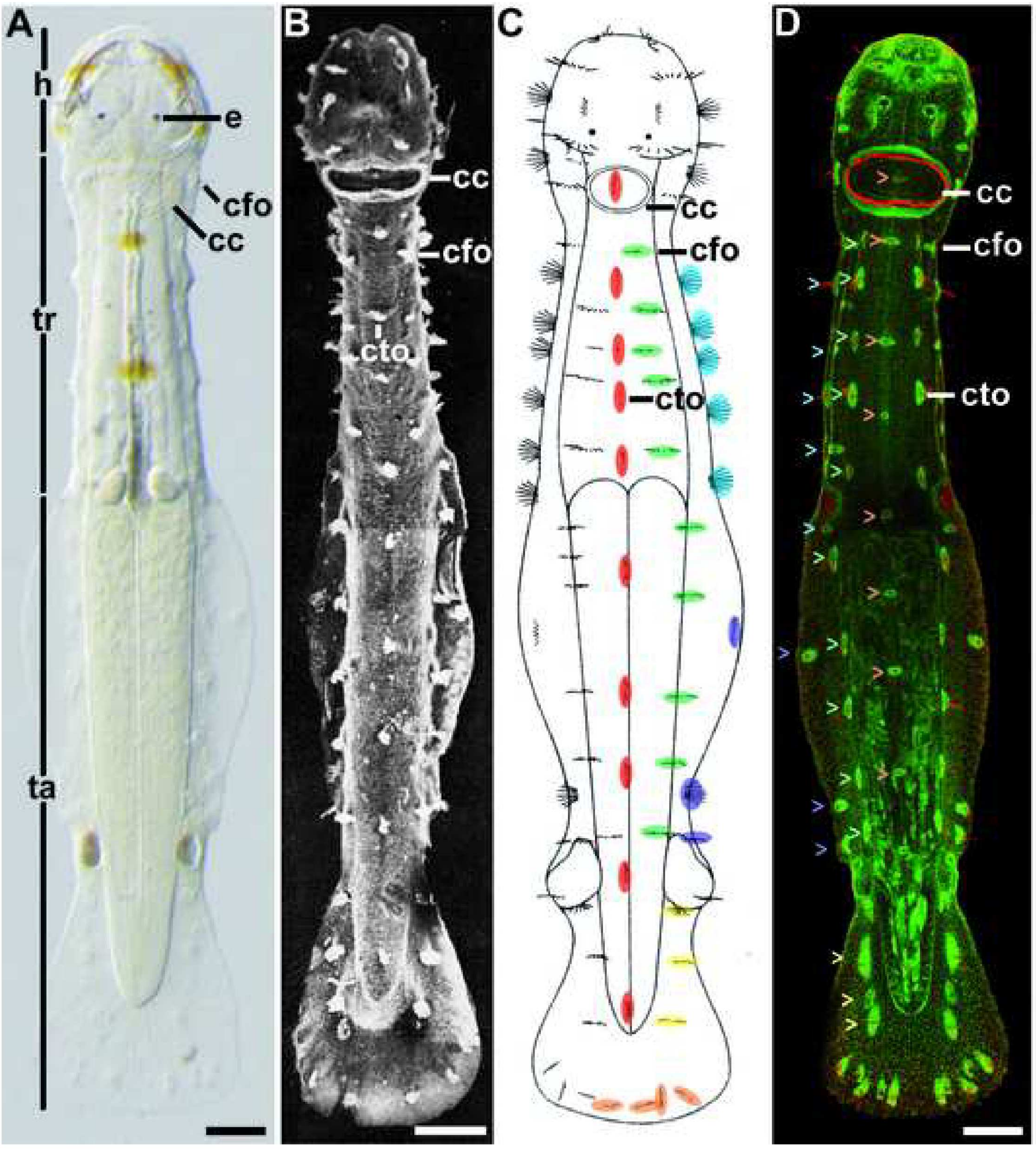
A
h
e
cfo
cc
tr
ta
B
cc
cfo
cto
C
cc
cfo
cto
D
cc
cfo
cto

Figure 2

Click here to download high resolution image

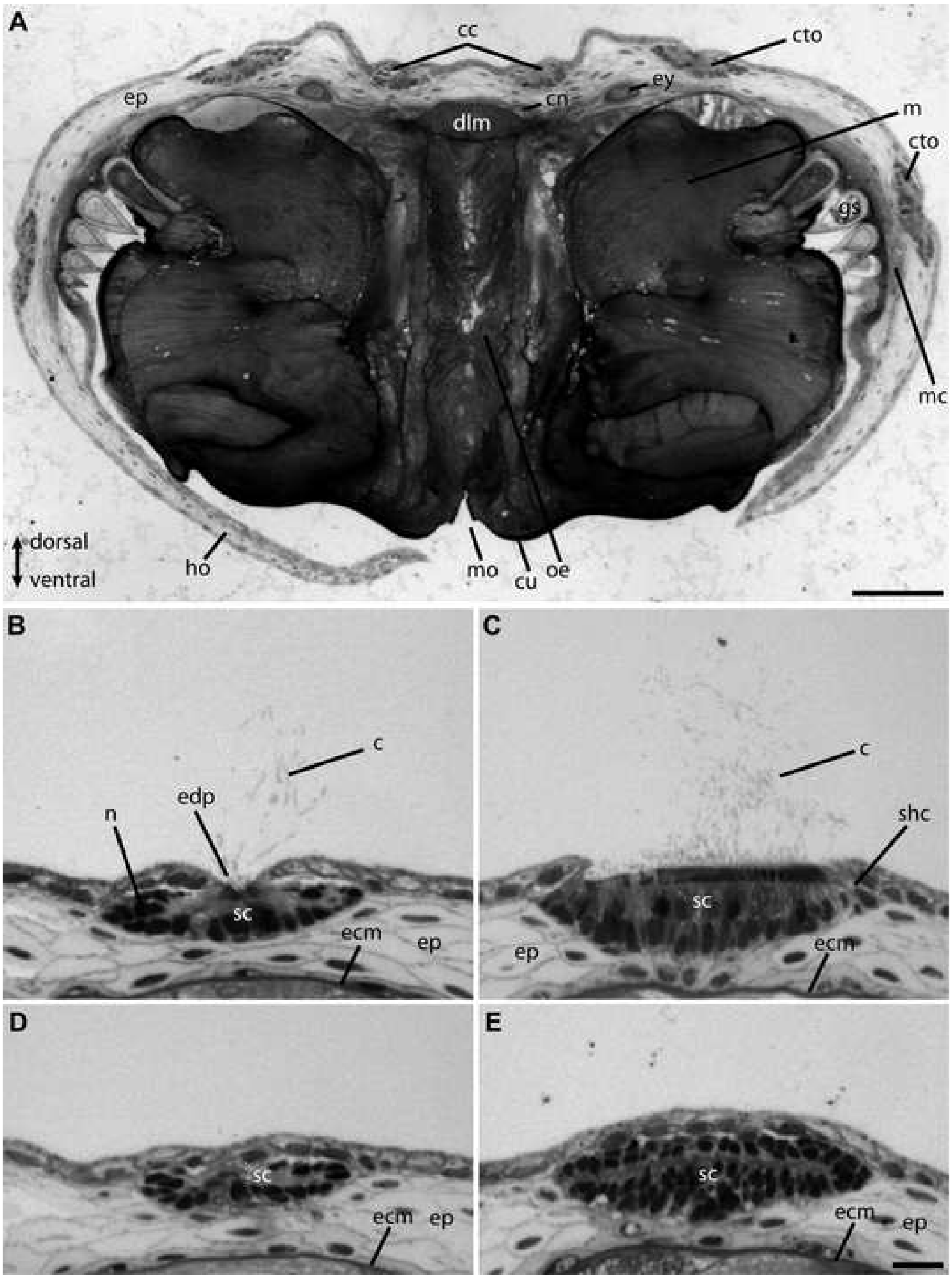
A
cc
cto
ep
ey
cn
dlm
m
cto
gs
mc
dorsal
ventral
ho
mo
cu
oe
B
c
edp
n
sc
ecm
ep
C
c
shc
sc
ep
ecm
D
sc
ecm
ep
E
sc
ecm
ep

Figure 3
Click here to download high resolution image

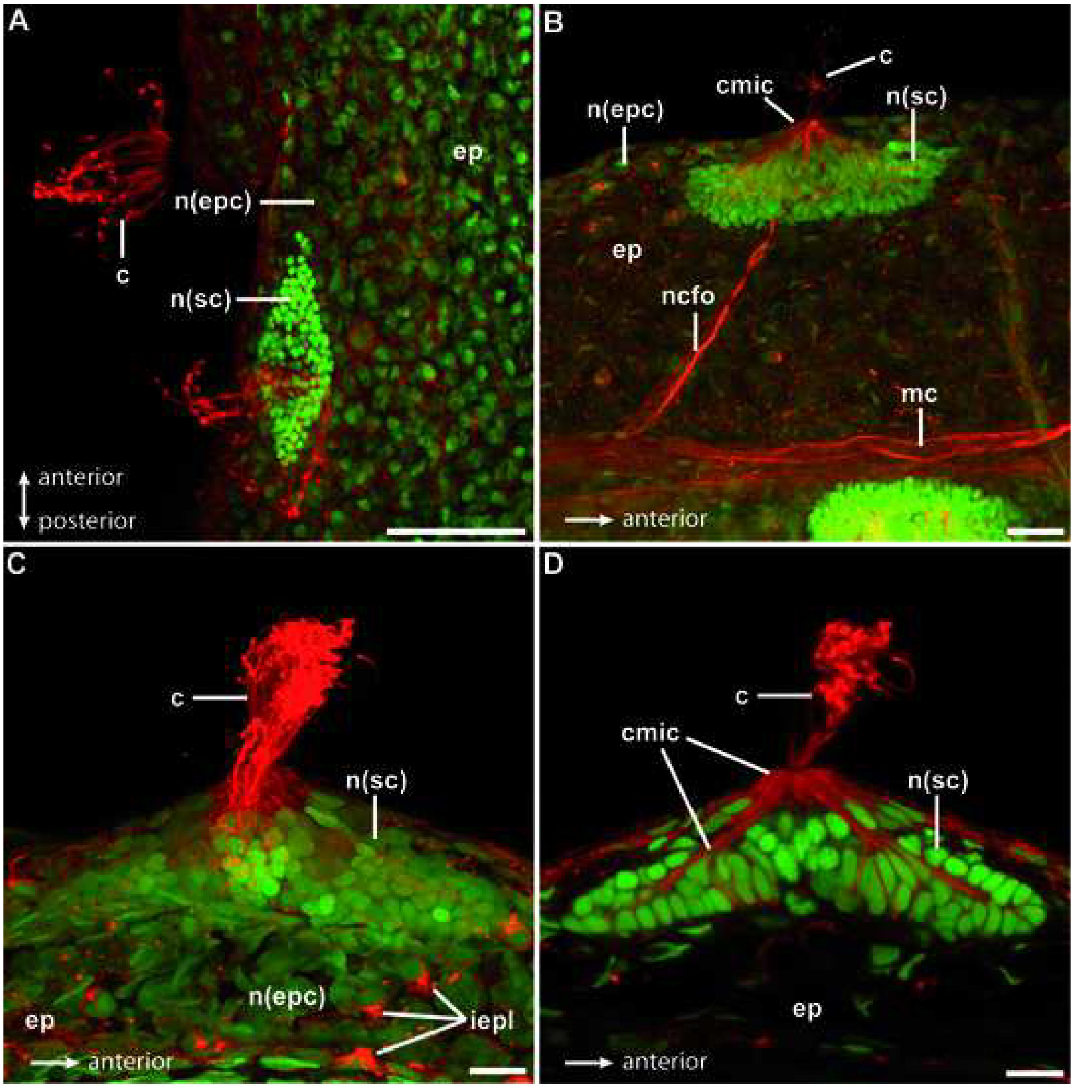
A
c
n(epc)
ep
n(sc)
anterior
posterior
B
c
cmic
n(epc)
n(sc)
ep
ncfo
mc
anterior
C
c
n(sc)
ep
n(epc)
iepl
anterior
D
c
cmic
n(sc)
ep
anterior

Figure 4
Click here to download high resolution image

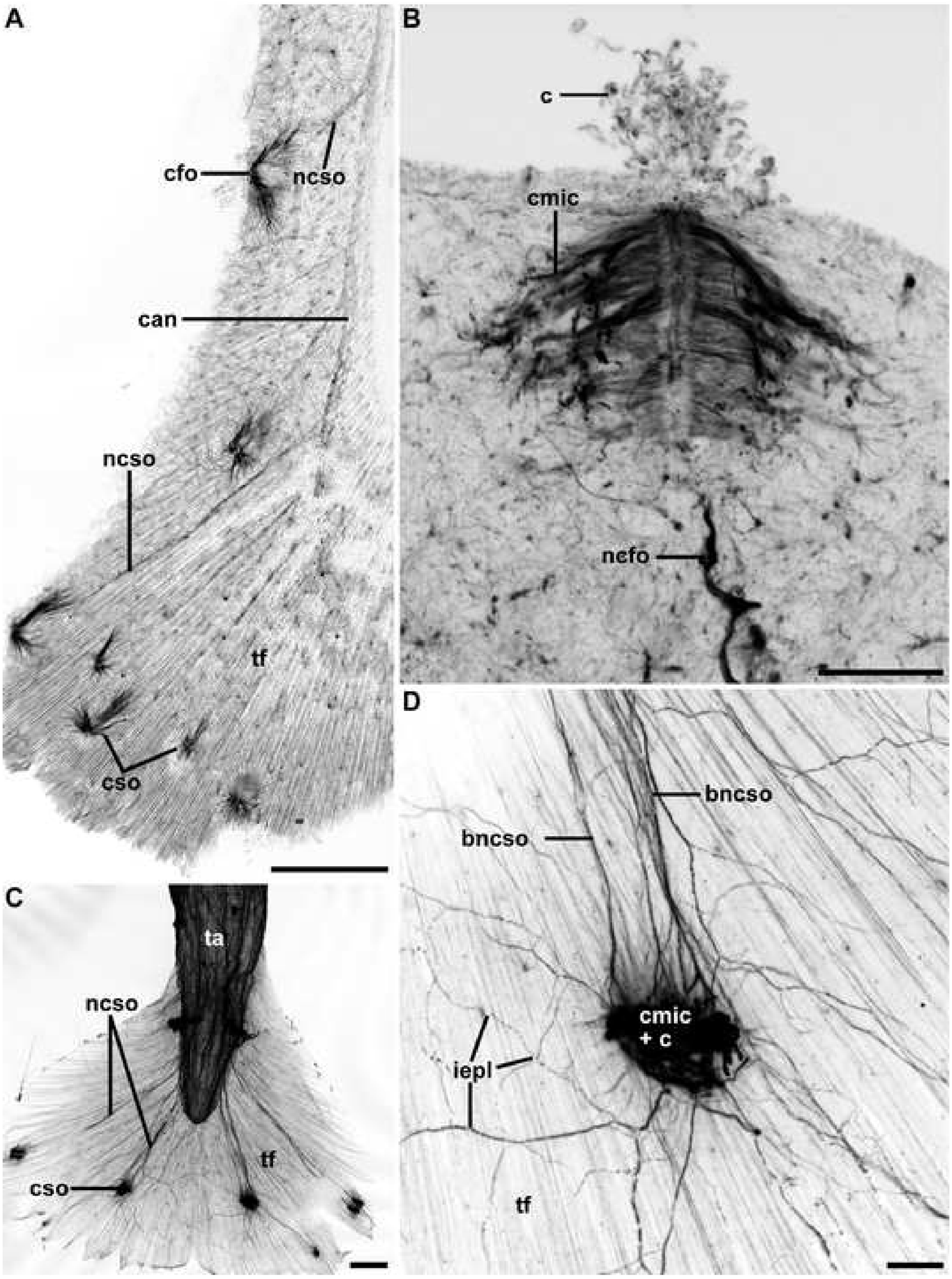
A
cfo
ncso
can
ncso
tf
cso
B
c
cmic
ncfo
C
ta
ncso
tf
cso
D
bncso
bncso
cmic
+ c
iepl
tf

Figure 5

Click here to download high resolution image

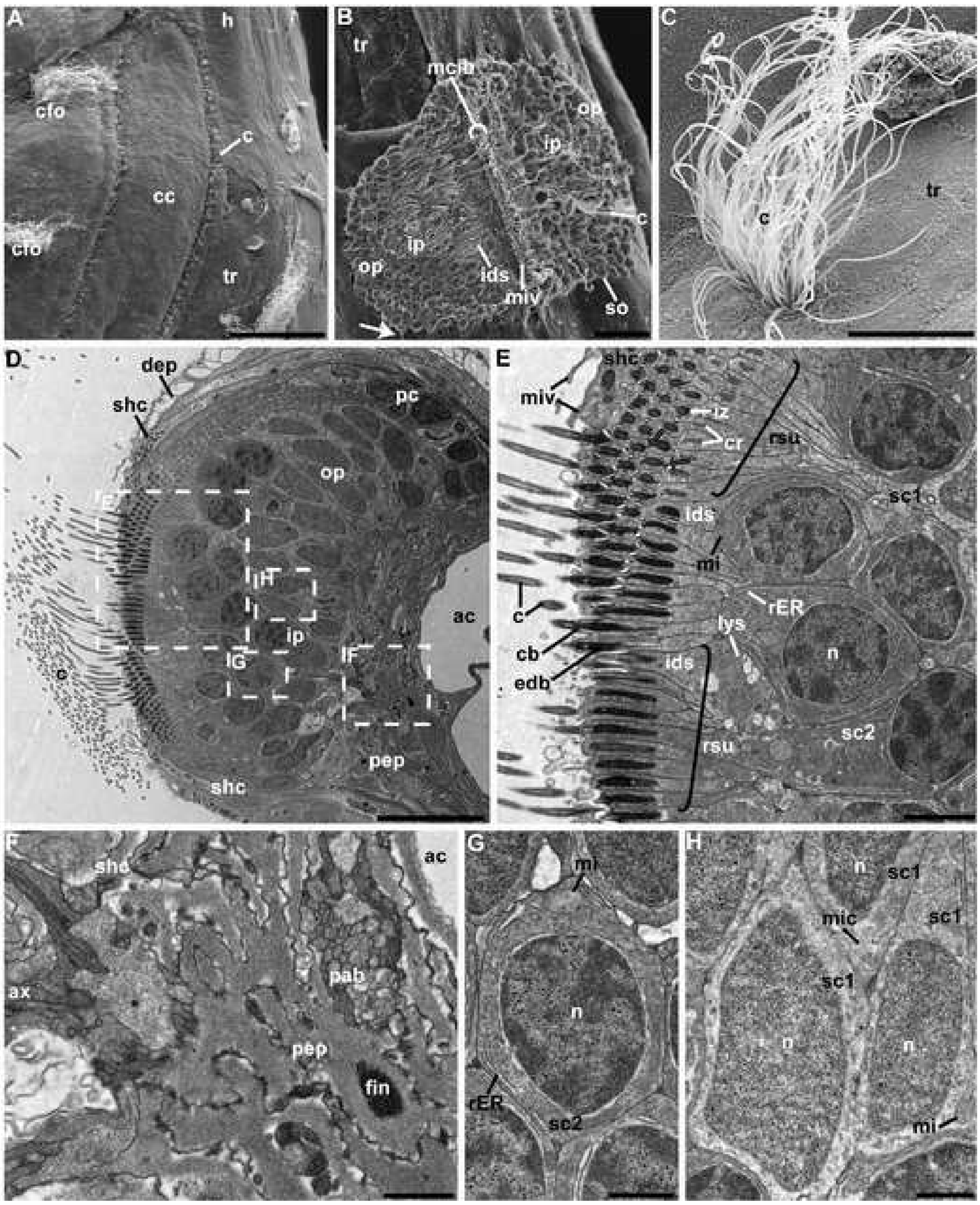
A
h
cfo
c
cc
cfo
tr
B
tr
mcib
op
ip
c
ip
op
ids
miv
so
C
c
tr
D
dep
shc
pc
op
E
H
ip
ac
G
F
c
pep
shc
E
shc
miv
iz
cr
rsu
sc1
ids
mi
rER
c
lys
cb
n
edb
ids
rsu
sc2
F
shc
ac
ax
pab
pep
fin
G
mi
n
rER
sc2
H
n
sc1
mic
sc1
sc1
n
n
mi

Figure 6

Click here to download high resolution image

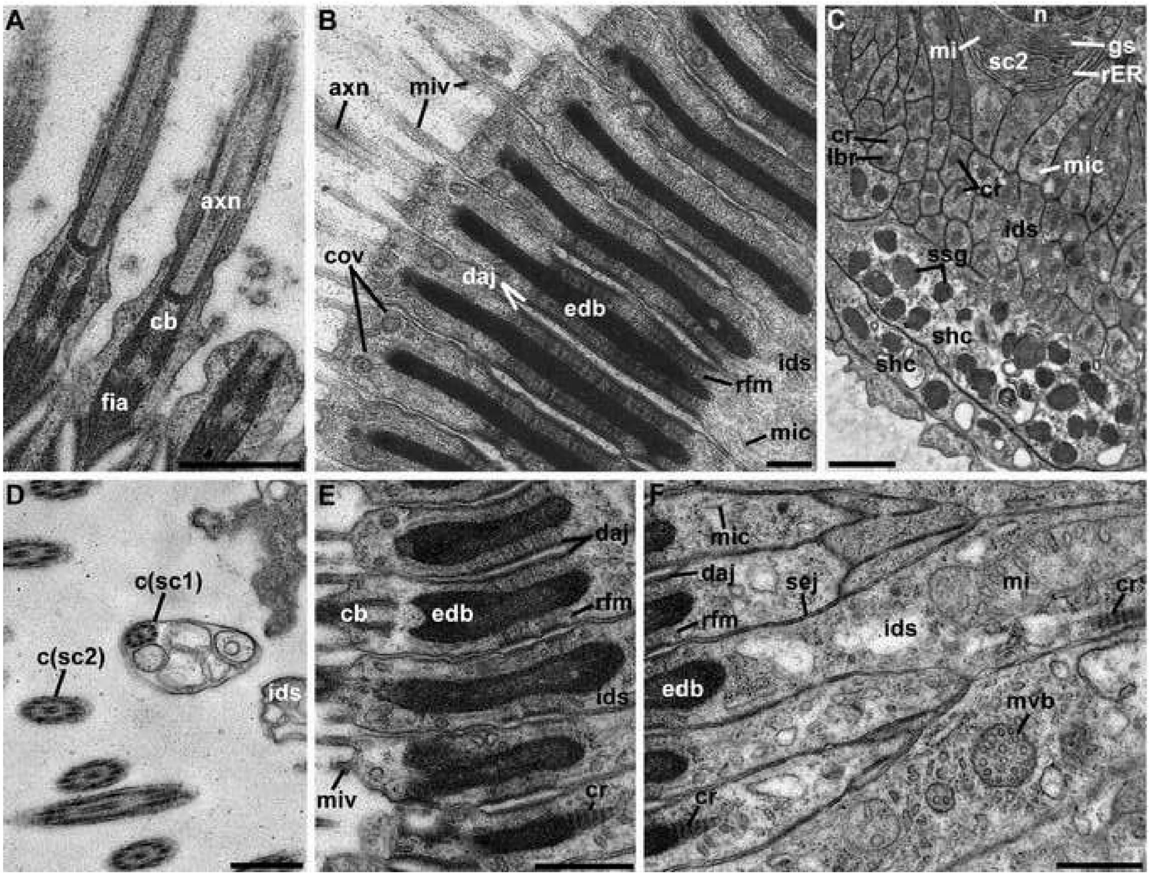
A
axn
cb
fia
B
axn
miv
cov
daj
edb
ids
rfm
mic
C
n
mi
sc2
gs
rER
cr
lbr
cr
mic
ids
ssg
shc
shc
D
c(sc1)
c(sc2)
ids
E
daj
cb
edb
rfm
ids
miv
cr
F
mic
daj
sej
mi
cr
rfm
ids
edb
mvb
cr

Figure 7

Click here to download high resolution image

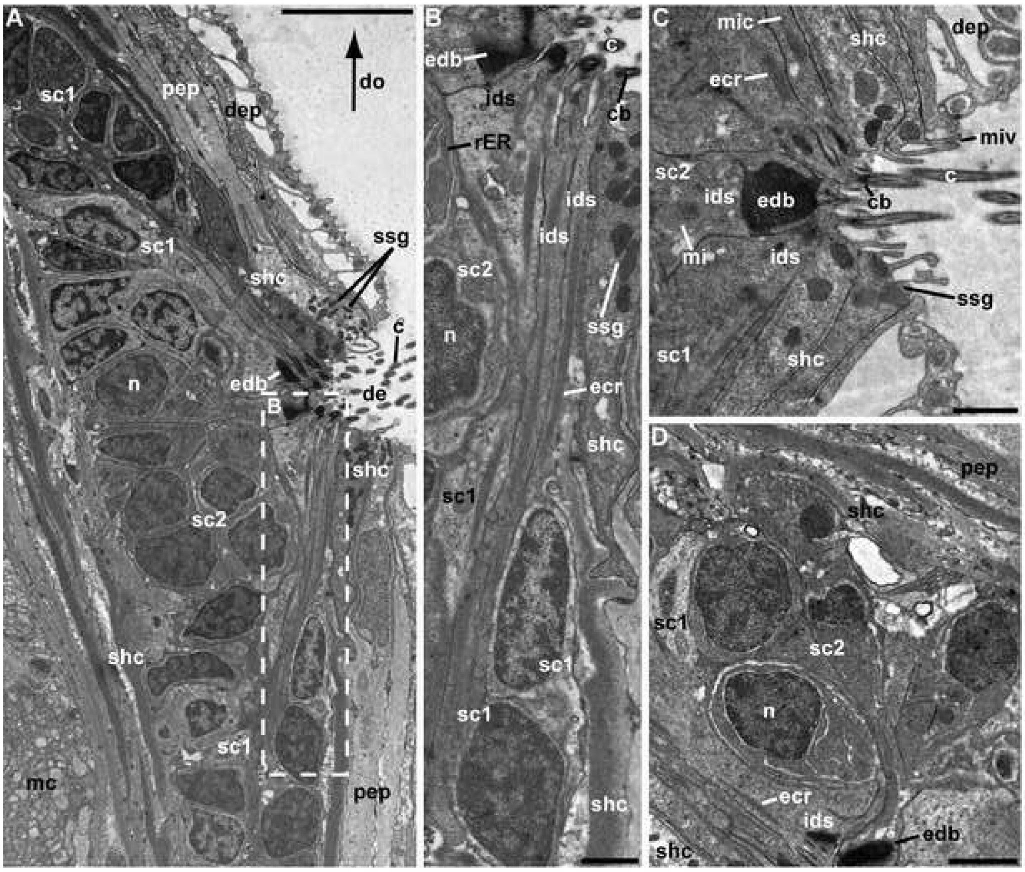
A
sc1
pep
dep
do
sc1
shc
ssg
c
edb
de
n
B
shc
sc2
shc
sc1
mc
pep
B
edb
c
ids
cb
rER
ids
ids
sc2
n
ssg
ecr
shc
sc1
sc1
sc1
shc
C
mic
shc
dep
ecr
miv
sc2
ids
edb
c
cb
mi
ids
ssg
sc1
shc
D
pep
shc
sc1
sc2
n
ecr
ids
edb
shc

Figure 8

Click here to download high resolution image

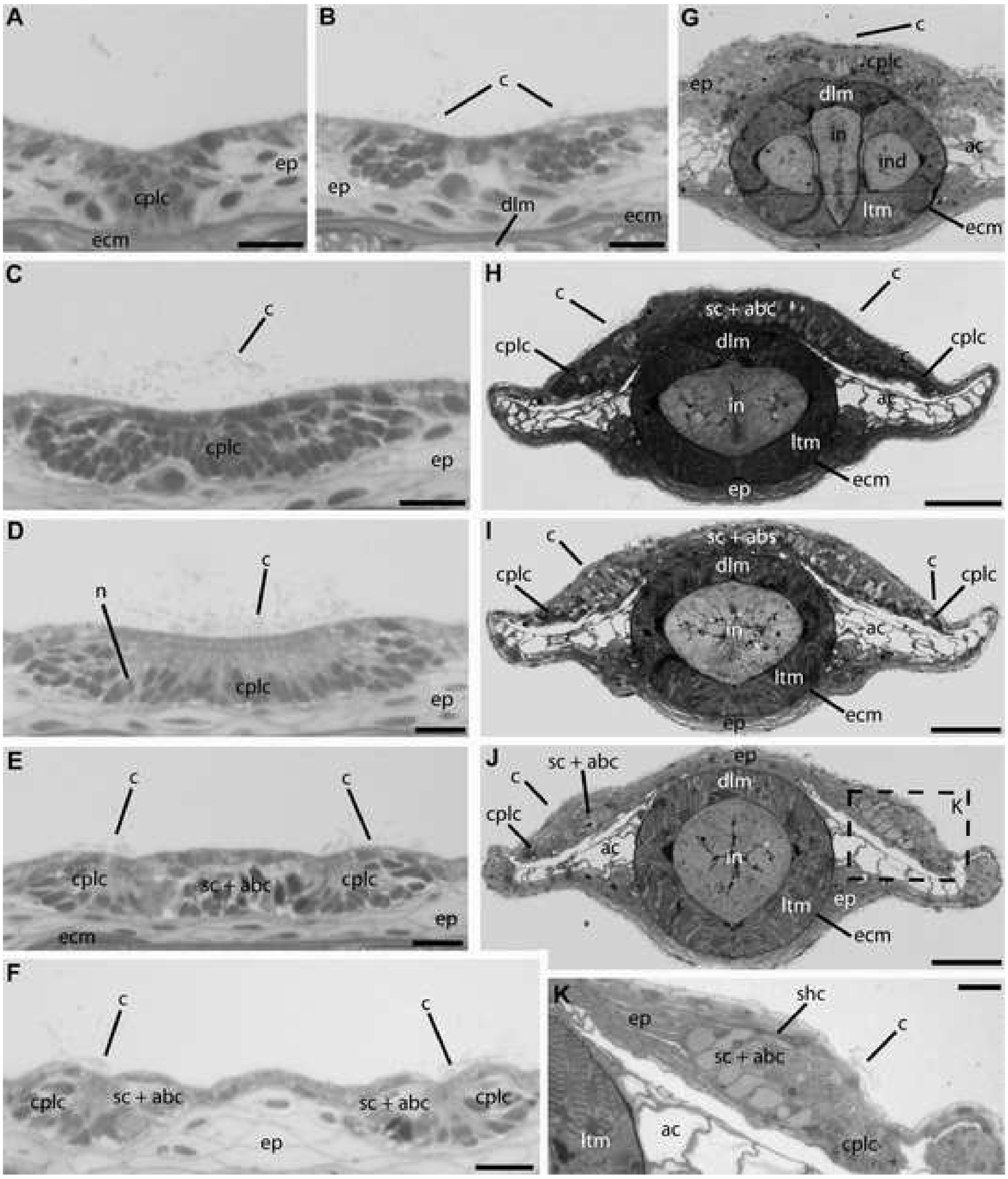
A
ep
cplc
ecm
B
c
ep
dlm
ecm
G
c
cplc
ep
dlm
in
ind
ac
ltm
ecm
C
c
cplc
ep
H
c
sc + abc
c
cplc
dlm
cplc
in
ac
ltm
ecm
ep
D
c
n
cplc
ep
I
c
sc + abs
dlm
c
cplc
cplc
in
ac
ltm
ecm
ep
E
c
c
cplc
sc + abc
cplc
ep
ecm
J
sc + abc
ep
c
dlm
cplc
K
ac
in
ltm
ep
ecm
F
c
c
cplc
sc + abc
sc + abc
cplc
ep
K
shc
ep
c
sc + abc
ac
ltm
cplc

Figure 9
Click here to download high resolution image

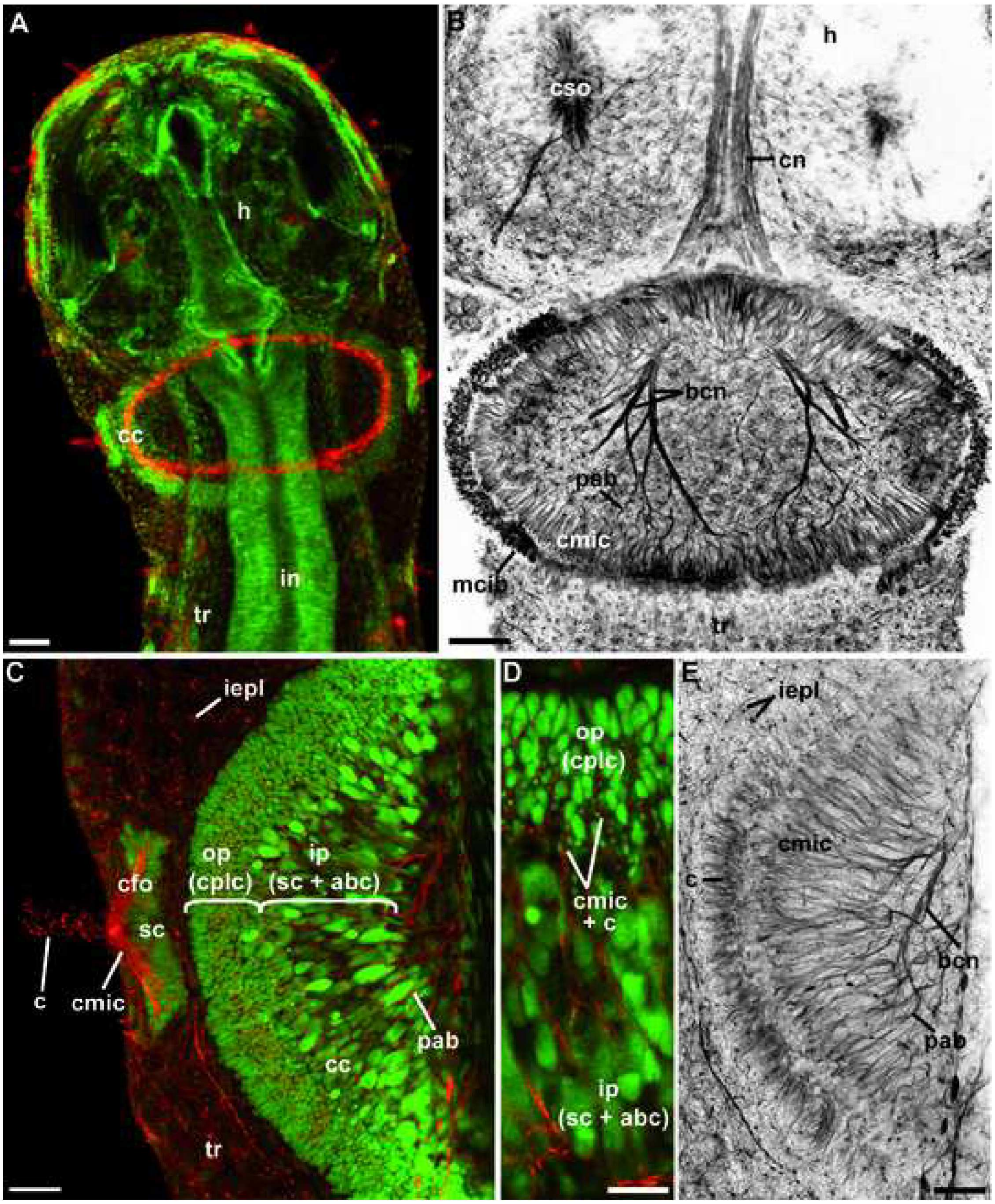
A
h
cc
in
tr
B
cso
h
cn
bcn
pab
cmic
mcib
tr
C
iepl
cfo
op
(cplc)
ip
(sc + abc)
sc
c
cmic
pab
cc
tr
D
op
(cplc)
cmic
+ c
ip
(sc + abc)
E
iepl
cmic
c
bcn
pab

Figure 10

Click here to download high resolution image

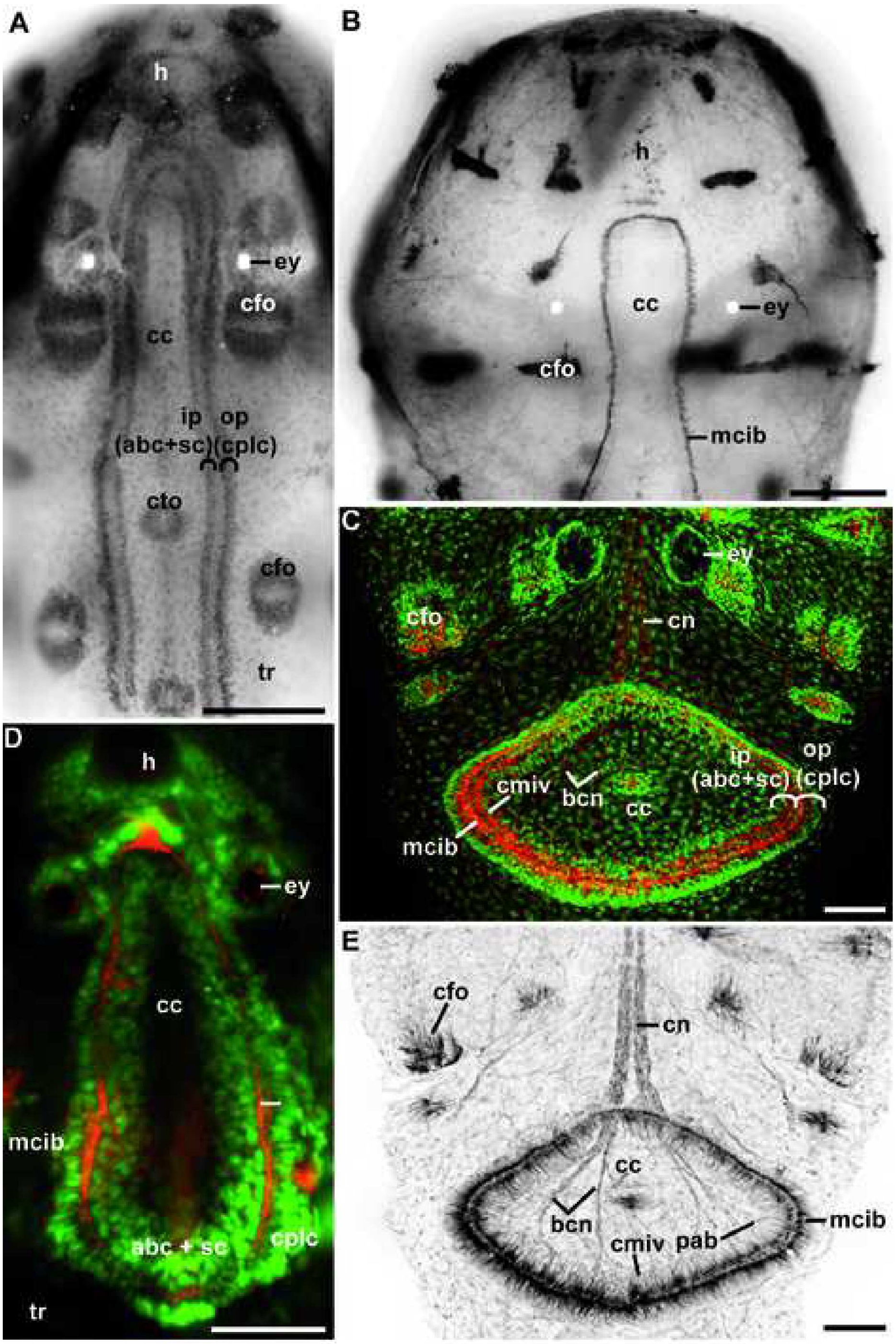
A
h
ey
cfo
cc
ip
op
(abc+sc)
(cplc)
cto
cfo
tr
B
h
cc
ey
cfo
mcib
C
ey
cn
cfo
ip
op
(abc+sc)
(cplc)
cmiv
bcn
cc
mcib
D
h
ey
cc
mcib
abc + sc
cplc
tr
E
cfo
cn
cc
bcn
cmiv
pab
mcib

Figure 11

Click here to download high resolution image

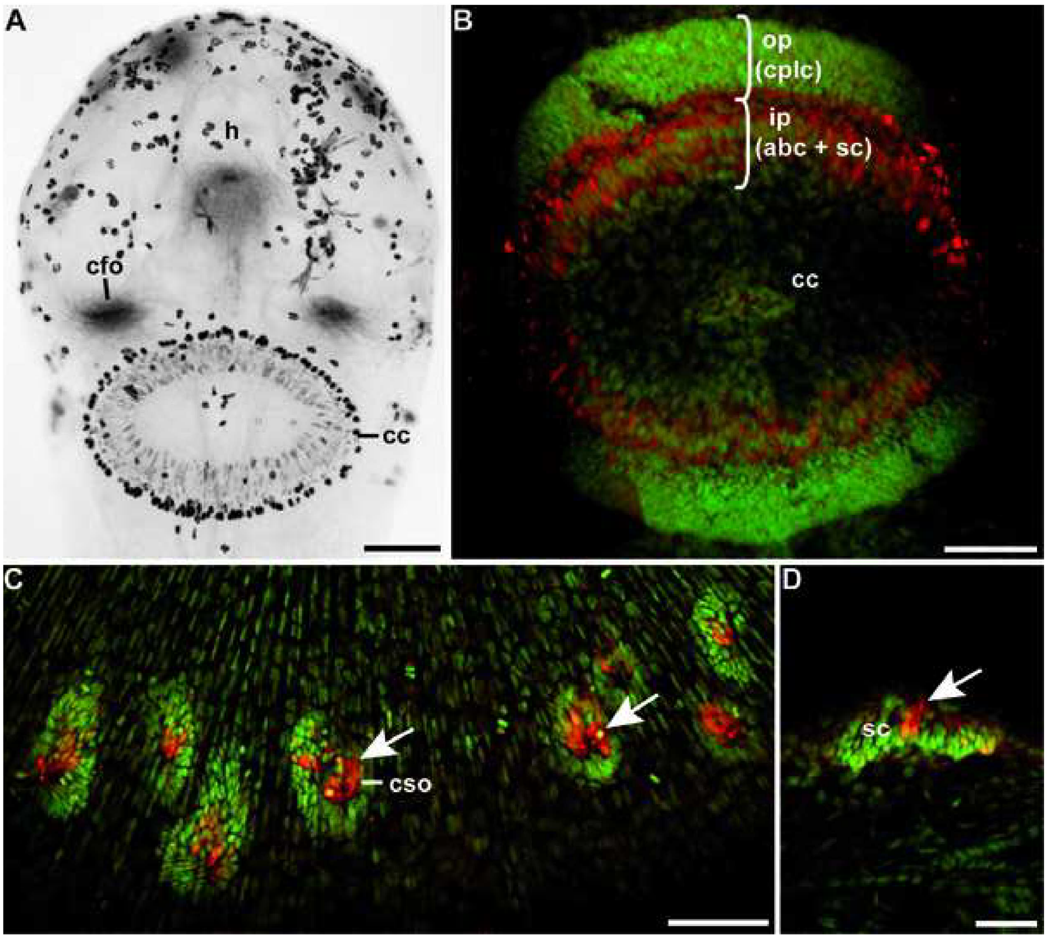
A
h
cfo
cc
B
op
(cplc)
ip
(abc + sc)
cc
C
cso
D
sc

Figure 12

Click here to download high resolution image

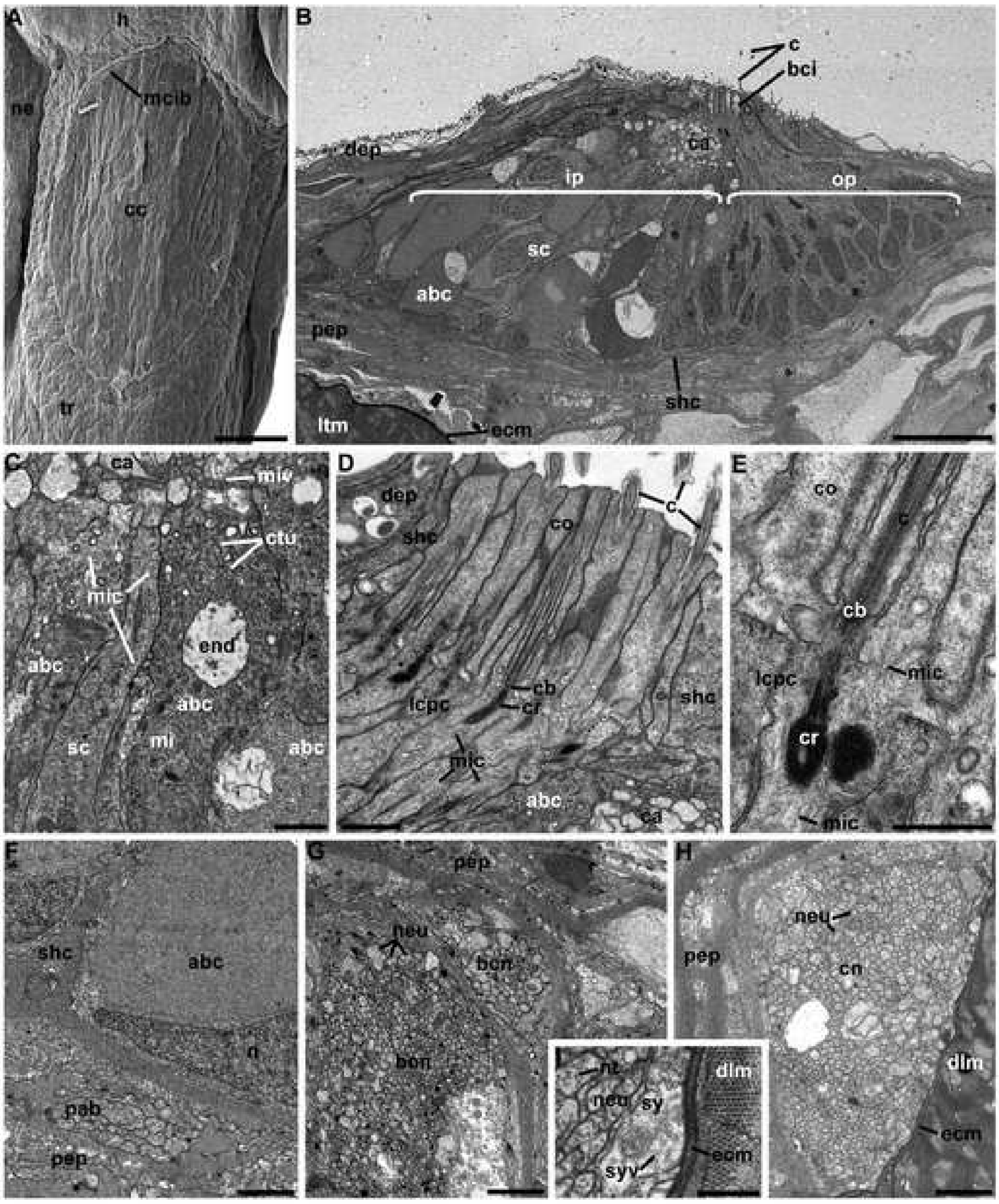
A
h
ne
mcib
cc
tr
B
c
bci
ca
dep
ip
op
sc
abc
pep
shc
ltm
ecm
C
ca
miv
ctu
mic
end
abc
abc
sc
mi
abc
D
dep
shc
co
c
cb
cr
lcpc
shc
mic
abc
ca
E
co
c
cb
lcpc
mic
cr
mic
F
shc
abc
n
pab
pep
G
pep
neu
bcn
bcn
nt
neu
sy
syv
dlm
ecm
H
pep
neu
cn
dlm
ecm

9. Selbständigkeitserklärung

Hiermit erkläre ich, dass diese Arbeit bisher von mir weder an der Mathematisch-Naturwissenschaftlichen Fakultät der Ernst-Moritz-Arndt-Universität Greifswald noch einer anderen wissenschaftlichen Einrichtung zum Zwecke der Promotion eingereicht wurde.

Ferner erkläre ich, dass ich diese Arbeit selbständig verfasst und keine anderen als die darin angegebenen Hilfsmittel und Hilfen benutzt und keine Textabschnitte eines Dritten ohne Kennzeichnung übernommen habe.

Verena Rieger

10. Acknowledgements

I am most grateful to my supervisor, Prof. Steffen Harzsch, who granted me the opportunity for this dissertation and was very supportive and extremely patient during every phase.

Prof. Roland Melzer gratiously agreed to be my second supervisor.

I also wish to thank Dr. A. Schmidt-Rhaesa, who was an invaluable help during my trip to Sylt where I was collecting gnathostomulids.

I want to express my gratitude towards Dr. Yvan Perez, who not only provided animals and hosted me during my visit to Marseille but also was a big help with his extensive knowledge and insight into the Chaetognatha.

Prof. Bill Hansson and the Max Planck Society provided an excellent working environment during the first two years of my project. The members of the Department of Evolutionary Neuroethology turned working in Jena into a very exiting, informative, and fun time. I am grateful to all of them.

I want to thank Dr. Carsten Müller, Dipl.-Biol. Franziska Glück, Dipl.-Biol. Charlotte Winkelmann, Dipl.-Biol. Helga Kapp, Dr. Andy Sombke and Dipl.-Biol. Elisabeth Lipke from Greifswald and Rostock for their insights, cooperation and help with my project.

My coauthors Prof. Thurston Lacalli and Prof. George Shinn deserve my gratitude for their valuable comments and their cooperation on our manuscripts.

I am also very grateful to the many other collaboration partners that contributed to my work by collecting specimens or providing antibodies: Hans Agricola, Andreas Bick, E. Buchner, Gisèle Champalbert, Anneke Denda, T. Leitz, Marc Pagano, Florian Peine, and Akihiro Shiroza.

Sincere thanks go to Dr. Bernd Christiansen, the research team, and the crew of the RV Meteor, cruise 79-3, who allowed me to join them in this great adventure. I learned a lot and had a marvelous time.

I am deeply indebted to the German Research Foundation (Deutsche Forschungsgemeinschaft) for their generous financial support (grant HA 2540/7-1/2/3).

A special mention and thank you is due for all members of the focus group ‘Deep Metazoan Phylogeny’, especially the members of the morphology group, for many useful discussions, new perspectives and excellent teamwork.

I am especially grateful to all of my friends, some of which also helped by proofreading: Elisabeth Zieger, Eva Blank, Thomas Schmidt, Christine Mißbach and Ewald Grosse-Wilde always had an open ear for my problems and patiently acted as my moral support along the way. You guys are the best.

Last but not least, I want to thank my family, especially my parents. They supported and encouraged me in every way and in all my endeavors and were of invaluable help, especially during the last months of writing.

11. Appendix:

11.1 Material & Methods

Material

Chaetognatha

Spadella cephaloptera was obtained during the summers of 2006-2008 by Yvan Perez (University of Provence, Marseille) at Sormiou near Marseille. They were collected by dragging a plankton-net over a meadow of *Posidonia* and were kept in seawater tanks at the laboratory. A more detailed description is available in (Rieger et al., 2010, 2011). The sampling of hatchlings took place in 2007 and 2008 as described in Rieger et al. (2011). For BrdU (Bromodeoxyuridine) experiments, hatchlings and adult specimens were incubated in BrdU-saline prior to fixation (see below), which was mainly done in July 2008.

A new species of *Spadella, Spadella valsalinae,* was discovered in the Mediterranean Sea near Pula, Croatia by Dr. C. Müller. Specimens were provided by Dr. C. Müller and Dipl.-Biol. Charlotte Winkelmann.

Some specimens *of Sagitta bipunctata, Pterosagitta draco, Flaccisagitta enflata*, and *Flaccisagitta hexaptera* were provided by several cooperation partners as detailed in Rieger et al. (2010). Several other specimens and species were collected during sampling trips in the Atlantic Ocean and the Mediterranean Sea.

The first trip was in May 2009 near the island of Madeira. Sampling took place as part of cruise 384 of the "R.V. Poseidon". Samples were taken by Dr. Florian Peine (Universität Rostock).

The second trip took place between July and August 2009 in the south Atlantic. The cruise number was M79/1 of the "R.V. Meteor". Samples were taken by PD Dr. Andreas Bick (Universität Rostock).

The third trip took place between September and October 2009 close to Cape Verde. The cruise number was M79/3 of the "R.V. Meteor". Samples were taken by me.

The fourth trip took place between July and October 2009 close to Cyprus. The cruise number was MSM 14/1 of the "R.V. Maria S. Merian". Samples were taken by Dipl.-Biol. Anneke Denda (Universität Hamburg).

All of the specimens obtained during the sampling trips were stored in 4% PFA. Information on sampling sites and methods was provided by Dipl.-Biol. Franziska Glück in Glück (2010).They were sorted and identified by Dipl.-Biol. F. Glück and Dipl.-Biol. Helga Kapp as described in greater detail in Glück (2010).

Gnathostomulida

Gnathostomulids were obtained on the island of Sylt during a stay at the "Wattenmeerstation" in List with the help and supervision of PD Dr. A. Schmidt-Rhaesa (Zoologisches Museum Hamburg) and the assistance of his students. Sand samples were taken from the tidal zone of the intertidal mudflats north of the Wattenmeerstation and gnathostomulids were discovered in a patch of sand at the edge of a colony of *Spionidae* (Polychaeta). The sand samples were taken with a shovel and consisted of the upper 15-20cm of substrate. The samples were processed by the seawater-ice method (Uhlig, 1964). Gnathostomulids in the extract were found using a stereomicroscope and extracted with a glass pipette. They were immobilized in a solution of 7% magnesium chloride ($MgCl_2$) before fixation in 4 % PFA and stored in PBS with sodium-azide.

Methods

Immunohistochemistry

Immunohistochemical experiments were conducted using the following standard protocol unless specified otherwise. Details on the antibodies and dilutions used are provided in tables 3-6. Details on the composition of the buffers and other solutions are also provided on page 220. All specimens were processed as whole mounts.

The samples were processed using the following protocol:

(1) Fix specimens in 4% paraformaldehyde (PFA) for at least 4 hours at room temperature
(2) Store specimens in the fixative or PBS (phosphate buffered saline) with added sodium-azide at 4°C
(3) Wash in several changes of PBS at room temperature
(4) Pre-incubate in PBS-TX (PBS with TritonX-100) for 45-60 minutes at room temperature
(5) Incubate in primary antibody (single staining) or a mix of two primary antibodies (double staining) diluted in PBS-TX overnight at room temperature
(6) Wash for at least 4 x 30 minutes in several changes of PBS at room temperature
(7) Incubate in a secondary antibody (single staining) or a mix of two secondary antibodies (double staining) and, if required, a nuclear marker for 4 hours at room temperature
(8) Wash for at least 4 x 30 minutes in several changes of PBS at room temperature
(9) Mount between two cover-slips in Mowiol

For anti-histamine experiments, immunohistochemistry specimens were fixed for 4 hours in a 4% EDAC (1-Ethyl-3-(3-dimethylaminopropyl) carbodiimide) solution prior to the fixation in PFA.

For Bromodeoxyuridine (BrdU) experiments animals were first incubated in BrdU-saline (seawater with added BrdU). The time of incubation (pulse) for the first set of experiments was 4 hours. It included adult specimens as well as hatchlings, all of which were fixed immediately after incubation. For the second set, the pulse/chase experiments, only hatchlings were used. They ranged in age from 1-6 days after hatching. The time of incubation was 10 minutes. Afterwards, a part of the hatchlings were fixed immediately while others were raised in seawater without BrdU for additional 1, 2, 4, 8 or 24 hours before fixation. During anti-BrdU immunohistochemistry, an additional step was required compared to the standard protocol described above. The specimens were incubated in 2N HCL for 20 minutes prior to the PBS-TX pre-incubation.

Primary antibodies:

Tab. 3: Details of applied primary antibodies

Antigen	Host	Clonality	Provider	Product-No.	Dilution
Acetylated Tubulin	mouse	mono	Sigma-Aldrich	T6793	1:2000
Allatostatin 1	rabbit	poly	Prof. Dr. H. Agricola, University of Jena		1:2000
Aspartate	rabbit	poly	MoBiTec	1011GE	1:2000
BrdU	mouse	mono	Amersham	RPN20	1:100
CCAP	rabbit	poly	Prof. Dr. H. Agricola, University of Jena		1:2000
FMRF-amide	rabbit	poly	Immunostar	20091	1:2000
GABA	rabbit	poly	Sigma-Aldrich	A2052	1:2000
Glutamate	rabbit	poly	MoBiTec	1014GE	1:2000
GLWamids	rabbit	poly	Prof. Dr. T. Leitz, TU Kaiserslautern		1:500
Histamine	rabbit	poly	Progen	16043	1:1000
Octopamine	mouse	mono	Jena Bioscience	ABD-029	1:1000
Perisulfakinin	rabbit	poly	Prof. Dr. H. Agricola, University of Jena		1:2000
SCPb	rabbit	mono	Laboratories of the Zoology Department, University of Washington		1:50
Serotonin	rabbit	poly	Immunostar	20080	1:1000
SubP	rabbit	poly	Immunostar	20064	1:5000
Synorf (Synapsin)	mouse	mono	Prof. Dr. E. Buchner, Universität Würzburg		1:30
Taurine	rabbit	poly	Gemacbio	AP042	1:2000
Tyramine	rabbit	poly	Millipore	AB124	1:500
Tyrosin Hydroxylase	mouse	mono	Immunostar	22941	1:1000
Tyrosinated Tubulin	mouse	mono	Sigma-Aldrich	T9028	1:1000
Ubiquitin	rabbit	poly	Chemicon(Millipore)	AB1690	1:500

Secondary antibodies:

Tab. 4: Details of applied secondary antibodies

Fluorochrome	Antigen	Host	Provider	Product-No.	Dilution
Alexa Fluor 488	rabbit IgG	goat	Invitrogen	A11008	1:500
Cy3	mouse IgG	goat	Jackson Immuno Research	115-165-003	1:500

Other labeling reagents

Tab. 5: Details of applied phallotoxin

Fluorochrome	Toxin	Provider	Product-No.	Dilution
Alexa Fluor 546	Phallotoxin	Invitrogen	A22283	1:51

Tab. 6: Details of applied nuclear dyes

Dye	Provider	Product-No.	Dilution
HOECHST (bisBenzimide)	Sigma-Aldrich	H 33258	0.5%
YOYO-1	Invitrogen	Y-3601	0.25%

Specificity of antibodies

The specificity of the most widely used antibodies is addressed in the attached publications (Harzsch et al. 2009; Rieger et al. 2010, 2011).

Microscopy

Overview images were obtained using a Zeiss Axioimager respective imaging software (see Rieger et al., 2010) or a Nikon Eclipse 90i with a DS-2MBWc camera and the NIS-Elements AR imaging software. Images of details were obtained with either a Zeiss LSM 410 with the respective imaging software (see Rieger et al., 2010) or a Leica TCS SP5 with the LAS AF imaging software (Version 2.3.1). The filter settings for the Nikon eclipse in respect to the emission and absorption spectrums of the most commonly used fluorochromes are detailed in figure 13 as an example.

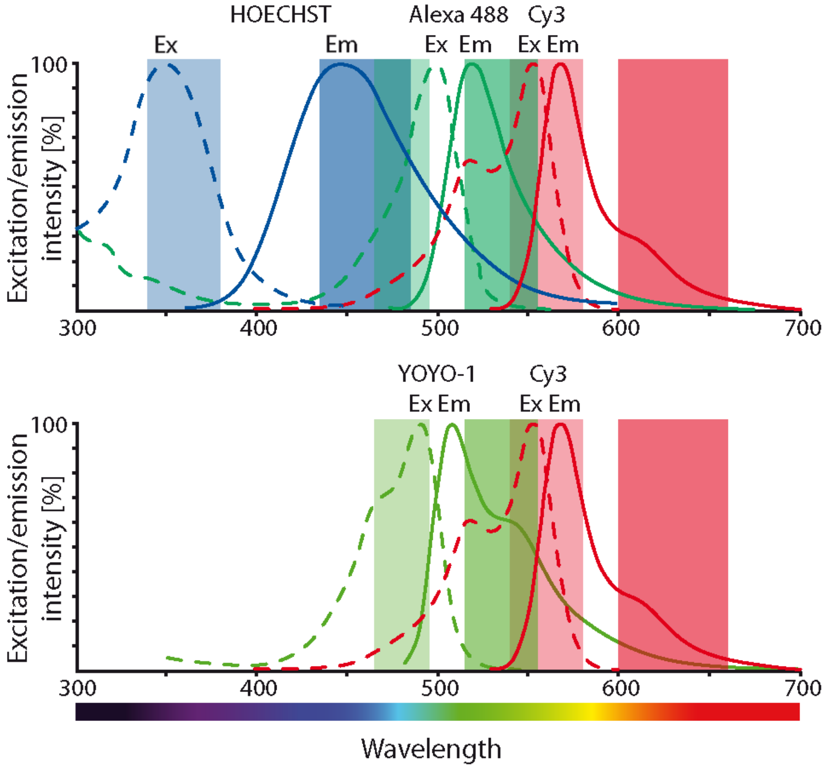

Fig. 13: Excitation (Ex, dotted line) and emission (Em, solid line) of commonly used fluorochromes. Blue: HOECHST (nuclear marker); dark green: Alexa 488 (conjugated to secondary antibody or phalloidin); light green: YOYO-1 (nuclear marker); red: Cy3 (conjugated to secondary antibody or phalloidin). Boxes indicate the wavelengths of filters for excitation (lighter color) and emission (darker color) on the Nikon Eclipse 90i.

Image processing

Adobe Photoshop CS4 was used to adjust the brightness of the colors using the ‘levels’ tool. In some cases images were black-white inverted. Figures were arranged using the Adobe Illustrator CS4 software.

Neuroanatomical Terminology

Where possible the terminology as suggested in Richter et al. (2010) was applied.

Buffers and solutions

Stock solutions for phosphate buffer:

Stock solution A: 33.9g $Na_2HPO_4 * 2 H_2O$ / 1000ml H_2O

Stock solution B: 25.9g KH_2PO_4 / 1000ml H_2O

PFA (paraformaldehyde) 4% in phosphate buffer:

Mix 4 g PFA in 50ml H_2O, stir solution, and heat to a maximum temperature of 60 °C. Stop heating and add a few drops of NaOH until the solution becomes clear. Add 40ml stock solution A and 10ml stock solution B, filter and store at -20°C.

PBS (phosphate buffered saline; 0.1M, pH 7.4):

Mix 40ml stock solution A, 10ml stock solution B, and 50ml H_2O. Add 580mg NaCl and 20µl Triton X-100.

PBS-TX (0.3% Triton, Na-Azide, 1% BSA):

Dissolve 30µl Triton X-100, 100mg bovine serum albumin (BSA), and 100 µl sodium azide (of a 5 % stock solution) in 10 ml PBS.

BrdU Saline (0.2mg/ml):

Dilute 350µl BrdU stock solution (from Amersham, RPN20 Proliferation Kit) in 5ml seawater.

4% EDAC solution

Dissolve 4g EDAC in 100ml PBS.

11.2 List of abbreviations

Technical and physical terminology

HPLC	high-performance liquid chromatography
Em	emission
Ex	excitation

Chemical terminology

BrdU	bromodeoxyuridin
BSA	bovine serum albumin
EDAC	1-ethyl-3-(3-dimethylaminopropyl) carbodiimide
PBS	phosphate buffered saline
PBS-TX	phosphate buffered saline with TritonX-100
PFA	paraformaldehyde

Neurotransmitters

ASTA	allatostatin
CCAP	crustacean cardioactive peptide
GABA	gamma-aminobutyric acid
PSK	perisulfakinin
SCPb	small cardiac peptide B
SubP	substance P

Neuroanatomical terminology

ap	adhesive papillae
bnp	bridge neuropil
cc	corona ciliata
cn	caudal nerve
cnp	core neuropil
con	coronal nerve
e	eye
fc	frontal connective
fh	frontal horn
fr	fence receptor
gs	grasping spines
int	intestine
-ir	immunoreactive, immunoreactivity
lf	lateral fin
lh	lateral horn
mc	main connectives
on	optical nerve
rs	receptaculum seminis
sv	seminal vesicle
tf	tail fin
vg	vestibular ganglion
VNC	ventral nerve center